Explaining temporal variability of and quantifying the impact of livestock grazing intensity on carbon and energy exchange in semi-arid near-natural and managed savanna ecosystems in South Africa

DISSERTATION

zur Erlangung des akademischen Grades eines

Doktors der Naturwissenschaften (Dr. rer. nat.)

in der Bayreuther Graduiertenschule für Mathematik und Naturwissenschaften (BayNAT)

der Universität Bayreuth

vorgelegt von

Kanisios Mukwashi

aus Buhera, Simbabwe

Bayreuth 2021

Die vorliegende Arbeit wurde in der Zeit von Dezember 2015 bis Juni 2021 in Bayreuth am Lehrstuhl für Mikrometeorologie unter der Betreuung von Herrn Professor Dr. Christoph Thomas angefertigt.

Vollständiger Abdruck der von der Bayreuther Graduiertenschule für Mathematik und Naturwissenschaften (BayNAT) der Universität Bayreuth genehmigten Dissertation zur Erlangung des akademischen Grades eines Doktors der Naturwissenschaften (Dr. Rer. Nat.)

Dissertation eingereicht am: 14.01.2020

Zulassung durch das Leitungsgremium: 05.02.2020

Wissenschaftliches Kolloquium: 01.06.2021

Amtierender Direktor: Prof. Dr. Markus Lippitz

Prüfungsausschuss:

Prof. Dr. Christoph Thomas   (Gutachter)

Prof. Dr. Steven Higgins   (Gutachter)

Prof. Dr. Cyrus Samimi   (Vorsitz)

Prof. Dr. Bettina Engelbrecht

Dedicated to my wife, children and whole family

Summary

This dissertation focuses on the responses of carbon and turbulent energy fluxes to land use disturbance and micro-climatic controls in semi-arid areas of South Africa using the eddy covariance method. Flux tower sites examined were Skukuza, a near-natural savanna ecosystem, and two Karoo sites (Karoo 1 and Karoo 2), managed under different livestock grazing intensities. Flux measurements at the Karoo sites were conducted over two years from November 2015 to October 2017 while six hydro-ecological years were assessed at Skukuza, from among the existing flux datasets from 2000 to 2014.

The main aims, investigated at both the Skukuza and Karoo sites, were: to better understand the rain-pulse driven 'hot moments' of ecosystem respiration (R_{eco}) efflux, as well as the connectivity of precipitation and net ecosystem carbon dioxide (CO_2) exchange (NEE) to explain the onset and end of vegetative functional seasons, and to study the temporal variation of ecosystem water use efficiency (EWUE). Additionally, site-specific issues were studied separately on individual sites in order to complement previous work and to derive new findings.

The phenomenon of 'hot moments' of CO_2 efflux or R_{eco} spikes, as well as the amount of precipitation required to trigger them, has not been explored before for these types of ecosystems. Ecosystem respiration spikes at Karoo sites responded to rain pulses that ranged in size from about 1 mm to less than 15 mm and falling within 1 day to a maximum of 5 days. The minimum precipitation thresholds that triggered R_{eco} spikes at Karoo 1 and Karoo 2 were 3 mm and 1 mm, respectively. The dissimilarity was most likely due to higher organic matter substrate for microbial activity at the Karoo 2 site, rested from livestock grazing, compared to the gently grazed Karoo 1 site. There were no distinct 'hot moments' of CO_2 efflux at Skukuza due to increased size of rain pulses, frequency of precipitation occurrence and amount of precipitation.

A novel approach to determine the onset and end of vegetative functional seasons at the study sites was introduced using connectivity between precipitation and NEE. The minimum precipitation thresholds to reach the onset of vegetative functional seasons at Karoo 1, Karoo 2 and Skukuza were 33.9 mm, 40.8 mm and 52.8 mm, respectively. However, it was noted that the end of vegetative functional seasons at Skukuza for successive hydro-ecological years were generally late as the deep-rooted plants continued to show a photosynthesis response a couple

of days or weeks after the cessation of rainfall. This indicates the need to consider plant functional types in determining the end of the vegetative functional seasons.

EWUE ranged from around 1 g C kg^{-1} H_2O at Karoo sites to about 2 g C kg^{-1} H_2O at Skukuza showing a rise with increasing rainfall and productivity between Karoo sites and Skukuza. Livestock grazing intensity (gentle grazing vs long-term resting) did not cause a significant difference in EWUE between Karoo 1 and Karoo 2 for two consecutive growing seasons.

In regard to the impact of livestock grazing intensity on annual carbon budgets, the annual NEE of Karoo 1 and Karoo 2 were similar. However, the long rest of 8 years at Karoo 2 relatively increased carbon sequestration compared to the gently grazed Karoo 1 site suggesting that land use management can potentially modify vegetation structure and function, which may cause variation in the magnitude of gross primary production. For instance, during the second year of measurement, the annual carbon budgets for Karoo 1 and Karoo 2 were 41 ± 74 g C m^{-2} yr^{-1} and -57 ± 83 g C m^{-2} yr^{-1}, respectively. Vegetation greenness and micro-meteorological conditions were similar between Karoo 1 and Karoo 2, allowing a rational comparison on the effect of livestock grazing intensity on carbon exchange components between the sites.

Using the thermal diffusion equation, soil heat storage above 10 cm depth was estimated and it improved energy balance closure (EBC) at Karoo 1 by 4 % and 3 % for year 1 and year 2, respectively. At Karoo 2, accounting for soil heat storage improved EBC slightly by 1 % for both year 1 and year 2. A comparison of ground heat flux between Karoo 1 and Karoo 2 showed no significant difference between the two sites.

At Skukuza, soil moisture was the main control of the variability of maximum photosynthetic capacity (GPP_{opt}) and net ecosystem CO_2 exchange offset (NEE_{offset}). GPP_{opt} and NEE_{offset} increased with increasing soil moisture, supporting the notion that photosynthesis and R_{eco} are higher during wet periods compared to dry periods. Air temperature and vapor pressure deficit did not show a clear relationship with GPP_{opt} at Skukuza. From this study, it is concluded that land management and climate related controls are influential in the temporal dynamics of carbon and energy exchange components at these semi-arid areas of South Africa.

Zusammenfassung

Die vorliegende Dissertation betrachtet die Reaktion turbulenter Kohlenstoff- und Energieflüsse semiarider Gebiete Südafrikas auf Störungen in der Landnutzung und auf mikroklimatische Einflussgrößen mit Hilfe der Eddy-Kovarianz-Methode. Die Messungen stammen vom ‚Skukuza'-Messturm in einem naturnahen Savannenökosystem, sowie von zwei Messtürmen in der Karoo (‚Karoo 1' und ‚Karoo 2'), die jeweils von unterschiedlich intensiver Weidewirtschaft geprägt waren. An den beiden Karoo-Standorten wurden jeweils über zwei Jahre, von November 2015 bis Oktober 2017, Flussmessungen vorgenommen, während insgesamt sechs hydro-ökologische Jahre als Teil der bestehenden Langzeitmessungen von 2000 bis 2014 am Skukuza-Turm im Rahmen dieser Arbeit betrachtet wurden.

Die Arbeit beschäftigt sich im Kern mit drei Phänomenen, die sowohl am Skukuza-Messturm, als auch an denen in der Karoo untersucht wurden: mit sogenannten ‚Hot moments' des Ökosystem-Respirationsflusses (R_{eco}), ausgelöst durch Niederschlagsimpulse nach der Trockenzeit; mit der Verknüpfung von Niederschlägen und dem Netto-Ökosystemaustauschs von Kohlenstoffdioxid (CO_2; NEE) zur Bestimmung der Vegetationsperioden; sowie mit der zeitlichen Variation in der ökosystemintegrierten Wassernutzungseffizienz (EWUE). Desweiteren wurden standortspezifische Themen separat für die individuellen Standorte untersucht, um frühere Arbeiten zu Ergänzen und neue Erkenntnisse abzuleiten.

Der Zusammenhang zwischen den sogenannten ‚Hot moments' der CO_2-Flüsse bzw. der R_{eco}-Spitzen und der benötigten Niederschlagsmenge, um solche auszulösen, wurde für die hier betrachteten Ökosysteme bislang nicht untersucht. In der Karoo wurden Spitzen in der Ökosystemrespiration als Antwort auf Niederschlagsereignisse mit einer Intensität von 1 mm bis weniger als 15 mm und einer Dauer von weniger als 1 bis zu 5 Tagen beobachtet. Der minimale Schwellenwert zur Auslösung von R_{eco}-Spitzen betrug 3 mm am Standort Karoo 1, beziehungsweise 1 mm am Standort Karoo 2. Der Unterschied ließ sich mit hoher Wahrscheinlichkeit auf die höhere Verfügbarkeit an organikreichem Substrat für mikrobielle Aktivität am ehemals beweideten Standort Karoo 2 zurückführen, verglichen mit dem auch heute noch schwach beweideten Standort Karoo 1. Am Skukuza-Turm wurden, wahrscheinlich

aufgrund des intensiveren und häufigeren Niederschlages, keine ‚Hot moments' im CO_2-Fluss beobachtet.

Ein neuartiger Ansatz zur Bestimmung von Anfang und Ende der Vegetationsperiode an den Messstandorten wurde vorgestellt, der auf der Verknüpfung von Niederschlagsmessungen und Messungen des NEE basiert. Die minimale Niederschlagsmenge um den Beginn der Vegetationsperiode zu erreichen betrug jeweils 33.9 mm, 40.8 mm und 52.8 mm an den Standorten Karoo 1, Karoo2 und Skukuza. Es wurde jedoch auch festgestellt, dass das Ende der Vegetationsperiode am Standort Skukuza für aufeinanderfolgende hydro-ökologische Jahre im Allgemeinen spät einsetzte, da die tiefwurzelnde Vegetation auch nach dem Ende der Regenzeit weiterhin einige Tage bis Wochen Photosyntheseaktivität zeigte. Zukünftig sollten daher gegebenenfalls Pflanzenfunktionstypen bei der Bestimmung des Endes der Vegetationsperiode berücksichtigt werden.

Die EWUE reichte von 1 g C kg^{-1} H_2O in der Karoo bis zu 2 g C kg^{-1} H_2O am Standort Skukuza und war somit durch die größere Niederschlagsmenge und Produktivität am Standort Skukuza gegenüber der Karoo erhöht. Über einen Zeitraum von zwei aufeinander folgenden Wachstumsperioden wurde kein signifikanter Unterschied in der EWUE zwischen Karoo 1 und Karoo 2 gefunden, der sich auf die unterschiedliche Beweidungsintensität (schwach beweidet vs. langfristig ruhend) zurückführen ließe.

Hinsichtlich des Einflusses der Beweidungsintensität auf die jährliche Kohlenstoffbilanz waren Karoo 1 und Karoo 2 im jährlichen NEE einander ähnlich. Die lange Beweidungsruhe von 8 Jahren am Standort Karoo 2 erhöhte jedoch relativ gesehen die Kohlenstoffsequestrierung verglichen mit dem schwach beweideten Standort Karoo 1, was darauf schließen lässt, dass die Landnutzung potenziell die Vegetationsstruktur und –funktion modifizieren und Variationen in der Höhe der Bruttoprimärproduktion verursachen kann. Während des zweiten Jahres der Messungen betrugen die jährlichen Kohlenstoffbilanzen beispielsweise 41 ± 74 g C m^{-2} yr^{-1} für Karoo 1 und -57 ± 83 g C m^{-2} yr^{-1} für Karoo 2. Dabei waren die mikrometeorologischen Bedingungen und die ‚greenness' der Vegetation zwischen beiden Standorten ähnlich, was eine

gute Vergleichbarkeit des Effekts der Beweidungsintensität auf den Kohlenstoffaustausch untereinander zuließ.

Die Wärmespeicherung im Boden oberhalb 10 cm Tiefe wurde mit Hilfe der Wärmeleitungsgleichung abgeschätzt und führte zu einer Verbesserung der Energiebilanzschließung (EBC) um 4 % im ersten und 3 % im zweiten Jahr für den Standort Karoo 1, während am Standort Karoo 2 die Berücksichtigung der Wärmespeicherung die EBC in beiden Jahren nur leicht um jeweils 1 % verbesserte. Der Bodenwärmestrom zeigte keine signifikanten Unterschiede zwischen Karoo 1 und Karoo 2.

Am Standort Skukuza wurde die Bodenfeuchte als primäre Steuergröße für die Variabilität der maximalen Photosynthesekapazität (GPP_{opt}) und des Offsets im Netto-Ökosystemaustausch von CO_2 (NEE_{offset}) identifiziert. GPP_{opt} und NEE_{offset} waren mit steigender Bodenfeuchte erhöht, was die Vorstellung erhöhter Photosyntheseleistung und R_{eco} während feuchter Perioden im Vergleich zu Trockenzeiten stützt. Ein klarer Zusammenhang zwischen GPP_{opt} und der Lufttemperatur bzw. dem Dampfdruckdefizit konnte für den Standort Skukuza nicht gefunden werden. Es wird aufgrund der vorliegenden Studie darauf geschlossen, dass sowohl Landbewirtschaftung, als auch klimatische Steuergrößen einen Einfluss auf die zeitliche Dynamik des Kohlenstoff- und Energieaustauschs in den hier betrachteten, semiariden Gegenden Südafrikas haben.

Acknowledgements

CONTENTS

List of abbreviations and notations

Abbreviation / Notation	Description
CO_2	Carbon dioxide
EC	Eddy covariance
ET	Evapotranspiration
EVI	Enhanced vegetation index
EWUE	Ecosystem water use efficiency (g C kg^{-1} H_2O)
FAPAR	Fraction of absorbed photosynthetically active radiation
G_o	Ground heat flux (W m^{-2})
GPP	Gross primary production (μmol m^{-2} s^{-1})
GPP_{opt}	Optimum gross primary production (μmol m^{-2} s^{-1})
GHGs	Greenhouse gases
H	Sensible heat flux (W m^{-2})
HEY	Hydro-ecological year
h_m	Measurement height of flux tower instruments (m)
IPCC	Intergovernmental Panel on Climate Change
LE	Latent heat energy (W m^{-2})
NDVI	Normalized difference vegetation index
NEE	Net ecosystem CO_2 exchange (μmol m^{-2} s^{-1})
NEE_{offset}	Offset of Net ecosystem CO_2 exchange
P	Precipitation
R_{eco}	Ecosystem respiration (μmol m^{-2} s^{-1})
EBC	Energy balance closure (%)
SHF	Soil heat flux (W m^{-2})
SM	Soil moisture (%)
SWB	Surface water balance
T_{air}	Air temperature
UN	United Nations

IX

USGCRP	United States Global Change Research Program
VFS	Vegetative functional season
VPD	Vapor pressure deficit (hPa)

List of definitions and explanations of key terms

Term	Definition and/or explanation
Biogeochemical cycle	Pathway by which matter moves through biotic (biosphere) and abiotic (atmosphere, lithosphere and hydrosphere) components of the Earth
Ecosystem water use efficiency	The ratio of gross primary production to amount of water loss through evapotranspiration at ecosystem scale
Eddy covariance method	A micro-meteorological technique to measure the exchange of greenhouse gases and energy between the Earth's surface and atmosphere over time scales of hours to years and spatial scales of hundreds to thousands square meters
Energy balance closure	The balance between turbulent energy fluxes (sensible and latent heat flux) and the available energy (net radiation minus energy stored) in an ecosystem
Flux	Quantity of something (e.g., gas, energy) that moves through a unit area per unit time
Global change	Changes that occur in discrete sites but are so widespread as to constitute a planetary-scale change. This includes human population dynamics and resource use, land use and land cover and encompass changes in climate, carbon cycle, water cycle, biodiversity, among others.
Greenhouse gases	Gases that contribute to the greenhouse effect by absorbing infrared radiation (e.g. carbon dioxide, water vapor, methane, nitrous oxide, ozone, chlorofluorocarbons and hydrofluorocarbons, and others)

Gross primary production	The amount of chemical energy that primary producers make in a given length of time. This can also be referred to as photosynthesis.
Hot moment of ecosystem respiration	Sudden temporal high CO_2 efflux after rewetting of soils following dry months
Hydro-ecological years	Rainfall years – (e.g., 01 August – 31 July) in order to capture an uninterrupted wet season, as rainfall occurs during summer months, usually from November to April. A calendar year is from January to December.
Net ecosystem CO_2 exchange (NEE)	The difference between ecosystem respiration and gross primary production
Soil heat capacity	The quantity of heat that is needed to raise the temperature of a unit volume of soil by one degree Kelvin
Surface water balance (SWB)	The difference between precipitation and evapotranspiration i.e. (SWB = Precipitation – Evapotranspiration)
Vegetative functional season	Season or period of physiologically active vegetation. This is synonymous to the growing season.
Veld	Open, uncultivated area or grassland usually with scattered shrubs and trees and normally used as pastureland or farmland in southern Africa
Vapor pressure deficit (VPD)	The difference between the amount of moisture in the air and the quantity of moisture the air can hold when it is saturated

List of Figures

List of Tables

1. Introduction

1.1 Climate change and Southern African ecosystems

It is generally acknowledged that the Earth's climate is changing and the globe becoming warmer (Blunden and Arndt, 2016; IPCC, 2013, 2007, 2001; Penner, 1994; USGCRP, 2017; Zachos et al., 2008). Over several decades there has been an increasing trend in Earth's surface temperature, melting of ice and general reduction in snow cover, among other global indicators, which is consistent with rising global warming (Blunden and Arndt, 2016). For instance, from 1986 to 2016, global mean annual temperature increased by more than 1.2°F (0.7°C) (USGCRP, 2017). Water vapor (H_2O) concentrations are also likely to increase in a warmer world, amplifying the climatic effects of other greenhouse gases (Held and Soden, 2000). Primary greenhouse gases (GHGs), including CO_2, H_2O, methane (CH_4), nitrous oxide (N_2O) and ozone (O_3), trap infrared radiation in the atmosphere causing global warming (Zachos et al., 2008). The dynamics of GHGs are controlled by natural processes and anthropogenic activities such as the use of fossil fuels, deforestation, land use change and biomass burning (IPCC, 2007; Li et al., 2016). Carbon dioxide is usually considered as the most important anthropogenic GHG, partly due to its longer lifetime (Penner, 1994). The global atmospheric concentration of CO_2 has increased prominently by 40 % since 1750, pre-industrial time, mainly due to human activities, which IPCC (2007) confirmed as the dominant cause of the observed global warming since the mid-20th century. As of mid-2013, atmospheric CO_2 concentration had just exceeded 400 parts per million (Wright et al., 2014).

Flux measurements by eddy covariance (EC) is one of the many ways to monitor GHG emissions. In some parts of the world, a wide network of flux observation sites have been established for that purpose (Feig et al., 2017). These include regional flux networks such as the Integrated Carbon Observation System (ICOS), the National Ecological Observatory Network (NEON), Ameriflux, AsiaFlux and Fluxnet-Canada, among others. In order to upscale and increase the scope of such GHG monitoring efforts, the work is also complemented by remote sensing efforts (Gillson et al., 2012; Vittek et al., 2014). Despite the flux network and abundance of GHG data, global coverage is still poor due to lack of measurements in regions such as Africa. In Africa, very few EC flux measurement sites are currently running (Ardö et al., 2008; López-Ballesteros et al., 2018; Williams et al., 2007). Among the African countries, South Africa is the country with the highest number of about 7 operational flux towers, with

1

the Skukuza tower in Kruger National Park being the longest running and active since 2000 (Feig et al., 2017). Most other countries in Africa have very weak flux measurement infrastructures. Ardö et al. (2008) considered the sparsity of the flux observation network in Africa to significantly hinder our understanding of the global carbon cycle.

Southern Africa is experiencing rates of warming that are higher than the global average (Davis-Reddy and Vincent., 2017). Davis-Reddy and Vincent (2017) also reported that between 1961 to 2014, temperatures have increased at a rate of 0.4 °C per decade. Consequences of climate change in Southern Africa include increased occurrence of droughts and floods and the general depletion of water resources (Kusangaya et al., 2014; Magadza, 1994). In Sub-Saharan Africa, Kotir (2011) reviewed reports and noted changes in average temperature, rainfall amount and patterns and the frequency and intensity of weather extremes.

Climate-driven droughts may increase inter-annual variability of carbon and water vapor fluxes in African savanna ecosystems. Climate change is also predicted to lead to vegetation shifts (Masubelele et al., 2014). Higgins and Scheiter, (2012) showed evidence that the increase in atmospheric CO_2 concentration is likely to shift ecosystems such as savannas to alternative states dominated by woody plants. This phenomenon, known as 'CO$_2$ fertilization', has been reported in literature and identified as a driver that can stimulate growth of woody plants, among a myriad of other drivers (Cernusak et al., 2013; Wigley et al., 2010).

Africa covers 20 % of the global land mass (Williams et al., 2007), while savannas cover about 12 % of the global land surface (Scholes and Archer, 1997) and 50 % of the African land area (Buitenwerf et al., 2011; Osborne et al., 2018). Savannas are tropical or sub-tropical summer rainfall ecosystems, having distinct wet and dry seasons, and characterised by the coexistence of a continuous herbaceous component and a discontinuous woody component (Frost et al., 1986; Kutsch et al., 2008). Due to extensive coverage of savannas, Africa is increasingly being recognized for its role in the global carbon cycle (IPCC, 2013). However, there is lack of adequate measurements in land-atmosphere CO_2 exchange in African savannas, which represents a deficiency in global carbon estimates (Merbold et al., 2009; Williams et al., 2007). Williams et al. (2007) reported that it was uncertain whether Africa is a net source or sink of CO_2 because of lack of adequate information to partition carbon sources and sinks. Bombelli et al. (2009) echoed the same sentiments and in their study found that African savanna net annual

carbon budget ranged from a slight carbon source to a sink. According to Valentini et al. (2014), Africa is a small sink of CO_2, while at a sub-regional level Southern Africa is a net CO_2 source.

Africa is considered the most susceptible continent to climate change and climate variability (Ciais et al., 2011; IPCC, 2013). The reason for its susceptibility is mainly in ecological and socio-economic factors (Bombelli et al. 2009); poverty, weak human assets (e.g., nutrition, health, education and literacy), high degree of economic vulnerability and frequent droughts (UN, 2002). Climate change and climate variability have compromised food security in Africa, where dependency on agriculture and natural resources is high and climate adaptation strategies are inadequate (Kotir, 2011).

1.2 Land-atmosphere exchange of carbon and water

Climatic change has significant consequences on biogeochemical cycles, especially in water-limited areas (Austin et al., 2004). A biogeochemical cycle is a pathway by which matter moves through biotic (biosphere) and abiotic (atmosphere, lithosphere and hydrosphere) components of the Earth. An example is the movement of CO_2: naturally, the CO_2 from the atmosphere is consumed by primary producers through the process of photosynthesis and is released back to the atmosphere by autotrophs and heterotrophs through the processes of respiration and organic matter decomposition. Additionally, some of the CO_2 accumulated and stored in the ground (e.g., within a rock substrate) is released slowly through processes such as weathering and volcanism (Svensen et al., 2004). With increased temperature and land disturbance, more CO_2 gets released into the atmosphere intensifying global warming. Through monitoring the net ecosystem carbon dioxide exchange (NEE) between the land surface and atmosphere, the carbon source/sink dynamics of an ecosystem can be ascertained and tracked.

Interest in land-atmosphere exchange of carbon and water has grown rapidly in the context of global change (Feig et al., 2017; IPCC, 2007; McGuire et al., 2001; Nelson et al., 2018). In particular, Chapin et al. (2006) reiterated the growing interest to understand the controls of carbon cycling components as it influences the atmospheric CO_2 concentration and the spatial and temporal dynamics of the global climate system.

In the semi-arid savannas of Africa, biogeochemical cycling of water is of particular importance (Merbold et al., 2009). Water sets a limit on maximum plant productivity and a constraint on types of plants that can survive alternating periods of dry and wet conditions in semi-arid areas (MacDonald et al., 1996). Where rainfall is seasonal, it can also be possible to use the connectivity between precipitation and NEE in determining the onset of vegetative functional seasons. The precipitation-carbon exchange-vegetation functional seasonality connectivity is poorly known in savanna ecosystems.

Furthermore, studies on ecosystem photosynthetic potential (GPP_{opt}) in African savannas scarcely exist due to the lack of continuous long-term data. Assessment of maximum photosynthetic carbon uptake at canopy level has been limited to short to moderate time periods in Africa (Ago et al., 2016; Brümmer et al., 2008; Kutsch et al., 2008; Merbold et al., 2009; Moncrieff et al., 1997). This also represents a general scarcity of comparative studies of carbon exchange related parameters such as GPP_{opt} and NEE_{offset} on similar ecosystems. Brümmer et al. (2008) suggested that long-term studies are required to get a better insight into the effect of climate change on carbon exchange of savanna ecosystems. The lack of long-term carbon flux data in Africa is also one of the major causes of uncertainty in global carbon budget estimation, as discussed in the previous section.

1.3 Controls of temporal dynamics of carbon dioxide exchange components in Africa

Africa contributes approximately half of the inter-annual variability of carbon balance on global scale due to climatic perturbations (e.g., El Niño) and anthropogenic disturbances (IPCC, 2007; Williams et al., 2007). Southern Africa, in particular, is characterized by high inter-annual variability of gross primary production (GPP) (Weber et al., 2009). Regions with highest variability of GPP are semi-arid areas where carbon balance is strongly associated with variations in precipitation and temperature (Ahlström et al., 2015; P. Ciais et al., 2011; Kutsch et al., 2008).

Considering the seasonality of rainfall, previous studies in semi-arid savanna ecosystems of Africa have found that water plays a key role in controlling functional processes like GPP (photosynthesis) and R_{eco} (Archibald et al., 2009; Kutsch et al., 2008; Merbold et al., 2009;

Williams et al., 2007). This concurs with other studies globally, for instance Thomas et al. (2009) study where plant-available soil water was the main determinant of carbon fluxes in central Oregon. Huang et al. (2016) reported drought, which is common in Southern Africa, as the main driver of inter-annual variability in global terrestrial net primary production. In similar ecosystems in northern China, precipitation, soil moisture and vapor pressure deficit (VPD) were among the main drivers of daily, seasonal and inter-annual variability of NEE (Jia, 2017).

In previous studies carried out in Skukuza, a near-natural semi-arid savanna area in South Africa, respiration showed a strong dependence on both temperature and soil moisture (Kutsch et al., 2008; Makhado and Scholes, 2011), while Williams et al. (2009) found no clear relationship between nighttime carbon fluxes and temperature. The main driver of NEE at Skukuza was water (Kutsch et al., 2008; Merbold et al., 2009). In a study to investigate the drivers of the inter-annual variability of NEE at Skukuza, the main correlates were absorbed photosynthetically active radiation (APAR), number of days of available soil moisture and growing season length (Archibald et al., 2008).

Elsewhere, Falge et al. (2002) investigated factors that control seasonal changes in GPP and R_{eco} in a wide range of terrestrial ecosystems. Their results showed that the seasonality of GPP can also be influenced by biological factors. In that regard, since the assimilation of carbon in an ecosystem is driven by photosynthesis, larger canopies that possess more photosynthetically active tissue could allow for more assimilation of carbon provided there is adequate soil moisture. In a study by Jin et al. (2013), Normalized difference vegetation index (NDVI) and enhanced vegetation index (EVI) were used to track the phenology of savanna woodlands in Southern Africa and linear relationships between the vegetation metrics and GPP were also observed.

Fraction of absorbed photosynthetically active radiation (FAPAR) has also been identified as a proxy for vegetation productivity and a good measure of assessing the biophysical relationship with GPP. In a study conducted by Jung et al. (2008), growing season FAPAR values correlated strongly with annual GPP. Hoffmann et al. (2015) also found a strong PAR dependency of GPP. In an African savanna, Archibald et al. (2009) found FAPAR as the most important predictor of GPP and ER.

VPD is also an important driver of photosynthesis. At the leaf level, higher VPD is associated with stomatal closure due to a relatively limited supply of water to the leaf compared to atmospheric demand and can substantially reduce photosynthesis from maximum rates especially in the afternoons (Jenerette et al., 2009).

The stochastic nature of environmental drivers in African savannas, the complexity of their interactions and the comprehensive network of linkages of ecological responses and feedbacks make it difficult to predict 'typical' functional behavior of these ecosystems using short-term records, emphasizing the need for long term flux datasets.

1.4 Land use and land cover change effects on carbon and energy exchange in African savannas

Land use and land cover change (LULCC) refers to all forms of land management and human-induced changes in land cover (Houghton et al., 2012; Kleemann et al., 2017). LULCC has gained increasing attention a few decades ago as scientists also discovered a strong link between land use change and climate (Lambin et al., 2003). Between 1990 to 2010 LULCC accounted for 12.5 % of global anthropogenic carbon emissions (Houghton et al., 2012). LULCC is driven by population growth, agriculture intensification, modification of pasturelands, deforestation, climate change and variability of annual precipitation, among others (Lambin et al., 2001; Lambin and Meyfroidt, 2011; Ramankutty and Foley, 1999).

Globally, there has been a considerable increase in human population, coupled with substantial agriculture intensification and expansion, during the period from 1700 to 1992 (Goldewijk, 2001; Ramankutty and Foley, 1999). It has been estimated that up to half of the Earth's land surface had been directly transformed by human action from natural ecosystems such as forests or wetlands into agricultural land (Vitousek et al., 1997) and these land transformations driven by population growth are still occurring (IPCC, 2013, 2007). By 2017, the global population reached about 7.6 billion (UN, 2017) and Lutz and Kc. (2010) predicted a global population projection to be around 8 to 10 billion by 2050, with higher population growth rates especially in Africa and Western Asia. Africa's population is ~17 % of the world population, and it has

been projected that its population will double from approximately 1.3 billion in 2017 to more than 2.5 billion by 2050 (UN, 2017).

In African savannas, the CO_2 emissions from land use change are higher than fossil fuel emissions (Valentini et al., 2014) and the largest contributor is the burning of forests (Williams et al., 2007). In Southern Africa, forests and woodlands were being cleared at a rate of 25 to 50 thousand km^2 per year by early 2000 (Scholes and Biggs, 2004). There is growing evidence that deforestation has increasingly become a major source of anthropogenic greenhouse gas emissions in natural systems (IPCC, 2007).

African savanna ecosystems are under pressure due to increasing human population, majority being pastoralists, increasing pressure on land and widespread over-exploitation of natural resources and changes in savanna structure and composition (Scholes and Archer, 1997). The increase in human population may cause rampant alterations of geochemical cycles (Ciais et al., 2011; Ramankutty and Foley, 1999; Vitousek et al., 1997). For instance, the conversion of native vegetation to disturbed vegetation has been associated with increased soil respiration (Raich and Schlesinger, 1992) as LULCC activities alter the rates of carbon uptake and carbon release (Hansis et al., 2015). Munang et al. (2013) observed that ecosystem degradation compromises the carbon sequestration ability of natural systems, and may turn these systems from carbon sinks to sources. The ability of disturbed ecosystems to store carbon in the future therefore remains uncertain considering the land use effects in many areas (IPCC, 2007).

Drivers that are causing rapid vegetation change across African savannas include climate change, grazing and browsing, land cover change and transformations (Skarpe, 1991). The joint effects of land use and climate change are seen to pose an immediate threat to savanna ecosystems (Higgins et al., 2010). Human-induced land use transformations have a direct influence on enhanced greenhouse gas emissions subsequently causing climate change (Vitousek et al., 1997). Lambin et al (2003) observed that anthropogenic factors such as grazing may interact with other climatic drivers of land cover changes. It would be important to understand the response of largely complex semi-arid savanna ecosystems to grazing under climate change (Lohmann et al., 2012).

Livestock grazing is a common land use practise that may affect carbon and energy exchange in semi-arid regions of Africa. It is one of the missing links in continental carbon budgets estimates as net carbon fluxes associated with land use practices are lacking (Williams et al., 2007). A recent review by Kgosikoma et al. (2013) has shown that there are generally few studies that have focused on grazing management in African ecosystems. Räsänen et al. (2017) observed a scarcity of carbon flux data in agricultural areas of South Africa, yet most of the savannas and grasslands are used for livestock grazing. Livestock grazing can be a sustainable land use in these areas but land degradation may occur in overgrazed areas (Vegten van, 1981). Over-stocking with domestic livestock has been, in general, the major cause of degradation of grasslands/rangelands in African ecosystems (Scholes and Biggs, 2004). A shift in plant community composition is a common effect of grazing in dry ecosystems (Scott et al., 2009). In the grassy biomes of South Africa, bush encroachment and/or woody invasion has been associated with intensive grazing (Wigley et al., 2010). Furthermore, a study by Jaweed et al. (2018) found more degradation by livestock especially around watering points where animals return frequently to drink water, around sheepfolds, areas of mineral licks, among other places of congregation – usually leaving the ground bare and exposed. It was also found that the reduction in above-ground biomass may negatively affect carbon sequestration (Jaweed et al., 2018).

Any land management practice which causes change in vegetation and soil properties may have a significant effect on surface energy balance components (Mallick et al., 2015; Wilson et al., 2002). Cava et al. (2008) and Foken (2008) found that surface energy imbalance is strongly dependent on site characteristics, exchange processes of ecosystems and measurement set up. In that regard, high grazing intensity may alter fluxes of mass and energy in an ecosystem (Gan et al., 2012). The effect of grazing on energy components can occur via alterations of evapotranspiration (ET) rates and heat storage, since grazing is associated with changes in vegetation, soil properties and surface characteristics (Jaweed et al., 2018; Wigley et al., 2010).

Human land use practices which have a direct impact on soil and vegetation may contribute to alteration of hydrological system components such as ET, which apart from being controlled by climatic elements, is also influenced by soil properties, surface characteristics and type of vegetation (Frost et al., 1986). ET is a link of the energy and hydrological cycles, with latent

heat of vaporization acting as a sink of heat in the atmosphere (Majozi et al., 2017). Ecosystem hydrological changes may therefore pose a global warming related threat (Vörösmarty et al., 2000). Rainfall and ET variability may also affect ecosystem surface water balance (SWB), which in this study is defined as the difference between precipitation and ET.

Considering the high inter-annual variability of rainfall and temperature (Ma et al., 2007) and land use disturbance on vegetation and soil properties in semi-arid savannas (Lohmann et al., 2012), it is also crucial to understand how efficient these ecosystems are in terms of using the limited water available. Ecosystem water use efficiency (EWUE), an indicator of the coupling of carbon and water cycle, is the ratio of ecosystem gross primary production (photosynthesis) to water loss through ET (He et al., 2017). EWUE is also a useful measure of vegetation functionality in semi-arid areas (Emmerich, 2007). The effects of land use management practices (e.g., livestock grazing) on EWUE remain unclear.

Surface energy balance closure (EBC) is an important indicator that can be used to assess the balance between turbulent energy fluxes (sensible and latent heat flux) and the available energy (net radiation minus energy stored) in an ecosystem. Non-closure of the energy balance is usually when the available energy is greater than the sum of the turbulent energy fluxes (Masseroni et al., 2014; Wilson et al., 2002). The degree of uncertainty in the measurement of turbulent energy fluxes by Eddy Covariance method (see section 1.6) may also have some implications on the estimation of CO_2 fluxes (e.g., Kidson et al., 2010), which demonstrates the need to perform energy balance assessments under different grazing regimes.

The effects of land use and climate change on biogeochemical cycling of carbon and water in African savanna ecosystems are poorly understood (Kutsch et al., 2008), yet localized land use disturbances are widespread across most areas (Devine et al., 2017). Relatively few measurements have been made on land-atmosphere CO_2 and energy exchange in natural/near-natural and managed savannas of Africa (e.g., Archibald et al., 2009; Baldocchi et al., 2016; Hui et al., 2003; Kutsch et al., 2008; Merbold et al., 2009; Räsänen et al., 2017; Williams et al., 2007). Earlier research by Raich and Schlesinger (1992) mentioned the scarcity of information on CO_2 exchange from savanna ecosystems.

1.5 Rainfall seasonality and hot moments of ecosystem respiration in African savannas

The importance of water availability to vegetation dynamics is well documented in literature (Adole et al., 2018; Foley et al., 2003; Hickler et al., 2005; Kutsch et al., 2008; Merbold et al., 2009; Scholes et al., 2001). As earlier discussed, the seasonality of rainfall is an important aspect in understanding the biotic and abiotic environment of the savanna ecosystem (Nel and Sumner, 2006). Southern African savanna ecosystems receive most rain during summer months from November to April (Archibald et al., 2009). While mean annual precipitation may give the productive potential of a region, in savannas it may also be important to look at aspects such as the amount of precipitation, its distribution, frequency of occurrence, intensity and inter-annual variability of rainfall as some years may receive above-average rainfall while other years may receive below-average rainfall.

The concept of 'hot moments' relates to period of time during which rates of biogeochemical processes are enhanced (McClain et al., 2003). In arid and semi-arid areas, the onset of the growing season is usually preceded by episodes of isolated rain showers of varying intensities and then followed by dry periods of variable lengths (Archibald et al., 2009; Arneth et al., 2006; Ati et al., 2002; Hess et al., 1995; Huxman et al., 2004; Leon et al., 2014; Räsänen et al., 2017; Snyder and Tartowski, 2006; Veenendaal et al., 2004; Verduzco et al., 2015; Williams et al., 2009). Such periods of pulse rain events cause a pulse response of ecosystem respiration (Williams et al., 2009). This concept of 'hot moments' of CO_2 efflux is also synonymous to a phenomenon known as the 'Birch effect', after the pioneering work of Birch, (1958) on stimulation of soil respiration when dry soils are rewetted. After rewetting of soils following dry months, there is reactivation and/or mobilization of accumulated reactants through soil microbial activity, leading to sudden temporal high fluxes due to increased rate of CO_2 emissions from terrestrial ecosystems to the atmosphere (Arneth et al., 2006; Leon et al., 2014; Veenendaal et al., 2004; Williams et al., 2009).

Adole et al. (2018) reported that there is usually a time lag for vegetation to green up following the onset of rains after which a larger proportion of vegetation would then become physiologically active and sequester more CO_2. Huxman et al. (2004) describe these pulsed rain events as important triggers for biological activity. To relate these rain pulses with pulse-like

CO_2 fluxes, it is crucial to study hot moments of CO_2 efflux at short time scales (e.g. daily). In a study conducted in a savanna ecosystem of South Africa by Räsänen et al. (2017), it was reported that there is a general increase in ecosystem respiration following early rains and then followed by increased carbon sequestration as precipitation increases into the growing season. In agricultural areas, where the onset of the growing season is crucial for planting purposes, Hess et al., (1995) referred to these periods of rain pulses as a 'false start' of the growing season.

The importance of water to vegetation dynamics in African savannas is well documented (Adole et al., 2018; Foley et al., 2003; Hickler et al., 2005; Kutsch et al., 2008; Merbold et al., 2009; Scholes et al., 2001). However, in spite of voluminous information on water-vegetation relations, there is limited information on the link between rain 'pulses' and CO_2 efflux in the semi-arid savanna ecosystems of Africa. The effects of rain pulses on CO_2 efflux deserves more scrutiny in the context of climate change and land use disturbance. For instance, after the rewetting of soils following dry months, it is not known how much water is required to trigger a hot moment of CO_2 efflux. It is also not known how long these ecosystem respiration pulses last after the occurrence of pulsed rain events and the magnitude of CO_2 efflux during pulsed rain events. Williams et al. (2009) found a deficiency in pulse models representing ecosystem carbon processes. Similarly, Archibald et al. (2009) also noted that pulsed CO_2 fluxes are not well-represented in standard gap-filling procedures (see section 2.4 for an example of a gap-filling approach).

1.6 Theory of eddy covariance

Eddy covariance (EC) is a micro-meteorological technique to measure the exchange of GHGs and energy between the Earth's surface and atmosphere over time scales of hours to years and spatial scales of hundreds to thousands square meters (Baldocchi, 2003; Burba, 2013; Burba and Anderson, 2010). The method has been widely applied in various fields (e.g., environmental science, agriculture and industry) and is robust in direct and fast measurements of gas fluxes (Aubinet et al., 2012; Baldocchi et al., 2001; Burba, 2013; Burba and Anderson, 2010). Fluxes are transported by turbulent eddies, comprising 3-D components that include an upward and downward 'vertical' air movement component. In this context eddies are air (currents) that moves and rotates in a circular manner. Detailed equations on how a flux is derived are widely

documented in literature (e.g., Aubinet et al., 2012; Baldocchi et al., 2001; Burba and Anderson, 2010). The infra-red gas analyser and sonic anemometer are part of the key measurement infrastructure, among others (see appendix 2). The high frequency measurements from the sonic anemometer and infra-red gas analyser are used to calculate the flux, which is the covariance of the vertical velocity (w) with any variable of interest (c). The following is a simplified equation for flux calculation.

$$F_c = \overline{\rho_a} \cdot \overline{w'c'} \qquad (1)$$

Where F_c is the flux of any gas species, ρ_a is the air density, w' is the vertical wind velocity and c' can be a scalar such as concentration of a gas (e.g., CO_2), temperature or any other variable of interest. Overbars means a time average and primes denote departure from the mean (turbulent fluctuations). A flux is therefore calculated as the product of mean air density and the mean covariance of deviations in fast vertical wind speed and measured gas concentration over the averaging period usually 30 minutes. However, a full mass balance approach considers measurement of all fluxes (turbulent vertical flux – by IRGA and sonic measurements; and advection fluxes for complex terrain – by setting up additional height profile flux measurements) plus the storage terms – also accomplished by setting a profile system of additional measurements.

The eddy covariance method has several assumptions which need to be satisfied including flux measurement in an ideal horizontal and uniform terrain where air density fluctuations and flow convergence and divergence are minimal, availability of adequate flux footprint, turbulent air flow, among others (Burba and Anderson, 2010). The various data quality procedures that are implemented in the eddy covariance method are meant to match the theoretical assumptions for the method, otherwise the method itself is very sound.

This study mainly focuses on the measurements of NEE and turbulent energy fluxes using the eddy covariance technique. Net ecosystem CO_2 exchange, a component of the carbon cycle measured directly at an EC flux tower where all measurements are done, is the difference

12

between CO_2 assimilated by photosynthesis (GPP) and CO_2 released back into the atmosphere by plants and microbial activity (R_{eco}) (Baldocchi, 2003; Chapin et al., 2006; Reichstein et al., 2005). Thomas et al. (2013) mentioned that NEE is the most important parameter to describe the ecosystem's carbon sink or source strength. The micro-meteorological sign convention is used in the interpretation of NEE results, where a negative NEE flux represents a net flux towards the surface (GPP / CO_2 uptake by the ecosystem), and a positive flux represents a net flux away from the surface (R_{eco} / CO_2 release to the atmosphere). In that regard, an ecosystem is referred to as a net source of CO_2 if the NEE is positive and a net sink if the NEE is negative.

1.7 Research aims, questions and objectives

This study was conducted under the ARS AfricaE (Adaptive Resilience of Southern African Ecosystems) project, a SPACES (Partnerships for the Adaptation/Adjustment to Complex Earth System Processes in Southern Africa) initiative whose overall goal was to understand the consequences of ecosystem changes in Southern Africa caused by multiple disturbances. Two major forms of disturbances that were identified in the overall project as a threat to semi-arid savanna ecosystems of Southern Africa were land use (change) and climate change. The study aims were: to provide better understanding of rain-pulse driven 'hot moments' of CO_2 efflux; to build on the knowledge of the connectivity of precipitation and NEE to explain onset and end of vegetative functional seasons; and to find out the temporal variation of EWUE at near-natural and grazed savanna sites in South Africa. Additionally, the study also aims to contribute towards development of sustainable grazing management practices that produce high carbon sequestration and to reduce the energy balance closure (EBC) error by inclusion of soil heat storage at the managed Karoo sites. Finally, the study aims to better understand climatic drivers (e.g., soil moisture (SM), air temperature (T_{air}), vapor pressure deficit (VPD)) and their influence on inter-annual variability of maximum photosynthetic potential (GPP_{opt}) and net ecosystem CO_2 exchange offset (NEE_{offset}) at the near-natural Skukuza site.

To fulfil the aims, the following research questions were set:

(i). How do the micrometeorological drivers influence the inter-annual variability of growing season GPP_{opt} and NEE_{offset} at a near-natural savanna site?

(ii). How do precipitation and temporal dynamics of NEE explain vegetative functional seasons at the near-natural and grazed semi-arid sites?

(iii). What is the effect of rain pulses on ecosystem respiration at the near-natural and grazed semi-arid sites?

(iv). How does water use efficiency vary between or across vegetative functional seasons at the near-natural and grazed semi-arid sites?

(v). What is the status and the drivers of the temporal dynamics of NEE and its eco-physiological fluxes of GPP and R_{eco} across a grazing intensity gradient from seasonal to annual time scales?

(vi). What is the effect of soil heat storage inclusion in surface energy balance closure estimation at the grazed sites?

In order to facilitate the achievement of the research aims and answer the research questions, the following objectives were undertaken:

(i). To explain inter-annual variability of growing season GPP_{opt} and NEE_{offset} and its drivers at the near-natural Skukuza site using long-term flux data

(ii). To determine connectivity between precipitation and temporal dynamics of NEE in explaining vegetative functional seasons at the near-natural and grazed semi-arid sites

(iii). To examine the effect of rain pulses on ecosystem respiration efflux at the near-natural and grazed semi-arid sites

(iv). To determine the temporal variability of EWUE during vegetative functional seasons at the near-natural and grazed semi-arid sites

(v). To determine and compare the temporal dynamics and drivers of NEE and its eco-physiological fluxes of GPP and R_{eco} across a grazing intensity gradient at the grazed sites from seasonal to annual time scales

(vi). To quantify and compare energy balance components and closure before and after inclusion of soil heat storage flux between two grazed sites at annual time scale

1.8 Conceptual model of land-atmosphere exchange of carbon and water

The main focus of this study is in observing land-atmosphere exchange of carbon and energy as driven by climate and anthropogenic land use activities. To simulate the different interactions that are the focus of this study, the conceptual framework of interactions by McGuire et al., (2001) was adapted (Fig. 1.1). This framework can be used to capture the dynamics of land-atmosphere exchange of CO_2 and turbulent energy as well as showing the drivers of ecosystem change. For the purposes of this study, the model was adapted to include additional components (in red) such as the land-atmosphere exchange of turbulent energy fluxes (i.e., latent heat energy (LE) and sensible heat flux (H)) as well as other drivers of ecosystem change and connections with the terrestrial carbon and water pools. There is a biophysical connection between biotic and abiotic components and ecosystem functional processes (Diaz et al., 2007; Falge et al., 2002; Nakano and Shinoda, 2015).

In McGuire et al. (2001) conceptual framework, the term net carbon exchange (NCE) was used to define net carbon balance of a terrestrial biosphere, from heterotrophic respiration (R_H) and net primary production (NPP), while also considering anthropogenic-driven carbon exports from the terrestrial pool, carbon movements through dissolved organic carbon (DOC), CO_2 emissions from fire, and other long-term decay processes. In this study, other carbon components accounted for by McGuire et al. (2001) were beyond the scope of this research work, which focused on the temporal dynamics of measured NEE and turbulent energy fluxes in near-natural and managed semi-arid savanna ecosystems.

Figure 1.1 also illustrates the cycling of water through the ecosystem. For instance, some of the water that is received on the land as precipitation flows to streams, rivers, lakes and oceans as water run-off and some infiltrates into the ground where it is taken in by the roots and used for photosynthesis, and later to be released back to the atmosphere through ET. Some of the water that infiltrates into the ground form aquifers or move along as groundwater flow.
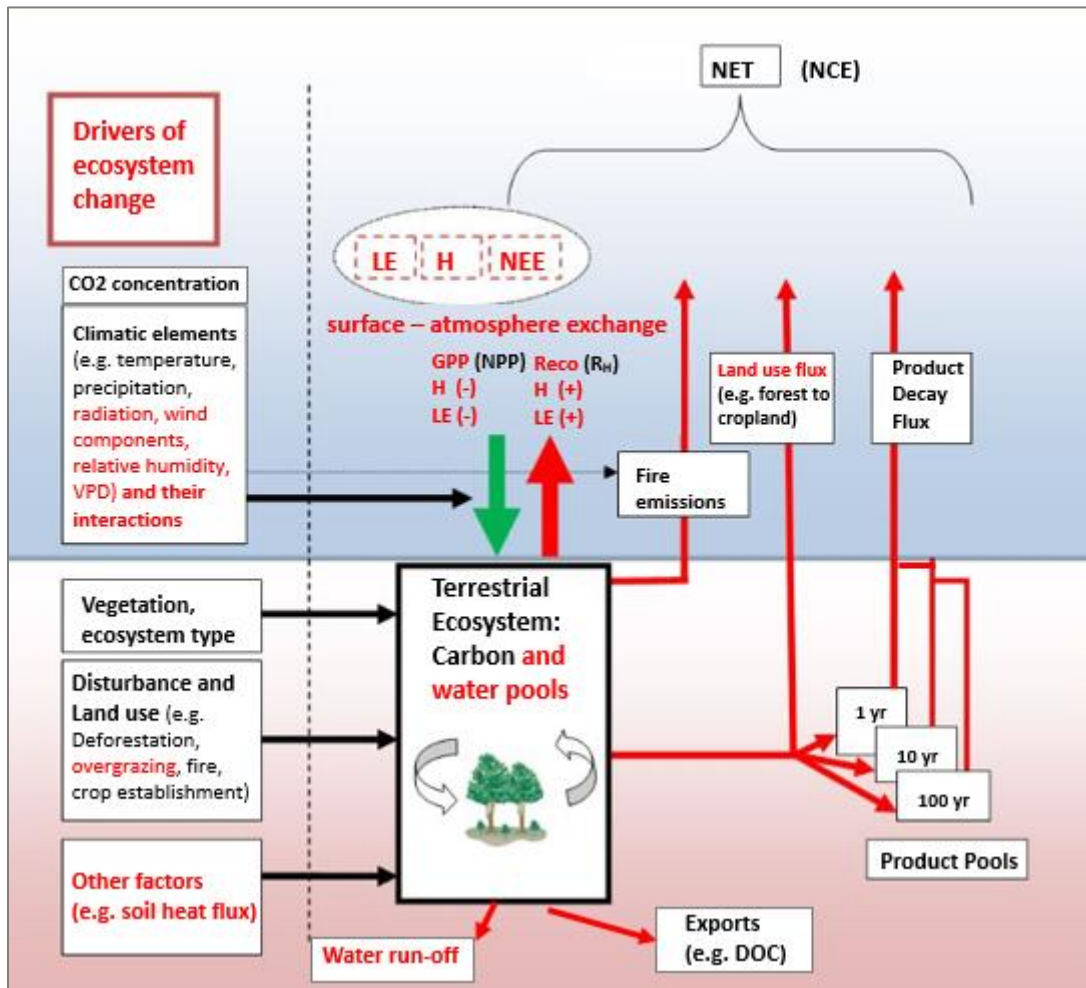
Figure 1. 1: Conceptual framework of land-atmosphere CO_2 and turbulent energy exchange and drivers of ecosystem change. An adaptation from McGuire et al. (2001).

Given the background that increased CO_2 concentration since pre-industrial times has been one of the major causes of global warming (IPCC, 2013), human activities and associated land disturbances that may continue to increase atmospheric CO_2 concentration may further exacerbate the effects of climate change on terrestrial ecosystems. Changes in temperature, rainfall and other climatic elements may directly have an effect on land-atmosphere carbon and energy exchange. Similarly, anthropogenic land use disturbances such as livestock overgrazing, fires, deforestation and other unsustainable land use practices may affect the components of the carbon and hydrological cycles. For example, climatic and land use effects on SWB (i.e., the difference between precipitation and water lost from the ecosystem through ET) and run-off. In the context of this study, hydrological components which were of paramount importance

were precipitation and ET, the latter providing a link to the water, energy and carbon cycles. Water run-off was not a major cause for concern in this study in the calculation of SWB as the Karoo and Skukuza study sites have low and moderate rainfall and experience high water infiltration and ET rates.

1.9 Thesis outline

The introduction provides the background, encompassing the relevant literature of current knowledge, aims and objectives of this research. The materials and methods section provide an overview of the theory of the EC method, description of the study sites, instrumentation and measurements, post-processing of EC data and all data management procedures. Various computations are also described in this section, including water use efficiency, surface energy balance and soil heat storage. Additionally, the methodology to describe the 'hot moments' of R_{eco} or periods of sudden temporal high CO_2 efflux after rewetting of soils following dry months in semi-arid savannas is also described. The results and discussion sections present and deliberate on the following issues; 1) inter-annual variability of GPP_{opt} and NEE_{offset}, which are the parameters derived from the light response of NEE at the near-natural savanna site; 2) the temporal variability of these parameters and the control by climatic drivers such as SM, T_{air} and VPD; 3) a comparison of the temporal dynamics of net carbon exchange components (NEE, GPP and R_{eco}) and their controls between two Karoo sites (karoo 1 and Karoo 2) with different livestock grazing intensities; 4) responses of R_{eco} to rain pulses, connection between precipitation and CO_2 fluxes in explaining vegetative functional seasons; 5) the dynamics of EWUE at the near-natural Skukuza site and the managed Karoo sites; and 6) comparison of the results of surface energy balance and the influence of soil heat storage inclusion in energy balance closure between the two Karoo sites. Finally, the conclusion section provides the summary of the main results, outlook and recommendations for future research. This study may contribute new knowledge to other studies related to the influence of climate change and land use disturbance on land-atmosphere exchange of carbon and turbulent energy fluxes in arid and semi-arid savanna ecosystems.

2. Methodology

2.1 Sites description

2.1.1 Skukuza location, vegetation, geology and soil and land use types

The Skukuza flux tower (25.0197°S, 31.4969°E) was established in February 2000 and is located in a semi-arid savanna in Kruger National Park, South Africa (Fig. 1). The site lies at 365 m above sea level (Kutsch et al., 2008) and rainfall is seasonally occurring mainly during summer months of November to April (Archibald et al., 2009). Mean annual temperature is 21.9 °C (Merbold et al., 2009) and the micro-climatic conditions are characterized by mild winters and warm to hot summers with temperatures that can reach up to 44 °C in summer (Makhado and Scholes, 2011). Mean annual precipitation is 550 ± 160 mm/year (Archibald et al., 2009).

The terrain of Skukuza is gently undulating and the plant community is dominated mainly by broad-leaved *Combretum apiculatum* on coarse sand crests and fine-leaved *Acacia nigrescens* savanna on sandy clay loam in the valleys (Scholes et al., 2001). The flux tower lies at the boundary of these two distinct savanna vegetation types. The grassy and herbaceous understory comprises of grasses such as *Panicum maximum*, *Digitaria eriantha*, *Eragrostis rigidor*, and *Pogonarthria squarrosa*. The underlying parent material is Archaean granite and gneiss (Kutsch et al., 2008). Soils are about 0.6 m deep; trees can reach 8-10 m height (Archibald et al., 2009) and the flux measurement instruments are at 16 m height (Ramoelo et al., 2014).

Skukuza's land use is wildlife conservation, characterised by grazing and browsing of wild ungulates. There is partial human interference on the ecosystem in the form of wildlife management and provision of water for game at some areas further away from the Skukuza flux tower. Of special mention is the management of megaherbivores such as elephants in the general park area (Scholes et al., 2001). In that regard, the drivers of ecosystem change at Skukuza flux site, apart from climatic factors, are as a result of natural processes. Figure 2.1 shows the location of Skukuza flux tower station within Kruger National Park, South Africa.
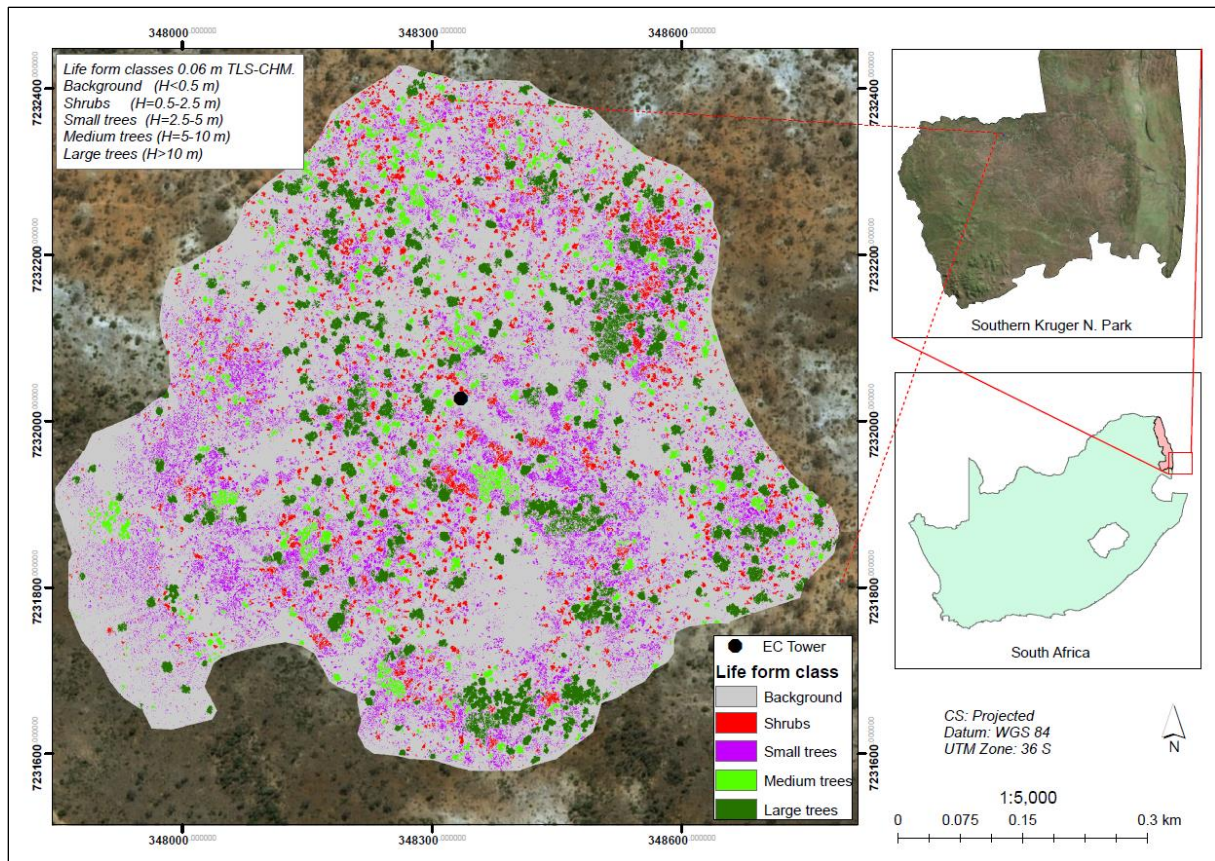
Figure 2. 1: Map of the study area showing the location of Skukuza eddy covariance flux tower within Kruger National Park, South Africa. TLS-CHM refers to terrestrial laser scanning - canopy height model, H is height and EC is eddy covariance. Source: Victor Odipo (ARS AfricaE Remote Sensing Work Package, University of Jena).

Skukuza is one of the few EC flux measurement sites in Africa providing long-term flux data. For the purpose of this study, EC data from the Skukuza site was used to observe: 1) The long-term carbon exchange and spatiotemporal responses of carbon balance constituents (i.e. GPP_{opt} and NEE_{offset}) to environmental drivers such as SM, T_{air} and VPD; 2) The relationship of vegetative functional seasons with fraction of absorbed photosynthetically active radiation (FAPAR), NDVI, EVI and SWB; 3) The variability of EWUE across two vegetative functional seasons (i.e. 2009/2010; 2010/2011); 4) The connection between precipitation and CO_2 fluxes in explaining vegetative functional seasons; 5) The response of R_{eco} to rain pulses that are a common occurrence in semi-arid regions.

2.1.2 Karoo location, vegetation, geology and soil and land use types

The two Karoo flux stations (coordinates: Karoo 1: 31.4253°S, 25.0294°E and Karoo 2: 31.4302°S, 25.0161°E; both 3 m high and at approximately 1265 m above sea level) were established in October 2015. The Karoo is categorized as a semi-arid ecosystem, and has a long-term mean annual rainfall (1889–2013) of 373 mm (du Toit et al., 2015; du Toit and O'Connor, 2014). Rainfall is seasonal and occurs in summer months usually from October to March. The area is characterized by long hot summers and moderate winters. The mean annual temperature for the site is about 15°C (Hagan et al., 2017). Vegetation is dominated by small-leaved dwarf shrubs, mainly *Eriocephalus ericoides*, grasses, some geophytes, herbs and few isolated trees occurring on the hill slopes (du Toit et al., 2015). Topography is generally flat and soils are shallow and weakly developed (Du Toit et al., 2011). According to Hagan et al. (2017) the soils are categorized as Aridisols with silt, clay and sand constituting about 13.5%, 19.9% and 64.7%, respectively. Livestock farming, dominated by sheep production, is considered as the main land use practise.

Karoo 1 paddock was a gently grazed site stocked with sheep and cattle at a recommended normal grazing capacity of approximately 16 hectares per livestock unit (LSU) for Upper Karoo systems according to Acocks (1988). Karoo 1 is 13 hectares in size and it was also considered as the 'benchmark'. Karoo 2 paddock, 5 hectares in size, was a rested site for the past eight years but heavily overgrazed by Dorper sheep (*Ovis aries*) before the resting. Karoo 1 treatment was the standard rotational grazing system adopted over the years in which the routine was that livestock would graze for three months, then be removed for six months, and the cycle repeated again. The treatment for Karoo 2 was continued resting from livestock grazing as from project start (i.e., 30 October 2015) until 15 July 2017 when the paddock was restocked with six Dorper sheep at a low stocking rate of one small stock unit (SSU) per hectare. The project end date was 31.10.2017 and the restocking of Karoo 2 towards the end of the data collection period coincided with the dry season when the vegetation was largely in a dormant state and physiologically inactive. Figure 2.2 shows the location of the Karoo sites in South Africa.
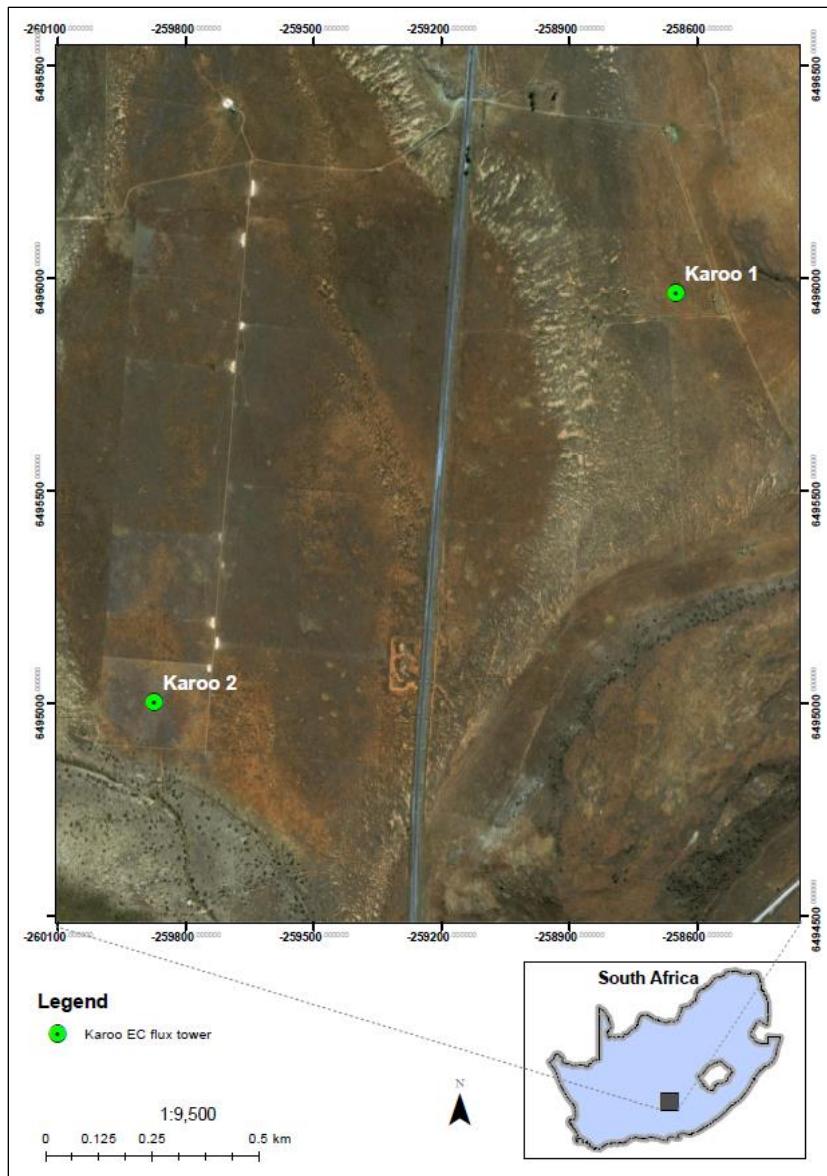
Figure 2. 2: Map of the study area showing the location of Karoo 1 and Karoo 2 eddy covariance (EC) flux towers in Middelburg, South Africa. Source: Victor Odipo (ARS AfricaE Remote Sensing Work Package, University of Jena).

Karoo rangelands of the Eastern Cape Province of South Africa occupy 35% of the land area of South Africa and are referred to as 'arid Nama Karoo' (Du Toit et al., 2011). The Karoo is not particularly rich in species or endemism but the flora and fauna of the ecosystem are well adapted to its climatic extremes (Dean and Milton, 1999). A small fraction (*less than 1 %*) of the Karoo is conserved (Barnard et al., 1998), and this has intensified the threats from pastoralism, exotic plants, mining and agriculture (Lovegrove and Siegfried, 1993). The major large-scale disturbance to the Nama Karoo ecosystem has been grazing by domestic sheep and goats confined within farm boundaries (Skead, 1982). High stocking rates of small stock in the

Karoo were found to have negative impacts on vegetation composition, basal cover and canopy cover of desirable plant species (Du Toit et al., 2011; Esler et al., 2006; Lovegrove and Siegfried, 1993).

The Nama-Karoo biome in South Africa has the longest history of livestock grazing as the main land use (Lubke et al., 1986). At Karoo (Middelburg), there are grazing trials that were initiated in the early 1930s by the then Grootfontein College of Agriculture, which is now called Grootfontein Agriculture Development Institute (GADI). The main livestock grazing systems in the Karoo are rotational grazing and continuous grazing systems.

The focus on the Karoo site was intended to gain understanding on the effects of livestock grazing intensity as one common form of land management and other controls such as EWUE, NDVI and EVI on land-atmosphere carbon and energy exchange components. Hot moments of ecosystem respiration and the connectivity between precipitation and CO_2 fluxes in describing vegetative functional seasons were also examined at the Karoo sites. The purpose was to gain better understanding of those aspects in the context of livestock grazing. Since grazing is also known to influence changes in soil properties and vegetation, surface energy balance components were also examined at Karoo 1 and Karoo 2. Since Karoo 1 was gently grazed, the site was constituted by a mixture of dwarf shrubs and palatable grass species. Nevertheless, Karoo 2 had a mixture of dwarf shrubs and mainly unpalatable grass species due to overgrazing in the past.

The Karoo sites are currently data deficient on ecosystem carbon metabolism and no study has been done on the associated impacts of livestock grazing on carbon and turbulent energy exchange.

2.2 Eddy covariance measurements and instruments at Skukuza and Karoo

The Skukuza and Karoo flux towers were equipped with various micro-meteorological instruments for measurement of carbon dioxide and turbulent energy fluxes; wind velocity;

radiation; humidity; air temperature; soil moisture; soil temperature; soil heat flux; among others. Digital signal processing for CO_2/H_2O data and integration of sonic data were accomplished by the LI-7550 Analyzer Interface Units (AIUs) compatible for the LI-7200 and LI-7500 CO_2/H_2O IRGAs at Karoo and Skukuza sites, respectively. The instruments and measurement details for Skukuza and Karoo flux tower stations are summarized in Appendix 2.

2.2.1 Skukuza flux tower and instruments

In order to investigate carbon and water fluxes, the EC technique was applied to measure gas species' exchange between the atmosphere and semi-arid savanna ecosystem sites in South Africa. The Skukuza flux tower was equipped with a fast-response closed-path infrared gas analyser (IRGA; model LI-6262, Li-Cor, Lincoln, NE, USA) for measurement of CO_2 and water vapour (H_2O) concentrations from 2000 to 2005. From 2006 the gas analyzer was changed to an open-path infrared gas analyser (IRGA; model LI-7500, Li-Cor, Lincoln, NE, USA). A three-dimensional sonic anemometer (Wind Master Pro, Gill Instruments), measuring wind velocity, was previously mounted on the flux tower but then replaced by a three-axis Sonic Anemometer (CSAT3, Campbell Scientific Inc., Logan, UT, USA) around 2006. The IRGA and the sonic anemometer were installed at a measurement height (h_m) of 16 m above ground level. Raw data from these fast-response instruments were collected at 20 Hz.

Flux measurements at Skukuza were accompanied by other ancillary measurements. These included soil moisture (SM), soil temperature (T_{soil}), incoming and outgoing shortwave radiation and incoming and outgoing longwave radiation, air temperature (T_{air}), relative humidity (RH), photosynthetically active radiation (PAR) and rainfall. Soil moisture was measured by frequency domain reflectometry sensors (CS615L, Campbell Scientific Inc., Logan, UT, USA). Soil temperature was measured by CS108 probes (Campbell Scientific Inc., Logan, UT, USA) at depths 6, 13, 29 and 58 cm. Incoming and outgoing shortwave radiation and incoming and outgoing longwave radiation were measured with a two-component net radiometer (CNR2: Kipp and Zonen B.V., Delft, The Netherlands) from 2000 to 2008 and replaced by wind speed corrected CNR4 Kipp and Zonen net radiometer in 2009. Air

temperature and relative humidity were measured at 16 m height by Vaisala HMP155 probe (Campbell Scientific Inc., Logan, UT, USA). Photosynthetically active radiation was measured using a quantum sensor (Licor LI 190R, Li-Cor Inc., Lincoln, NE, USA). Rainfall was measured with a tipping bucket rain gauge (Texas TR525M, Campbell Scientific Inc., Logan, UT, USA) at the tower top. For this study, we used only the SM at the depth of 6 cm (average of two replicates). PAR (μmol m^{-2} s^{-1}) was only used when there were no shortwave radiation measurements, and was converted to shortwave/global radiation (Rg, Wm^{-2}) by a factor of 0.5. Ancillary measurements were recorded by the CR1000 logger (Campbell Scientific Inc., Logan, UT, USA) at 1 Hz and stored every 30 minutes. Figure 2.3 shows Skukuza flux tower in South Africa.
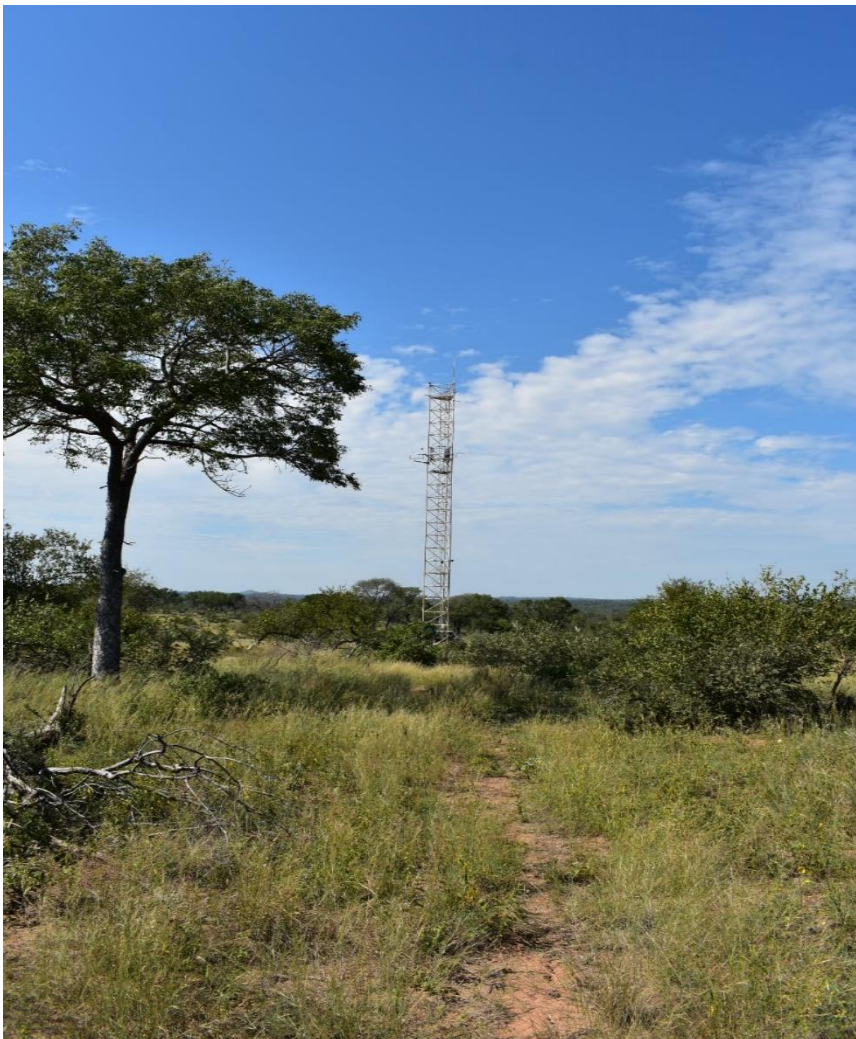
Figure 2. 3: Skukuza flux tower, Kruger National Park, South Africa. (Source: Dr. Gregor Feig, South African Environmental Observation Network (SAEON))

Bio-physical controls of GPP_{opt} and NEE_{offset} that were investigated at Skukuza (i.e., SM; T_{air}; VPD; SWB, NDVI, EVI and FAPAR) were derived from site measurements and other data sources from satellite remote sensing products.

2.2.2 Karoo flux towers, experiment set-ups and instruments

Karoo 1 and 2 flux towers (Fig. 2.4), installed at measurement height 3 m above ground level, were approximately 1 km apart and were equipped with an enclosed path fast-response infra-red gas analyzers (IRGA; model LI-7200, Li-Cor, Lincoln, NE, USA) for CO_2 and H_2O measurements and a CSAT3 Sonic Anemometer (Campbell Scientific Inc., Logan, UT, USA) for wind velocity measurements. The LI-7200 enclosed path system collected data at 20 Hz and calculated fluxes in real time by the SMARTflux unit using the EddyPro software. The LI7550 AIU for the LI-7200 IRGA also compressed the raw data (metadata, flux and biomet data) into .ghg file format, which were archived for later processing.

Ancillary measurements at the Karoo sites were soil temperature, soil heat flux, soil moisture, rainfall, relative humidity, air temperature and rainfall. Soil temperature was measured by UMS TH3 sdi12 sensors at depths 3, 5, 7, 10, 17 and 30 cm at Karoo 1 and at 2, 4, 6, 8, 18 and 35 cm at Karoo 2. Soil heat flux was estimated by HFP01 (non-self-calibrating) and HFP01 (self-calibrating) plates at depths 10 cm and 20 cm. Soil moisture was measured by ML3x Delta T probes at depths 8 cm and 16 cm. Rainfall was measured by tipping bucket rain-gauge (Texas Electronics TR 525) at the top of the 3 m flux towers. Relative humidity and air temperature were measured by Rotronic HC2S3 probe. Figure 2.4 shows Karoo flux towers and monitoring instruments.

Figure 2. 4: Karoo flux towers and monitoring instruments

2.3 Eddy covariance post-field data processing

Fluxes of mass and energy were calculated from raw high frequency data (20 Hz) at 30 minutes averaging period to generate half hourly fluxes using conventional methodology described in detail by authors (e.g., Aubinet et al., 2000; Burba, 2013; Moncrieff et al., 1997). For Skukuza, post-processing of eddy covariance datasets from 2000 to 2014 was done by EddySoft software package. A hydro-ecological year (HEY) was a period from 01 August to 31 July. At Karoo sites, half hour flux averages were calculated by EddyPro 6.1.0 (Li-Cor, Lincoln, NE, USA) software package, and a hydro-ecological year (HEY) was a period from 01 November to 31 October.

Flux processing options followed appropriate data processing scheme for EddySoft and included double rotation for proper alignment of anemometers' axes (i.e., tilt correction) (Wilczak et al., 2001), lag correction for CO_2 and water vapour concentrations, spectral response corrections (Eugster and Senn, 1995), and the Webb-Pearman-Leuning (WPL) correction (Webb et al., 1980) for open-path system (Li-7500) at Skukuza post 2005. The NEE sign follows the micrometeorological convention, being negative for net CO_2 uptake by the ecosystem and positive for net CO_2 release into the atmosphere.

Karoo data was subjected to data quality procedures for EddyPro 6.1.0 and included correction for high frequency spectral losses (i.e., spectral response correction) (Moncrieff et al., 2004, 1997), double rotation for anemometer's axis tilt correction, quality control checks following

flagging policy by Mauder and Foken. (2004), among others. Although standard quality criteria were applied, datasets were again screened for uncertain values (e.g., skewness and kurtosis). Table 2.1 shows post-processing procedures at Skukuza and Karoo sites.

Table 2. 1: Post-processing procedures at Skukuza and Karoo sites

Post-processing procedure	Skukuza	Karoo
30 min flux averaging interval	x	x
Angle of attack correction for wind components	x	
Axis rotation for tilt corrections	x	x
Time lags compensation	x	x
Detrending	x	x
Rotation	x	x
Spectral response corrections	x	x
WPL corrections	x	
Quality flux check	x	x
Footprint estimation	x	x
Ustar filtering	x	x
Despiking	x	x
Random uncertainty estimation	x	x
Gap filling	x	x

2.4 Data gap-filling, partitioning of NEE and error estimation

Gap-filling of data and partitioning of NEE were accomplished by the online flux data processing tool (REddyProc package), administered by the Max Planck Institute for Biogeochemistry, that implements standardized methods of Reichstein et al. (2005) and Lasslop

et al. (2010). Details about NEE flux data availability for Skukuza and Karoo sites are presented on sections 2.5.1 and 3.2.3, respectively. Long data gaps at flux measurement stations mainly occur due to instrument failure (e.g., as a result of lightning strikes / storms) and power failure. Short data gaps may result due to exclusion of bad data (e.g., during low turbulence), among other reasons.

Due to long gaps of precipitation measured at the site, the daily precipitation used in the calculation of SWB was obtained from South Africa Weather Services (SAWS) and European Reanalysis (ERA)-Interim databases. Gap-filling of precipitation followed the method proposed by Vuichard and Papale (2015).

The Lasslop et al. (2010) flux partitioning method was used across all sites to partition NEE into GPP and R_{eco}. The method uses a light response curve approach and taking into consideration the temperature sensitivity of respiration and VPD effects on CO_2 assimilation. The curves are fit to daytime NEE measurements and ecosystem respiration estimates are derived from the intercept of the y-axis (Lasslop et al., 2010). The Lasslop approach has shown good agreement with other flux partitioning methods, with variability of less than 10% at annual scale in estimates of GPP and R_{eco} with other methods (Lasslop et al., 2010). The input parameters are optimized to reproduce daytime NEE, but if the parameter values are uncertain or missing for a specific time window the algorithm uses the parameter values of the previous window(s).

The interpretation of the Lasslop et al. (2010) method is as follows:

$$NEE_{observed} = R_{eco} - GPP + Res \qquad (2)$$

Where Res is the residual, which is the difference between modelled and observed parameters.

However, the Lasslop et al. (2010) algorithm for NEE flux partitioning did not represent well during the periods of rain pulses and the estimated R_{eco} values were not good at these times.

However, during these rain pulse periods fluxes were mainly representing ecosystem respiration since vegetation was largely dry and physiologically inactive. Therefore, in order to better represent CO_2 spikes using the Lasslop et al. (2010) approach, Res (on Equation 2) was assumed to be equal to zero but only during the short periods of rain pulses when GPP was very small or zero.

EC measurements are also subject to errors that can contribute to total uncertainty in NEE estimates including bias errors emanating from gap-filling approaches, random errors associated with inadequate sample size, systematic errors associated with instrumentation precision or insensitivity to high-frequency turbulence and issues related to vertical and horizontal advection (Finkelstein and Sims, 2001; Loescher et al., 2006; Lucas-Moffat et al., 2018; Moffat et al., 2007). Estimation of error is an important criterion when reporting annual sums of NEE to obtain a confidence interval for the annual estimates of NEE (Archibald et al., 2009). In EC flux measurements we also aim to reduce the uncertainty of NEE estimates (Loescher et al., 2006). The approach by Finkelstein and Sims (2001) of estimating random errors is implemented in EddyPro software and was applied in this study. In addition, bias errors from gap-filling of EC data were also considered. Lucas-Moffat et al. (2018) and Moffat et al. (2007) describe the equations to calculate bias and random errors, which are then summed up to give a measure of uncertainty of annual sums. The offset on the annual sum (δASum) resulting from gap-filling of the eddy covariance data is given by the formula:

$$\delta\text{ASum} = \text{Np} \cdot \text{BE} \tag{3}$$

Where δASum is the offset on the annual sum NEE, Np is number of gap-filled days; and BE is the bias error. Moffat et al. (2007) investigated the effect of gap filling techniques on the annual sums of NEE using 10 benchmark datasets and the bias error span between the upper and lower quartiles for most of the gap-filling techniques based on medium gaps was less than 0.25 g C m^{-2} d^{-1}. By using 0.25 as the bias error (BE) constant, equation 3 becomes:

$$\delta\text{ASum} = \text{Np} \cdot 0.25 \text{ g C } m^{-2} \text{ year}^{-1} \tag{4}$$

The random error of the annual sum (εASum) developed by Lucas-Moffat et al. (2018) over the gap-filled days is:

$$\varepsilon ASum = \sqrt{Np \cdot RMSE^2} \qquad (5)$$

Where RMSE is root mean square error - which is a measure for normally distributed random errors (Lucas-Moffat et al., 2018). Since random error estimates for each half hour were obtained from EddyPro software using the method by Finkelstein and Sims (2001), equation 5 from Lucas-Moffat et al. (2018) was modified to produce εASum based on Finkelstein and Sims. (2001) over the duration of gap-filled days. The random error of the annual sum (εASum) is therefore:

$$\varepsilon ASum = \sqrt{\sum \varepsilon_{eddyp}} \qquad (6)$$

Where, after Finkelstein and Sims (2001), ε_{eddyp} is random error from EddyPro software for each half hour.

To get the NEE uncertainty estimate for the year, equation 4 and 6 were summed up to give:

$$NEE_{uncertainty} = \delta ASum + \varepsilon ASum \qquad (7)$$

The other potential sources of error, apart from bias and random errors, were not included in the estimation of annual NEE uncertainty of the Karoo sites.

2.5 Technical steps

For the Skukuza datasets, vegetative functional seasons (VFS) were first identified for each hydro-ecological year. This was then followed by stratification of data into moisture and air temperature classes, where parameters GPP_{opt} and NEE_{offset} were determined from light response curve fittings of NEE and global radiation (Rg) using long-term EC data (from 2000 to 2014).

2.5.1 Identifying vegetative functional seasons at Skukuza

Vegetative functional seasons (growing seasons) were targeted because that is when the ecosystem is physiologically active. Onset and end of a growing season of an ecosystem can be determined on the basis of the transition from net carbon loss to net carbon uptake and vice versa (Law et al., 2002). This was the approach taken for the Skukuza data to identify vegetative functional seasons. Figure 2.5 shows the approximate duration of vegetative functional seasons (shaded and unshaded panels) within a hydro-ecological year. However, these vegetative functional seasons were to some extent confined by data availability. The shaded panels show the approximate duration when there was available data of good quality and the unshaded panels are data gaps for each vegetative functional season.

| | Vegetative periods confined by data availability | | | Mar Jun Sep Dec Mar Jun Sep | | | | | | | | Possible number of half hour fluxes | Percentage (%) of Good quality data used |
	Year	Good data: Onset to End dates	Good data: Duration	Q1	Q2	Q3	Q4	Q1	Q2	Q3	Q4		
1	2000/2001	06.11.00 - 30.05.01	206d									9888	21
2	2001/2002	12.11.01 - 24.03.02	133d									6384	24
3	2002/2003	13.01.03 - 27.05.03	135d									6480	43
4 *	2003/2004	17.01.04 - 05.05.04	110d									5280	33
5 *	2004/2005	01.11.04 - 15.04.05	167d									8016	8
6 *	2005/2006	18.11.05 - 26.12.05	(39d)									1872	73
7 *	2006/2007	31.12.06 - 19.02.07	(51d)									2448	42
8 *	2007/2008	01.12.07 - 29.01.08	(60d)									2880	63
9	2008/2009	14.11.08 - 30.04.09	168d									8064	53
10	2009/2010	01.11.09 - 28.05.10	211d									10128	74
11	2010/2011	13.11.10 - 23.05.11	192d									9216	80
12	2011/2012	19.11.11 - 24.04.12	158d									7584	59
13	2012/2013	23.09.12 - 10.05.13	230d									11040	70
14	2013/2014	01.11.13 - 17.04.14	168d									8064	74
15													

■ Length of periods with available good quality flux data within a vegetative functional season
☐ Data gaps compromising/impeding appropriate definition of vegetative functional season
* Periods with critical data gaps which could not be used for further data analysis

Figure 2. 5: Duration of periods with available good quality flux data for each vegetative functional season at Skukuza

It is acknowledged that data gaps (unshaded panels) compromised the appropriate definition of a vegetative functional season but still yielding valuable information. The data gaps were caused by bad quality data, which could not be used for further analysis, or coincided with periods when there were no measurements due to system failure. In a study by Majozi et al. (2017a) data availability at Skukuza ranged between 13 % (2001) and 58 % (2010), with a mean and standard deviation of 36 % and 15 %, respectively. Out of the 14 years in this study, 9 years remained with good data. However, with further screening and after the assessment of GPP$_{opt}$ and NEE$_{offset}$, 6 years remained (i.e., 2001/2002; 2002/2003; 2009/2010; 2010/2011; 2012/2013; and 2013/2014).

For the task to determine the estimates of GPP$_{opt}$ and NEE$_{offset}$ within the vegetative functional seasons, good quality (non-gap filled) data were used. The focus was to explain the inter-annual

variability of GPP_{opt} and NEE_{offset} and the influence of climatic elements such as SM, T_{air} and VPD.

2.5.2 Data stratification procedure for Skukuza

Half hourly data from ancillary measurements were used during stratification of data into soil moisture and air temperature classes for each vegetative functional period from 2000 to 2014 from which GPP_{opt} and NEE_{offset} were calculated. Data were classified into the three SM classes, i.e., wet (SM > 9%), drying (6% ≤ SM ≤ 9%) and dry periods (SM < 6%), which were also previously identified according to a study by Archibald et al. (2009) at Skukuza. Stratification by SM for each vegetative functional period was meant to separate biologically functional periods from 'non-active' periods of water constraints. For each SM class data were further sub-classified into narrow *a priori* temperature sorted classes of 275.65 K bins between 20 °C and 35 °C in order to separate air temperature (T_{air}) effects on NEE response to light. Vapor pressure deficit (VPD, hPa) was calculated from T_{air} and relative humidity (RH) and VPD means for the stratified periods were also used for further analysis.

2.5.3 Deriving the parameters GPP_{opt} and NEE_{offset} from light response curve fittings for Skukuza

GPP_{opt} is a parameter that describes the maximum photosynthetic rate at saturating global radiation (Kato et al., 2004). GPP_{opt} is an analogue of A_{max} or C_{max} or P_{max}, as described in other studies at leaf to ecosystem-scale level (Ago et al., 2014; Arora, 2002; Fei et al., 2017; Whitehead and Gower, 2001). NEE_{offset} is defined as the intercept (at $Rg = 0$ W m^{-2}) of the light response relationship of NEE against global radiation (R_g). GPP_{opt} and NEE_{offset} are important carbon metabolism constituents that serve as indexes of ecosystem photosynthesis potential and respiratory losses, respectively.

A non-linear least squares regression model (NLSR) was used in R software to estimate GPP_{opt} and NEE_{offset}, from the fundamental relationship of NEE vs Rg. The Michaelis-Menten model (e.g., Michaelis and Menten, 1913) was adapted to simulate the response of NEE to Rg at ecosystem scale using the formula:

$$NEE = NEE_{offset} - \left(\frac{\alpha * GPP_{opt} * Rg}{\alpha * Rg + GPP_{opt}}\right) \qquad (8)$$

where NEE was taken from the flux tower measurements, α was the initial slope of the best fitted regression line of the ecosystem light response curve (also a measure of light use efficiency i.e., LUE), GPP_{opt} was the maximum photosynthetic rate, NEE_{offset} was a parameter that relates to CO_2 release at zero light, Rg was global radiation. By subtracting NEE_{offset} from Equation 8, the function is forced through zero and GPP_{opt} is thereby estimated. Only good quality half hourly NEE data and daytime measurements between 0530 hrs and 1900 hrs were used for this analysis.

For the vegetative functional seasons, GPP_{opt} and NEE_{offset} were derived from the light response curve fits in each SM and T_{air} class. Although light use efficiency (LUE) is another important parameter, it was not used in further analysis because it is driven by a complex and wide range of stressors ranging from short-term to longer-term stressors (Coops et al., 2010). For that reason, it was beyond the scope of this study to consider it. Figure 2.6 is a schematic illustration of the NEE vs Rg relationship.
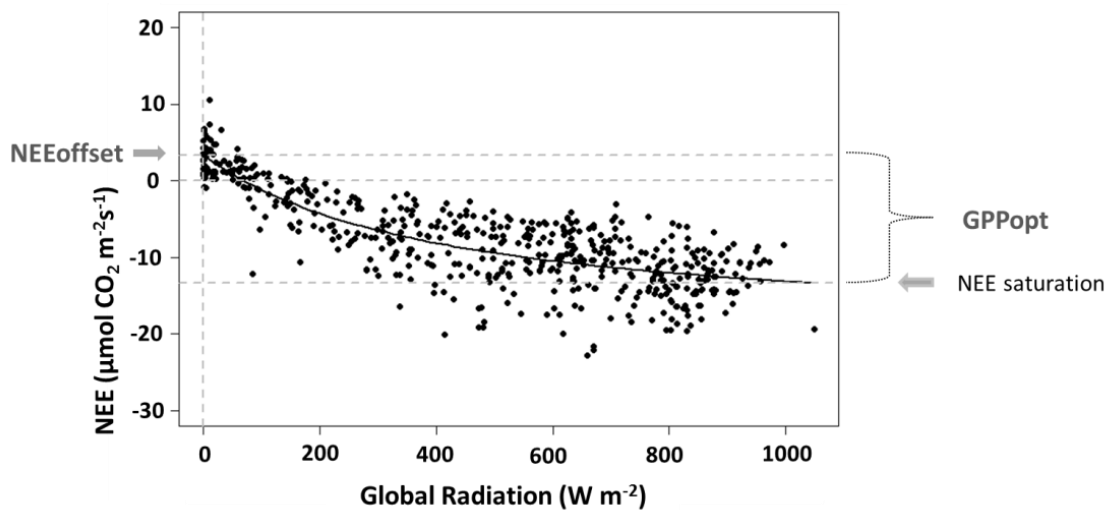
Figure 2. 6: Illustration of the relationship between net ecosystem CO_2 exchange (NEE) and global radiation at ecosystem level. The NEE light response curve was generated from equation 8 using data from 2012/2013 vegetative functional season.

The response of NEE to global radiation exhibited a rectangular hyperbolic relationship. At NEE saturation, the maximum value of GPP_{opt} is attained and light is no longer the factor limiting the overall rate of photosynthesis. The data that were used to derive GPP_{opt} and NEE_{offset} estimates were from the selected periods (based on flux data availability) (Fig. 5) and classes of soil moisture and air temperature within VFSs from 2000 to 2014. The only periods that achieved significant fitting of regression parameters (with P-value < 0.05 and sample size (n) > 40) were selected for further analyses to characterize the inter-annual variability of growing season GPP_{opt} and NEE_{offset}.

2.6 Assessing the temporal dynamics of CO_2 exchange at Karoo

Temporal patterns of CO_2 can be assessed by observing the daily and seasonal components of land-atmosphere carbon exchange processes (Mitchell et al., 2018). Gross primary production is a reflection of ecosystem biological process of carbon assimilation while R_{eco} is a reflection of both biological processes and anthropogenic activities that emits CO_2 into the atmosphere.

At Karoo, one of the aims was to show how NEE and its physiological components (GPP and R_{eco}) vary between the grazed site and the rested site at seasonal and annual timescales, and to show how other climatic elements and factors (e.g., NDVI, EVI, precipitation and EWUE) influence site differences. The temporal progression of NEE, GPP and R_{eco} were presented through time series plots, with two major seasons (i.e., winter and summer) being recognized rather than the four conventional seasons.

Over the course of the year, periods where Karoo 1 and Karoo 2 showed differences in terms of NEE were identified by analysing the differences between half-hourly NEE values of Karoo 1 and Karoo 2 (i.e., delta NEE = $Karoo1_{NEE} - Karoo2_{NEE}$). The delta NEE pattern was used to show the critical periods when the two sites differed, otherwise for the rest of the periods when the NEE difference was very small to non-existent, the two sites were behaving in a similar way. The identified period (in summer), when Karoo 1 was behaving differently from Karoo 2,

35

were used for further analyses that included showing the influence of NDVI and EVI on NEE site differences.

The annual carbon budgets of Karoo 1 and Karoo 2 were calculated as annual sums of the half-hourly NEE gap-filled flux data. Two datasets used were for estimating annual carbon budgets i.e.; (i) NEE gap-filled data after strict data quality control (flag 0 – of (Mauder and Foken, 2004) used plus additional skewness and kurtosis) and (ii) NEE gap-filled data after moderate data quality control (flag 0 and 1 – of (Mauder and Foken, 2004) used). The uncertainty of the annual NEE sum was calculated based on standard methods described in section 2.4 (Finkelstein and Sims, 2001; Lucas-Moffat et al., 2018; Moffat et al., 2007).

2.7 Biophysical connection between functional seasonality and carbon dynamics at Skukuza and Karoo

2.7.1 Identifying hot moments of CO_2 efflux at Skukuza and Karoo

In order to explore 'hot moments' of CO_2 efflux, gap-filled datasets for Skukuza and Karoo were used. Important attributes that were considered in characterizing the hot moments of CO_2 efflux were; 1) the size of the rain pulse (i.e., the amount of precipitation over a rain pulse event); 2) the duration of rain-induced ecosystem respiration (R_{eco}) pulse (i.e., how long the R_{eco} pulse/spike would last in response to a rain pulse event; and 3) the magnitude of a R_{eco} pulse (i.e., R_{eco} sum over the duration of a R_{eco} pulse). R_{eco} responded immediately after a rain-pulse event.

In order to identify the hot moments of R_{eco}, the initial step was to select isolated rain pulse events, which occurred within the period from the first day of rains following dry months to the onset of the vegetative functional season (growing season). Isolated rain pulse events were either single rain events or constituted by a maximum of two to three rain pulse events, falling in consecutive days or distributed across a maximum of five days. Isolated rain pulse events followed by dry days or intermittent dry periods > 7 days were selected in order to observe the effect of the rain pulse events on R_{eco}. A dry day refers to a day without any precipitation. For

36

each isolated rain pulse event, the duration of the subsequent R_{eco} pulse response was determined and used as the basis to determine the average duration for the control treatments.

This study adopted the approach developed by Sivakumar (1988), where the onset of a growing season was determined when accumulated rainfall over three consecutive days was at least 20 mm with no dry spells exceeding 7 days within the next 30 days, otherwise it would be considered as a 'false' start of a growing season. In this study, false starts of the growing season coincided with these periods of rain-induced R_{eco} pulses.

2.7.2 Connectivity between precipitation and carbon dynamics in determining vegetative functional seasons at Skukuza and Karoo

By determining how quickly NEE responds to changes in precipitation and SWB, a biophysical connection between carbon dynamics and functional seasonality can be established. After the phase of rain pulses and R_{eco} spikes, an increase in precipitation that follows subsequently triggers the onset of the growing season. In a study conducted in central Oregon, functional seasons of a semi-arid mature ponderosa pine forest were determined on the basis of site hydrology (Thomas et al., 2009).

To achieve that connectivity, the temporal progression of precipitation and SWB from dry to wet phases was linked to the temporal progression of NEE. Through tracking the connectivity, the magnitude of precipitation and SWB that can trigger the onset of a vegetative functional season was quantified. The onset of a vegetative functional season is that point when the ecosystem begins to transform from a large positive NEE (as a result of R_{eco} spikes during the period of rain pulse events) to systematic transition towards a more negative NEE as vegetation physiological activity increases with increased water availability.

In order to separate a 'false start' of the growing season and the onset of productive rains, well established methods of determining the onset of a growing season were adopted (e.g., Marteau et al., 2009; Sivakumar., 1988). Marteau et al. (2009) described the onset of a growing season as the first wet day (> 1 mm) of one or two consecutive days totaling at least 20 mm without any dry spell of 7 days receiving less than 5 mm in the following 20 days. These approaches by

Marteau et al. (2009) and Sivakumar (1988) were useful in defining the onset of productive rains in this study but the start of the vegetative functional seasons considered the coupling of precipitation and CO_2 fluxes, and the lag time of photosynthesis response by vegetation. The end of the vegetative functional season was based on systematic transition from a net carbon sink to a net carbon source (Law et al., 2002).

2.8 Measurement of remote sensing products

2.8.1 Acquisition of NDVI, EVI and FAPAR

Data were also acquired through satellite remote sensing. More specifically, data products provided by the MODIS satellite sensor were obtained with the aim to identify vegetation greenness or biophysical parameters that relate to photosynthesis (GPP) and to track temporal changes thereof. These data products comprise the NDVI, EVI and FAPAR. Where necessary, a second order polynomial regression was used to gap-fill FAPAR data in order to obtain robust average estimates of FAPAR measured for each VFS.

Statistics were computed to derive mean, minimum, maximum and standard deviation for the MODIS time series of EVI and NDVI for each VFS (Fig. 5). These statistics were derived from the following data products: (i) MOD13Q1 MODIS NDVI 16-day composites (dimensionless; for period from 03/2000 to 06/2014) at 250 m pixel resolution, (ii) MOD13Q1 MODIS EVI 16-day composites (dimensionless; for period from 03/2000 to 06/2014) at 250 m pixel resolution. For each data product and each acquisition date, the above statistics were extracted for those MODIS pixels falling within a 500 m radius around the Skukuza eddy covariance flux tower.

FAPAR data (dimensionless; for period from 07/2000 to 05/2015) were extracted from Multi-angle Imaging Spectro Radiometer (MISR) data, by converting it first to MISR High Resolution (MISR-HR) according to the method described in (Verstraete et al., 2012). FAPAR data were extracted every 16 days from grids within MISR-HR blocks (P167B111, P168B110 and P169B10) that were falling within the 500 m radius around the flux tower. Statistics were also computed to derive mean, minimum, maximum and standard deviation for the FAPAR time series.

However, FAPAR was missing for 2010/2011 and 2011/2012 VFSs at Skukuza and data for those periods was obtained from the Joint Research Centre of the European Commission (JRC-EC). The dataset was based on an analysis of visible (0.3–0.7 nm) and near-infrared (0.7–3.0 nm) broadband white sky albedo values (calculated under the assumption of an isotropic illumination of the surface) available from MODIS collection V005 products (MCD43B3) at 0.01° spatial resolution for successive 16-day periods. The two-stream model simulated accurately the partitioning of the solar fluxes based on a one-dimensional approach using effective state variables to overcome the unavoidable difficulties arising from the significant subpixel unresolved spatial variability (Pinty et al., 2006, 2011a, 2011b).

For the Karoo sites, a similar approach was used to determine NDVI and EVI and multi-temporal statistics for the pixels representing vegetation in the two paddocks. The vegetation greenness indices for the growing season were also compared between Karoo 1 and Karoo 2 (section 3.4.2).

2.8.2 Mathematical definition of NDVI and EVI

Vegetation indices are arithmetic combination of two or more bands related to the spectral characteristics of vegetation. The indices have been widely used for phonologic monitoring, vegetation classification, and biophysical derivation of radiometric and structural vegetation parameters. Among the commonly used vegetation indices in monitoring vegetation condition and vigor are Normalized Difference Vegetation Index (NDVI) and Enhanced Vegetation Index (EVI).

i.   Normalized Difference Vegetation Index (NDVI)

NDVI has gained most use in vegetation condition monitoring because of its operationalization on the global scale. Its ratio properties enable it to cancel out a large proportion of the noise caused by changing sun angles, topography, clouds or shadow, and atmospheric conditions (Matsushita et al., 2007; Huete et al., 1999). Mathematically, NDVI is defined as the ratio

between the difference and sum of the red band in the visible wavelength and the near infrared wavelength (Rouse et al., 1974), and is expressed as:

$$NDVI = \frac{\rho_{nir} - \rho_{red}}{\rho_{nir} + \rho_{red}}$$

(9)

With the ρ_{red}, and ρ_{nir} representing reflectance in the red (0.6 - 0.7μm), and Near-Infrared (NIR) wavelengths (0.7-1.1μm), respectively. Despite its simplicity and usefulness in providing vegetation condition, NDVI is however susceptible to large sources of error and uncertainty over variable atmospheric, canopy and soil background conditions (Xue and Su, 2017). To counter these issues, EVI was proposed to factor in the effects of background soil and canopy on the vegetation index.

ii.   Enhanced Vegetation Index

EVI is a modified NDVI with and aim of reducing attenuation of NDVI to high biomass levels through de-coupling of the canopy and soil background signal and a reduction in atmospheric influences (Huete et al., 1999). Unlike the NDVI, the EVI includes a soil adjustment factor L, in its denominator, making it possible to include a term without a band ratio format. Mathematically, EVI can be expressed according to Liu and Huete (1995), thus:

$$EVI = G \; x \; \frac{\rho_{nir} - \rho_{red}}{\rho_{nir} + (C_1 \; x \; \rho_{red} - C_2 \; x \; \rho_{blue}) + L}$$

(10)

where L is a soil adjustment factor, and C_1 and C_2 are coefficients used to correct aerosol scattering in the red band by the use of the blue band. The ρ_{blue}, ρ_{red}, and ρ_{nir} represent reflectance at the blue (0.45 - 0.52μm), red (0.6 - 0.7μm), and Near-Infrared (NIR) wavelengths (0.7 - 1.1μm), respectively. In general, $G = 2.5$, $C_1 = 6.0$, $C_2 = 7.5$, and $L = 1$.

2.9 Computing ecosystem water use efficiency

Data from vegetative functional seasons were used for computing the EWUE of Skukuza and Karoo ecosystems. EWUE is the ratio of gross primary production to ET (He et al., 2017; Huang et al., 2017) or gross ecosystem production (GEP) normalized by ET (Scott et al., 2010). Since it relates the ecosystem's carbon exchange and its water use, it is a useful measure of the functionality of ecosystems (Emmerich, 2007). The expression for ecosystem water use efficiency is as follows;

$$EWUE = \frac{GPP}{ET} \qquad (11)$$

Where EWUE is ecosystem water use efficiency, GPP is gross primary production and ET is evapotranspiration. To characterize the EWUE dynamics over the vegetative functional seasons, weekly GPP and ET were plotted. The ET was calculated from half hourly latent heat flux (LE, W m^{-2}) values, derived from the eddy covariance measurements, and summed for each day to obtain daily ET (mm), and for each week to obtain weekly ET (mm).

2.10 Computing surface water balance

SWB refers to the difference between the amount of water (precipitation) received in an ecosystem and the amount of water lost through ET and other means. SWB was calculated as follows:

$$SWB = P - ET \qquad (12)$$

Where P is precipitation, and ET is evapotranspiration. The cumulative daily SWB was integrated over the length of each vegetative functional season for each hydro-ecological year. In this study, only ET loss was considered in SWB calculation and measurement of other

potential water losses in the Karoo ecosystem was beyond the scope of this work. Run-off, in particular, was assumed to be negligible.

A positive SWB entails that water could still be added to soil water storage in the ecosystem and there would be more water for use by vegetation. If SWB becomes negative, soil water storage gets more depleted and at high soil water deficit vegetation will become limited.

2.11 Computing surface energy balance closure

Surface energy balance in an ecosystem is closed when available energy equals turbulent energy plus any energy storage change (Kidson et al., 2010). According to Wilson et al. (2002) the energy balance closure requires that the sum of turbulence energy fluxes be equivalent to available energy as follows;

$$LE + H = Rn - G - S - Q \tag{13}$$

Where LE is the latent heat flux (W m^{-2}), H is the sensible heat flux (W m^{-2}), Rn is the net radiation flux (W m^{-2}), G is the soil heat flux (W m^{-2}), S is the storage heat flux (W m^{-2}) and Q the sum of all additional energy sources and sinks.

The Q parameter is a small term and usually neglected. Similarly, heat storage (S) in the ecosystem is also neglected at times and the surface energy balance equation, or energy conservation equation (Mintz and Walker, 1993), would be written as follows;

$$LE + H = Rn - G \tag{14}$$

The left-hand side of equation (14) represents the turbulent fluxes measured by EC (LE + H) and the right-hand side represents the available energy (Rn − G) measured by independent meteorological instruments.

Heat storage (S) comprises of above-ground and below-ground soil heat storage. Soil heat storage estimation was taken into consideration in surface energy balance assessments at the Karoo sites. However, since the average height of vegetation was around 30 cm, the above-ground heat storage was not considered and was assumed to be negligible. For short vegetation of less than 8 m tall, canopy heat storage is expected to be small (Sánchez et al., 2010; Wilson et al., 2002). After considering the soil heat storage, the following energy balance closure equation was applied:

$$LE + H = Rn - Go \tag{15}$$

Where Go is the ground heat flux (i.e., soil heat flux from soil heat flux plates at a certain depth + soil heat storage).

Energy balance closure residual occurs when the left-hand side and the right-hand side of the above equation do not balance. The ideal EBC is attained when the slope and coefficient of determination are one and intercept of the regression fit is zero (Majozi et al., 2017a).

2.11.1 Computing soil heat storage

Change in soil heat storage (∂G) between the surface and soil heat flux plates buried at 10 cm was calculated between the gently grazed site and the rested site. The aim was to examine if livestock grazing intensity had an influence in altering soil heat storage and surface energy balance. Grazing may affect soil thermal properties which may have a significant impact on heat storage in the soil between the heat flux plates at a certain depth and the soil surface. Soil heat storage was calculated on the basis of integrating parameters such as soil temperature (K), soil heat capacity (J m^{-3} K^{-1}), time (s), soil thickness/depth (m) and measured soil heat flux (G) using thermal diffusion equation (TDE) (Guan et al., 2009; Yang and Wang, 2008; Zhang and Huang, 2004). As mentioned in section 2.2.2, soil measurements were taken at depths 3, 5, 7, 10, 17 and 30 cm and 2, 4, 6, 8, 18 and 35 cm for Karoo 1 and Karoo 2, respectively. Soil heat flux plates were buried at 10 cm and 20 cm at both sites. The influence of soil moisture on soil

thermal properties such as soil heat capacity (e.g., Abu-Hamdeh, 2003; Liu et al., 2008), was neglected due to inadequate soil moisture profiling at the Karoo sites. The calculations to estimate soil heat capacity and heat storage were as follows:

$$Cs = \frac{(G1 - G2)}{\partial z(\frac{\partial Tg}{\partial t})} \tag{16}$$

$$\frac{Cs\partial T}{\partial t}\partial z = \partial G \tag{17}$$

Where C_s is soil heat capacity; G1 and G2 are average soil heat fluxes at 10 and 20 cm below the land surface; ∂z is the soil thickness/depth between the levels at which the soil heat fluxes were measured; $\partial Tg/\partial t$ is the change in soil temperature over time (half hour), which was calculated for the layer between 10 cm and 20 cm soil depths for the purpose of estimating soil heat capacity; $\partial T/\partial t$ is the rate of change in soil temperature for the soil layer between the surface and soil heat flux plates at 10 cm depth; and ∂G is the soil heat storage. For the computation of $\partial Tg/\partial t$, soil temperature measurements at (10 cm and 17 cm) and (8 cm and 18 cm) were used to calculate the changes in soil temperature for the layer between 10 cm and 20 cm at Karoo 1 and Karoo 2, respectively. For the computation of $\partial T/\partial t$ in the calculation of heat storage above 10 cm soil depth, time derivative of soil temperature at 5 cm and 4 cm soil depths were used at Karoo 1 and Karoo 2, respectively. Average soil heat capacity between 10 and 20 cm soil depths was used in the calculation of soil heat storage above 10 cm soil depth. The calculated soil heat storage (∂G) and average soil heat flux (G) at 10 cm depth constituted the ground heat flux (G_0), which was used in computations of energy balance closure (see equation 15).

2.12 Data analyses

Analyses and interpretation of data were done in R software package (R Core Team, 2013).

To achieve objective (1); To explain inter-annual variability of growing season GPP_{opt} and NEE_{offset} and the influence of its drivers at Skukuza using long-term flux data;

A 3-dimensional functional relationship between a dependent variable (GPP_{opt}/NEE_{offset}) and independent variables (soil moisture and air temperature) was represented in 2-dimensional surface plots showing inter-annual variability of the functional relationships over six vegetative functional seasons. The vegetative periods for each hydro-ecological year used (i.e., 2001/2002, 2002/2003, 2009/2010, 2010/2011, 2012/2013 and 2013/2014) are shown on Figure 5. To aid in the interpretation of these surface plots, additional descriptive variables such as EVI, NDVI, FAPAR, and SWB were also used to describe each vegetative functional season.

In a further step, scatter plots of GPP_{opt}/NEE_{offset} against SM, T_{air} and VPD were used to explore the functional relationships and to determine the main variables that explain the inter-annual variability of GPP_{opt} and NEE_{offset}. A quadratic function was fitted to the relationships of GPP_{opt} and SM; GPP_{opt} and T_{air}; and GPP_{opt} and VPD. Similarly, linear and quadratic functional relationships of NEE_{offset} and SM; and NEE_{offset} and T_{air} were also determined. Relationships were considered significant at the $P < 0.05$ level and the coefficient of determination (R-square) was also used to explain the model fits.

To achieve objective (2); To determine connectivity between precipitation and temporal dynamics of net ecosystem CO_2 exchange in explaining vegetative functional seasons at Skukuza and Karoo sites;

The response of NEE to changes in precipitation and SWB was tracked using time series plots of precipitation, SWB, NEE and its partitioned components (GPP and R_{eco}). Cumulative precipitation and SWB from the beginning of productive rains (the dry-wet transition phase) up to the change point in NEE response from a larger positive NEE (reflecting non-active vegetative period) to transition towards negative NEE (reflecting active vegetative period) was quantified. Since precipitation is not a continuous variable (Thomas et al., 2009), the end of the

vegetative functional season was determined by the transition from negative NEE to positive NEE according to Law et al. (2002), as the soil moisture values could not be used.

To achieve objective (3); To examine the effect of rain pulses during periods of 'hot moments' of ecosystem respiration at Skukuza and Karoo sites;

Statistics that were computed for hot moments of ecosystem respiration and control treatments were; the size of rain pulse, the duration of a R_{eco} pulse in response to a rain-pulse event and the magnitude of R_{eco} pulse following a rain pulse event. Scatter plots and were used in order to relate rain pulse events (precipitation) and R_{eco} pulses.

To achieve objective (4); To determine EWUE for vegetative functional seasons between/across years at Skukuza and Karoo sites;

EWUE for the natural site (Skukuza) and the managed sites (Karoo 1 and Karoo 2) were evaluated through the regression slope value of weekly GPP vs. weekly ET. The approach is widely used in the Eddy Covariance community and the slope of the regression line is a measure of EWUE (Baldocchi et al., 2001). A more negative slope represents a greater EWUE, with the opposite also true for lower EWUE. Relationships were considered significant at the $P < 0.05$ level and regression coefficients were also determined.

To achieve objective (5); To determine and compare the temporal dynamics and drivers of NEE and its eco-physiological fluxes of GPP and R_{eco} across a grazing intensity gradient (Karoo 1, Karoo 2) from seasonal to annual time scales;

In order to test the significance of the differences in carbon exchange components and the influence of site vegetation greenness using vegetation indices (NDVI and EVI) between the grazed site (Karoo 1) and the rested site (Karoo 2), Welch's Two Sample t-test was performed.

The Shapiro-Wilk normality test was used to test the normality of data in order to satisfy the assumptions of Welch's Two Sample t-test.

To achieve objective (6); To quantify and compare energy balance components between Karoo 1 and Karoo 2 at annual time scale;

Energy balance closures for the Karoo sites were evaluated through the ordinary least squares (OLS) regression method (Wilson et al., 2002) by plotting statistical linear regression plots of (Rn − Go) against (LE + H), with the percentage (%) closure of the energy balance determined from the slope of the regression line.

3. Results and discussion

3.1 Long-term dynamics of carbon exchange parameters at Skukuza

3.1.1 Inter-annual variability of GPP_{opt} and NEE_{offset} across the years

Surface plots are powerful tools to visualize relationships among variables. Across the vegetative functional seasons (growing seasons), increases in GPP_{opt} with increasing soil moisture from dry (SM < 6 %) to drying (6 % ≤ SM ≤ 9 %) to wet (SM > 9 %) soil moisture conditions were observed (Fig. 3.1). GPP_{opt} also increased with increasing air temperature but then started to decrease at higher temperatures above approximately 27.5 to 30 °C for the drying and wet vegetative functional seasons across the hydro-ecological years. For the dry SM classes across the years, productivity was generally affected across the air-temperature classes although no solid conclusion about the GPP_{opt} pattern could be made due to lack of significant GPP_{opt} values for some of the T_{air} classes.

Apart from the GPP_{opt} variability across the different SM/T_{air} classes for each hydro-ecological year, GPP_{opt} also varied across the vegetative functional seasons of the different hydro-ecological years. However, two major distinctions in productivity were between the drought year (2002/2003) and other relatively wetter years (i.e., 2001/2002; 2009/2010; 2010/2011; 2012/2013 and 2013/2014). For instance, during the wet period in 2010/2011 vegetative functional season, highest GPP_{opt} of 29.47 ± 2.3 µmol CO_2 m^{-2} s^{-1} was observed whilst the lowest GPP_{opt} of 13.3± 2.1 µmol CO_2 m^{-2} s^{-1} was witnessed in the wet season of the drought year. Otieno et al. (2010) associated drying periods with low biomass production and reduced ecosystem CO_2 exchange, which can have an impact on GPP_{opt}. Yu et al. (2017) also reported an intensive reduction in GPP following a drought.

In contrast, higher GPP_{opt} values that were attained during wetter periods give an insight of the potential of the Skukuza ecosystem in terms of carbon assimilation (GPP) when soil moisture conditions are favourable. Ago et al. (2016) mentioned that GPP_{opt} increases following the growth of vegetation. In that regard, biophysical controls that were used to describe the hydro-ecological years in relation to the inter-annual variability of GPP_{opt} and NEE_{offset} at Skukuza

were vegetation status related (i.e., EVI, NDVI, FAPAR) and water availability related (i.e. SWB). The 2002/2003 drought year, which received an annual rainfall of 303 mm (Archibald et al., 2009), coincided with the lowest SWB, EVI, NDVI and FAPAR (Fig. 3.1), and its growing season was very dry (Kutsch et al., 2008). Wetter years have been generally associated with improved NDVI, EVI, FAPAR and SWB. In a study conducted by Zoungrana et al. (2014) in a savanna ecosystem in Burkina Faso, NDVI and EVI showed significant and strong positive correlation with rainfall indicators for all land cover types. Figure 3.1 shows a 2D surface plot of inter-annual variability of growing season integrated GPP_{opt} across air temperature and soil moisture gradients as well as information on other biophysical attributes at Skukuza.
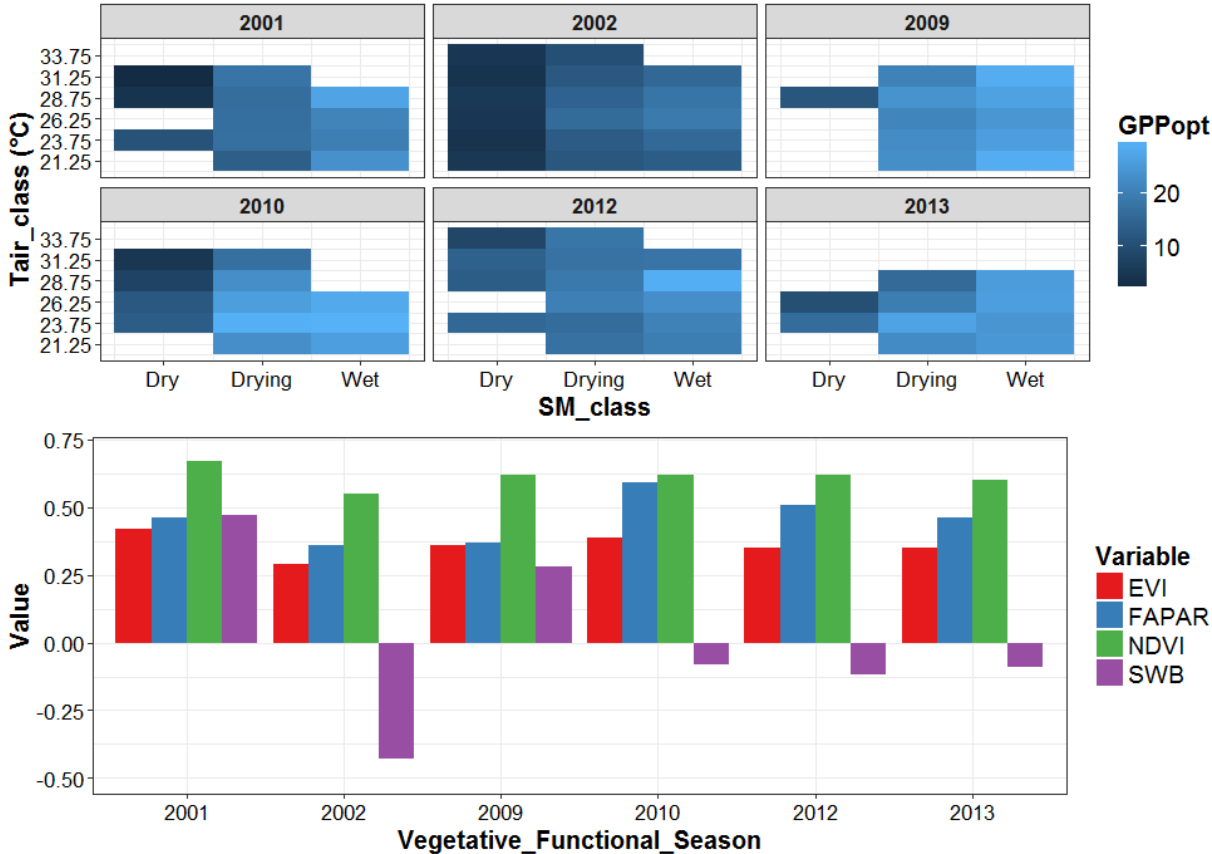
Figure 3. 1: 2D surface plot of inter-annual variability of growing season integrated (i) optimum gross primary production (GPP_{opt}) across soil moisture (SM) and air temperature (T_{air}) classes and; (ii) bar plot of annual variation of enhanced vegetation index (EVI), fraction of photosynthetically active radiation (FAPAR), normalized difference vegetation index (NDVI) and surface water balance (SWB) at Skukuza. SWB was integrated over the length of each vegetative functional season for each hydro-ecological year and normalized by dividing it with

the duration of each period. The general pattern of GPP_{opt}, across the classes, is represented by the colour changes as shown on the colour scale.

The observed variability of GPP_{opt} at Skukuza, across the vegetative functional seasons, is consistent with expectations that there is high inter-annual variability of carbon balance parameters in semi-arid areas. The high inter-annual variability of carbon fluxes has been linked to the remarkable variability in climate variables (Ahlström et al., 2015; Archibald et al., 2009; Ciais et al., 2011; Kutsch et al., 2008; Merbold et al., 2009; Nakano and Shinoda, 2015; Niu et al., 2017).

The GPP_{opt} values obtained for Skukuza (GPP_{opt} ranges for dry SM class; $2 - 16$ µmol CO_2 m^{-2} s^{-1}; drying SM class; $10 - 29$ µmol CO_2 m^{-2} s^{-1}; and wet SM class; $13 - 29$ µmol CO_2 m^{-2} s^{-1}) generally converges with those found in other studies in dry and semi-arid areas with mean annual rainfall ranging from 320 to 560 mm (e.g., Ago et al., 2014; Arneth et al., 2006; Hanan et al., 2010; Kutsch et al., 2008; Merbold et al., 2009; Scanlon and Albertson, 2004; Veenendaal et al., 2004). For instance, previous studies at Skukuza focused on light response curves of NEE above *Combretum* and *Acacia* vegetation and maximum canopy photosynthesis observed during the growing season were in the range between 17 and 22 µmol CO_2 m^{-2} s^{-1} (shown here as positive sign) (Hanan et al., 2010; Kutsch et al., 2008; Merbold et al., 2009). Elsewhere, across the Kalahari sands of Southern Africa – with mean annual rainfall ranging from 365 to 407 mm, Scanlon and Albertson (2004) obtained values of canopy-scale carbon dioxide fluxes at light saturation in the range of 15 to 20 µmol CO_2 m^{-2} s^{-1}. At a degraded woodland at Nangatchori site in Sudan, with an annual precipitation of about 850 mm observed in 2006, (Ago et al., 2014) found ecosystem level A_{max} of about 14.0 ± 1.8 µmol m^{-2} s^{-1} for the wet season.

At Demokeya, a scarce acacia savanna site that receives a mean annual rainfall of 320 mm, maximum photosynthesis capacity (Fp_{max}) was 18 µmol m^{-2} s^{-1} (Merbold et al., 2009). Wet season net ecosystem maximum photosynthesis capacity ranged from $14 - 23.5$ µmol m^{-2} s^{-1} in a woodland savanna ecosystem in Maun (Botswana), which receives mean annual rainfall of 464 mm (Merbold et al., 2009; Veenendaal et al., 2004). Wankama, a fallow bush with mean annual rainfall of 560 mm, reached a maximum photosynthesis capacity of 22 µmol m^{-2} s^{-1} (Merbold et al., 2009). Maximum photosynthesis rates (A_{max}) ranged between 12–14 µmol m^{-2} s^{-1} after about two months into the active season and continued to peak thereafter to 15 µmol

$m^{-2} s^{-1}$ in a *Colophospermum Mopane* -dominated semi-arid savanna ecosystem with annual precipitation of about 460 mm in Botswana, (Arneth et al., 2006).

However, there were some few periods where the observed GPP_{opt} values at Skukuza were slightly higher than those of other similar environments, for instance the wet period of 2010/2011 that reached a maximum GPP_{opt} value of 29 ± 2.3 µmol CO_2 $m^{-2} s^{-1}$. The likelihood of over-estimating the GPP_{opt} values cannot be ruled out as Tagesson et al. (2016) noted the possibility of getting out of range values of CO_2 uptake at light saturation due to possible over-estimation by hyperbolic equations. It was also interesting to observe that the maximum GPP_{opt} values observed for the drying and wet SM classes at Skukuza were similar, suggesting that even at lower soil moisture conditions, plants with deeper roots could still use underground water to achieve higher carbon sequestration. Archibald et al. (2009) had previously reported the occurrence of maximum carbon uptake rates during low soil moisture conditions when green leaves were still present.

Similar to the variability pattern of GPP_{opt}, NEE_{offset} also generally increased when moisture conditions increased from dry to drying to wet. However, the drought year showed signs of water constraint as shown by generally lower NEE_{offset} compared to the values obtained for wetter years (Fig. 3.2). Figure 3.2 shows a 2D surface plot of inter-annual variability of growing season integrated NEE_{offset} and other biophysical attributes across air temperature and soil moisture gradients at Skukuza
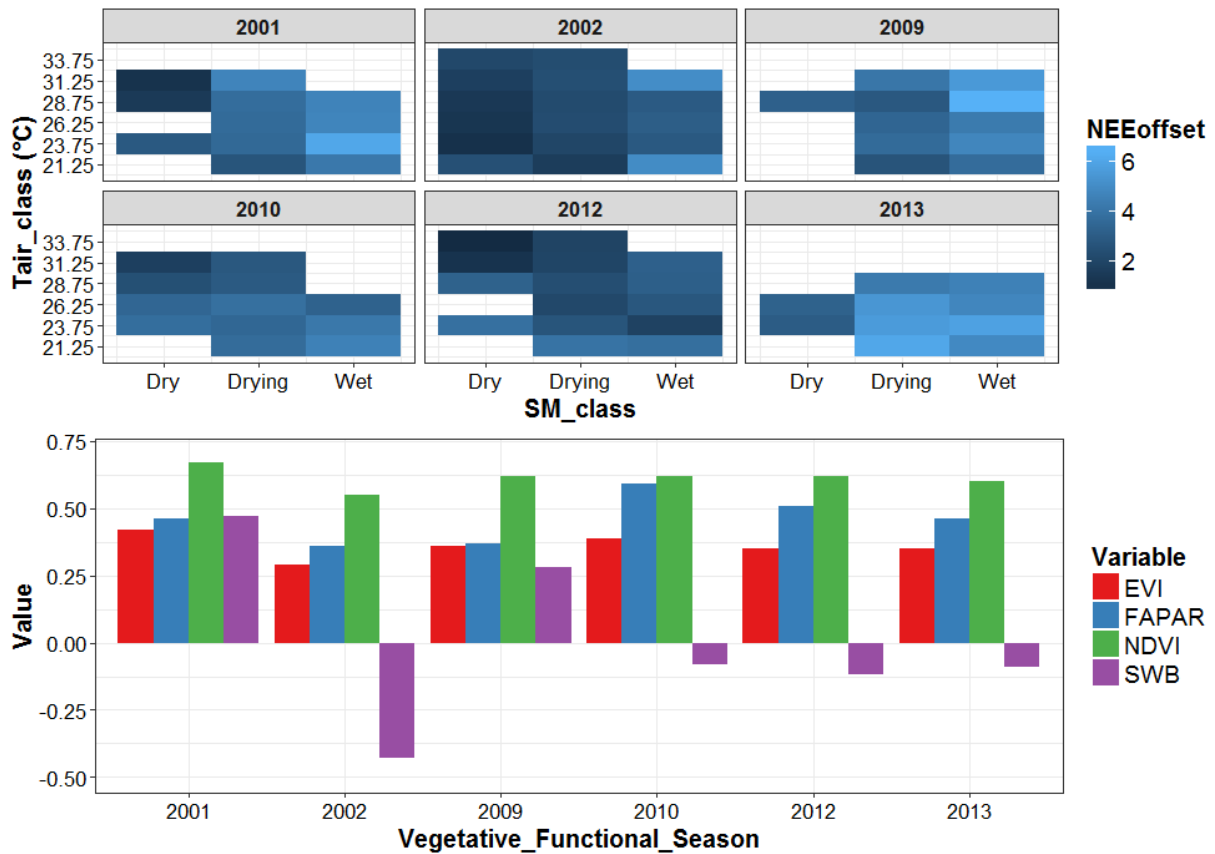
Figure 3.2: 2D surface plot of inter-annual variability of growing season integrated (i) net ecosystem CO_2 exchange offset (NEE_{offset}) across soil moisture (SM) and air temperature (T_{air}) classes and (ii) bar plot of annual variation of enhanced vegetation index (EVI), fraction of photosynthetically active radiation (FAPAR), normalized difference vegetation index (NDVI) and surface water balance (SWB) at Skukuza

For most of the vegetative functional seasons, NEE_{offset} did not show a clear pattern in response to air temperature increase, which is in agreement with Williams et al. (2009) who found no clear relationship between nighttime fluxes and temperature. There are generally few studies that have delved much on NEE_{offset} and its controlling factors (Ago et al., 2016; Gilmanov et al., 2003). Most studies on application of the non-rectangular hyperbolic model of light response curves have put much emphasis on maximum photosynthesis capacity than NEE_{offset} (Kutsch et al., 2008; Merbold et al., 2009). This study therefore provided some insights on this parameter as an index of ecosystem respiratory losses, for it has also been observed that periods that exhibit higher ecosystem respiration also show higher offsets of NEE (Ago et al., 2016). Gilmanov et al. (2003) has described NEE_{offset} as the respiration term of light response curves which is a measure of the average daytime ecosystem respiration. In the Lasslop et al. (2010)

52

NEE flux partitioning approach, daytime NEE data is used to fit light-response curves and ecosystem respiration is derived from the intercept of the ordinate (NEE_{offset}).

Due to the fact that periods which exhibit higher ecosystem respiration also show higher offsets of NEE (Ago et al., 2016), it was also interesting to explore other studies in Skukuza that investigated the relationship of ecosystem respiration or its components and controlling factors. Ecosystem respiration comprises of soil to atmosphere carbon flux (i.e., soil respiration) and the aboveground plant respiration (Barba et al., 2018). We found a study by Makhado and Scholes. (2011) which reported a temperature threshold for soil respiration at Skukuza, with soil respiration increasing to maximum at around 28 °C and then starts to decline beyond that temperature. However, the relative contribution of soil respiration to ecosystem respiration at Skukuza could not be confirmed although Makhado and Scholes. (2011) generalized that soil respiration contributes the largest carbon flux from savanna ecosystems to the atmosphere.

Since there is generally a lack of NEE_{offset} comparative studies with similar environments, an attempt was made to look at other sites elsewhere. For instance, at a savanna site at Nalohou (West Africa), with a high mean annual precipitation of 1303 mm, Ago et al. (2016) found values of NEE_{offset} (referred to as dark respiration) in the range from 1.0 ± 0.4 to 6.8 ± 1.1 µmol m^{-2} s^{-1}, which were comparable to the range of $NE_{Eoffset}$ values obtained at a relatively drier Skukuza flux site with $NE_{Eoffset}$ ranges: $1 - 4$ µmol CO_2 m^{-2} s^{-1}; $2 - 6$ µmol CO_2 m^{-2} s^{-1}; and $4 - 5$ µmol CO_2 m^{-2} s^{-1} for the dry, drying and wet SM classes.

3.1.2 Functional relationships of light response parameters (GPP_{opt} and NEE_{offset}) and soil moisture, air temperature and vapor pressure deficit

3.1.2.1 Functional relationship of GPP_{opt} vs soil moisture

Figure 3.3. shows the functional relationship between GPP_{opt} and soil moisture across a soil moisture gradient during vegetative functional seasons at Skukuza. During the years of above-average annual precipitation (wetter years) there were significant relationships between GPP_{opt}

and soil moisture at air temperature classes in sub-figures (b – e) ($P < 0.05$), but the relationship was not significant at air temperature class 20 to 22.5 °C ($P > 0.05$; $R^2 = 0.39$). Generally, as soil moisture increased GPP_{opt} also increased until it reached its peak, but the GPP_{opt} saturation that is attained could be an indication of the effects of other controlling variables. A similar shape of the curve was also observed for the drought year although it was very clear that the GPP_{opt} range for the drought year was on a much lower level compared to the range of GPP_{opt} values for wetter years combined, showing the effects of water limitation on productivity. It was observed that at a given soil moisture, higher assimilation rates were achieved during years of above-average annual precipitation and lower assimilation rates were observed during the drought year. The possible reason being that more water stress associated with drought might have led to a decrease in overall vegetation growth as revealed by the vegetation greenness metrics (Fig. 3.2) because annual rainfall received during 2002/2003 (303 mm) was about 55 % less than the long-term annual average for Skukuza.
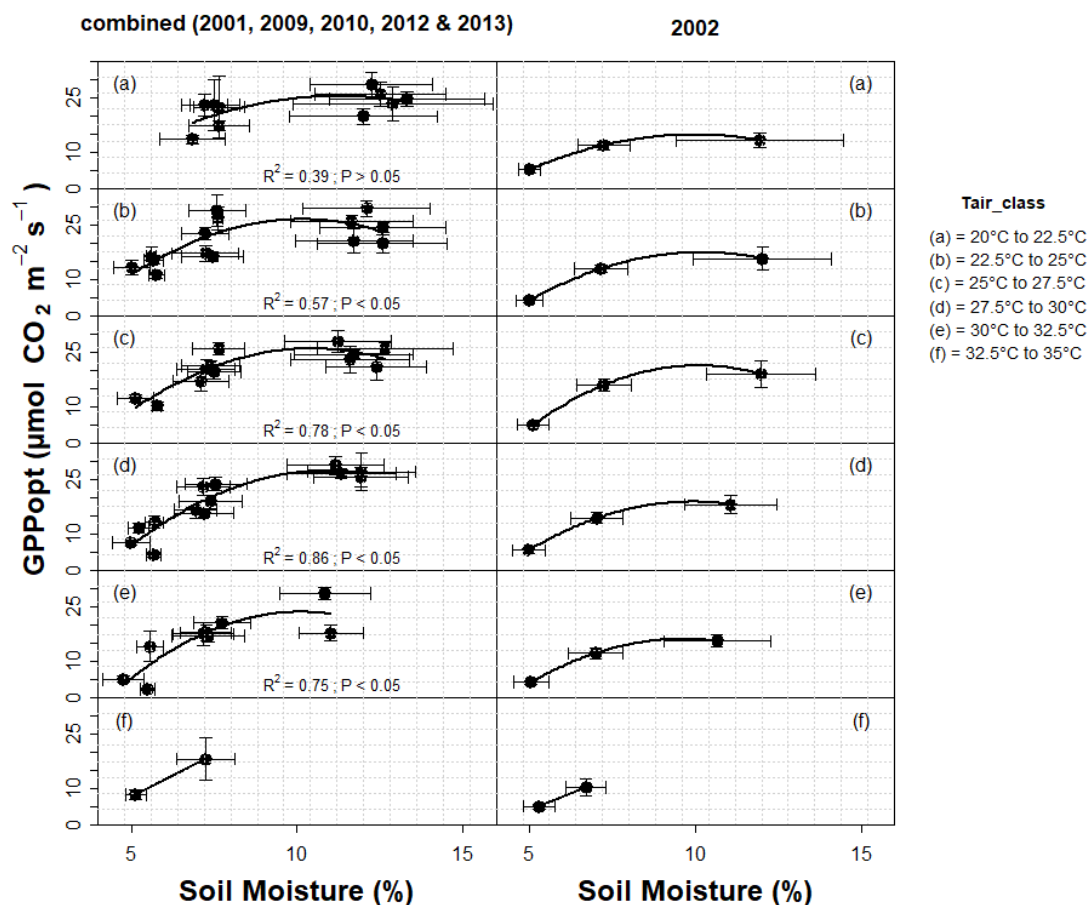
Figure 3. 3: Functional relationship between optimum gross primary production (GPP_{opt}) and soil moisture across air temperature gradient and vegetative functional seasons at Skukuza.

Coefficient of determination (R^2) and statistical significance level (P), where suitable, are shown on the bottom of sub-figures.

The decline in carbon uptake as soil moisture conditions deteriorates agrees with the observation of Archibald et al. (2009) that limited carbon uptake coincide with drought years even at the peak of the growing season. In a semi-arid grassland in Mongolia, Nakano and Shinoda. (2015) observed that carbon sequestration is effectively reduced during the drought year. The increase in carbon assimilation as soil moisture increases is consistent with results from previous studies at Skukuza (Kutsch et al., 2008; Merbold et al., 2009). In a photosynthesis model by Archibald et al. (2009), soil moisture was very significant in predicting GPP. Higher rainfall also supports a higher above-ground biomass than under dryer soil moisture conditions. Law et al. (2002) pointed out that there is a strong positive correlation between GPP and water availability. In arid and semi-arid regions, soil moisture strongly influences primary production (Qi and Xu, 2004) while drought is known to alter vegetation structure and function including the cycling of carbon and water in ecosystems (Scott et al., 2010).

From 2000–2014, precipitation at Skukuza showed high inter-annual variability (Fig. 3.4). Hydro-ecological years with precipitation below the long-term annual mean (drought years) were 2002/2003; 2006/2007 and 2007/2008. Peak precipitation was observed in 2005/2006 and 2012/2013. The pattern of the functional relationships between GPP_{opt}/NEE_{offset} and air temperature, soil moisture and vapour pressure deficit (graphs not presented here) were similar for the years with precipitation above the long-term annual average (i.e., 2001, 2009, 2010, 2012 and 2013). The drought year (2002) behaved differently from the other wetter years and that was the reason for combining these years (2001, 2009, 2010, 2012 and 2013) and jointly comparing them with 2002. Such comparison of wetter vs drier years is crucial to better understand ecosystem physiological responses to wetter periods and extreme climatic events such as severe droughts. Fig. 3.4 shows the inter-annual variability of precipitation at Skukuza from 2000 – 2014.
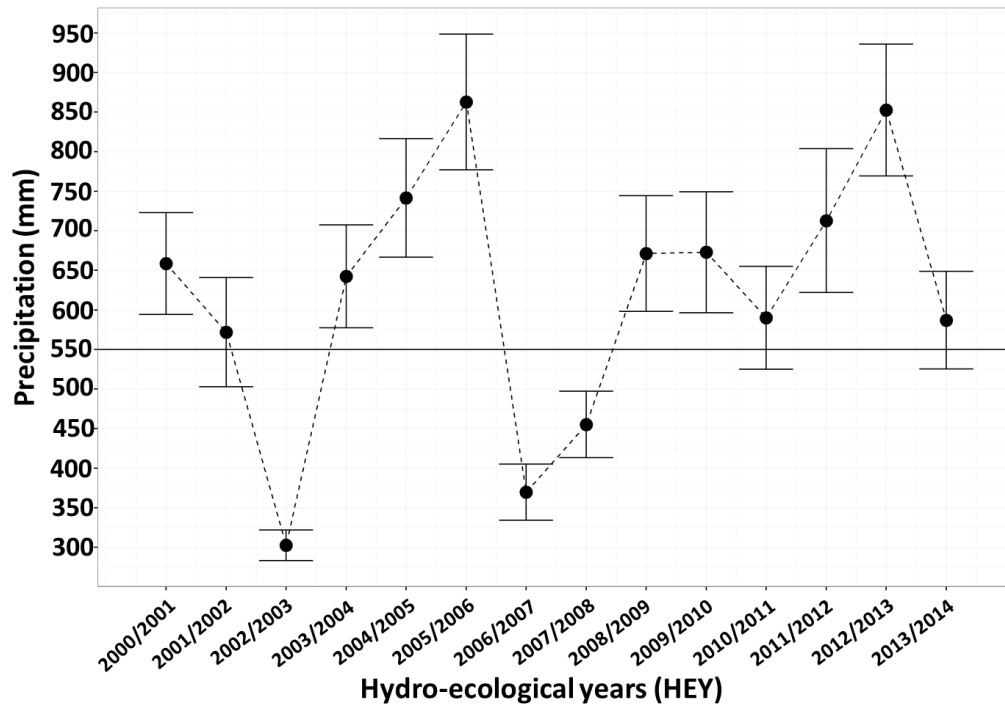
Figure 3. 4: Inter-annual variability of precipitation at Skukuza from 2000–2014, according to hydro-ecological years. The error bars indicate ± standard deviation.

3.1.2.2 Functional relationship of GPP$_{opt}$ vs air temperature

Figure 3.5 shows the functional relationship between GPP$_{opt}$ and air temperature across soil moisture gradient during vegetative functional seasons at Skukuza. The functional relationship of GPP$_{opt}$ and air temperature was not significant for all soil moisture classes during wetter years ($P > 0.05$; dry SM_class $R^2 = 0.40$; drying SM_class $R^2 = 0.09$; wet SM_class $R^2 = 0.02$). For the drought year, there was a significant relationship between GPP$_{opt}$ and air temperature at drying SM class ($P < 0.05$; $R^2 = 0.88$) but not at dry ($P > 0.05$; $R^2 = 0.01$) and wet ($P > 0.05$; $R^2 = 0.93$) SM classes. For the dry SM class during the drought year, it appeared that there was no relationship between GPP$_{opt}$ and air temperature due to water limitation. The relationships of GPP$_{opt}$ and air temperature across the SM classes during the drought year (2002/2003) illustrated that under varying soil moisture conditions contrasting patterns of the GPP$_{opt}$ and air temperature relationship can be experienced. Overall, these relationships of GPP$_{opt}$ and air temperature for years of above-average and below-average annual precipitation showed that air temperature is a less important driver of carbon uptake at Skukuza.
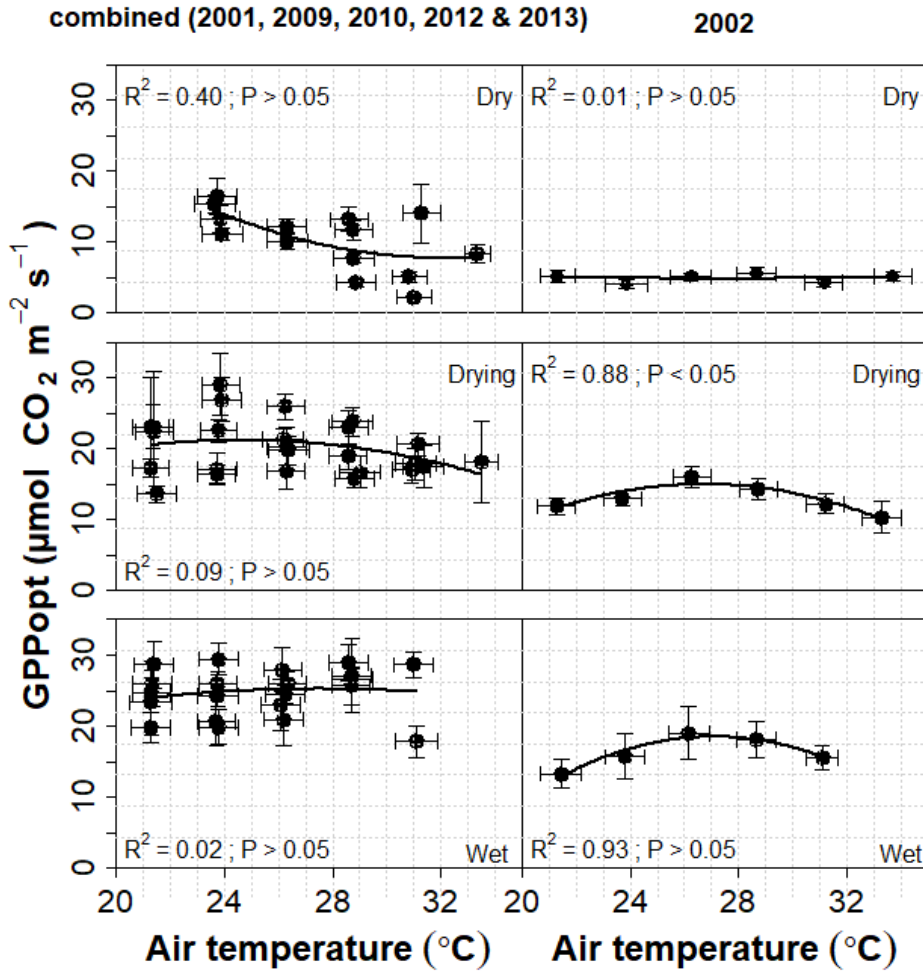
Figure 3. 5: Functional relationship between optimum gross primary production (GPP$_{opt}$) and air temperature across soil moisture gradient and vegetative functional seasons at Skukuza

In Skukuza, previous studies have demonstrated that air temperature is not the main determinant of CO_2 fluxes (Archibald et al., 2009; Kutsch et al., 2008; Merbold et al., 2009). Daily temperature variation over the course of the growing season is small and what deviates much is soil moisture which impacts on plant metabolism (Archibald et al., 2009). However, in some regions at an annual scale a linear relationship between GPP and mean annual air temperature was reported (Chen et al., 2013). At Mongu flux measurement site in Zambia, which receives an annual precipitation of 879 mm, air temperature beyond 27 °C decreased carbon uptake from daytime carbon uptake values > 20 µmol CO_2 m^{-2} s^{-1} to < 10 µmol CO_2 m^{-2} s^{-1} (Scanlon and Albertson, 2004).

3.1.2.3 Functional relationship of GPP_{opt} vs VPD

Figure 3.6 shows the functional relationship between GPP_{opt} and vapor pressure deficit across soil moisture gradient and vegetative functional seasons at Skukuza. VPD plays an important regulatory role in leaf gas exchange and diurnal evolution of transpiration. For wetter years, the relationship of GPP_{opt} and VPD was not significant ($P > 0.05$) for all SM classes as was the case between the relationship of GPP_{opt} and air temperature. Although the effect of VPD on GPP_{opt} under wetter vegetative functional seasons was not clear, the increase in soil moisture conditions seemed to delay the effects of VPD on GPP_{opt} as compared to the scenario during the drought year. Kutsch et al. (2008) noted that the sensitivity of plants to VPD increases with dryness.
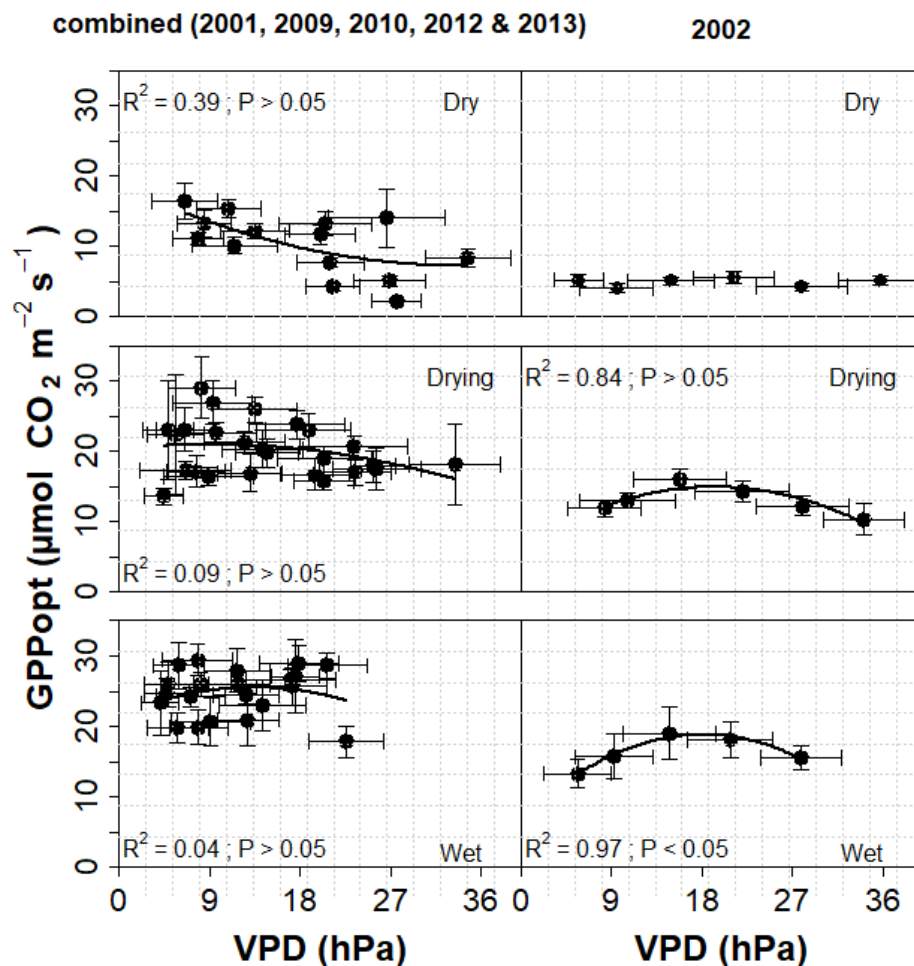
Figure 3. 6: Functional relationship between optimum gross primary production (GPP_{opt}) and vapor pressure deficit (VPD) across soil moisture gradient and vegetative functional seasons at Skukuza.

During the wet period of the drought year, the relationship of GPP_{opt} and VPD was significant ($P < 0.05$; $R^2 = 0.97$) and GPP_{opt} rose rapidly from values of around 13 µmol m^{-2} s^{-1} to close to 18 µmol m^{-2} s^{-1}, but at VPD of around 18–20 hPa photosynthesis begun to show signs of constraint. This is consistent with authors who have observed a strong decrease in photosynthesis rates when VPD goes above 2 kPa (i.e., 20 hPa) across a range of ecosystems (Liu et al., 2011; Merbold et al., 2009). Fei et al. (2017) reported a negative correlation between carbon exchange parameters and VPD at higher levels of VPD. The sensitivity of GPP_{opt} to VPD is linked to the underlying physiological mechanism of VPD effects on photosynthesis.

Although the GPP_{opt} and VPD relationship of the drying SM class of the drought year was not significant ($P > 0.05$; $R^2 = 0.84$), the pattern of relationship was also similar to that of GPP_{opt} vs air temperature at drying SM class of the drought year. Similarly, the relationship of GPP_{opt} and VPD at the dry SM class of the drought year was comparable to the GPP_{opt} and air temperature relationship of the drought year, showing a proxy relationship between VPD and air temperature.

The general pattern of lower VPD range under wet compared to dry soil moisture conditions at Skukuza is consistent with findings from Majozi et al., (2017a). The author observed a decrease in daily average VPD during rainy days or times of high soil water availability and an increase in VPD during times of little or no rain. Over a 15-year period (i.e., from 2000 – 2014), Majozi et al. (2017a) found an overall mean VPD of 1.28 ± 0.62 kPa; annual daily mean VPD range of 0.024 to 4.03 kPa; and annual average VPD ranges of 1.34 to 1.98 kPa and 2.77 to 2.97 kPa wetter years and drought years, respectively. Such VPD range of values are comparable to the VPD ranges obtained for the vegetative functional seasons of wet years (2001, 2009, 2010, 2012, 2013) and the dry year (2002).

3.1.2.4 Functional relationship of NEE$_{offset}$ vs soil moisture

Figure 3.7 shows the functional relationship between NEE$_{offset}$ and soil moisture across an air temperature gradient and vegetative functional seasons at Skukuza. During wetter years, the functional relationship between NEE$_{offset}$ and soil moisture showed a significant positive linear relationship ($P < 0.05$; $R^2 = 0.47$, $R^2 = 0.52$, respectively) at air temperatures between 27.5-30°C and 30-32.5°C (sub-figures d and e), but the relationships were not significant at other air temperatures (sub-figures a – c, f). During the drought year, the functional relationships between NEE$_{offset}$ and soil moisture showed a similar linear pattern, although not statistically significant ($P > 0.05$), for all air temperature classes, since the number of possible NEE$_{offset}$ samples were few. At each air temperature class, there were three soil moisture means (i.e., one for each of the dry, drying and wet soil moisture classes) hence there were three NEE$_{offset}$ estimates shown for each sub-plot on Fig.3.7. The sample size was higher for wetter years because the years were combined.

Figure 3. 7: Functional relationship between net ecosystem CO_2 exchange offset (NEEoffset) and soil moisture across air temperature gradient and vegetative functional seasons at Skukuza.

The general pattern was that NEE_{offset} increased with increasing soil moisture, supporting the notion that ecosystem respiration is higher during wet periods compared to dry periods (Ago et al., 2016; Williams et al., 2009; Williams and Albertson, 2004). Although the wetter years and drought year showed a similar pattern of NEE response to soil moisture, the difference was that the drought year had lower NEE_{offset} due to lower precipitation compared to the wetter years. Arneth et al. (2006) observed that respiration rates were higher at a given temperature when soil moisture measured at 10 cm depth exceeded 9%, compared to respiration rates when soil moisture was between 5 and 9% and < 5%. These soil moisture classes identified by Arneth et al. (2006) were similar to those used by Archibald et al. (2009) and used in this study for the analyses of GPP_{opt} and NEE_{offset} at Skukuza.

In deriving GPP_{opt} and NEE_{offset}, daytime half-hourly NEE measurements of between 0530 hrs and 1900 hrs were used to construct the light response curve fits of the relationship of NEE against global radiation. However, there was a possibility of slightly increasing the NEE_{offset} range in this study due to use of a fixed time criterion for daytime. In savanna ecosystems of South Africa, sunset and sunrise may vary slightly across the days during the summer period. It may therefore be necessary for future studies to use a threshold for defining daytime data for low latitudes (such as $Rg > 20$ W m^{-2}) (Lasslop et al., 2010), and cross-check it against sunrise and sunset local time information.

3.1.2.5 Functional relationship of NEE_{offset} vs air temperature

Particularly in Skukuza, contrasting views on the functional relationship of ecosystem respiration and air temperature have been reported (Archibald et al., 2009; Kutsch et al., 2008; Makhado and Scholes, 2011; Merbold et al., 2009; Williams et al., 2009) and there is no consensus on the exact form of the relationship. Some studies have shown a strong dependence of ecosystem respiration on both temperature and soil moisture (Kutsch et al., 2008; Merbold et al., 2009), whereas others found no clear relationship between nighttime fluxes and temperature (Williams et al., 2009).

Figure 3.8 shows the functional relationship between NEE_{offset} and air temperature across a soil moisture gradient and vegetative functional seasons at Skukuza. There was no clear relationship between NEE_{offset} and air temperature for most of the strata, with the exception of the drying

SM class of the drought year which showed a significant NEE_{offset} and air temperature relationship ($P < 0.05$; $R^2 = 0.95$). The pattern revealed for the drying SM class of the drought year was that NEE_{offset} initially increased with an increase in temperature and then dropped off at high temperatures. The NEE_{offset} and air temperature relationship also seemed to have become much more unclear with increases in soil moisture, as soil moisture is also known to moderate the effects of other factors such as temperature on respiration processes (Yan et al., 2011).
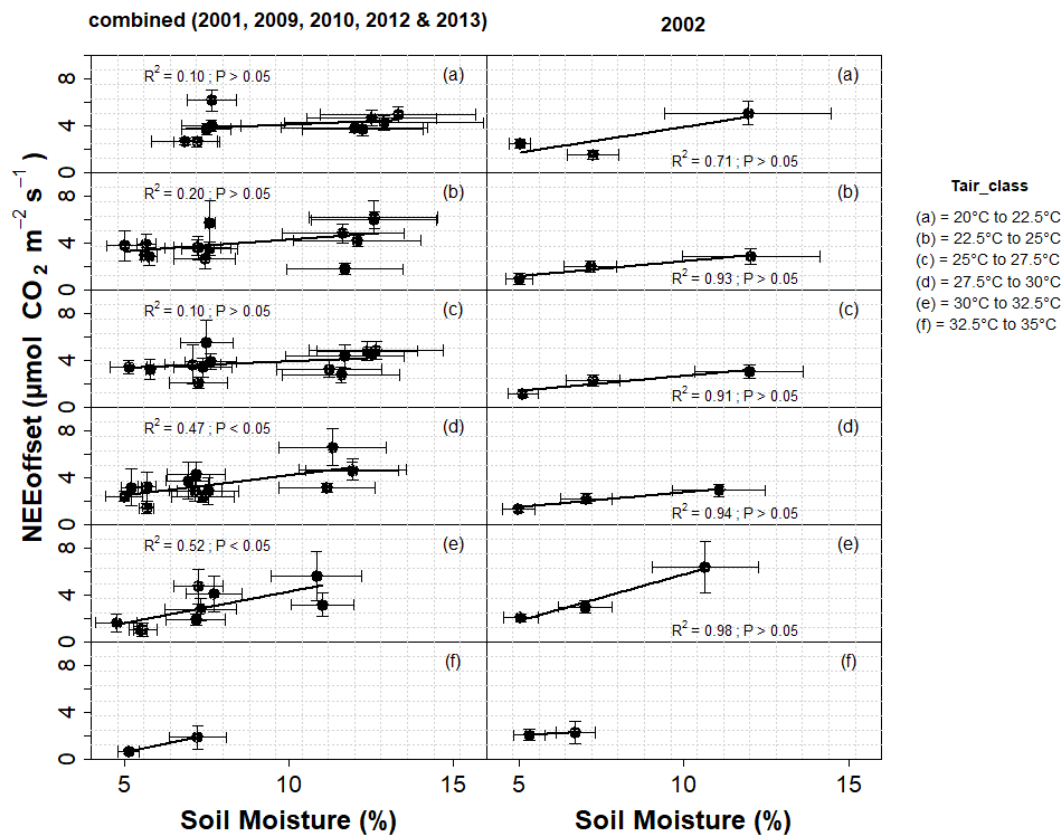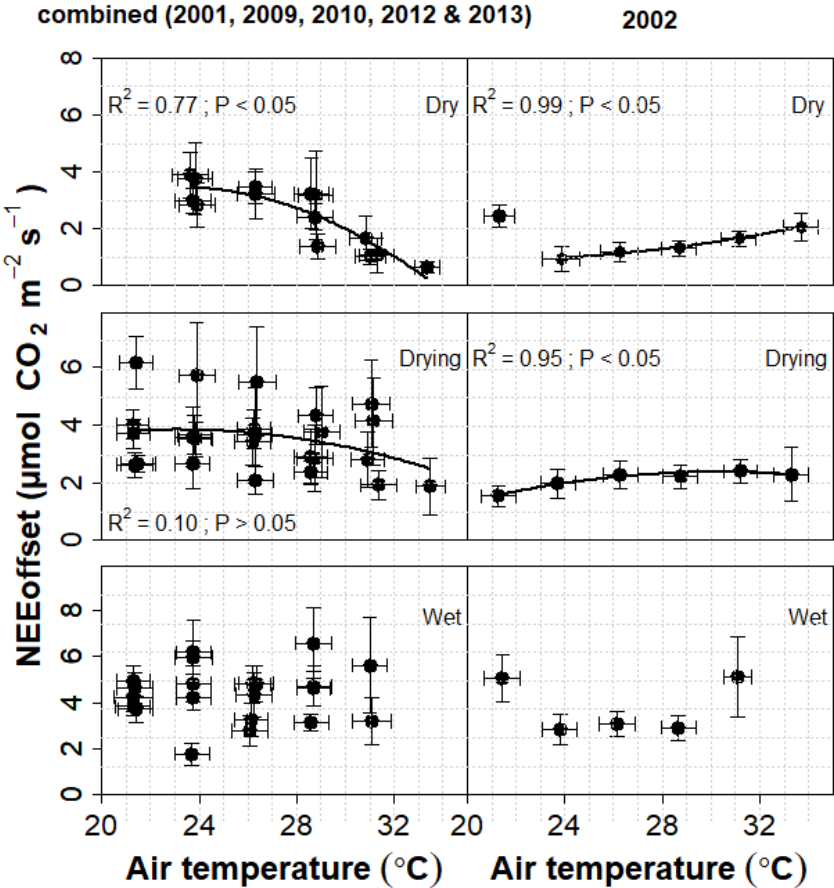

Figure 3. 8: Functional relationship between net ecosystem CO_2 exchange offset (NEE_{offset}) and air temperature across a soil moisture gradient and vegetative functional seasons at Skukuza.

3.1.2.6 Functional relationship of GPP$_{opt}$ vs NEE$_{offset}$

Figure 3.9 shows the relationship between light response parameters GPP$_{opt}$ and NEE$_{offset}$ between wetter years and the drought year and the influence of soil moisture on the relationship at Skukuza. GPP$_{opt}$ and NEE$_{offset}$ showed an initial linear relationship as both parameters agreed to a larger extent in their responses to driving environmental factors between the wetter and drier hydro-ecological years. Since GPP$_{opt}$ parameter relates to photosynthetic uptake process and NEE$_{offset}$ relates to respiratory release process, supporting results were also found by Yang and Zhou (2013) who observed ecosystem respiration responding to gross primary production in a linear manner. Similarly, Moyana et al. (2008) and Bahn et al. (2009) also found a linear relationship between soil respiration and plant photosynthesis. In another study, GPP was described as a driver of ecosystem respiration (Wang et al., 2010). However, the linear relationship weakened as air temperature increased beyond 27.5 to 30 °C and GPP$_{opt}$ dropped while NEE$_{offset}$ continued to increase slightly due to plants often responding to high day-time temperatures by way of closing their stomata in response to increasing VPD. It appeared that even when conditions are no longer conducive for optimum photosynthesis higher values of NEE$_{offset}$ can still occur and that could be ascribed to continued soil respiration activity.
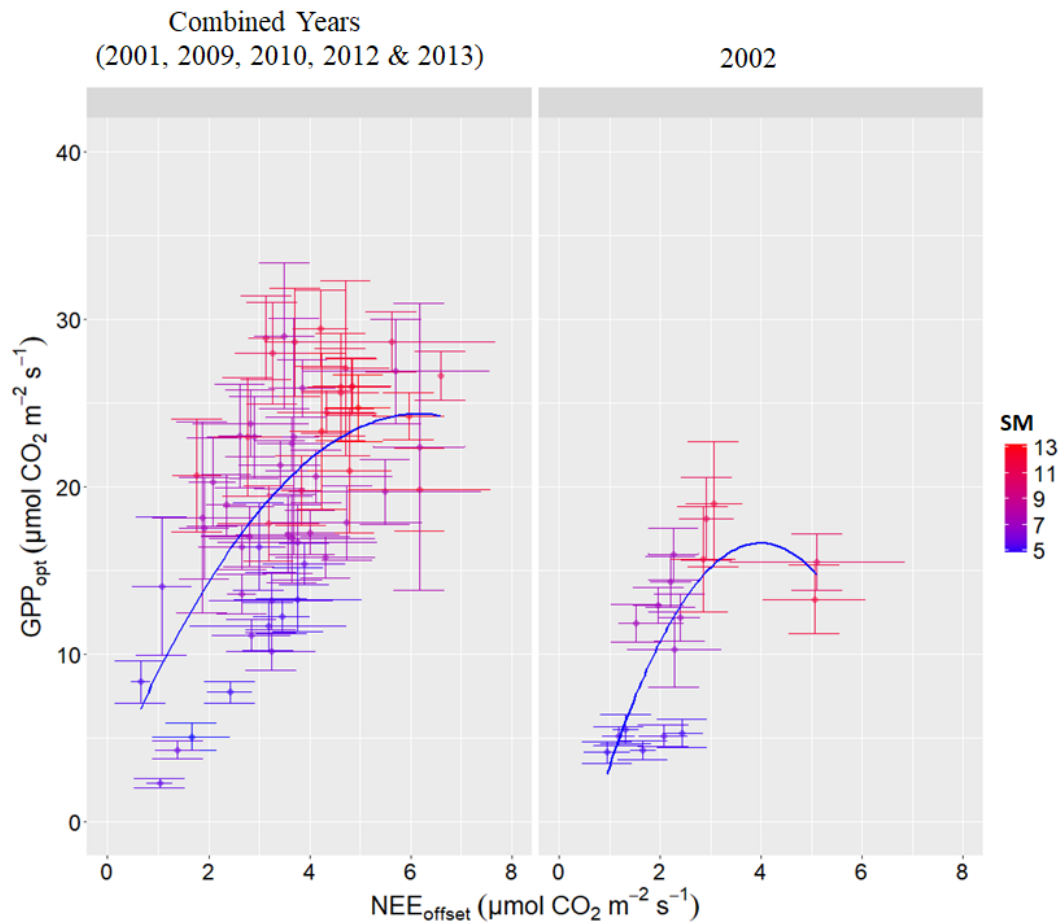
Figure 3. 9: Relationship between light response parameters GPP_{opt} and NEE_{offset} between wetter years and the drought year and the influence of soil moisture on the relationship at Skukuza. GPP_{opt} is optimum gross primary production. NEE_{offset} is net ecosystem CO_2 exchange offset.

Soil moisture also appeared to regulate productivity and average daytime ecosystem respiration, with increases in soil moisture generally resulting in increases in GPP_{opt} and NEE_{offset}. The comparison between the wetter years and the drought year also showed that ecosystem processes can be remarkedly limited by water availability.

3.2 Short-term dynamics of carbon exchange components at Karoo sites

3.2.1 Time series of NEE and meteorological measurements at Karoo sites

The Karoo system is characterized by seasonal rainfall, usually occurring from November to April. The dry period is from May to October, and to a large extent vegetation is in dormancy state. Most of the rains are received mid- to late-summer (Du Toit. 2010) between January and March (Fig. 3.10). Annual precipitation for Karoo 1 and Karoo 2 differed slightly during the two years of measurement but can generally be considered to be similar. Year 1 (November 2015 to October 2016) and year 2 (November 2016 to October 2017) precipitation for Karoo 1 were measured as 352 mm and 429 mm, respectively. Year 1 and year 2 precipitation for Karoo 2 were 371 mm and 406 mm, respectively. Rainfall for year 1 was below the long-term annual mean precipitation of 374 mm at both sites, while year 2 was relatively wetter with annual rainfall above the long-term annual mean. Cumulative precipitation for Karoo 1 and Karoo 2 for the two years of measurement were 781 mm and 777 mm, respectively. Year 1 was constituted by 50 and 48 rainfall days at Karoo 1 and Karoo 2, respectively, while year 2 comprised 49 and 46 rainfall days for Karoo 1 and Karoo 2, respectively.

Soil water content during the peak dry season months (October 2016 and September 2017) was ranging from 7 - 10% and maximum soil moisture values during peak rainy season months (January to March) were reaching 33 %. The wilting point for arid and semi-arid savanna ecosystems is around 5 % (Ardö et al., 2008). However, the soil water content values appeared to be over-estimated for the dry Karoo site. The ML3x Theta Probes, capable of measuring soil moisture and soil temperature, are temperature dependent in the estimation of soil moisture and it caused spurious diurnal soil moisture fluctuations even without rain being involved due to daytime high temperature amplitudes of 19°C to 35°C at the study site. A temperature correction algorithm is needed to address this problem of spurious daytime soil moisture measurements by the ML3x Theta Probes especially in open or sparse vegetation areas (Goodchild et al., 2018; Verhoef et al., 2006). In this study, a centered simple moving average technique with a window size of one day (RcppRoll package in R, R Core Team. (2013)) was used to smoothen and correct the diurnal soil moisture increases, although the soil moisture values from the sensors were generally higher than expected and therefore could not be used for further analyses.

Carbon uptake predominantly occurred in the rainy season when water was available, while the dry season was characterized by a net carbon loss. The daily mean NEE showed that initially, there was a net release of CO_2 into the atmosphere at the early phases of the rainy season during year 1 and year 2. This release was triggered by rain pulses described in detail in section 3.6. This was followed by transition to net CO_2 uptake as soil moisture conditions and vegetation physiological activities increased at Karoo 1 and Karoo 2, coinciding with the peak rainfall period of January to March. Between November and April, the daily mean NEE range for Karoo 1 and Karoo 2 during year 1 were -1 to 3 μmol m^{-2} s^{-1} and - 2 to 2 μmol m^{-2} s^{-1}, respectively. This was an indication that the gently grazed site (Karoo 1) released slightly more CO_2 to the atmosphere compared to the rested site (Karoo 2). The daily mean NEE at both locations between November and April during year 2 were in the similar range of - 3 to 2 μmol m^{-2} s^{-1}. The dormancy state of the dry season is reflected by very low daily mean NEE values at both sites, oscillating around the carbon neutral state (i.e., NEE = 0 μmol m^{-2} s^{-1}) but overall showing a slight net release of CO_2 into the atmosphere. For instance, a similar range of daily mean NEE of - 0.3 to 0.8 μmol m^{-2} s^{-1} was attained by both Karoo 1 (year 1) and Karoo 2 (year 1) between May and September. The means of daily NEE for Karoo 1 and Karoo 2 between May and September during year 2 were similar in the range of 0 – 0.9 μmol m^{-2} s^{-1}.

To understand the hydroclimate regime and daily mean NEE at the Karoo sites, a time series of daily precipitation, soil water content and daily mean values of NEE from November 2015 to October 2017 are shown in Figure 3.10.
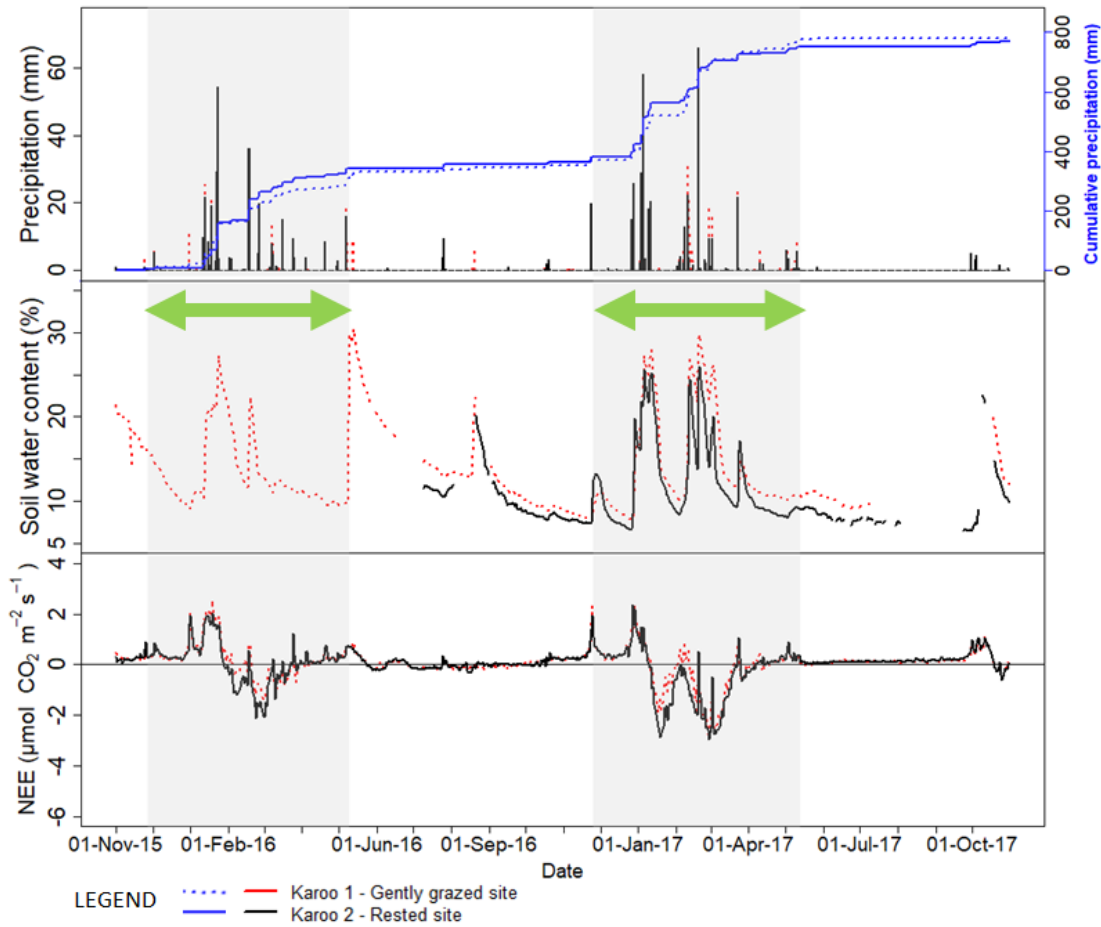
Figure 3. 10: Time series of daily precipitation, soil water content and daily mean net ecosystem CO_2 exchange (NEE) from November 2015 to October 2017 at Karoo sites

3.2.2 Seasonal pattern of daily integrated NEE, GPP and R_{eco}

The temporal dynamics of NEE, GPP and R_{eco} along a grazing intensity gradient between Karoo 1 (the gently grazed site) and Karoo 2 (the rested site) were investigated from seasonal to annual time scales. Figure 3.11 shows the daily sums of NEE, GPP and R_{eco} between November 2015 and October 2017 at Karoo 1 and Karoo 2.
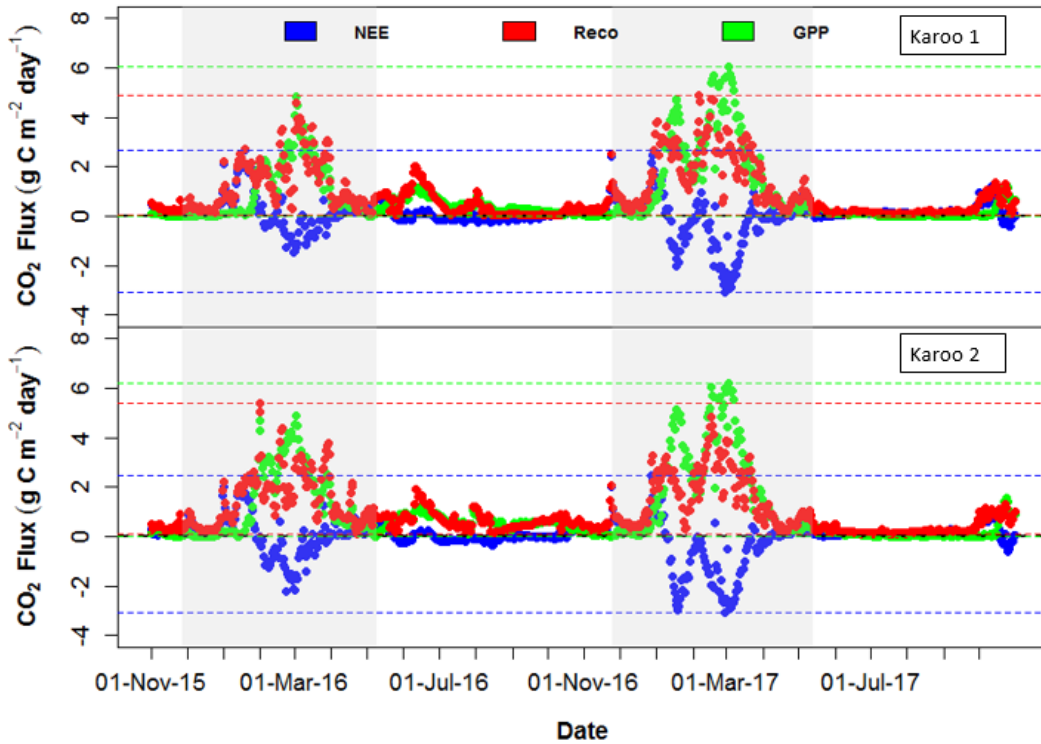
Figure 3. 11: Daily sums of net ecosystem CO_2 exchange (NEE), gross primary production (GPP) and ecosystem respiration (R_{eco}) between November 2015 and October 2017 at Karoo 1 and Karoo 2

NEE, R_{eco}, and GPP indicate net ecosystem CO_2 exchange, ecosystem respiration, and gross primary production, respectively. Shaded areas indicate calendar-fixed wet season (November – May) and the rest of the figure area is the dry season (June – October). Hydro-ecological year (HEY) 1 is from 01.11.2015 to 31.10.2016 and HEY 2 is from 01.11.2016 to 31.10.2017.

At Karoo 1, the amplitude of the daily NEE during the growing season of year 1 ranged from -1.5 g C m^{-2} d^{-1} (maximum net carbon uptake attained on 29.02.2016) to 2.7 g C m^{-2} d^{-1} (maximum net carbon release reached on 19.01.2016). During the same year, the mean daily carbon uptake at Karoo 1 for peak carbon uptake periods (February and March 2016) was -0.4 g C m^{-2} d^{-1}. In year 2, Karoo 1 amplitude of daily NEE ranged from -3.1 g C m^{-2} d^{-1} (maximum net carbon uptake reached on 28.02.2017) to 2.5 g C m^{-2} d^{-1} (maximum net carbon release attained on 29.12.2016). The mean daily carbon uptake at Karoo 1 during year 2 for peak carbon uptake periods (February and March 2017) was -0.9 g C m^{-2} d^{-1}. The peak daily net carbon release at Karoo 1 was higher compared to the peak daily net carbon release at Karoo 2 during

68

year 1. However, peak daily net carbon uptake was higher at Karoo 2 compared to the peak daily net carbon uptake at Karoo 1 during year 1. For Karoo 2 during year 1, the amplitude of the daily NEE ranged from -2.2 g C m^{-2} d^{-1} (maximum net carbon uptake attained on 23.02.2016) to 2.1 g C m^{-2} d^{-1} (maximum value of net carbon release reached on 19.01.2016). The mean daily carbon uptake at Karoo 2 during year 1 for peak carbon uptake periods (February and March 2016) was -0.7 g C m^{-2} d^{-1}. At Karoo 2 during year 2, the amplitude of daily NEE ranged from -3.1 g C m^{-2} d^{-1} (maximum net carbon uptake reached on 28.02.2017) to 2.5 g C m^{-2} d^{-1} (maximum net carbon release attained on 27.12.2016). The mean daily carbon uptake at Karoo 2 during year 2 for peak carbon uptake periods (February and March 2017) was -1.2 g C m^{-2} d^{-1}. The amplitudes of the daily NEE of Karoo 1 were similar to those of Karoo 2 during year 2. Peak and mean daily net carbon uptake, however, increased at both Karoo sites from year 1 to year 2 as rainfall increased.

At a similar dry ecosystem at Demokeya (Sudan), a sparse savanna site with mean annual rainfall of about 320 mm, the mean daily NEE observed during the wet season was -1.8 g C m^{-2} d^{-1} (Ardö et al., 2008). The mean daily net carbon uptake range at Karoo sites (-0.4 to -1.2 g C m^{-2} d^{-1}) were lower than the mean daily NEE observed at Demokeya in a wet season. At Maun (Botswana), a savanna woodland with mean annual rainfall of 464 mm, mean net carbon uptake during a wet season in 1999 varied between -0.6 to -2.4 g C m^{-2} d^{-1} (Veenendaal et al., 2004). Karoo 2 (year 1) mean net carbon uptake (i.e., -0.7 g C m^{-2} d^{-1}), Karoo 1 and Karoo 2 (year 2) mean net carbon uptakes (i.e., -0.9 and -1.2 g C m^{-2} d^{-1}, respectively) were in the range of mean net carbon uptake range obtained at Maun, although Maun generally showed a higher carbon uptake. Mean daily carbon uptake range obtained at Hapex (Niger), a Sahelian fallow savanna with mean annual rainfall of 495 mm, was 0.6 to -3.6 g C m^{-2} d^{-1} (Hanan et al., 1998). The Karoo sites mean daily net carbon uptake ranges were also in the similar range to that at Hapex although the Hapex site seemed to sequester more CO_2 than the Karoo sites due to its relatively higher rainfall. The total annual rainfall received at Karoo 1 and Karoo 2 during year 2, which was relatively wetter than year 1, were 429 and 406 mm, respectively. At the peak wet season, the Maun and Hapex sites had higher carbon uptake rates (NEE < -1.2 g C m^{-2} d^{-1}) compared to the Karoo sites.

At Baja California (Mexico), a desert shrub ecosystem which received annual precipitation of 147 and 197 mm in 2002 and 2003, respectively, a mean daily net carbon uptake of -0.48 g C m^{-2} d^{-1} was attained during the wet season of 2003 (Hastings et al., 2005). The mean daily carbon uptake for the Karoo sites during year 1 and year 2 were generally higher than at Baja California, with the exception of Karoo 1 during year 1, which received an annual precipitation of 352 mm and attained a mean daily carbon uptake of -0.4 g C m^{-2} d^{-1}.

Findings of mean carbon uptake for the Karoo sites and other dry and semi-arid areas during the wet season suggest that while rainfall is a major factor determining net carbon uptake it may also be crucial to look at the influence of other aspects/attributes on net carbon exchange, such as plant water strategies, water use efficiency, and land disturbance, among others. For instance, despite the Baja California desert site being drier than the Karoo sites, its mean daily carbon uptake was higher than the mean daily carbon uptake at Karoo 1 during year 1. An intercomparison of NEE at an annual time-scale between Karoo sites and other dry and semi-arid areas is presented in section 3.2.3.

GPP and R_{eco} at the Karoo sites varied seasonally, with peak values for both observed during the summer months (January to March). The dry period is generally characterized by low GPP and R_{eco}, with CO_2 efflux dominating the net carbon exchange due to activities of heterotrophs. The Karoo is also known for higher termite activity during the dry season. After rewetting of soils following the dry months, there was a sudden high imbalance between R_{eco} and GPP fluxes with high R_{eco} triggered by occurrence of rain pulses, resulting in higher R_{eco} than GPP. However, photosynthesis surpassed ecosystem respiration at the most physiologically active vegetative period in the summer. Elsewhere, at Kendall grassland, a seasonal semi-desert grassland, NEE also showed a similar seasonal pattern, with a much stronger carbon uptake and ecosystem respiration associated with wet season compared to the dry period (Scott et al., 2010).

During year 1 at Karoo 1, peak R_{eco} of 4.5 g C m^{-2} d^{-1} was attained during the vegetative functional season when water availability was adequate. Similarly, the highest GPP of 4.8 g C m^{-2} d^{-1} was reached during the vegetative functional season, while the lowest GPP values were

observed in non-vegetative periods. At Karoo 2 during year 1, R_{eco} reached a peak of 5.0 g C m^{-2} d^{-1}, and as expected, R_{eco} values reduced in the dry season due to soil moisture constraints. The highest daily GPP value in the vegetative functional season of year 1 at Karoo 2 was 4.9 g C m^{-2} d^{-1}. In general, higher R_{eco} and GPP peak values were reached at Karoo 2 compared to Karoo 1 during the vegetative functional season of year 1. In year 2 at Karoo 1, R_{eco} reached a maximum of 4.9 g C m^{-2} d^{-1} while GPP attained its peak value of 6 g C m^{-2} d^{-1} during the vegetative functional season. At Karoo 2 during year 2, R_{eco} and GPP peaks were 4.8 and 6.2 g C m^{-2} d^{-1}, respectively, during the vegetative functional season. Again, peak daily net carbon uptake increased at both Karoo sites from year 1 to year 2 as rainfall increased.

The differences in NEE, GPP and R_{eco} between Karoo 1 and Karoo 2 were relatively higher especially during the period from January to March for both Karoo sites and years. The period coincided with higher above-ground biomass due to warmer and wetter conditions conducive for maximum vegetation growth. This is also the period where Karoo 1 and 2 were behaving differently in terms of NEE progression (see Figs. 3.14 and 3.15).

3.2.3 Annual carbon budgets of Karoo 1 and Karoo 2

In this section, the annual carbon budgets (NEE) at Karoo sites are presented using both, high quality data (Flag 0 of Mauder and Foken. (2004) plus additional skewness and kurtosis) and moderate quality data (Flag 0 and 1 of (Mauder and Foken, 2004)). The selection of quality flags and filtering is crucial for getting annual carbon balances, which were calculated in order to determine the status of the two Karoo sites in terms of carbon source/sink strength. The data from Karoo 1 (gently grazed site) and Karoo 2 (rested site) for two consecutive hydro-ecological years (HEYs) (i.e., 2015/2016 and 2016/2017) and the annual NEE sums between the two Karoo sites exhibited some similarity.

Using high quality data, the NEE sum for Karoo 1 (Fig.3.12) spanned in the order of magnitude from 54 ± 72 g C m^{-2} in 2015/2016 (HEY 1) to 8 ± 86 g C m^{-2} yr^{-1} in 2016/2017 (HEY 2). For

simplicity, the term 'HEY 1' and 'HEY 2' would be referred to as year 1 and year 2, respectively. At Karoo 1, the above values give an annual NEE range of -18 to 126 g C m^{-2} yr^{-1} for year 1 and -78 to 94 g C m^{-2} yr^{-1} for year 2. The NEE sum for Karoo 2 changed from 30 $\pm$ 87 g C m^{-2} yr^{-1} in year 1 to annual NEE of -26 $\pm$ 87 g C m^{-2} yr^{-1} in year 2. This gives an annual NEE range of -57 to 117 g C m^{-2} yr^{-1} at Karoo 2 for year 1 and an annual NEE range of -113 to 61 g C m^{-2} yr^{-1} for year 2. Despite relative differences in annual NEEs between the Karoo sites for each year and between the years for each site, the annual NEEs were not significantly different after considering the uncertainties of the annual NEE estimates.

The first year of observation was drier compared to the second year which was relatively wetter. At Karoo 1, year 1 was marked by a total rainfall of 352 mm and it increased to 429 mm in year 2. Rainfall at Karoo 2 increased from 371 mm in year 1 to 406 mm in year 2. A slight increase in carbon uptake in response to an increase in precipitation was noticeable at both Karoo 1 and Karoo 2, although the change in annual NEE from year 1 to year 2 was not statistically significant as a result of an overlap of confidence intervals in the estimate of annual NEE. However, with the unpredictable nature and high inter-annual variability of precipitation in semi-arid areas of Africa, there is need to continuously monitor Karoo ecosystem's carbon budgets in response to meteorological forcings. Elsewhere, Miao et al. (2015) observed a linear increase in above-ground herbage biomass with increasing precipitation. Figure 3.12 shows the annual carbon budgets for Karoo 1 and Karoo 2 for year 1 and year 2 using high quality data.
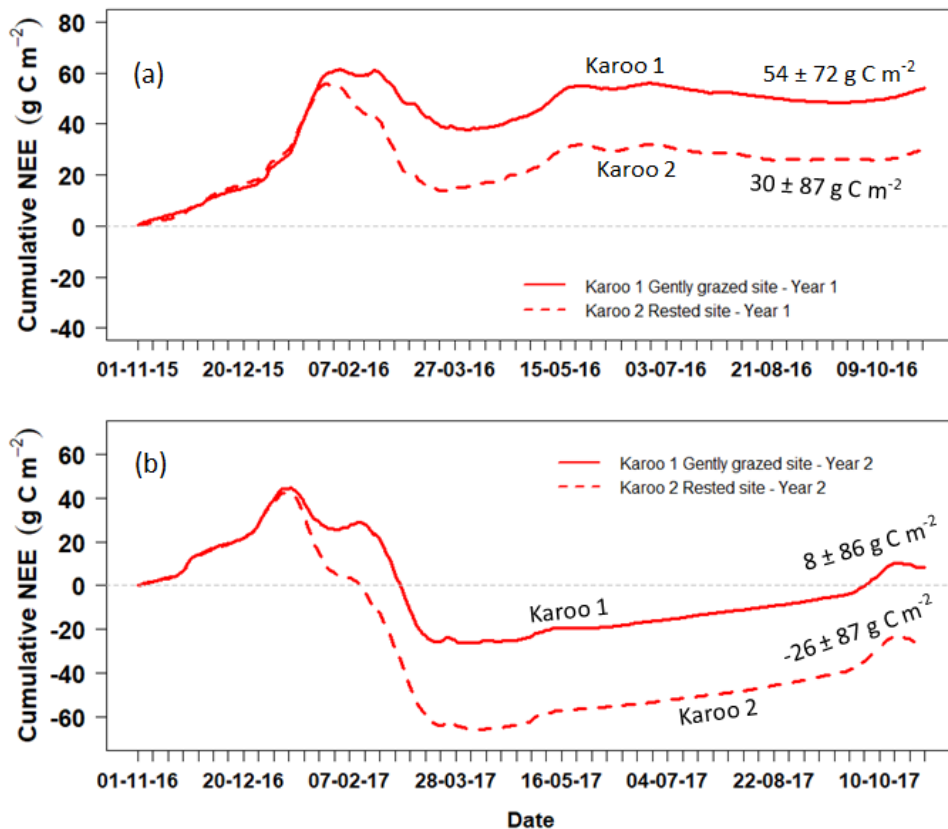
Figure 3. 12: Annual carbon budgets for Karoo 1 and Karoo 2 for (a) 2015/2016 and (b) 2016/2017 hydro-ecological years using high quality data

Site comparison between Karoo 1 and Karoo 2 showed that the livestock grazing regimes subjected to the two sites did not cause a significant difference in NEE between the sites. Notwithstanding the observed similarities in NEE between the Karoo sites for year 1 and year 2, the relative NEE differences between Karoo 1 and Karoo 2 should not be overlooked. As such, Karoo 2 sequestered relatively higher CO_2 compared to Karoo 1 for both year 1 and year 2. For instance, during year 1 the annual rainfall at Karoo 2 was 19 mm higher than the annual rainfall at Karoo 1 and carbon uptake at Karoo 2 was relatively higher than that at Karoo 1 (Fig. 3.12). However, despite the rainfall at Karoo 2 being lower than the rainfall at Karoo 1 by 23 mm during year 2, CO_2 sequestration still remained relatively higher at Karoo 2 compared to Karoo 1. Based on the findings of other comparison studies elsewhere (e.g., Ago et al., 2016), the magnitude of the differences in annual rainfall between Karoo 1 and Karoo 2 for both year 1 (19 mm) and year 2 (23 mm) is considered as small – suggesting similar meteorological conditions at Karoo 1 and Karoo 2. The possible reasons of Karoo 2 having a slightly higher carbon uptake compared to Karoo 1 include (i) livestock grazing intensity could have

73

contributed to the relative differences in annual NEE between the two Karoo sites to some extent or (ii) considering annual precipitation alone could be misleading. For instance, Guo et al. (2015) emphasized the importance of precipitation characteristics (e.g., size, interval, seasonal distribution, frequency, intensity) as sites may have similar amounts of annual precipitation but having remarkably different number of heavy precipitation events which may have an influence on annual GPP.

Further studies are needed to investigate the impact of livestock grazing intensity on CO_2 exchange at Karoo sites in order to come up with concrete conclusions. Karoo 2 was heavily overgrazed by sheep and goats in the past until 8 years ago, and the site has been gradually recovering from land degradation and dominance by small-leaved dwarf shrubs. The slightly higher carbon uptake at Karoo 2 could be an indication that resting highly degraded paddocks for a longer period may improve carbon sequestration in the semi-arid Karoo ecosystem, which is generally characterised by low recovery to disturbance. Du Toit et al. (2011) reported that a resting period of 11 months could be sufficient to restore a degraded Karoo rangeland to a state which can be ideal for livestock grazing. In a study by Seymour et al. (2010), twenty years of resting brought back the grazing potential of a Karoo rangeland although palatable plant diversity did not return.

In the grazing trials conducted in the Karoo ecosystem in 1995 and 1996, basal cover of the herbaceous layer decreased in 1995 at the heavy stocking rate of 16 small stock units per hectare (SSU/ha). Similarly, basal cover also decreased with increasing stocking rates of 4, 8 and 16 SSU/ha in 1996 (Du Toit et al., 2011). The heavy stocking rate reduced canopy cover by 53 % in 1995 (Du Toit et al., 2011). A relatively lower basal cover and canopy cover was expected at the gently grazed site (Karoo 1), stocked at 16 hectares per large stock unit (ha/LSU) (equivalent of approximately 16 hectares per 7 SSU) while a relatively higher basal and canopy cover was expected at the rested site (Karoo 2). Fixed-point photos of vegetation biomass comparison between Karoo 1 and Karoo 2 from 25.07.2016 to 23.10.2017 showed that Karoo 2, because of resting, had accrued relatively more vegetation cover compared to Karoo 1 (see Appendix 1) – hence the slight differences in annual NEE.

Using high-quality data, the total uncertainty of NEE sums (based on random and bias errors) for Karoo 1 site were 72 and 86 g C m^{-2} year^{-1} for year 1 and year 2, respectively. Total uncertainty of NEE sums for Karoo 2 was 87 g C m^{-2} year^{-1} for both year 1 and year 2, respectively. The high-quality control procedure was meant to have more reliable data than just a huge sample size although it created gaps in the range from 60 – 68 %, which was slightly higher than the expected range. Typically, after quality control, 20 – 60 % gaps are common in annual datasets (Moffat et al., 2007; Papale et al., 2006). Table 3.1 shows the uncertainty of annual NEE and data availability using high quality data control procedure (i.e., Flag 0 of (Mauder and Foken, 2004) plus additional skewness and kurtosis).

Table 3. 1: Uncertainty of annual net ecosystem CO$_2$ exchange (NEE) using high data quality control procedure

	Random Error (g C m^{-2} year^{-1})	Bias Error (g C m^{-2} yr^{-1})	Total uncertainty (g C m^{-2} yr^{-1})	% Gap
Karoo 1 (Year 1)	10 (0.2)	62	72 (62)	68
Karoo 1 (Year 2)	30 (0.3)	56	86 (56)	61
Karoo 2 (Year 1)	27 (0.3)	60	87 (60)	66
Karoo 2 (Year 2)	32 (0.4)	55	87 (55)	60

The overall uncertainty values of Karoo 1 and Karoo 2 using high quality data (Table 3.1) and moderate data quality control procedure (Table 3.2) were in the similar range from 72 to 87 g C m^{-2} year^{-1}. However, the difference was that the high quality data (flag 0 + skewness and kurtosis) led to more rejection of 'bad' data and created more gaps (> 50%) on the dataset while the moderate data quality (flag 0 and 1) reduced data gaps to less than 40 %. High quality data resulted in higher bias errors (from gap-filling) but lower random errors while moderate quality data resulted in lower bias errors but higher random errors due to inclusion of flag 1 data (see Table 3.2). Typically, high quality data (flag 0) is associated with random errors less than 20 % while moderate quality data (flag 1) is associated with random errors in the range from 15 % to 50 % (Mauder et al., 2013). The differences in annual NEE sums for the Karoo sites between using datasets from high data quality procedure and the moderate data quality procedure could

be a reflection of these differences in random errors and bias errors in the data time series. Table 3.2 shows the uncertainties of annual NEE sums using high and moderate quality data (Flag 0 and 1 of (Mauder and Foken, 2004)).

Table 3. 2: Uncertainty of annual net ecosystem CO_2 exchange (NEE) using moderate data quality control procedure

	Random Error ($\mathbf{g\ C\ m^{-2}\ yr^{-1}}$)	Bias Error ($\mathbf{g\ C\ m^{-2}\ yr^{-1}}$)	Total uncertainty ($\mathbf{g\ C\ m^{-2}\ y^{-1}}$)	% Gap
Karoo 1 (Year 1)	47	32	79	35
Karoo 1 (Year 2)	53	21	74	23
Karoo 2 (Year 1)	53	34	87	37
Karoo 2 (Year 2)	58	25	83	28

The uncertainty on annual NEE sums at the Karoo sites may increase if other additional sources of errors are included. However, compared to other studies the range of uncertainty of the annual NEE at the less productive Karoo sites, ranging from $74 - 87$ g C m^{-2} yr^{-1}, is within the expected limits for a site with a long-term mean annual rainfall of 373 mm yr^{-1}. The long-term mean annual NEE uncertainty obtained at a similar semi-arid savanna ecosystem, with a slightly higher mean annual precipitation of 550 mm yr^{-1}, was $\pm$ 105 g C m^{-2} yr^{-1} (Archibald et al., 2009). At a south-western savanna site in Burkina Faso, with a higher long-term mean annual rainfall of 926 mm, Brümmer et al. (2008) found uncertainties of annual NEE in the range of $98 - 100$ g C m^{-2} yr^{-1}.

Using the moderate data quality control procedure, NEE annual sums showed no significant differences between Karoo 1 and Karoo 2 for year 1 (Fig. 3.13a). The NEE annual sums for Karoo 1 and Karoo 2 for year 1 were 28 ± 79 g C m^{-2} yr^{-1} and 28 ± 87 g C m^{-2} yr^{-1}, respectively. In year 2, the annual NEE sums for Karoo 1 and Karoo 2 were 41 ± 74 g C m^{-2} yr^{-1} and -57 ± 83 g C m^{-2} yr^{-1}, respectively (Fig. 3.13b). However, the difference in NEE annual sums between Karoo 1 and Karoo 2 was also considered statistically insignificant using moderate quality data due to overlapping confidence intervals. It also appeared that the increase in precipitation from

year 1 to year 2 did not increase net carbon sequestration at Karoo 1 but rather increased ecosystem respiration. From the annual NEE ranges at Karoo 1 for year 1 and year 2, it can be depicted that the site was more of a carbon source. Interestingly, there was a notable increase in the carbon sink strength at Karoo 2 compared to Karoo 1 from year 1 to year 2, despite that Karoo 1 had received relatively higher rainfall than Karoo 2 during year 2, as previously mentioned. Again, the potential influence of livestock grazing intensity on carbon exchange was revealed. Usually there is a high correlation between carbon assimilation rates and annual precipitation (Merbold et al., 2009), as more rainfall supports a larger biomass. Earlier claims by Roux and Vorster. (1983) suggest that the cause of ecosystem changes in the Karoo is over-exploitation by sheep and climate related changes only enhance vegetation instability. Interestingly, Seymour et al. (2010) reported that while rainfall is the main determinant of vegetation cover in the Karoo, grazing intensity explain differences in vegetation composition. The carbon budgets using moderate data quality control procedure are shown in figure 3.13.
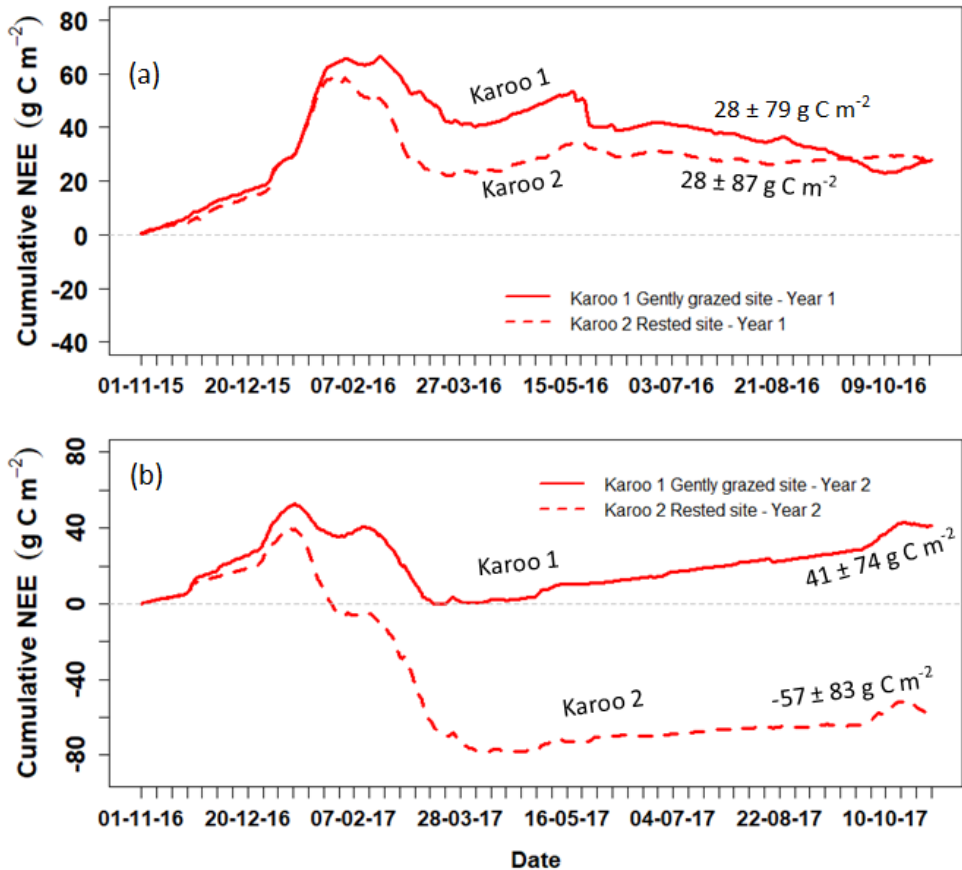
Figure 3. 13: Annual carbon budgets for Karoo 1 and Karoo 2 for (a) year 1 and (b) year 2 using moderate quality data

While gap-filled data from the high data quality control procedure (i.e., flag 0 + additional skewness and kurtosis) can be used for other purposes, flags 0 and 1 are usually used as the standard for reporting annual carbon budgets. The flags 0 and 1 of Mauder and Foken. (2004) data quality control procedure are recommended for fundamental research and long-term observation programs (Mauder et al., 2013). In that regard, the results using moderate data quality control procedure are compared with annual net carbon balance of other similar environments. There are no other studies on net carbon exchange that have been conducted in a similar Karoo ecosystem in Africa but studies on annual carbon balance in other dry and semi-arid areas of similar rainfall were used for comparison purposes.

The annual NEE of Karoo 1, being more of a carbon source for both year 1 (i.e., NEE = 28 ± 79 g C m^{-2} yr^{-1}) and year 2 (41 ± 74 g C m^{-2} yr^{-1}) can be compared to the 1999/2000 annual NEE of 12 g C m^{-2} yr^{-1} at Maun (Botswana), which had received a mean annual rainfall of 462 mm. However, the differences in annual NEE between the Karoo sites and Maun could also partly be ascribed to the differences in annual precipitation, land use and vegetation. The Karoo sites are dominated by dwarf shrubs and grasses whilst Maun is a semi-arid open savanna woodland. The net carbon uptake at Karoo 2 in year 2 (i.e., -57 ± 83 g C m^{-2} yr^{-1}) was higher than that reported at Hapex (Niger) (- 32 g C m^{-2} yr^{-1}) – a Sahelien fallow savanna which had received a mean annual rainfall of 495 mm (Hanan et al., 1998). The Karoo 2 net carbon balance for year 2 also compared to those estimated at a more drier desert shrub ecosystem in Baja California, Mexico. In 2002 and 2003, the desert site received precipitation of 147 and 197 mm, respectively, but annual carbon balance estimates were -39 and -52 g C m^{-2} yr^{-1}, respectively (Hastings et al., 2005), which is a reflection of the efficient conservative water storage mechanisms and water use strategies that plants in dry environments undertake. Therefore, magnitude of annual rainfall alone may not be adequate to explain differences in annual carbon budgets among sites but consideration of other ecosystem characteristics and functional properties may also need to be explored.

3.3 Comparing cumulative NEE and precipitation between Karoo 1 and Karoo 2

Given the nature of the hydroclimate regime of the Karoo sites (Fig 3.10), understanding the critical periods when there were site differences in NEE was an essential step in order to capture

those exciting moments when the two Karoo sites were behaving differently in relation to NEE and precipitation pattern. It was found that NEE differences between Karoo 1 and Karoo 2 mainly occurred during the (wet) vegetative functional seasons for both year 1 and year 2, otherwise the two sites were behaving in a similar manner for the rest of the periods. During year 1, site differences were observed for both NEE and precipitation as from 09.01.2016 to 03.04.2016 (approximately 86 days) while during year 2 the site difference was from 26.12.2016 to 08.04.2017 (approximately 104 days) (Fig. 3.14). Although the sites had generally similar number of precipitation events for both years (Fig. 3.10), the precipitation events were generally distributed over a relatively longer period during year 2 compared to year 1 – hence NEE site differences were also observed for a relatively longer period during year 2 (104 days) compared to year 1 (86 days). Figure 3.14 shows the differences in cumulative NEE and precipitation between Karoo 1 and Karoo 2 during year 1 and year 2.
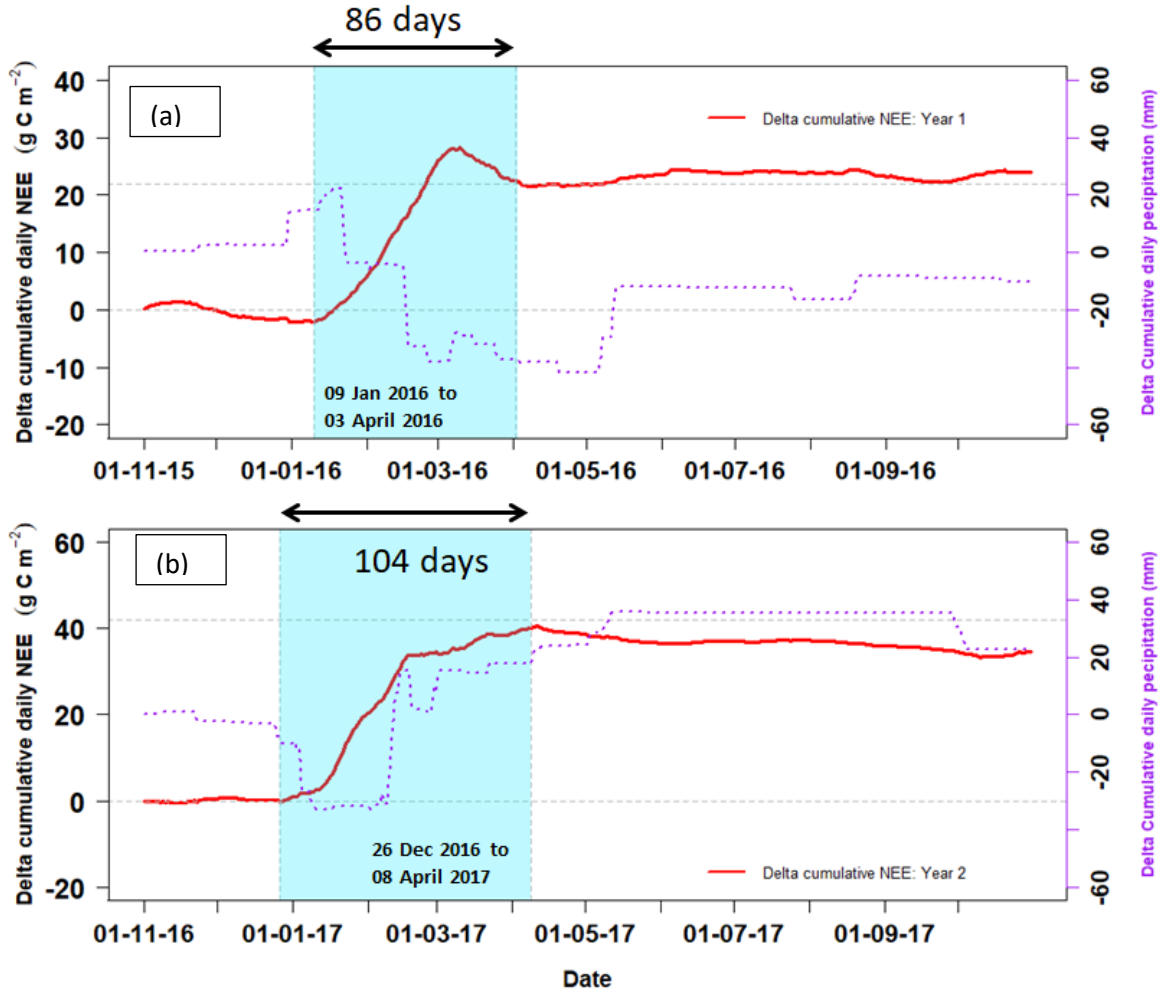
Figure 3. 14: Delta cumulative NEE and precipitation between Karoo 1 and Karoo 2 during (a) year 1 and (b) year 2, based on high quality data. NEE is net ecosystem CO_2 exchange. Delta

cumulative NEE is equal to Karoo 1 cumulative NEE minus Karoo 2 cumulative NEE., and same applies for delta cumulative precipitation.

As mentioned earlier on, Karoo 1 and Karoo 2 had generally similar meteorological conditions at the annual scale. However, by looking at differences in precipitation between Karoo 1 and Karoo 2 during the vegetative functional seasons of year 1 and year 2 and the corresponding site differences in NEE, two possible explanations can be drawn from the results on Fig. 3.14.

Firstly, sub-figure 3.14 (a) shows that when precipitation of Karoo 2 was increasing more than the precipitation of Karoo 1 (delta cumulative precipitation slope decreasing), a correspondingly higher carbon uptake was also observed at Karoo 2 compared to Karoo 1. This indicates that differences in ecosystem productivity can be linked to slight differences in precipitation characteristics (e.g., precipitation size, intensity, distribution, e.t.c.).

Secondly, sub-figure 3.14 (b) shows that even when Karoo 1 precipitation was increasing more than the precipitation of Karoo 2 (delta cumulative precipitation slope increasing), Karoo 2 still showed a correspondingly higher carbon uptake compared to Karoo 1, suggesting that the role of other factors, including livestock grazing intensity, influenced carbon exchange at the Karoo sites.

Using moderate quality data (Fig. 3.15), Karoo 1 and Karoo 2 also behaved differently in terms of NEE especially during the (wet) vegetative functional seasons of year 1 and year 2 and the two sites generally behaved similarly during the rest of the period. Site differences in precipitation were also observed, especially during the vegetative functional seasons. Nevertheless, unlike when high-quality data was used (Fig. 3.14), a slightly different pattern of delta NEE was observed during year 1 from around 07 May 2016 until 31 October 2016 when moderate quality data was used (Fig. 3.15). Using high quality data, the two Karoo sites generally behaved similarly in terms of NEE after the vegetative functional season of year 1 despite the observed incidences of precipitation differences between Karoo 1 and Karoo 2 such

as that from 7 to 12 May 2016. Figure 3.15 shows delta cumulative NEE and delta cumulative precipitation between Karoo 1 and Karoo 2 during year 1 and year 2.
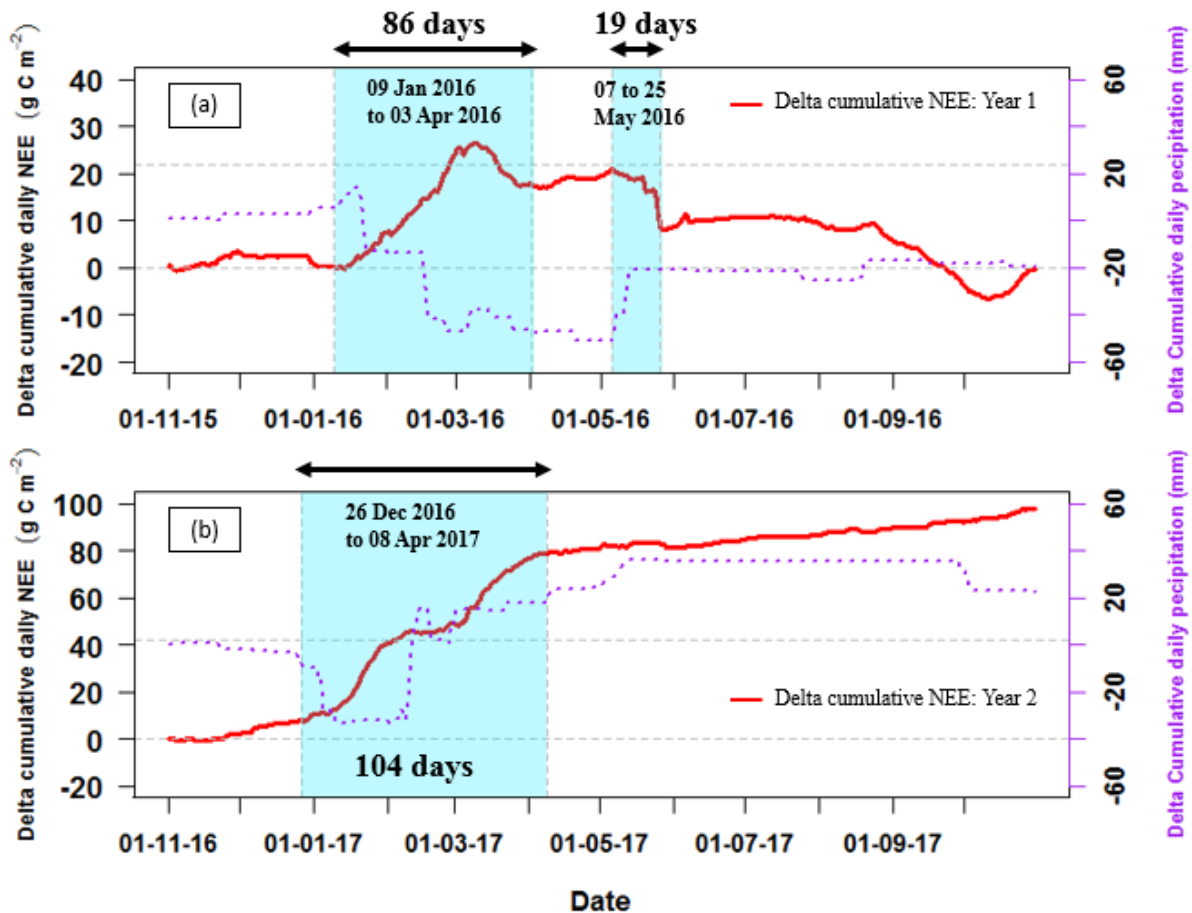
Figure 3. 15: Delta cumulative NEE and precipitation between Karoo 1 and Karoo 2 during (a) year 1 and (b) year 2 using moderate quality data. NEE is net ecosystem CO_2 exchange. Delta cumulative NEE is equal to Karoo 1 cumulative NEE minus Karoo 2 cumulative NEE., and same applies for delta cumulative precipitation.

Despite the noticeable deviation in delta NEE after 07 May 2016 during year 1 using moderate quality data (Fig. 3.15a), both high and moderate quality data generally showed similar steeper slopes in delta NEE during the vegetative functional seasons of year 1 and year 2 showing that Karoo 1 and Karoo 2 behaved differently in terms of NEE mainly during the wet period when differences in precipitation characteristics between the two sites were more pronounced. In that regard, the vegetative functional period was also quite crucial in examining the factors that influence this different behaviour between Karoo 1 and Karoo 2. The deviation in delta NEE after 25 May 2016 (year 1) using moderate quality data (Fig. 3.15a), which was slightly

81

different from the delta NEE pattern observed for the same period using high quality data (Fig. 3.14), could be ascribed to the differences in the two datasets as a result of the different data quality procedures undertaken, apart from other possible factors mentioned earlier on.

3.4 Aspects influencing temporal dynamics of carbon exchange at Karoo sites

3.4.1 Livestock grazing intensity

The effects of livestock grazing intensity on carbon exchange were clearly shown in this study. The results showed no significant differences in annual NEE sums between the two grazing treatments at Karoo. Still, the small relative differences in NEE between the gently grazed site (Karoo 1) and the rested site (Karoo 2) indicated that livestock grazing has the potential to influence land-atmosphere carbon exchange components as evidenced by the rested site sequestering relatively more CO_2 than the gently grazed sited at the annual scale. In order to disentangle the effects of livestock grazing intensity on NEE, other possible drivers of ecosystem change such as precipitation and vegetation greenness metrics (NDVI and EVI) (section 3.4.2), and the temporal variation of EWUE (section 3.7) were also further explored and discussed.

3.4.2 Vegetation greenness

Apart from water, other factors that can also exert direct effect on GPP include leaf area and greenness of vegetation (Archibald et al., 2009; Baldocchi et al., 2016; Hashimoto et al., 2012; Jin et al., 2013; Pan et al., 2015; Sjöström et al., 2009). Jin et al. (2013) and Hashimoto et al. (2012) found a strong NDVI and EVI dependency of GPP. In modelling GPP, Archibald et al. (2009) found green leaf material to be the most important predictor. Sjöström et al. (2009) reported a linear relationship between EVI/NDVI and GPP. In the grazing context, Blanco et al. (2008) found that grazing may affect NDVI differently for different sites and in a high rainfall humid subtropical system, Junges et al. (2016) observed that vegetation indices may differentiate moderate grazing intensity from low and high grazing intensities under normal hydro-climatic conditions.

82

NDVI and EVI values were MODIS products derived for successive day 16 periods during the period from (09.01.2016 to 06.04.2016) and (26.12.2016 to 08.04.2017) for year 1 and year 2, respectively. The GPP/R_{eco} values were sums over 3 days – including a day before, during and a day after the EVI and NDVI measurement. Delta_GPP, Delta_R_{eco}, Delta_NDVI and Delta_EVI were the differences in GPP, R_{eco}, NDVI and EVI between Karoo 1 and Karoo 2.

A comparison of EVI and NDVI between Karoo 1 and Karoo 2 during the vegetative functional seasons was performed in order to ascertain the impact of livestock grazing intensity on the greenness indices. The NDVI values during year 1 were in the ranges; (0.3 - 0.4) and (0.3 – 0.6) for Karoo 1 and Karoo 2, respectively. The NDVI ranges in this study were similar to those of a temperate forest (0.2 – 0.5) reported by Pettorelli (2013). EVI values were around 0.2 and (0.2 – 0.4) for Karoo 1 and Karoo 2, respectively. In general, the temporal variability patterns of NDVI and EVI over the vegetative functional seasons were similar, the only difference being that EVI values were smaller than the NDVIs.

GPP and R_{eco} differences between Karoo 1 and Karoo 2 (i.e., delta_GPP and delta_R_{eco}, Figs 3.16 and 3.17) were relatively higher for measurement periods (01 - 03.02.2016) and (17 - 19.02.2016) compared to the rest of the periods - with Karoo 2 having higher GPP and R_{eco} than Karoo 1. The GPP/R_{eco} values were 3-day GPP/R_{eco} sums, including GPP/R_{eco} values of a day before, during and a day after the EVI / NDVI measurement. These periods of distinct GPP and R_{eco} differences also coincided with relatively higher differences in NDVI and EVI between the two sites, based on NDVI and EVI measurements on 02.02.2016 and 18.02.2016 – with Karoo 2 having higher NDVI and EVI than Karoo 1. Higher values of GPP and R_{eco} were associated with higher values of NDVI and EVI.

The high precipitation (> 49 mm over 16 days) received during the periods (18.01.2016 to 02.02.2016) and (03.02.2016 to 18.02.2016) contributed to higher NDVI and EVI differences between Karoo 1 and Karoo 2. NDVI and EVI measurements were done on 02.02.2016 and 18.02.2016. For the other periods with lower precipitation (< 49 mm over 16 days), differences in NDV, EVI and GPP between Karoo 1 and Karoo 2 were lower. Figures 3.16 shows a comparison of EVI, NDVI and GPP between Karoo 1 and Karoo 2 during the vegetative functional seasons of year 1.

Figure 3. 16: Comparison of EVI, NDVI and GPP between Karoo 1 and Karoo 2 for vegetative functional season of year 1. EVI is enhanced vegetation index, NDVI is normalized difference vegetation index and GPP is gross primary production. Delta_EVI is equal to Karoo 1 EVI minus Karoo 2 EVI. Delta_NDVI is equal to Karoo 1 NDVI minus Karoo 2 NDVI. Delta_GPP is equal to Karoo 1 GPP minus Karoo 2 GPP.

Figures 3.17 shows a comparison of EVI, NDVI and R_{eco} between Karoo 1 and Karoo 2 during the vegetative functional seasons of year 1.
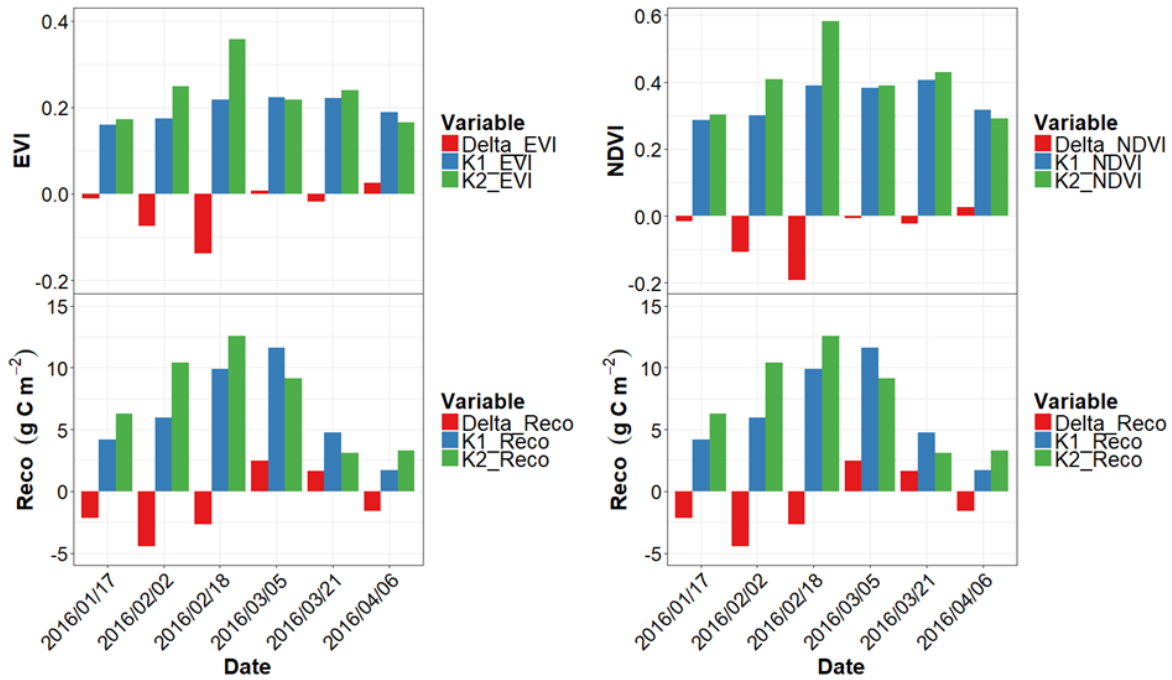
Figure 3. 17: Comparison of EVI, NDVI and R_{eco} between Karoo 1 and Karoo 2 for vegetative functional season of year 1. EVI is enhanced vegetation index, NDVI is normalized difference vegetation index and R_{eco} is ecosystem respiration. Delta_EVI is equal to Karoo 1 EVI minus Karoo 2 EVI. Delta_NDVI is equal to Karoo 1 NDVI minus Karoo 2 NDVI. Delta_R_{eco} is equal to Karoo 1 R_{eco} minus Karoo 2 R_{eco}.

The EVI and NDVI of Karoo 1 and Karoo 2 showed no significant differences either on year 1 or year 2 (Welch's two sample t-test significant levels, $P > 0.05$). Similarly, GPP also showed no significant differences ($P > 0.05$) between the two Karoo sites over the measurement periods (Figures 3.17; 3.18; 3.19).
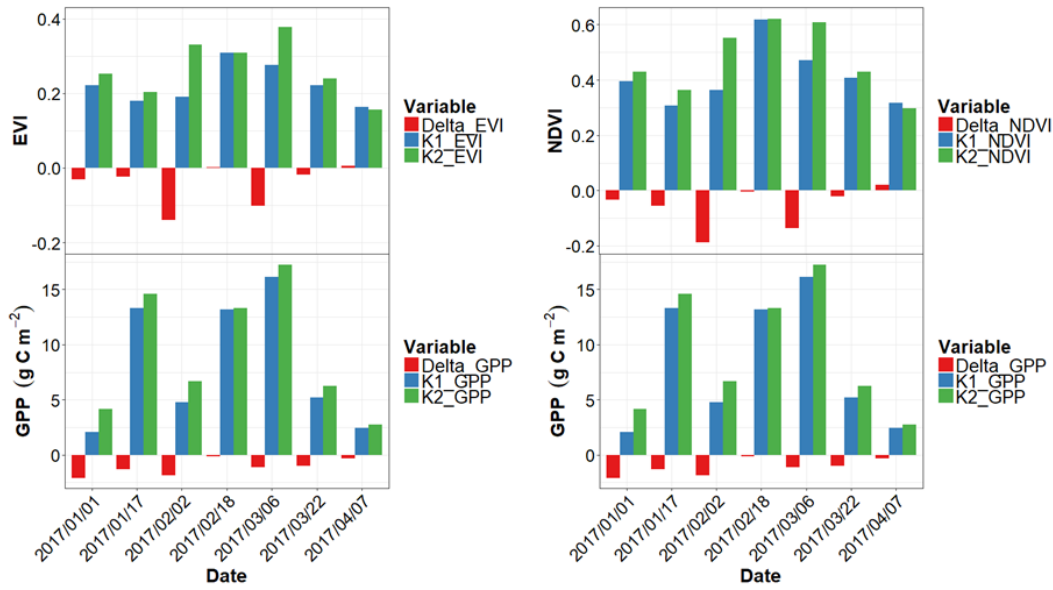
Figure 3. 18: Comparison of EVI, NDVI and GPP between Karoo 1 and Karoo 2 for vegetative functional season of year 2. EVI is enhanced vegetation index, NDVI is normalized difference vegetation index and GPP is gross primary production. Delta_EVI is equal to Karoo 1 EVI minus Karoo 2 EVI. Delta_NDVI is equal to Karoo 1 NDVI minus Karoo 2 NDVI. Delta_GPP is equal to Karoo 1 GPP minus Karoo 2 GPP.
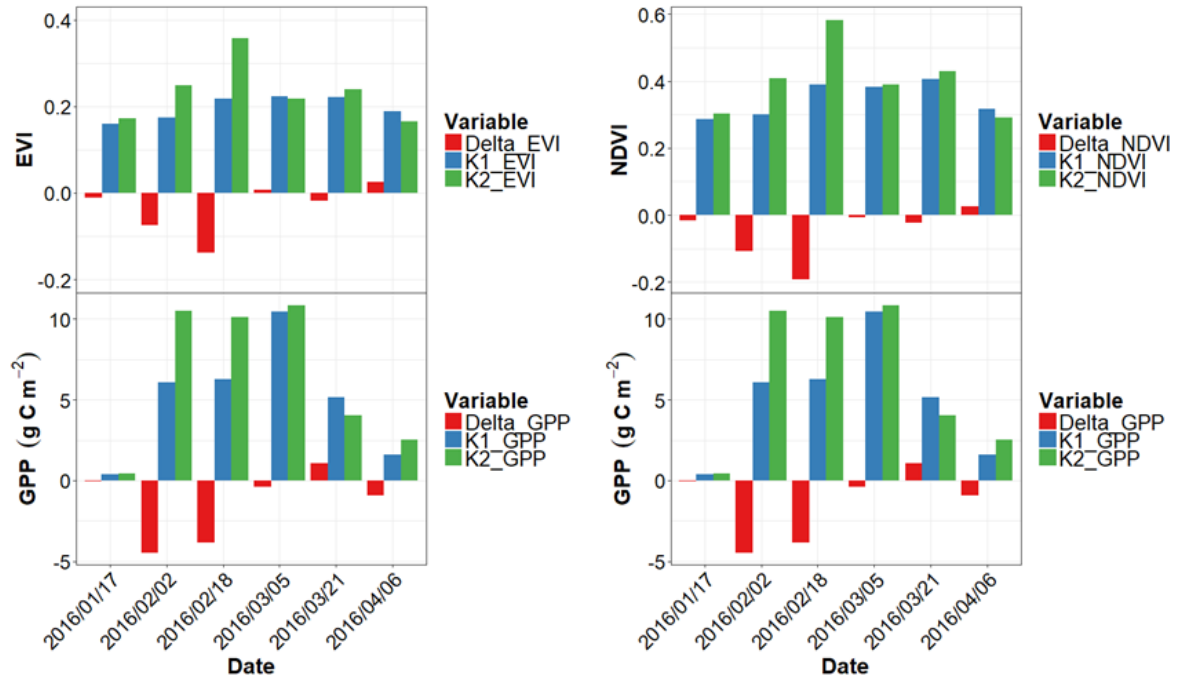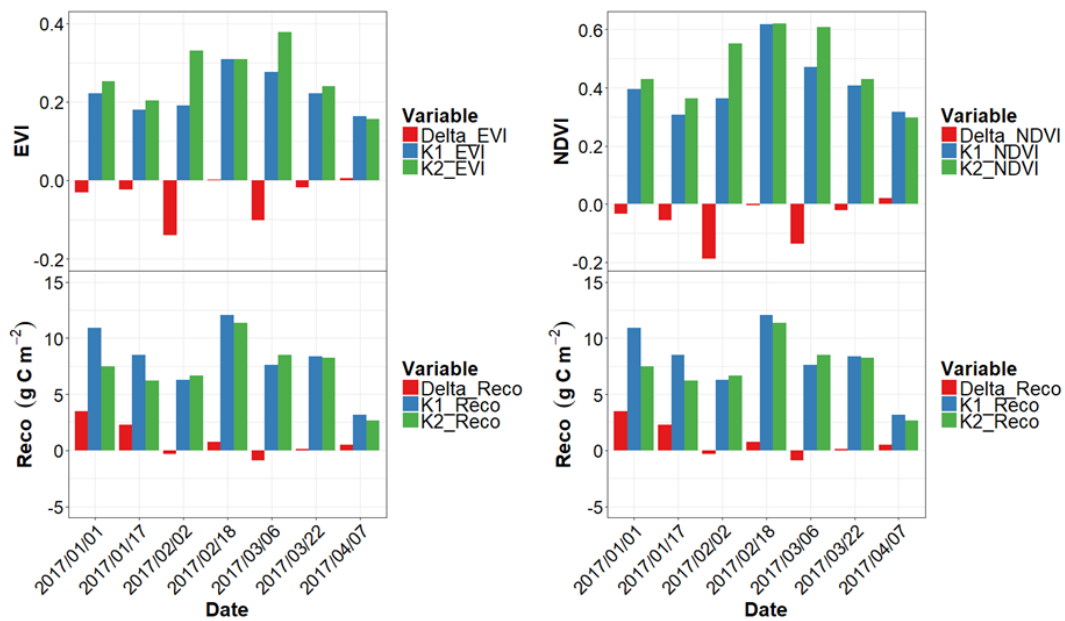

Figure 3. 19: Comparison of EVI, NDVI and R_{eco} between Karoo 1 and Karoo 2 for vegetative functional season of year 2. EVI is enhanced vegetation index, NDVI is normalized difference vegetation index and R_{eco} is ecosystem respiration. Delta_EVI is equal to Karoo 1 EVI minus

Karoo 2 EVI. Delta_NDVI is equal to Karoo 1 NDVI minus Karoo 2 NDVI. Delta_R_{eco} is equal to Karoo 1 R_{eco} minus Karoo 2 R_{eco}.

In general, the changes in NDVI and EVI did not consistently correspond to the changes in GPP and R_{eco}. Although the temporal changes in vegetation greenness did not seem to differ significantly between the two Karoo sites, the rested site seemed to have slightly higher vegetation cover compared to the gently grazed site (see Figures 3.16 and 3.18; Appendix 1). This is consistent with the fact that the rested site sequestered slightly more CO_2 compared to the gently grazed site, although the difference was not significant between the two Karoo sites. Thus, vegetation greenness metrics are yet to fully demonstrate their ability to detect even small vegetation changes brought by variation in livestock grazing intensity in the dry Karoo ecosystem.

In arid and semi-arid rangelands of Iran, Jafari et al. (2016) found stronger predictions of vegetation cover and rangeland condition by NDVI and EVI. Using FLUXNET La Thuile datasets, Verma et al. (2014) reported that 40 – 60% of interannual variability of annual GPP in dry biomes were explained by remotely sensed vegetation greenness metrics. Vicca et al. (2016) observed that while NDVI can generally detect changes in vegetation greening, it may fail to reflect decreases in plant activity caused by dry conditions. Junges et al. (2016) found no NDVI and EVI differences among sites with low, moderate and high grazing intensities during drought years while Bajgain et al. (2015) reported smaller variations of NDVI and EVI under dry conditions.

In this study, neither the impact of grazing nor the difference in rainfall between the two measurement years were reflected as differences in NDVI and EVI between Karoo 1 and Karoo 2. Since the remotely sensed MODIS products (NDVI and EVI) may not detect small changes in vegetation greenness under the typical dry climatic conditions of the Karoo system, additional field measurements and observations are needed. In that case, inferences regarding the temporal patterns of NDVI and EVI at the Karoo sites at this stage should be made with caution.

3.4.2.1 Long-term time series of EVI and NDVI at Karoo 1 and Karoo 2

There were no significant differences in NDVI and EVI between Karoo 1 and Karoo 2 for the observed short periods in the vegetative seasons of year 1 and year 2. However, Welch Two Sample T-Test showed significant site differences in NDVI and EVI ($P < 0.05$) between the two sites using long-term datasets. Long-term EVI means for Karoo 1 and Karoo 2 were 0.14 and 0.17, respectively. The long-term NDVI mean for Karoo 1 was 0.28 while that for Karoo 2 was 0.31. Figure 3.20 shows EVI and NDVI time series using annual means from 2000 to 2017 for Karoo 1 and Karoo 2.
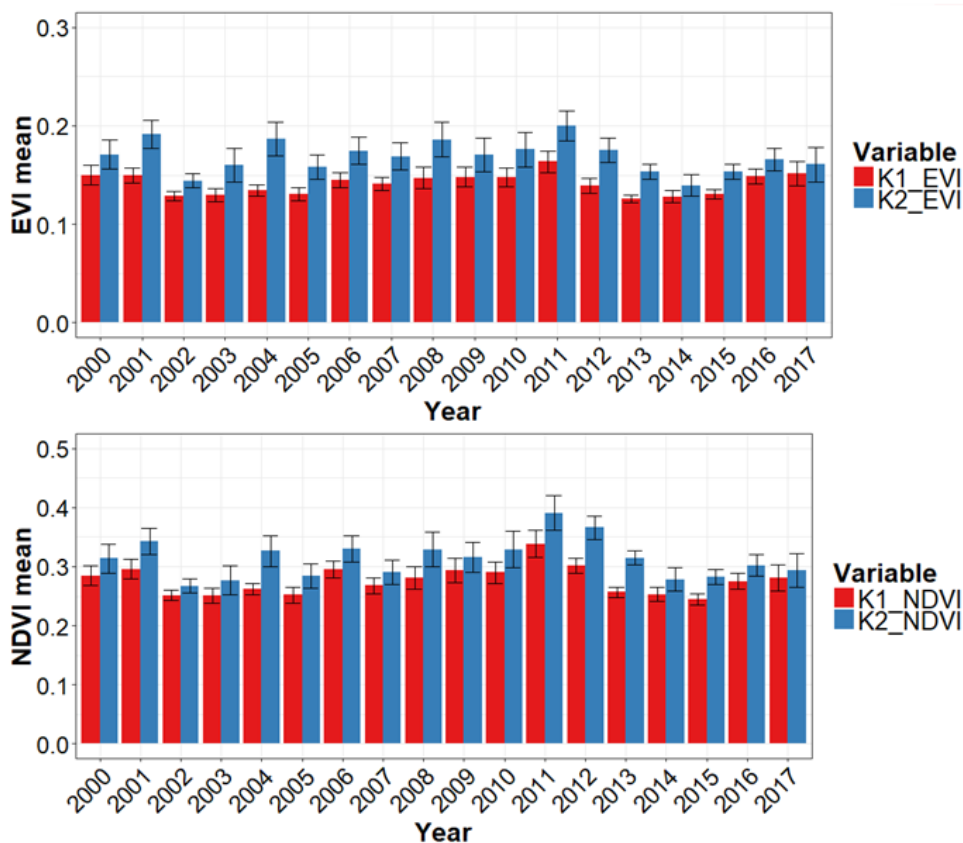
Figure 3. 20: EVI and NDVI time series from 2000 to 2017 (Annual means ± standard error) at Karoo 1 and Karoo 2. EVI is enhanced vegetation index and NDVI is normalized difference vegetation index.

Using January – April (vegetative season) NDVI and EVI means over the period from 2000 – 2017, Welch Two Sample t-tests showed that there were also significant site differences in

NDVI and EVI (P < 0.05) between Karoo 1 and Karoo 2. Similarly, EVI and NDVI showed significant differences (P < 0.05) between the Karoo sites. The long-term EVI means for Karoo 1 and Karoo 2 were 0.18 and 0.22, respectively, while the long-term NDVI means for Karoo 1 and Karoo 2 were 0.34 and 0.41, respectively. Figure 3.21 shows EVI and NDVI time series (using January to April means) from 2000 to 2017 for Karoo 1 and Karoo 2.
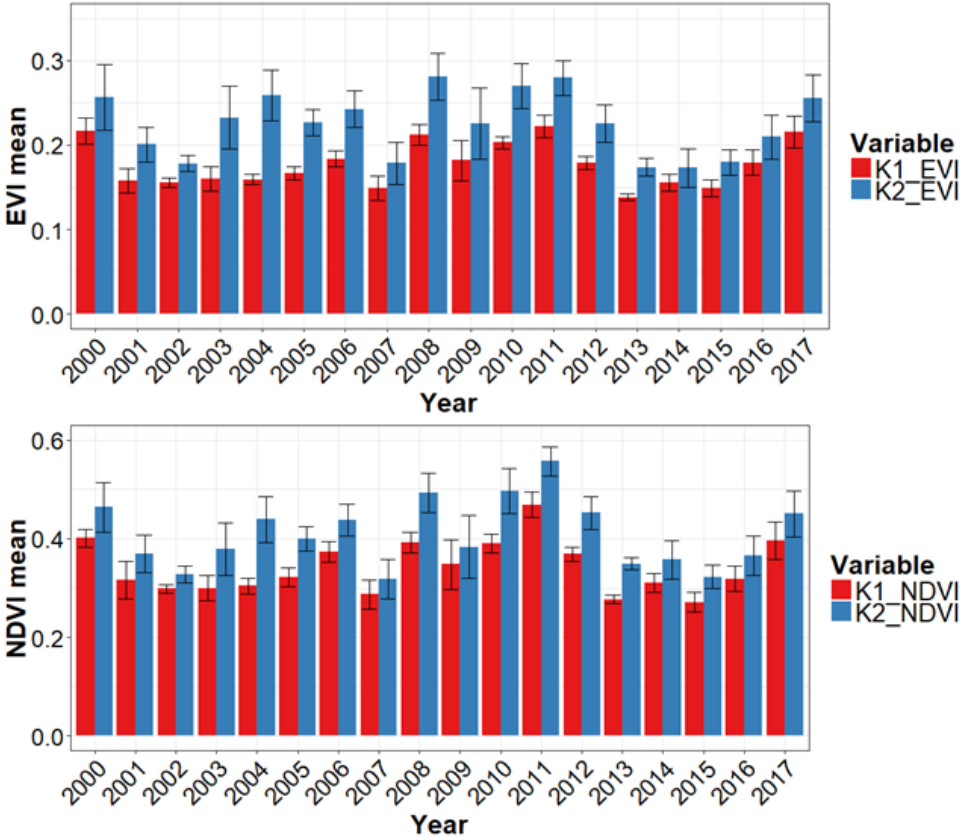
Figure 3. 21: EVI and NDVI time series from 2000 to 2017 (January – April means ± SE) at Karoo 1 and Karoo 2. EVI is enhanced vegetation index and NDVI is normalized difference vegetation index.

It appeared that site differences in NDVI and EVI between Karoo 1 and Karoo 2 were reflected when long-term NDVI and EVI averages (i.e., annual and; January to April means) were used compared to when NDVI and EVI values of vegetative functional seasons of the measurement period in this study. Long-term averaging of vegetation greenness metrics seemed to reflect the long-term changes in vegetation growth and cover well. Verma et al. (2014) found remotely

sensed MODIS vegetation metrics appropriate in explaining inter-annual variability of annual GPP.

3.5 Connection between precipitation, carbon dynamics and vegetative functional seasons at Karoo and Skukuza sites

Data from the high-quality control procedure was used in this section to establish the connection between water (precipitation and SWB) and NEE in determining the onset and end of vegetative functional seasons. The timing of growing season is one of the important seasonal rainfall metrics that is critical and decisive for favorable vegetation growth (Zhang et al., 2018). A strong coupling between carbon dynamics and water has been observed in arid and semi-arid ecosystems (Ago et al., 2016; Archibald et al., 2009; Kutsch et al., 2008; Merbold et al., 2009; Parton et al., 2012; Reichstein et al., 2005; Thomas et al., 2009; Verduzco et al., 2015). For instance, in Asia, Chen et al. (2013) observed a sigmoidal relationship between GPP and mean annual precipitation. In Sub-Saharan Africa, Merbold et al. (2009) found an exponential relationship between maximum canopy photosynthesis and mean annual precipitation.

This study tracked the temporal response of NEE in the Karoo ecosystem and linked it to the temporal dynamics of precipitation and SWB on a seasonal scale. For instance, the onset of rains, before the greening up of vegetation, was characterized by isolated and sporadic rain pulses which enhanced the CO_2 efflux. Rain pulse events that occurred in consecutive days or were separated by one or two days were combined together and considered as one rain pulse event; the maximum consecutive rain pulse events combined were 3, occurring within a period of 5 days. Even when such incidences resulted in relatively larger rain pulse sizes compared to individual rain pulses, they were still considered as dry periods because in-between all isolated rain pulse events there were long dry-days (> 7 days) which were basically drying up the soil through ET. For instance, after the rains of 02.12.2015 (i.e., 5.7 mm) at Karoo 1 there was no rain until 31.12.2015. The site received a total of 12.3 mm from precipitation events of 31.12.2015 (11.4 mm) and 01.01.2016 (0.9 mm) but it was followed by 9 dry days until the rain on 11.01.2016. Rain pulse sizes at Karoo 1 and Karoo 2 during these periods are presented in section 3.6.

To summarize the important periods shown on Fig. 3.22 and other similar plots (e.g., Figs 3.23 – 3.27), the dry phase was the dormancy period while the dry + isolated rain pulses phase was also part of the dry season but characterized by rain pulses at the early stages of the rainfall season. The dry-wet transition phase (a) shows a period of shift from dry to wet period as rainfall increased and became regular. At this stage, despite rainfall having increased during this period, ecosystem respiration was still dominating the NEE. The wetting phase (b) occurred when increased plant available water resulted in pronounced vegetation growth and greening, with CO_2 assimilation starting to increase as the carbon sink developed. The wet phase (c), was the period when the carbon sink had become much stronger as wet conditions increased, coupled with a further increase in vegetation growth and greenness.

At Karoo 1 during the 2015/2016 hydro-ecological year, the lag time for photosynthesis to start dominating the net carbon balance since the onset of productive rains was 13 days. Karoo 1 begun to receive rainfall at regular intervals (at least after every 1 – 2 days, i.e., with no dry-days > 7 days in-between precipitation events) from 11.01.2016, and the onset of the vegetative functional season was reached on 24.01.2016. During the dry-wet transition phase, rain pulse sizes comprised largely of intense precipitation events > 10 mm d^{-1}, which highly contributed to the resumption of vegetation growth and greening up. The peak NEE that was reached during the dry-wet transition phase until the onset of the vegetative functional season was 2.7 g C m^{-2} day^{-1}. Figure 3.22 shows the connection between the temporal dynamics of precipitation, SWB and carbon fluxes at Karoo 1 during the 2015/2016 hydro-ecological year, which had a total precipitation of 352 mm.

Figure 3. 22: Connectivity among precipitation, surface water balance and carbon fluxes in explaining the vegetative functional season at Karoo 1 during 2015/2016 hydro-ecological year. Cum = cumulative and SWB = surface water balance.

A precipitation threshold of 132 mm, received during the period from 11.01.2016 to 24.01.2016 (i.e., dry-wet transition, phase a), triggered the gently grazed site (Karoo 1) to reach the onset of vegetative functional season, described as the change point when NEE begun to transition towards a net carbon sink. At the change point, GPP begins to gradually take over and dominates the net carbon balance (see wetting phase b, Fig. 3.22). During the wetting phase (b), it took about 11 days (i.e., from 24.01.2016 to 04.02.2016) from the change point of NEE transitioning towards a net carbon sink to the point when NEE became neutral or negative (i.e., NEE ≤ 0 g C m^{-2} d^{-1}). Thus, at Karoo 1 during year 1, the total number of days from the onset

of productive rains (i.e., 11.01.2016) to the onset of vegetative functional season (i.e., 24.01.2016) was 13 days, while it took 24 days from the onset of productive rains to the point when the ecosystem changed from a net carbon source to a net carbon sink.

In semi-arid Sudan, in the Sahel region of Africa, it took approximately 30 days from the onset of significant rains for the system to turn from a carbon source to a carbon sink (Ardö et al., 2008). Towards the end of the growing season, number of dry days were systematically increasing and limiting photosynthesis. Zhang et al. (2018) observed that productivity is significantly affected after above 14 consecutive dry days. The end of the vegetative functional season at Karoo 1 was around 03.04.2016, giving a growing season length of about 71 days (i.e., from 24.01.2016 to 03.04.2016).

The small carbon uptake that was observed following the end of the vegetative functional season was in response to sporadic rainfall events that occurred thereafter, with some of them exceeding 5 mm per day. Du Toit (2010) noted that a rainfall event that exceeds 5 mm per single day can be considered as 'effective' and likely to infiltrate the soil and be available to the plants. It is also unsurprising that even when most of the herbaceous vegetation quickly dried out by the end of the growing season, some limited photosynthesis may still occur from dwarf shrubs that would still be green but gradually drying up in the forthcoming days. Ecosystem respiration from heterotrophs dominated during the dry season while photosynthesis took over during the wet season. At Karoo 1 during year 1, the cumulative growing season NEE was $= -18$ g C m^{-2} d^{-1} while the dry season cumulative NEE was 72 g C m^{-2} d^{-1}.

In addition to linking the temporal dynamics of precipitation and carbon fluxes, SWB connectivity with carbon fluxes was also examined between the gently grazed site and the rested site, as rainfall alone could be a poor indicator of water availability to plants (Scholes et al., 2004). Nevertheless, precipitation is frequently used as a proxy for water availability while SWB is used to account for water losses through ET, runoff and drainage losses (Biederman et al., 2016). Taking into account ET losses in drier ecosystems is crucial as evaporation dominates water balance during dry years (Everson, 2001). Since grazing may have a direct impact on the controls of SWB, such as vegetation cover and leaf area index (Asner et al., 2004), it was important to also consider SWB in explaining the temporal dynamics of NEE, GPP and R$_{eco}$ along the grazing intensity gradient.

At Karoo 1 during the 2015/2016 HEY, from the onset of productive rains to the onset of the vegetative functional season, SWB was about 103 mm. At the end of the growing season, as water availability got depleted, there was quicker cessation of physiological activity than ecosystem respiration, with vegetation drying out and leaves falling down. However, cumulative SWB still showed a positive value at the end of the vegetative functional season, suggesting that more research may be needed in the Karoo ecosystem to further explore on plant-water relations and mechanisms that the plants employ to conserve water. For that reason, SWB could not be used to determine the end of the growing season, but rather the initial approach that was applied at the Skukuza site was used, where the growing season end was determined based on transition from a net carbon uptake to a net carbon loss, according to Law et al. (2002).

At Karoo 2 (rested site) during 2015/2016, the dry-wet transition period (phase a) was 8 days (from 11 – 19.01.2016) compared to 13 days (from 11 – 24.01.2016) at Karoo 1 (gently grazed site). The amount of precipitation that triggered the ecosystem to reach the onset of the vegetative functional season at Karoo 2 was 60.6 mm while at Karoo 1 it was 132 mm. The overall annual difference in total precipitation between the two Karoo sites during the 2015/2016 HEY was 19 mm. Karoo 2 and Karoo 1 had total annual precipitation of 371 mm and 352 mm, respectively. Although the rainfall means between the two sites were similar, the observed differences in growing season precipitation thresholds required to trigger the onset of vegetative functional season indicate that future studies are required to explore site differences in terms of rainfall characteristics and how the vegetation responds to precipitation in the Karoo. Rainfall characteristics include size of rain pulses, frequency of rainfall occurrence, distribution of precipitation events, among others. Figure 3.23 shows the connectivity among precipitation, SWB and carbon fluxes in explaining vegetative functional season at Karoo 2 during the 2015/2016 HEY.

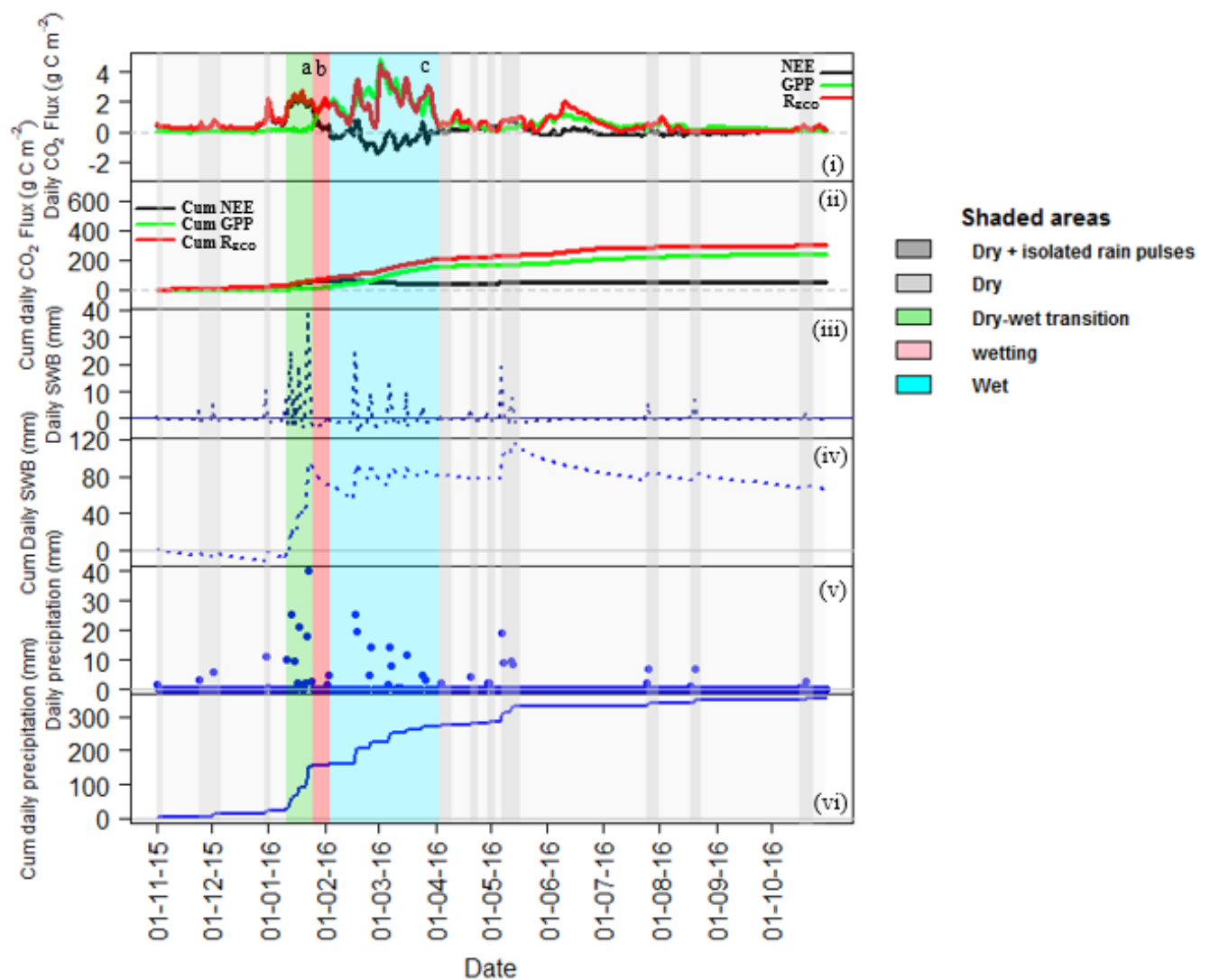Figure 3. 23: Connectivity among precipitation, surface water balance and carbon fluxes in explaining vegetative functional season at Karoo 2 during 2015/2016 hydro-ecological year. Cum = cumulative and SWB = surface water balance.

At Karoo 2 it had rained on 31.12.2015 (9 mm) and 01.01.2016 (0.6 mm), which is a total precipitation of 9.6 mm, after a long dry spell of about 23 days, after which, there was no rain until the onset date of productive rains on 11.01.2016. The 8-day period during the dry-wet transition period at Karoo 2 (from 11 – 19.01.2019) was the lag time of delayed photosynthesis since the onset of productive rains. Usually, leaf material development is enhanced as precipitation increases and becomes more regular. At the Skukuza site, Archibald et al. (2009) reported a lag time of 5–7 days after a wetting event for photosynthesis to reach its maximum, depending on the leaf material present.

At Karoo 2, it took 10 days (19 - 29.01.2016) from the change point of NEE transitioning towards a net carbon sink to the actual point when NEE became neutral or negative (i.e., NEE ≤ 0 g C m^{-2} d^{-1}) – compared to 11 days at Karoo 1. The total number of days from the onset of productive rains to the point when Karoo 2 became a carbon sink was 18 days (compared to 24 days at Karoo 1). The length of the growing season at Karoo 2 was 76 days (19.01.2016 to 03.04.2016) – compared to 71 days at Karoo 1 (24.01.2016 to 03.04.2016).

The findings of 2015/2016 HEY showed that Karoo 2 (rested site) was triggered by relatively lower amount of productive rainfall to reach the onset of the vegetative functional season compared to Karoo 1 (gently grazed site). Karoo 2 also became a net carbon sink earlier than Karoo 1 during the early stages of the vegetative functional season and its growing season length was longer by 5 days. At Karoo 2, cumulative NEE during the wet season of year 1 was - 30 g C m^{-2} d^{-1} while the cumulative NEE during the dry season was 60 g C m^{-2} d^{-1}, using high quality data.

At Karoo 2, SWB from the onset of productive rains to the onset of the vegetative functional season was approximately 42.2 mm (compared to 103 mm at Karoo 1) due to the shorter dry-wet transition phase at Karoo 2 compared to Karoo 1. Like at Karoo 1, cumulative SWB also showed a positive value at the end of the vegetative functional season of 2015/2016 HEY, suggesting that the mechanisms that the plants employ to conserve water between the two Karoo sites could be similar.

In the second year, the onset of the vegetative functional season at Karoo 1 was reached on 29.12.2016. The amount of precipitation that was required to reach the onset of the active vegetative season was 33.9 mm, and it comprised of only two major rainfall events of 26.12.2016 (10.2 mm) and 28.12.2016 (23.7 mm). The lag time for photosynthesis to resume was only 4 days since the onset of productive rains, which was even shorter than the time lags observed in other semi-arid areas (e.g., Archibald et al., 2009). This also further emphasizes the importance of precipitation characteristics in determining the onset of the vegetative functional season. For instance, Guo et al. (2015) reported that heavy precipitation events (> 10 mm d^{-1}) recharged deeper soils and increased gross primary production in a temperate steppe. In the

Sahel and northern Sudanian region, a rainfall intensity of ~ 13 mm day^{-1} was found optimum for quick accumulation of above-ground net primary production (Zhang et al., 2018).

Prior to the onset of productive rains on 26.12.2016, the Karoo 1 (gently grazed site) had experienced a very long dry spell of about 32 dry-days since the precipitation event of 23.11.2016, which was about 16.8 mm. From the onset of the vegetative functional season to the point when NEE reached neutral or negative (i.e., NEE $\leq$ 0 g C m^{-2} d^{-1}), it took about 12 days (i.e., from 29.12.2016 to 10.01.2017). The vegetative functional season at Karoo 1 for year 2 was from 29.12.2016 to 18.04.2017 resulting in a growing season length of about 111 days, which was longer than the growing season lengths of Karoo 1 and Karoo 2 during the first year. Figure 3.24 shows the connectivity among precipitation, SWB and carbon fluxes in explaining vegetative functional season at Karoo 1 during the 2016/2017 HEY.
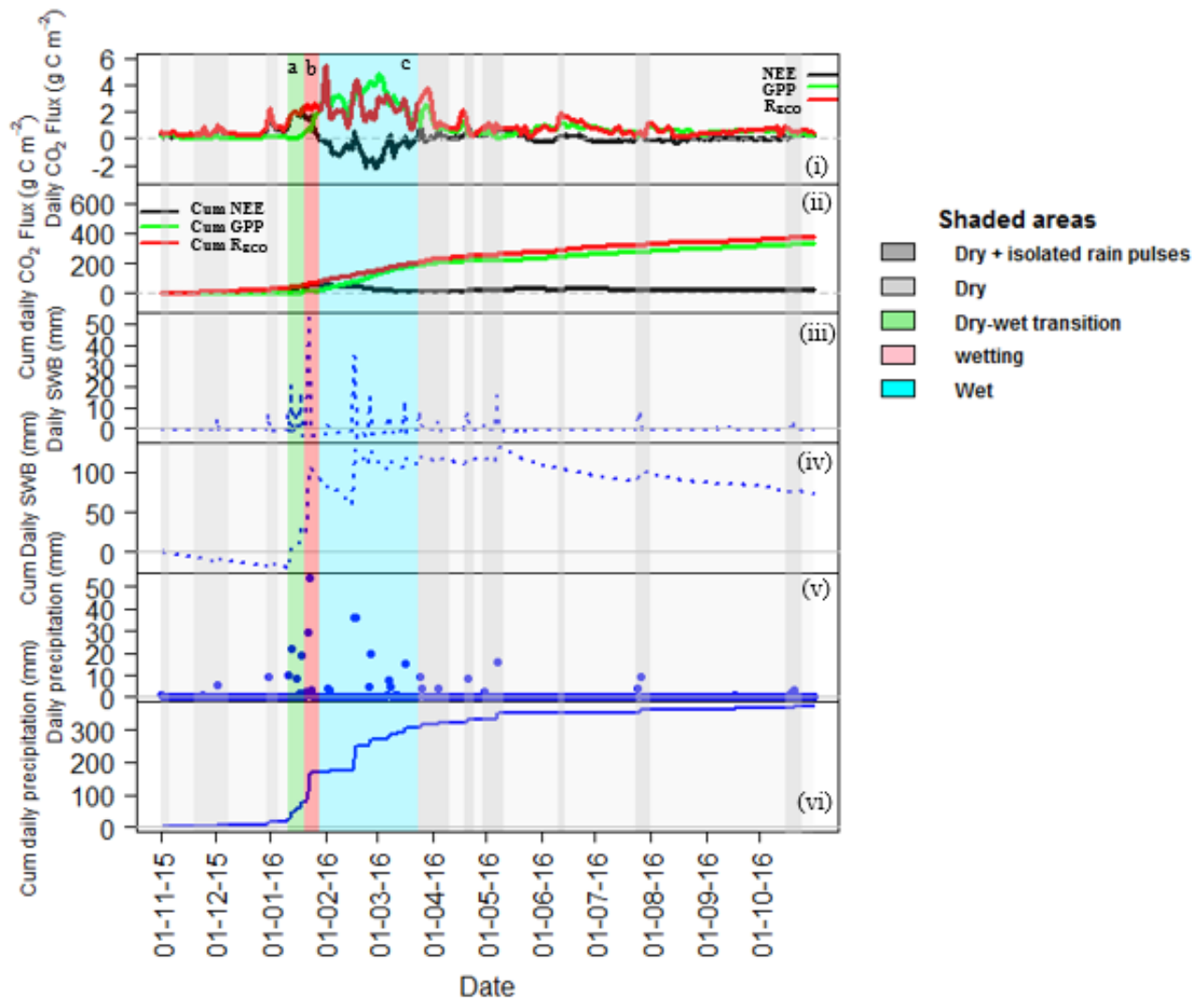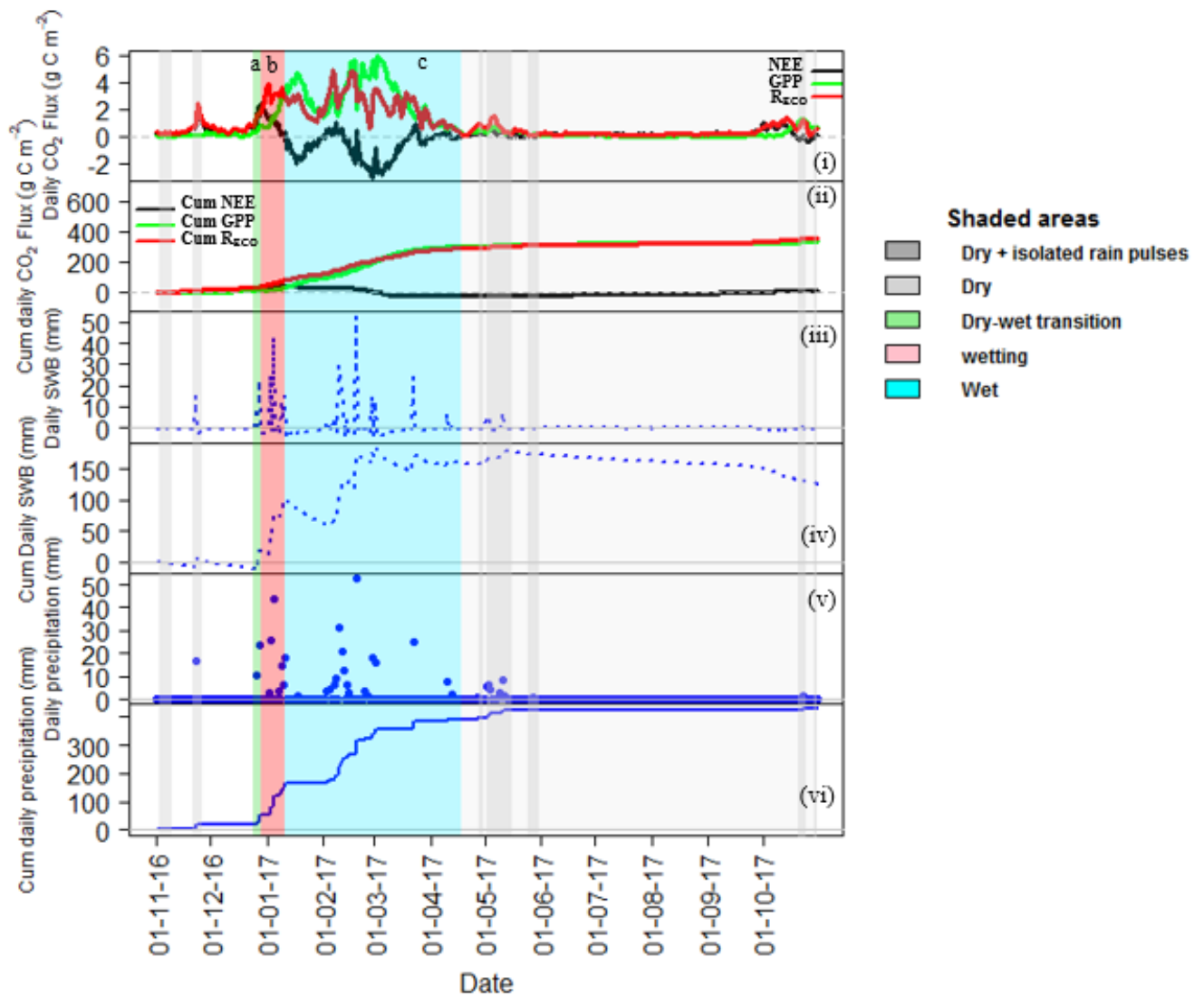
Figure 3. 24: Connectivity among precipitation, surface water balance and carbon fluxes in explaining vegetative functional season at Karoo 1 during 2016/2017 hydro-ecological year. Cum = cumulative and SWB = surface water balance.

The longer growing season length at Karoo 1 was also accompanied by relatively higher precipitation of 429 mm in 2016/2017 HEY compared to the 2015/2016 HEY precipitation of 352 mm. Cumulative SWB from the onset of productive rains to the onset of the vegetative functional season (dry-wet transition phase) was 26.7 mm, indicating availability of water for use by vegetation at Karoo 1. Daily SWB reached its peak during the mid-growing season.

The onset of vegetative functional season at Karoo 2 was triggered by a total of 40.8 mm of productive rains over a period of 4 days during year 2. This was slightly higher than the precipitation threshold of 33.9 mm for the onset of vegetative functional season at Karoo 1 during the same period. The period from the onset of productive rains to the onset of the vegetative functional season (i.e., dry-wet phase) at Karoo 2 was from 26 – 29.12.2016. Two major rainfall events of 26.12.2016 (15 mm) and 28.12.2016 (25.8 mm) constituted the dry-wet transition phase. The lag time of photosynthesis was therefore only 4 days, similarly to Karoo 1. It took approximately 11 days from the onset of the vegetative functional season on 29.12.2016 to the point when NEE reached neutral or negative (i.e., NEE ≤ 0 g C m^{-2} d^{-1}) on 09.01.2017. The length of the vegetative functional season at Karoo 2 for year 2 was 108 days, covering the period from 29.12.2016 to 15.04.2017. The growing season length for Karoo 2 was similar to that of Karoo 1 (i.e., 111 days) during year 2. Cumulative NEE at Karoo 2 for the vegetative functional season during year 2 was - 95 g C m^{-2} compared to the dry season cumulative NEE of 69 g C m^{-2}. Figure 3.25 shows the connectivity among precipitation, SWB and carbon fluxes in explaining vegetative functional season at Karoo 2 during the 2016/2017 HEY.
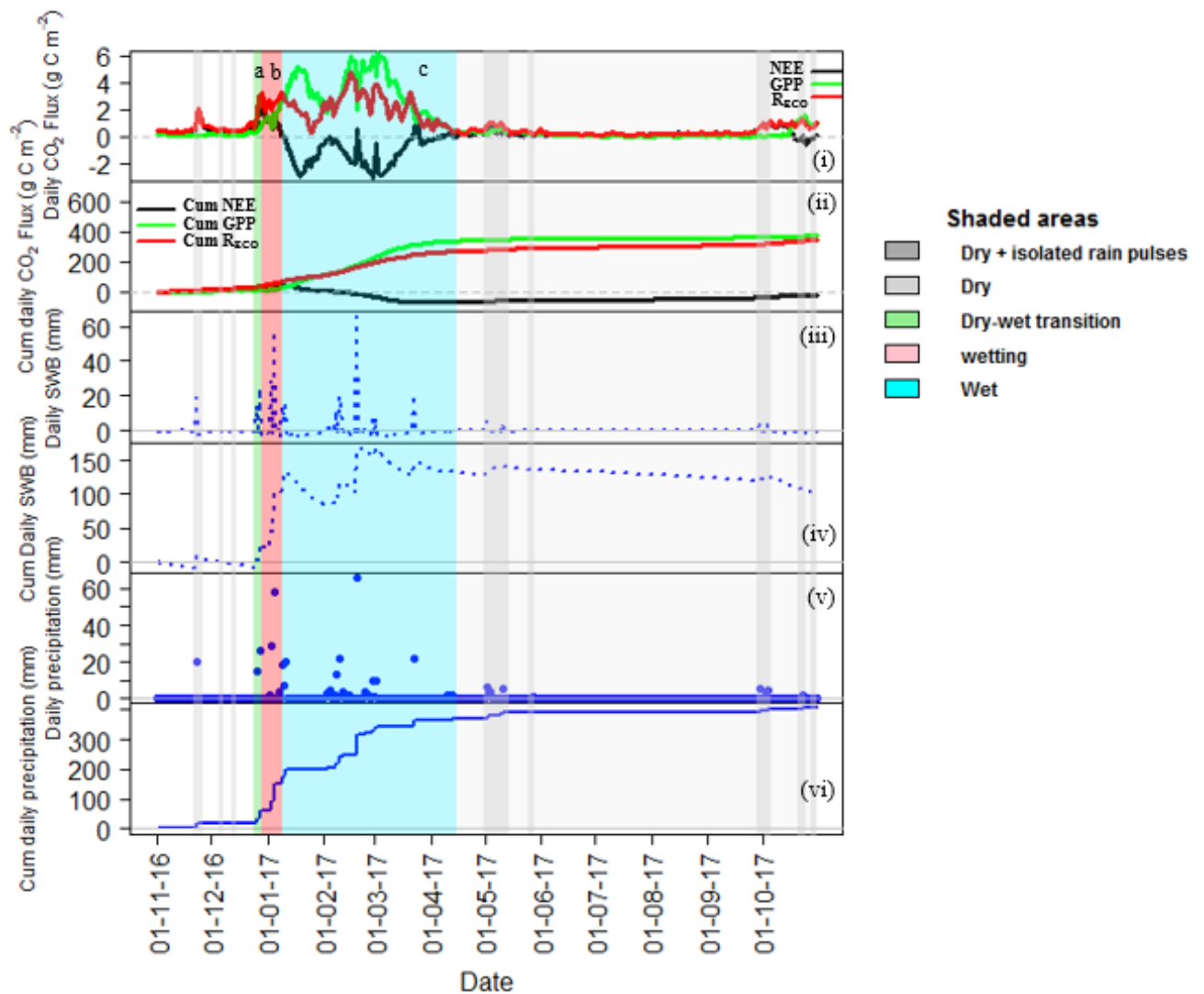
Figure 3. 25: Connectivity among precipitation, surface water balance and carbon fluxes in explaining vegetative functional season at Karoo 2 during 2016/2017 hydro-ecological year. Cum = cumulative and SWB = surface water balance.

A positive SWB of 33 mm also characterised the dry-wetting phase of Karoo 2 during year 2. This was slightly higher than the SWB of 26.7 mm attained at Karoo 1 during the same period. Karoo 2, like Karoo 1, also showed an overall positive SWB by the end of the vegetative functional season.

In summary, the amounts of precipitation that triggered the gently grazed site (Karoo 1) and the rested site (Karoo 2) to reach the onset of the vegetative functional season during year 1 were 132 mm and 60.6 mm, respectively. The difference in precipitation thresholds between the sites

was due to the fact that Karoo 1 had a relatively longer dry-wet phase than Karoo 2. During year 2, the amounts of precipitation that triggered Karoo 1 and Karoo 2 to reach the onset of the vegetative functional season were 33.9 mm and 40.8 mm, respectively. Less amount of water triggered the Karoo sites to reach the onset of the vegetative functional season during year 2 compared to year 1. During the first year of measurement, it took about 13 days from the onset of productive rains to the onset of vegetative functional season at Karoo 1 while it took about 8 days at Karoo 2. For the second year, both Karoo 1 and Karoo 2 took about 4 days to reach the onset of vegetative functional season from the onset of productive rains. Water-stress of plants during year 1, which was a drought year, could have contributed to a higher amount of precipitation required to trigger the onset of the growing season. During year 1, the onset of productive rains was towards mid-January at Karoo 1 and Karoo 2 while significant rains were received towards end of December during year 2.

The growing season lengths for Karoo 1 and Karoo 2 during year 1 were 71 days and 76 days, respectively. In year 2, with annual precipitation above the long-term average, the growing season lengths were 111 days and 108 days for Karoo 1 and Karoo 2, respectively. At the Karoo sites, it took approximately 15 days from the onset of significant rains during year 2 for the ecosystems to turn from a carbon source to a carbon sink. During year 1, it took about 24 days and 18 days from the onset of productive rains to the point when the ecosystems became net sinks of CO_2 at Karoo 1 and Karoo 2, respectively. SWB was probably over-estimated by failure to account for other water losses, apart from ET, and the connectivity of the variable to the temporal dynamics of CO_2 fluxes could have been compromised. As a result, no solid conclusion could be made based on SWB and its connectivity with CO_2 fluxes.

Using the coupling of precipitation and CO_2 fluxes in determining key events such as the onset of vegetative functional seasons is a unique approach that has not been explored in South Africa. By such coupling of precipitation and CO_2 fluxes, precipitation thresholds that may be required to trigger the onset of vegetative functional seasons and the switch from a net ecosystem carbon source to a net ecosystem carbon sink can be established. For instance, in a semi-arid dry forest in southern Sonora (Mexico), with long-term mean annual precipitation of 647mm yr^{-1}, Verduzco et al. (2015) discovered a threshold of ~350 to 400 mm of precipitation that triggered a switch of the dry forest ecosystem from a net source (+102 g C m^{-2} yr^{-1}) to a net sink (-249 g C m^{-2} yr^{-1}).

At Skukuza (the near-natural site) during the 2009/2010 HEY, the onset of productive rains and vegetative functional season were on 13.11.2009 and 20.11.2009, respectively. The observed time lag of 7 days for the Skukuza ecosystem to respond to photosynthesis was consistent with the observations by Archibald et al. (2009). The amount of precipitation that triggered the onset of the vegetative functional season was 91.5 mm and from that point it took only 3 days (21 – 23.11.2009) for the site to shift from being a net carbon source to a net carbon sink. After 109 days from the onset of the growing season, the system was very dry and physiological activity was briefly disrupted for about a week until the site received about 47.6 mm of precipitation in 4 consecutive days from 17–20.03.2010. Such periods of very low soil moisture within a vegetative functional period are common (Kutsch et al., 2008). Again, the site experienced the dry-wet transition, wetting and wet phases (Fig. 3.26).

The total growing season length for the 2009/2010 HEY was about 189 days (i.e., from 21.11.2009 to 28.05.2010). Growing season NEE at Skukuza during 2009/2010 HEY was -119 g C m^{-2} and the dry season NEE was 89 g C m^{-2}. At Skukuza, there were two rainfall peaks in November 2009 and April 2010 that also reflected higher productivity associated with those rainfall periods. The total annual rainfall at Skukuza for the 2009/2010 HEY was 685 mm. Figure 3.26 shows the connectivity among precipitation, SWB and carbon fluxes in explaining vegetative functional season at Skukuza during 2009/2010 HEY.

Figure 3. 26: Connectivity among precipitation, surface water balance and carbon fluxes in explaining vegetative functional season at Skukuza during 2009/2010 hydro-ecological year. Cum = cumulative and SWB = surface water balance.

Cumulative SWB that had accrued from the onset of productive rains to the onset of vegetative functional season during the 2009/2010 HEY at Skukuza was 67.8 mm. The second dry-wet phase had a total SWB of 33.9 mm since the onset of rains on 17.03.2010. Unlike at the Karoo sites, ET seemed to be higher at Skukuza. In a study conducted at Skukuza, Majozi et al. (2017b) also mentioned about high ET during summer as latent heat flux exceeded sensible heat flux during the wet season.

In 2010/2011 HEY, the Skukuza site received rains earlier as compared to the 2009/2010 HEY. The amount of precipitation that was required to reach the onset of the vegetative functional season on 10.11.2010 since the onset of productive rains on 04.11.2010 was 52.8 mm. The lag time of vegetation response to photosynthesis was therefore 6 days, which was similar to that of 2009/2010 (i.e., 7 days). Most of the rains in 2010/2011 were received between December 2010 and January 2011. After the onset of the vegetative functional season, it took only 2 days for the ecosystem to change from a net carbon source to a net carbon sink. The 2010/2011 vegetative functional season also experienced a dry phase which limited photosynthesis from around 16.02.2011 to 21.03.2011. The precipitation of about 32.8 mm on 22.03.2011 was the second trigger of photosynthesis, and by 28.03.2011 NEE began to transform towards negative. The ecosystem slightly changed from a net carbon source to a net carbon sink by 06.04.2011. The end of the vegetative functional season at Skukuza during the 2010/2011 HEY was around 23.05.2011, giving a growing season length of about 195 days (i.e., from 10.11.2010 to 23.05.2011). The total precipitation of the 2010/2011 HEY was about 606 mm, which was lower than that received in 2009/2010 (i.e., 685 mm). The growing season lengths at Skukuza (the near-natural site) were longer compared to the Karoo sites due to higher annual precipitation at Skukuza than at Karoo. Figure 3.27 shows the connectivity between precipitation, SWB and carbon fluxes in explaining vegetative functional season at Skukuza during 2010/2011 HEY.
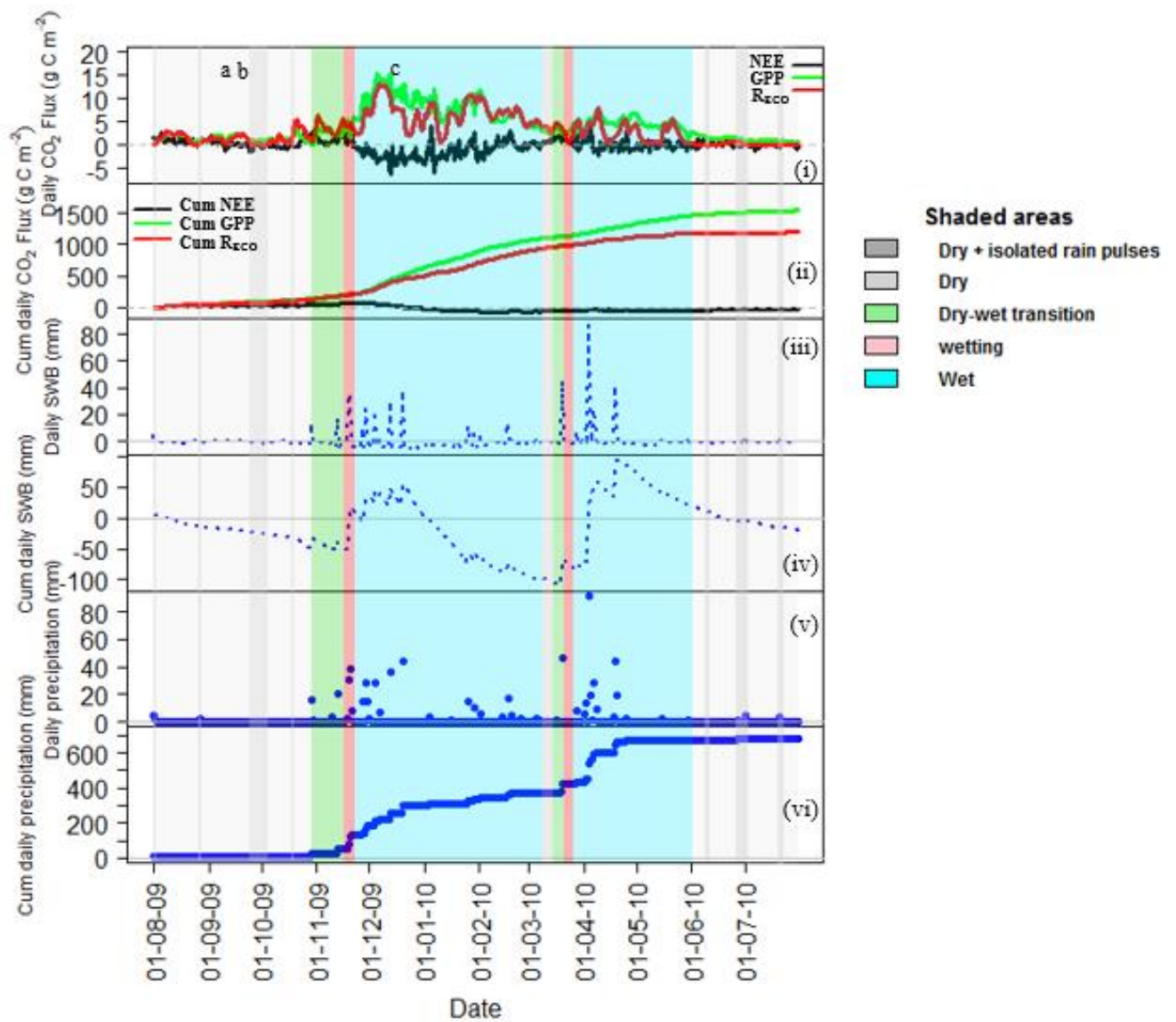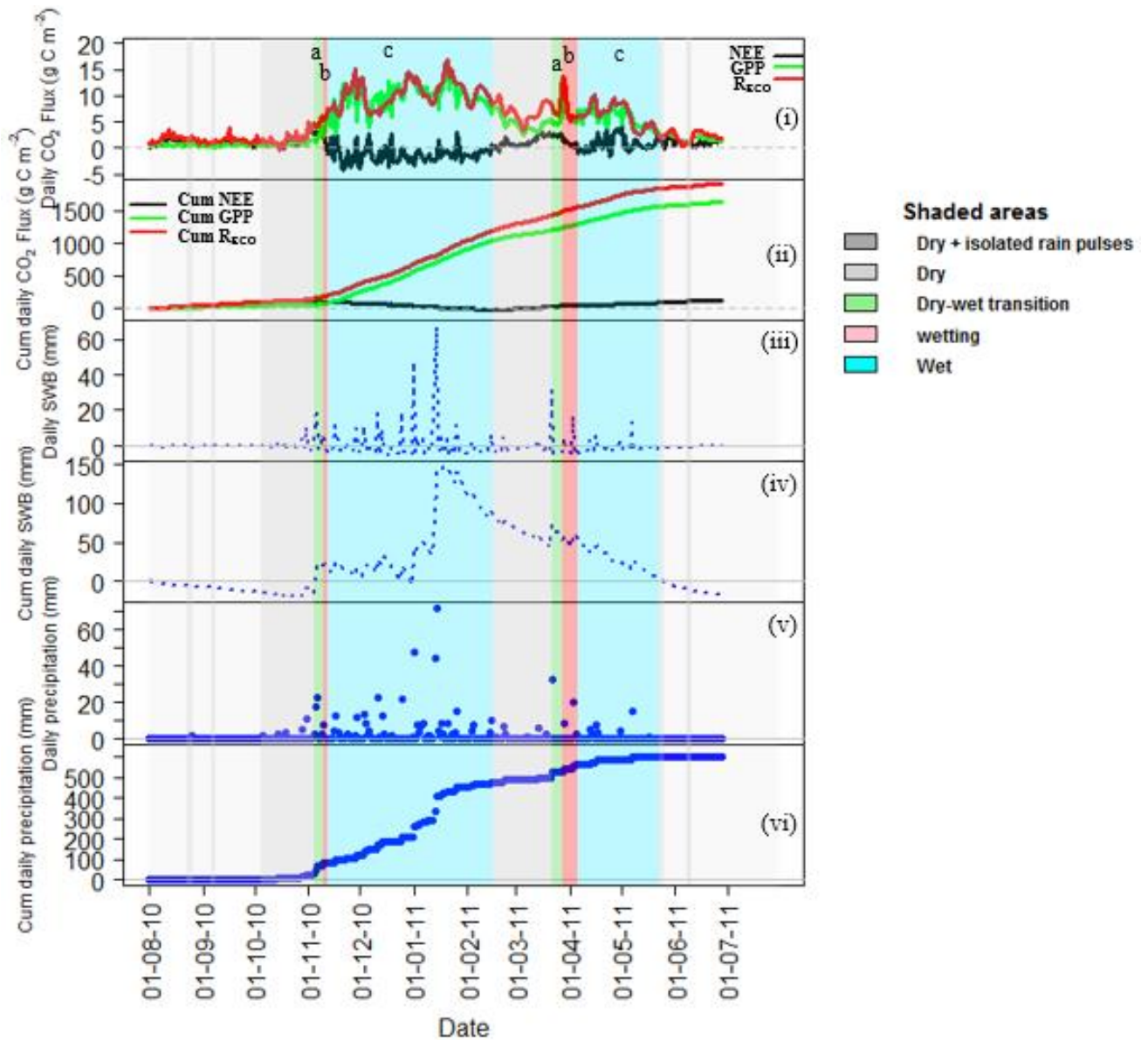
Figure 3. 27: Connectivity among precipitation, surface water balance and carbon fluxes in explaining vegetative functional season at Skukuza during 2010/2011 hydro-ecological year. Cum = cumulative and SWB = surface water balance.

The cumulative SWB between the period from the onset of productive rains to the onset of the vegetative functional season at Skukuza for the 2010/2011 HEY was about 37.4 mm. Like during the 2009/2010 HEY, there was also a dry period during the vegetative functional season giving rise to two dry-wet phases (Fig. 2.27). The second dry-wet phase was characterized by cumulative SWB of 11 mm. During the 2010/2011 HEY plant available water was at its peak around the mid-growing season. The dry season showed a negative SWB (Fig. 3.27, panel iv).

Cumulative SWB is also showing the influence of high ET at Skukuza as was also reflected during the 2009/2010 HEY. Although SWB can be a proxy of soil moisture (Yu et al., 2017), the lack of good soil moisture measurements in this study limited further analyses to also relate CO_2 fluxes with soil moisture.

Table 3.3 summarizes the findings of this section showing the magnitude of all the key variables related to the connectivity of water and CO_2 fluxes in explaining vegetation functional seasons at Karoo sites and Skukuza. Variables included precipitation thresholds that triggered the onset of vegetative functional seasons, SWB estimates between the onset of productive rains and the onset of vegetative functional seasons, time lags of vegetation physiological activity response to productive precipitation, growing seasons lengths, among others.

Table 3. 3: Summary of precipitation attributes in defining onset, cessation and length of vegetative functional seasons at Karoo sites and Skukuza

Year	Variable	Karoo 1	Karoo 2
2015/2016	Precipitation threshold to reach onset of vegetative functional season (mm)	132	60.6
	Time lag response of photosynthesis (days)	13	8
	Onset of vegetative functional season (Date)	24.01.2016	19.01.2016
	End of vegetative functional season (Date)	03.04.2016	03.04.2016
	Duration between onset of productive rains and attainment of net carbon uptake state (days)	24	18
	Cumulative surface water balance from onset of productive rains to onset of vegetative functional season (mm)	103	42.2
	Growing season length (days)	71	76
	Annual precipitation (mm)	352	371
2016/2017	Precipitation threshold to reach onset of vegetative functional season (mm)	33.9	40.8
	Time lag response of photosynthesis (days)	4	4
	Onset of vegetative functional season (Date)	29.12.2016	29.12.2016
	End of vegetative functional season (Date)	18.04.2017	15.04.2017

	Duration between onset of productive rains and attainment of net carbon uptake state (days)	15	15
	Cumulative surface water balance from onset of productive rains to onset of vegetative functional season (mm)	26.7	33
	Growing season length (days)	111	108
	Annual precipitation (mm)	429	406

Site	Variable		
		2009/2010	2010/2011
Skukuza	Precipitation threshold to reach onset of vegetative functional season (mm)	91.5	52.8
	Time lag response of photosynthesis (days)	7	6
	Onset of vegetative functional season (Date)	21.11.2009	10.11.2010
	End of vegetative functional season (Date)	28.05.2010	23.05.2011
	Duration between onset of productive rains and attainment of carbon uptake state (days)	10	8
	Cumulative surface water balance from onset of productive rains to onset of vegetative functional season (mm)	67.8	37.4
	Growing season length (days)	189	195
	Annual precipitation (mm)	685	606

The onsets of vegetative functional seasons were generally reached quicker at the Skukuza site compared to the Karoo sites. Meteorological conditions such as the amount of precipitation may also influence the onset of the vegetative functional season. For instance, at the Karoo sites the onset of the vegetative functional season was reached in January during the drought year (2015/2016 HEY) and in December when annual precipitation was above the long-term average (2016/2017 HEY). At Skukuza, with relatively higher precipitation than the Karoo sites, the onset of the growing seasons for the two hydro-ecological years were reached in November. At the Karoo sites, the growing season lengths were also longer during year 2 compared to year 1 because the onset of vegetative functional seasons were earlier during year 2 compared to year 1. The end of the vegetative functional seasons at Karoo sites were generally similar for year 1 and year 2 but the onsets of the growing seasons from year 1 to year 2 shifted by some 21 – 26 days at Karoo 2 and Karoo 1, respectively. This could also be the reason why both Karoo 1 and Karoo 2 sequestered relatively more CO_2 during year 2 compared to year 1. However, despite the noticeable relative differences in annual NEE between the years at Karoo sites, the annual NEE estimates were similar for both HEYs in light of the uncertainty of annual NEE estimates.

Shifts in the onset and end of the growing season and growing season length may or may not occur inter-annually at different areas. For instance, in a study carried out in a semi-arid area of Southern Zimbabwe, Mupangwa et al. (2011) reported no significant changes in the start, end and growing season length over a period of 50–74 years. Most importantly, if the date of growing season onset, end and precipitation characteristics are known, the success or failure of a season can be approximated. Ngetich et al. (2014) mentioned that the amount of water available to plants is strongly dependent on the onset and length of a growing season.

The approach used here, of determining the onset of the vegetative functional season by tracking the nexus between precipitation and the changes in NEE, was more robust in explaining vegetative functional seasons compared to the initial approach that was also used in this study for the long-term flux datasets at Skukuza (see sub-section 2.5.1). However, the approach to determine the end of the growing season by observing when the ecosystem systematically shifts from a net carbon sink to a net carbon source may have a bias or uncertainty at times when a subjective decision has to be made in situations when there are multiple oscillations of NEE values around the carbon neutral state (i.e., NEE = 0). This can happen when a site receives some sporadic rains after long dry days towards the end of the rainfall season. In determining the end of vegetative functional season of woodland savanna areas like Skukuza, there might also be need to consider the plant-water relations of the deep rooted broad-leaved *Combretum apiculatum* and fine-leaved *Acacia nigrescens* trees, as the plants may still continue to photosynthesize for some days or weeks after the cessation of rainfall (Archibald and Scholes, 2007; Archibald et al., 2009). For that reason, the end of the vegetative functional season at Skukuza was generally late (towards end of May) compared to Karoo sites (early to mid-April). It is therefore crucial to develop ecosystem-specific, standardized, reliable, robust and more precise approaches of determining the onset and cessation of vegetative functional seasons that can be widely applied in monitoring inter-annual shifts of these important dates. Ardö et al. (2008) noted that comparability among studies can be affected due to varying definitions on when the dry/wet seasons start and end.

3.6 Hot moments of ecosystem respiration at Karoo and Skukuza sites

The 'hot moments' of ecosystem respiration were characterized by high-frequency 'spikes' of CO_2 efflux immediately after the flux sites experienced isolated rain pulse events early in the rainfall season. These R_{eco} spikes during such periods are a general feature of arid and semi-arid savanna ecosystems. At Karoo 1 during year 1, about four hot moments of CO_2 efflux were identified and characterized in terms of precipitation size, duration and magnitude of R_{eco} pulses/spikes. Figure 3.28 shows hot moments of ecosystem respiration at Karoo 1 for hydro-ecological year 2015/2016.
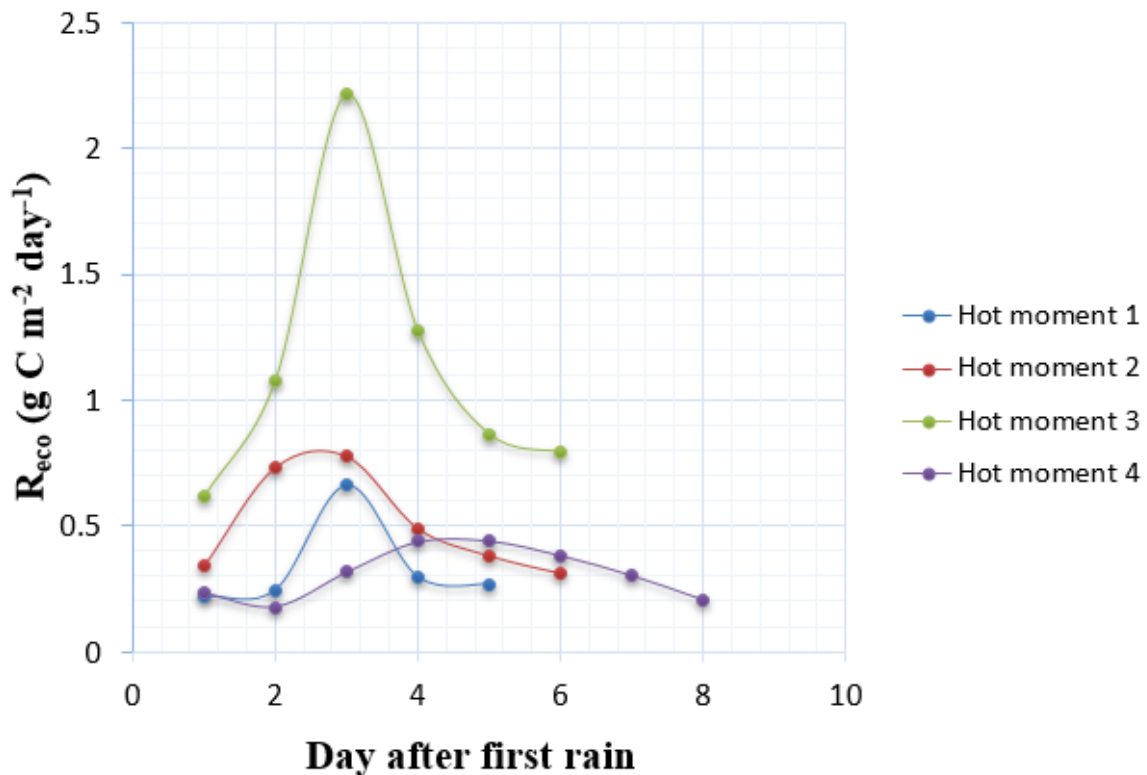
Figure 3. 28: Response of ecosystem respiration to rain pulses at Karoo 1 for hydro-ecological year 2015/2016. Dates of hot moments of CO_2 efflux (plus rain pulse size) and control treatments were as follows: Hot moment 1: 23.11.2015 to 27.11.2015 (3.3 mm); Hot moment 2: 01.12.2015 to 06.12.2015 (5.7 mm); Hot moment 3: 30.12.2015 to 04.01.2016 (14.3 mm); Hot moment 4: 15.10.2016 to 22.10.2016 (4.5 mm) and 6 days control treatments: Control 1: 04.11.2015 to 09.11.2015; Control 2: 15.11.2015 to 20.11.2015; Control 3: 09.12.2015 to 14.12.2015; Control 4: 15.12.2015 to 20.12.2015; Control 5: 21.12.2015 to 26.12.2015; Control 6: 09.10.2016 to 14.10.2016.

The scatterplot (Fig. 3.28) shows daily R_{eco} over the entire duration of the hot moment. Each hot moment of CO_2 efflux was constituted by either a single isolated rain pulse event or a maximum of 3 combined rain pulse events close to each other, either falling on consecutive days or within a maximum of a 5-day period in cases where there were 3 rain pulse events. The single/first rain pulse was falling on/from day 1 (Fig.3.28). For instance, hot moment 1 comprised a single rain pulse event of 3.3 mm of rainfall that was received on 24.11.2015. In most of the cases, after a rain pulse event, the response by heterotrophs was very quick and CO_2 efflux was already increasing within one day of the precipitation event, which is in line with Sponseller (2006) who observed CO_2 efflux increasing immediately after soil rewetting in a Sonoran Desert ecosystem.

With the rain pulse sizes of 3.3 mm to 14.3 mm at Karoo 1, R_{eco} would reach its peak and gradually return to its background levels in 2 to 6 days after the rainfall event(s) (Fig. 3.28). Respectively, Yan et al. (2014) observed soil respiration pulses following precipitation sizes of 0.4 mm to 31 mm returning to background levels in 2.93 to 27.9 days after the rainfall events. The peak R_{eco} attained during CO_2 efflux hot moments 1 to 4 at Karoo 1 during year 1 were 0.7 g C m^{-2} d^{-1}, 0.8 g C m^{-2} d^{-1}, 2.2 g C m^{-2} d^{-1} and 0.4 g C m^{-2} d^{-1}, respectively (Fig.3.28). With similar rain sizes and duration of R_{eco} pulses, peak R_{eco} values obtained at Karoo 1 during year 1 contradicts with those obtained by Yan et al. (2014) at a similar arid region in north-eastern Inner Mongolia, China. For instance, with a rain size of 5.4 mm, Yan et al. (2014) obtained a soil respiration peak of ~ 1.6 g C m^{-2} d^{-1}, twice as much as the R_{eco} peak of 0.8 g C m^{-2} d^{-1} observed at Karoo 1 at rain size of 5.7 mm. Again, at 16.4 mm rain size Yan et al. (2014) found a soil respiration peak of ~ 1.5 g C m^{-2} d^{-1} while a higher R_{eco} peak of 2.2 g C m^{-2} d^{-1} was obtained at a rain size of 14.3 mm at Karoo 1. Both areas have similar annual precipitation (i.e., 374 mm yr^{-1} at Karoo 1 vs 377 mm yr^{-1} at the north-eastern Inner Mongolia site) but they differ in temperature, the Karoo 1 site having a mean annual temperature of 15°C (Hagan et al., 2017) while the north-eastern Inner Mongolia site has a mean annual temperature of 3.3^{o} C. This implies that other pre-conditions (e.g., soil temperature, soil moisture) also play a key role in microbial response to rewetting of soils, apart from rainfall.

The daily R_{eco} values (from day 1 to the last day when R_{eco} returned to background levels) were summed over the duration of the hot moment of CO_2 efflux and control treatments. The average duration of R_{eco} pulses at Karoo 1 and Karoo 2 were 6 days and 5 days, respectively. Figure

3.29 shows the size of precipitation pulse(s) and the summed daily R_{eco} values of each hot moment at Karoo 1 for hydro-ecological year 2015/2016.
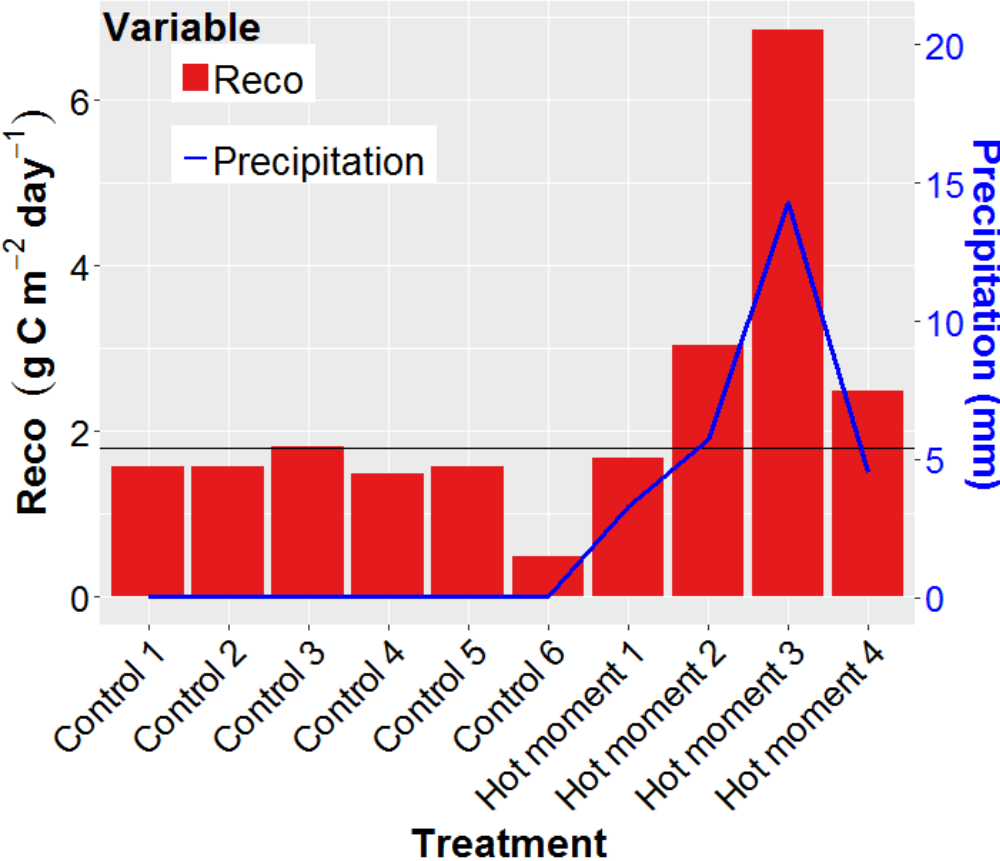
Figure 3. 29: Precipitation pulses and ecosystem respiration pulses at Karoo 1 for hydro-ecological year 2015/2016

At Karoo 1, depending on rain pulse size, CO_2 effluxes were in the range from 1.7 g C m^{-2} d^{-1} to maximum of 6.8 g C m^{-2} d^{-1} – with the largest rain pulse size of 14.3 mm inducing the greatest pulse effect of R_{eco}. The rainfall pulse sizes for the identified hot moments of CO_2 efflux ranged between 3.3 – 14.3 mm. Three of the four hot moments of CO_2 efflux occurred during light rains (below 6 mm). According to a rainfall size classification by Du Toit (2010), rainfall < 10 mm day^{-1} can be considered as light rain.

When ET losses were accounted for, the SWB during hot moments of CO_2 efflux ranged from 0.7 – 6.4 mm at Karoo 1 during year 1. Figure 3.30 shows SWB and ecosystem respiration pulses at Karoo 1 for hydro-ecological year 2015/2016.
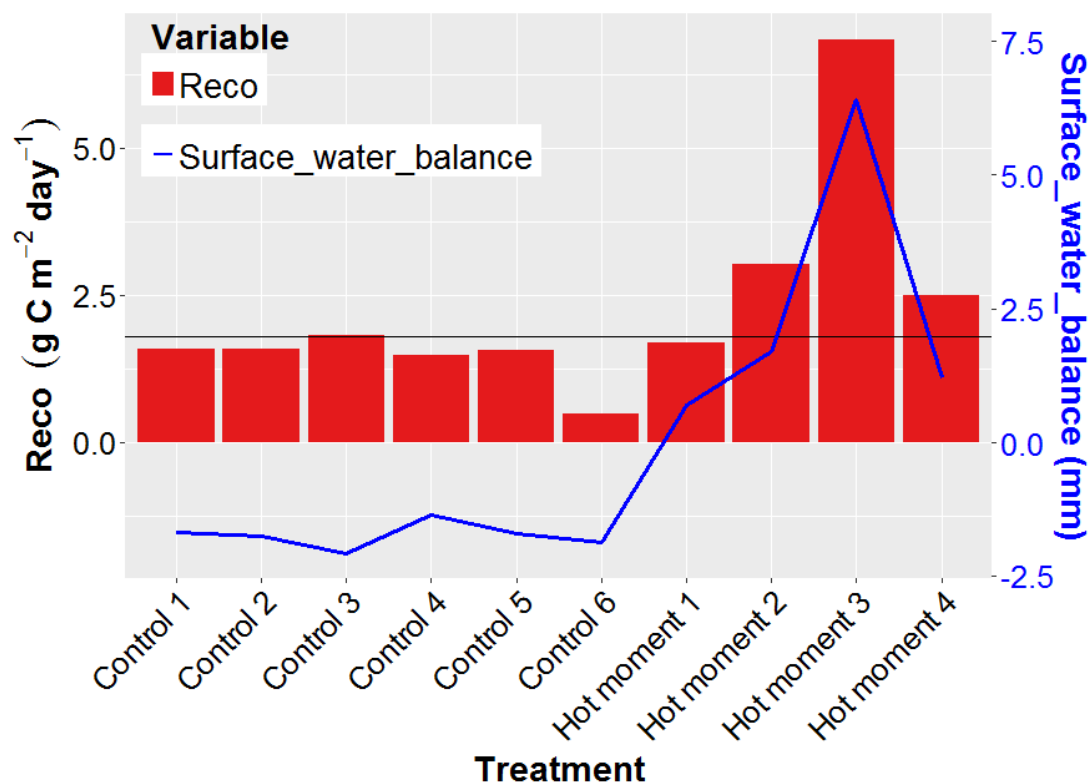
Figure 3. 30: Surface water balance and ecosystem respiration pulses at Karoo 1 for hydro-ecological year 2015/2016

The maximum R_{eco} value that was attained by control 3 was 1.8 g C m^{-2} d^{-1}. The lowest rain pulse size of 3.3 mm yielded a R_{eco} pulse size of 1.7 g C m^{-2} d^{-1}, which was similar to those observed at control treatments. For that reason, a rain size threshold of > 3 mm was required to trigger a hot moment of CO_2 efflux at the gently grazed site (Karoo 1) during year 1. In reference to the work of Guo et al. (2015), precipitation > 1 mm in one day was considered as one precipitation event and precipitation < 1 mm was regarded as a dry day. Zhang et al. (2018) also defined a rainy day as precipitation >= 1 mm. Rainfall of 1 – 3 mm did not cause significant R_{eco} spikes at Karoo 1 site during year 1. In the second year, which was relatively wetter than the first year, there were no adequate rain pulses following the dry season at Karoo 1 to perform a meaningful analysis. Figure 3.31 shows a scatter plot of isolated rain pulse sizes and the magnitude of R_{eco} at Karoo 1 for the 2015/2016 hydro-ecological year.
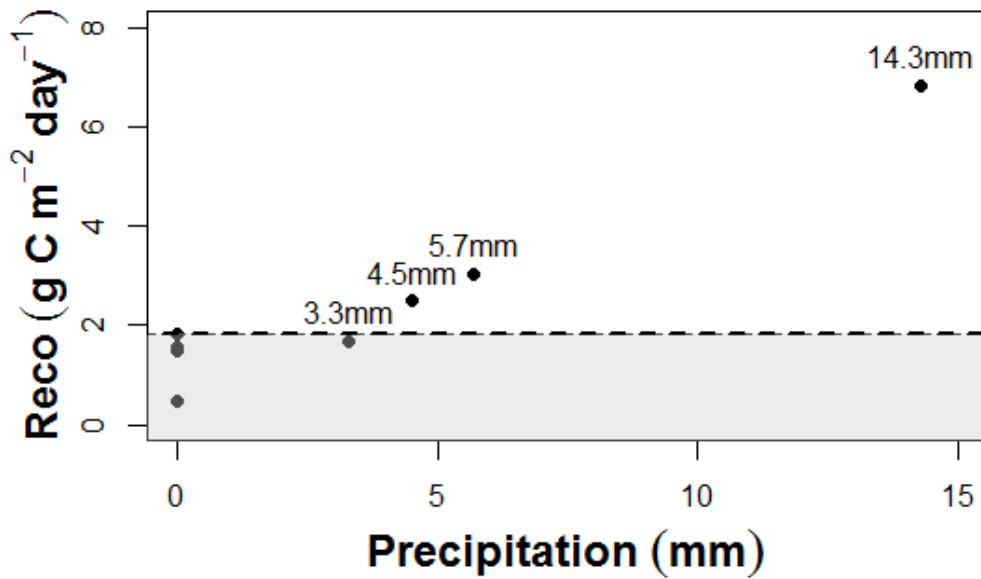
Figure 3. 31: Scatter plot of isolated rain pulses vs magnitude of ecosystem respiration response at Karoo 1 for hydro-ecological year 2015/2016

At the rested site (Karoo 2) during year 1, three hot moments of CO_2 efflux were identified. The peak R_{eco} attained during CO_2 efflux hot moments 1 – 3 at Karoo 1 during year 1 were 0.9 g C m^{-2} d^{-1}, 1 g C m^{-2} d^{-1} and 2.2 g C m^{-2} d^{-1}, respectively (Fig.3.32). With the rain pulse sizes of range 0.9 – 9.6 mm at Karoo 2, R_{eco} pulse effect would last for 4 – 5 days after rain pulse event(s). Figure 3.32 shows the response of ecosystem respiration to rain pulses at Karoo 2 for hydro-ecological year 2015/2016.
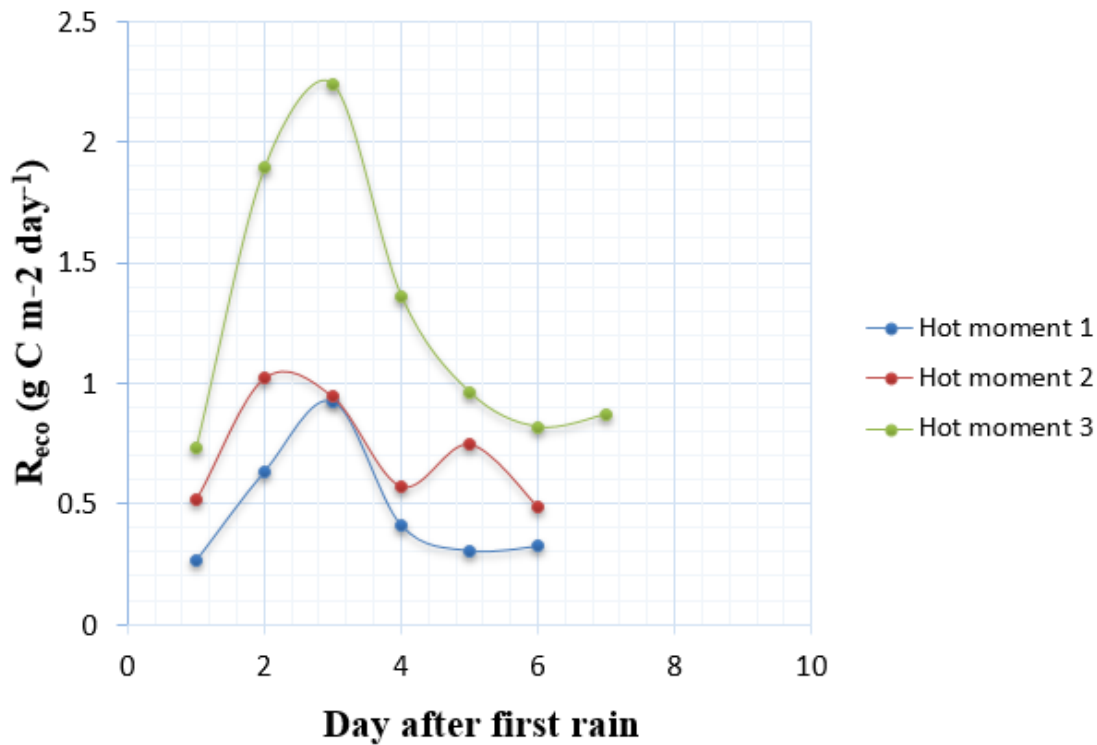
Figure 3. 32: Response of ecosystem respiration to rain pulses at Karoo 2 for hydro-ecological year 2015/2016. Dates of hot moments of CO_2 efflux (plus rain size) and control treatments were as follows: Hot moment 1: 23.11.2015 to 28.11.2015 (0.9 mm); Hot moment 2: 01.12.2015 to 06.12.2015 (5.4 mm); Hot moment 3: 30.12.2015 to 05.01.2016 (9.6 mm); and 5 days control treatments: Control 1: 08.11.2015 to 12.11.2015; Control 2: 13.11.2015 to 17.11.2015; Control 3: 13.12.2015 to 17.12.2015; Control 4: 18.12.2015 to 22.12.2015; Control 5: 23.12.2015 to 27.12.2015; Control 6: 10.10.2016 to 14.10.2016; Control 7: 27.10.2016 to 31.10.2016.

After summing R_{eco} values over the duration of each control treatment, a maximum R_{eco} of 2.9 g C m^{-2} d^{-1} was attained at Karoo 2 (compared to 1.8 g C m^{-2} d^{-1} at Karoo 1). The highest rain pulse size of 9.6 mm also caused the greatest R_{eco} pulse effect of 8.9 g C m^{-2} d^{-1}. Rainfall of 0.9 mm and 5.4 mm caused R_{eco} effluxes of 2.9 g C m^{-2} d^{-1} and 4 g C m^{-2} d^{-1}, respectively. Figure 3.33 shows rain pulses and ecosystem respiration pulses at Karoo 2 for hydro-ecological year 2015/2016.
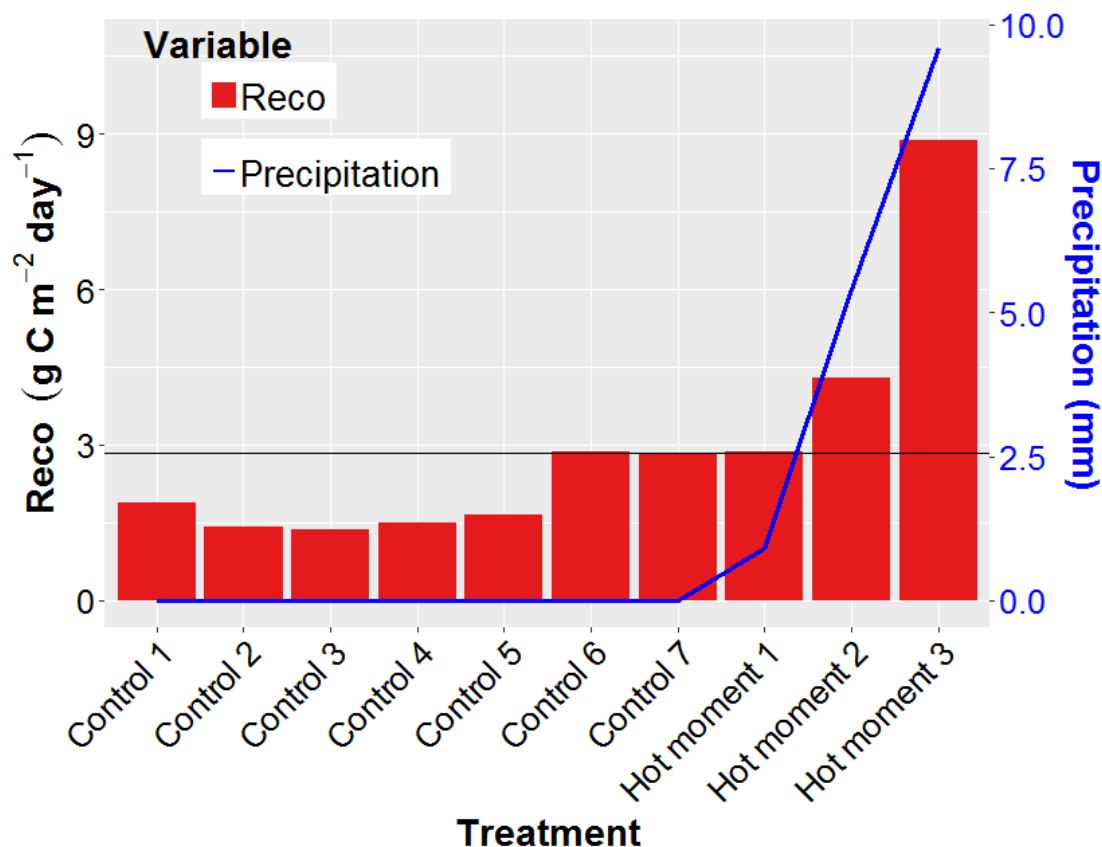
Figure 3. 33: Precipitation pulses and ecosystem respiration pulses at Karoo 2 for hydro-ecological year 2015/2016

It was found that at relatively lower rainfall, the rested site (Karoo 2) had higher R_{eco} effluxes compared to the gently grazed site (Karoo 1). For instance, the rain pulse of 9.6 mm caused a R_{eco} pulse of 8.9 g C $m^{-2} d^{-1}$ at Karoo 2, while a higher rain pulse of 14.3 mm at Karoo 1 resulted in a lower R_{eco} pulse of 6.8 g C $m^{-2} d^{-1}$. Again, a smaller rain pulse of 0.9 mm caused a relatively larger R_{eco} pulse of 2.9 g C $m^{-2} d^{-1}$ at Karoo 2 during year 1, yet a larger rain pulse of 3.3 mm produced a lower R_{eco} pulse of 1.7 g C $m^{-2} d^{-1}$. From these statistics, it can be pointed out that quicker microbial response to soil re-wetting was associated with the rested site than the gently grazed site. A similar result was also found by Chen et al. (2008) in a semi-arid steppe ecosystem in Inner Mongolia, where an ungrazed site achieved a higher soil respiration rate compared to a grazed site. The author mentioned that while the rate of soil respiration is largely dependent on rain pulse size, the interactive effects of precipitation pulses and grazing may also alter soil respiration rates (Chen et al., 2008). Land degradation due to grazing may therefore reduce CO_2 efflux, as grazing is associated with changes in vegetation, soil properties and surface characteristics (Jaweed et al., 2018; Wigley et al., 2010).

Figure 3.34 shows SWB and ecosystem respiration pulses at Karoo 2 for hydro-ecological year 2015/2016. SWB during hot moments of CO_2 efflux was in the range from -2.9 to 1.4 mm at Karoo 2 during year 1.
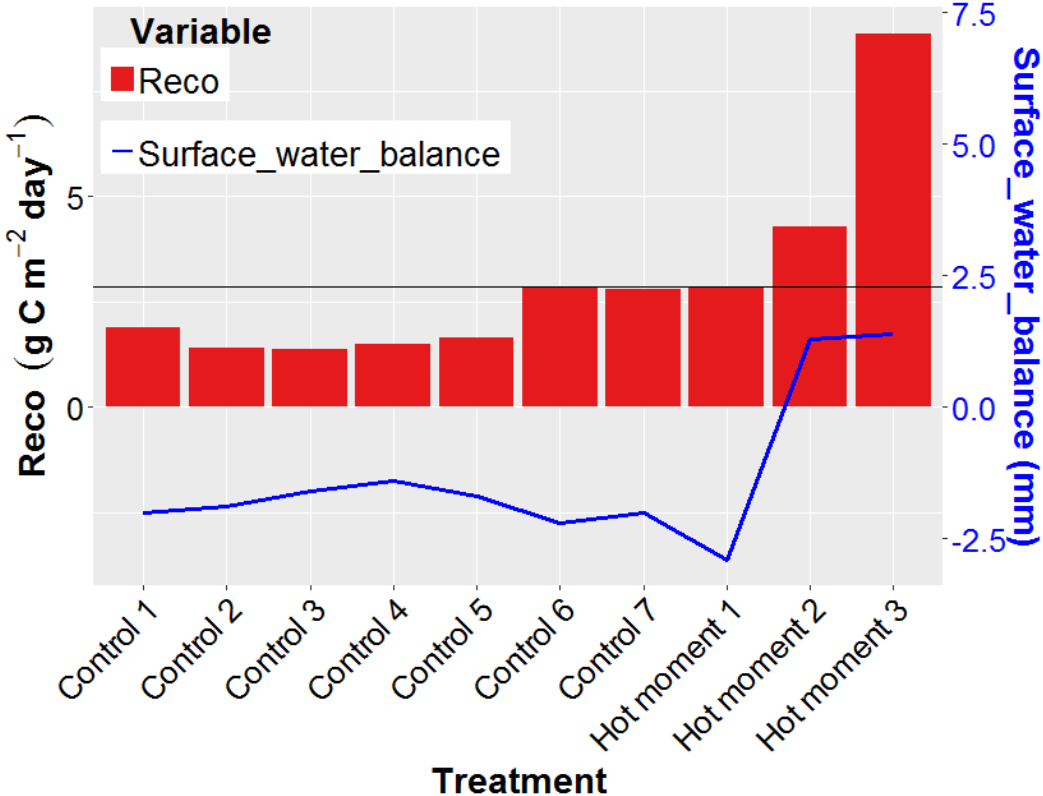
Figure 3. 34: Surface water balance and ecosystem respiration pulses at Karoo 2 for hydro-ecological year 2015/2016

Figure 3.35 shows the scatter plot of isolated rain pulses and magnitude of ecosystem respiration response at Karoo 2 for hydro-ecological year 2015/2016. The lowest rain pulse of 0.9 mm induced a R_{eco} pulse of 2.9 g C m^{-2} d^{-1}, which was similar to the maximum R_{eco} efflux that was observed at control treatments. For small rain pulse sizes, Chen et al. (2008) mentioned that the response of soil respiration to precipitation only lasts for very short periods. For that reason, a rain size threshold of > 0.9 mm was required to trigger a hot moment of CO_2 efflux at the rested site (Karoo 2) during year 1 (compared to rain size threshold of > 3 mm observed at Karoo 1. During year 2, there were no adequate rain pulses following the dry season at Karoo 2.

116
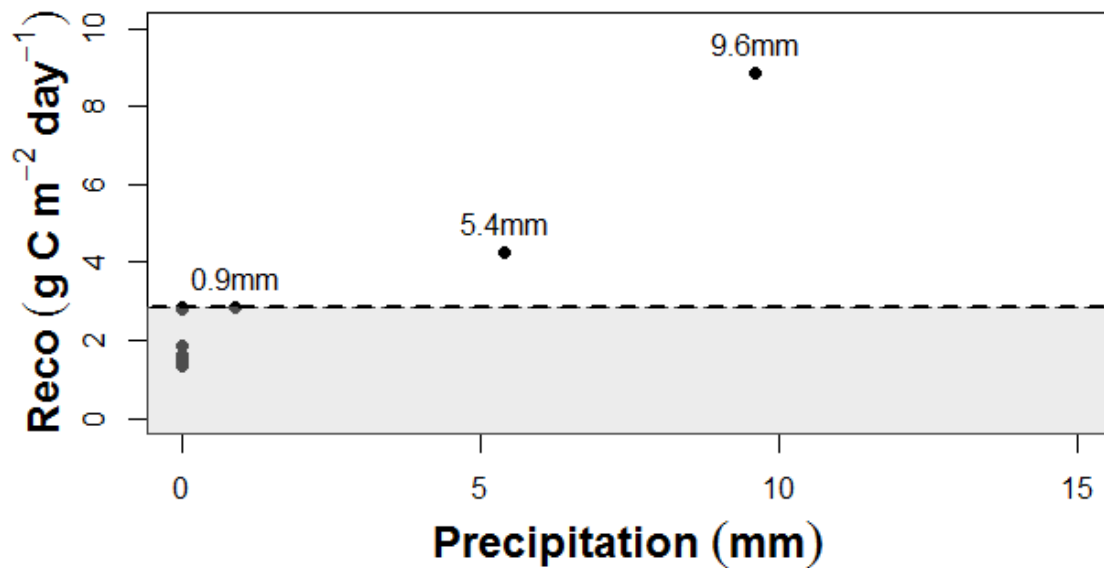
Figure 3. 35: Scatter plot of isolated rain pulses vs magnitude of ecosystem respiration response at Karoo 2 for hydro-ecological year 2015/2016

At Karoo 2 during year 1, rain pulse size associated with the identified hot moments of CO_2 efflux did not exceed 10 mm. Precipitation events > 10 mm d^{-1} are considered large and they promote carbon uptake while precipitation events < 10 mm d^{-1} are regarded as small and associated with increased heterotrophic respiration (Parton et al., 2012).

It can still be noted that there were few available isolated rain pulse events that were identified in this study and long-term measurements may still be needed in order to check consistency of these preliminary results that can be used as the baseline. It may also be necessary to examine the influence of other micro-meteorological controls on R_{eco} pulse effect, as Yan et al. (2014) mentioned that rain pulse effects can be intensified not only by larger individual precipitation events, but also by other elements or pre-conditions such as soil temperature, soil moisture and soil organic matter content. Soil CO_2 efflux response to soil re-wetting under mild conditions was also found to be smaller than under severe drought conditions (Unger et al., 2010). Similarly, Carbone et al. (2011) also reported higher soil respiration pulses when soil water content prior to a rain pulse was at its driest.

At Skukuza there were no distinct hot moments of ecosystem respiration that could be identified, possibly due to relatively higher rainfall compared to the Karoo sites. Pulsed rain events are more associated with dry regions.

117

3.7 Ecosystem water use efficiency during vegetative functional periods at Skukuza and Karoo

The inter-annual variability of ecosystem water use efficiency (EWUE) was assessed for the Karoo sites and Skukuza using datasets for two consecutive vegetative functional seasons at each site. Karoo 1 and Karoo 2 sites have similar climatic conditions (both semi-arid ecosystems), similar vegetation (mixed grasses, herbs, dwarf shrubs and few scattered trees) but are under different livestock grazing management regimes as explained in sub-section 2.2.2. The Skukuza site is a near-natural site managed for wildlife conservation and a semi-arid open woodland savanna but relatively wetter than the Karoo sites.

The motivation for this assessment was to observe the magnitude of EWUE under different site characteristics, for example differences in climate, vegetation type and land use management. As EWUE is the ratio of GPP to ET, these processes can be affected differently by site meteorological conditions (e.g., Brümmer et al., 2012) and land use management regimes. Huizhi and Jianwu (2012) cited several environmental factors (including wind velocity, solar radiation, atmospheric water demand, humidity, air temperature, ground cover characteristics) and biological factors that control ET which may need to be further investigated in detail in future studies.

Figure 3.36 shows the EWUE of Skukuza for vegetative functional season of 2009/2010. At Skukuza, during the vegetative functional season of 2009/2010, EWUE was 2.2 g C kg^{-1} H$_2$O. The 2009/2010 hydro-ecological year was wetter with annual precipitation above the average (see Fig. 3.4). The maximum weekly ET and GPP during the 2009/2010 growing season were 37 kg H$_2$O m^{-2} and 96 g C m^{-2}, respectively. There was a strong linear correlation between weekly GPP and weekly ET values maintaining a fairly constant EWUE. The constancy of EWUE at Skukuza was also reported by Kutsch et al. (2008) during 2002/2003.

Figure 3. 36: Skukuza ecosystem water use efficiency for vegetative functional season 2009/2010. Period of assessment from 09 November 2009 to 29 May 2010.

Figure 3.37 shows the EWUE of Skukuza for the vegetative functional season of 2010/2011. For the vegetative functional season of 2010/2011, EWUE was 2.1 g C kg^{-1} H$_2$O. From 2009/2010 to 2010/2011, EWUE did not change much and there was no significant difference (P > 0.05) between EWUE of the two hydro-ecological years. The annual precipitation for 2010/2011 was above the long-term annual average for Skukuza, although it was lower than that of 2009/2010. The maximum weekly ET attained during the 2010/2011 growing season was 35 kg H$_2$O m^{-2} (compared to a weekly maximum ET of 37 kg H$_2$O m^{-2} during the 2009/2010 growing season). A weekly GPP peak of 64 g C m^{-2} was reached during 2010/2011 growing season (compared to a maximum weekly GPP of 96 g C m^{-2} attained during the 2009/2010 growing season).

Figure 3. 37: Skukuza ecosystem water use efficiency for vegetative functional season 2010/2011. Period of assessment from 13 November 2010 to 22 April 2011.

Figure 3.38 shows the EWUE of Karoo 1 for the vegetative functional season of 2015/2016. Ecosystem water use efficiency was about 1.1 g C kg^{-1} H_2O. Year 1 was a drought year – as precipitation was below the long-term annual average for the Karoo. The maximum weekly ET attained during the 2015/2016 growing season was 21 kg H_2O m^{-2} while weekly GPP reached a peak of 25 g C m^{-2}.

Figure 3. 38: Karoo 1 ecosystem water use efficiency for vegetative functional season 2015/2016. Period of assessment from 27 January to 03 April 2016.

Figure 3.39 shows the EWUE of Karoo 2 for the vegetative functional season of 2015/2016. During this period, EWUE was about 1.2 g C kg^{-1} H_2O (compared to 1.1 g C kg^{-1} H_2O at Karoo 1 during the same period). The maximum weekly ET attained during the 2015/2016 growing season at Karoo 2 was 23 kg H_2O m^{-2} (compared to 21 kg H_2O m^{-2} at Karoo 1 during the same period). Peak weekly GPP reached at Karoo 2 was 29 g C m^{-2} (compared to 25 g C m^{-2} reached at Karoo 1 during the same period). There was no significant difference in EWUE ($P > 0.05$) between Karoo 1 and Karoo 2 during year 1.
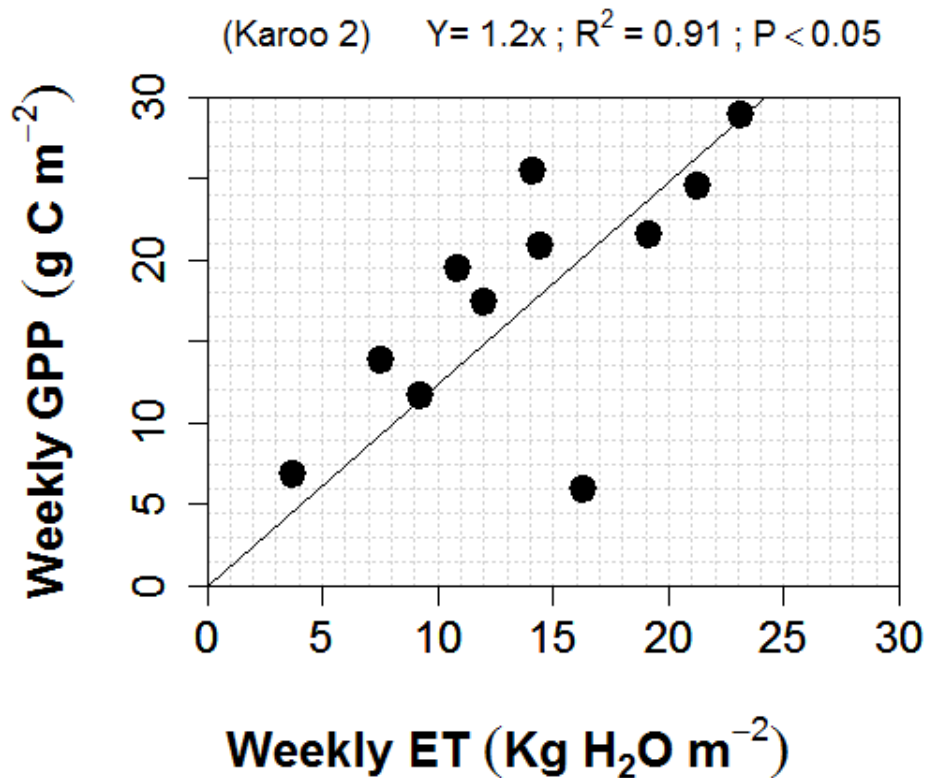
Figure 3.39: Karoo 2 ecosystem water use efficiency for vegetative functional season 2015/2016. Period of assessment from 20 January to 03 April 2016.

Figure 3.40 shows the EWUE of Karoo 1 for the vegetative functional season of 2016/2017. Ecosystem water use efficiency was about 1.5 g C kg^{-1} H_2O, which was a slight increase given that year 1 EWUE was 1.1 g C kg^{-1} H_2O. However, the EWUE of year 1 and year 2 at Karoo 1 were not significantly different (P > 0.05). The maximum weekly ET attained at Karoo 1 during year 2 growing season was 23 kg H_2O m^{-2}, which was again a slight increase from year 1 peak weekly ET of 21 kg H_2O m^{-2}. Similarly, a peak weekly GPP of 37 g C m^{-2} was reached at Karoo 1 during year 2 (compared a maximum weekly GPP of 25 g C m^{-2} attained during year 1). The slight increase in peak values of weekly ET and GPP at Karoo 1 from year 1 to year 2 is a reflection of the relative increase in assimilation rates that occurred from year 1 to year 2 as a result of the increase in annual rainfall.
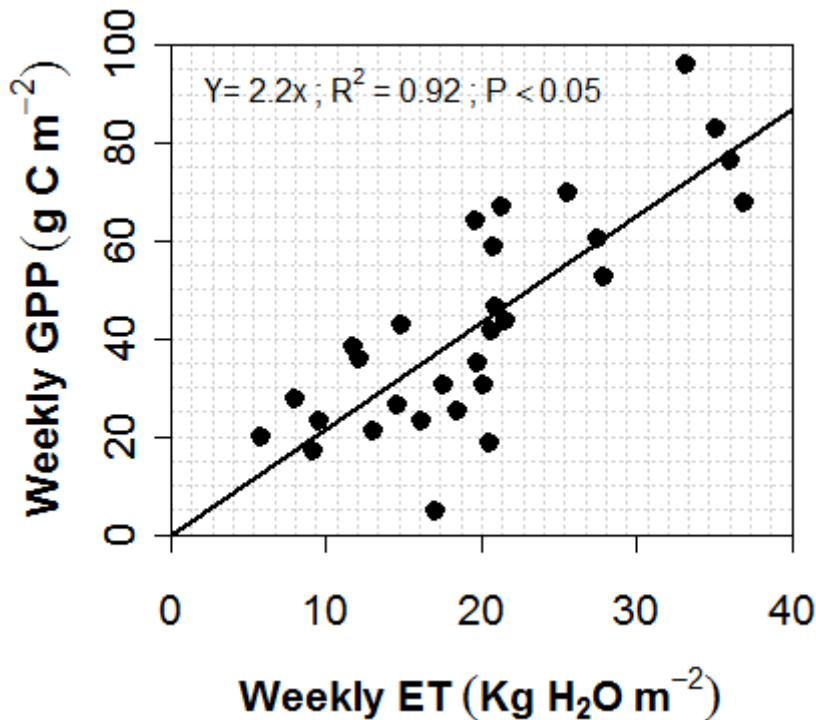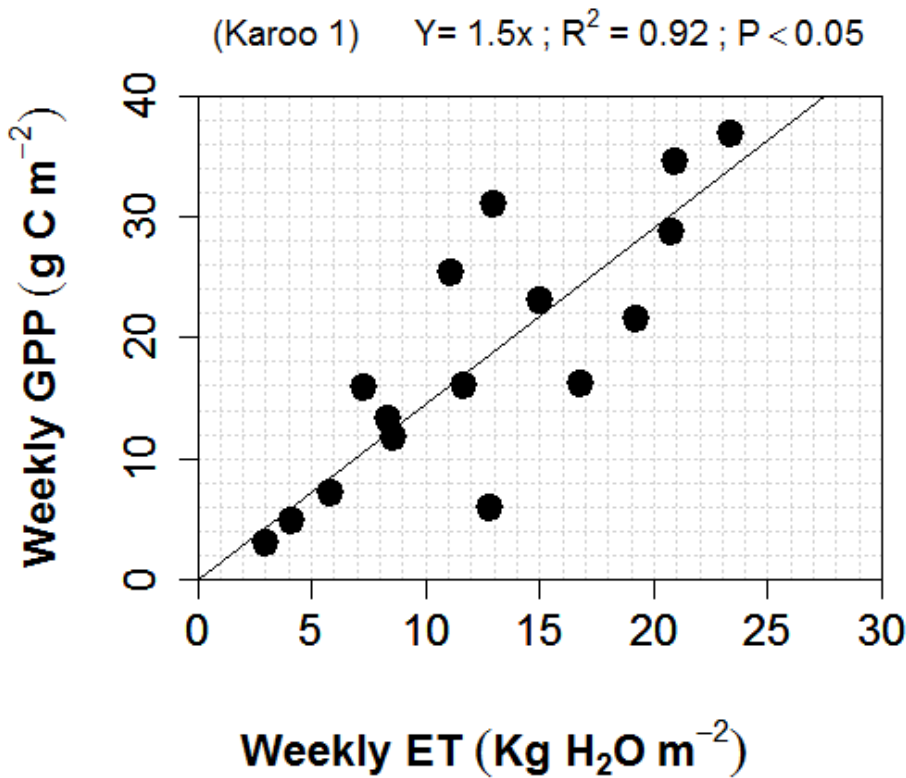
Figure 3. 40: Karoo 1 ecosystem water use efficiency for vegetative functional season 2016/2017. Period of assessment from 29 December 2016 to 18 April 2017.

Figure 3.41 shows the EWUE of Karoo 2 for the vegetative functional season of 2016/2017. Ecosystem water use efficiency was about 1.6 g C kg^{-1} H$_2$O (Fig. 3.40) compared to 1.5 g C kg^{-1} H$_2$O at Karoo 1 during the same period. The maximum weekly ET attained during the growing season of year 2 at Karoo 2 was 23 kg H$_2$O m^{-2}, which was the same weekly ET peak that was observed at the site during year 1 and also at Karoo 2 during year 2. Peak weekly GPP reached at Karoo 2 during year 2 was 39 g C m^{-2} (compared to a lower peak weekly GPP of 29 g C m^{-2} attained at the same site during year 1). Comparing the peak (weekly) GPP values of the two Karoo sites during year 2, Karoo 1 had a lower GPP peak (i.e., 37 g C m^{-2}) than that at Karoo 2 (i.e., 39 g C m^{-2}). However, the difference in EWUE between Karoo 1 and Karoo 2 during year 2 was not significant (P > 0.05).
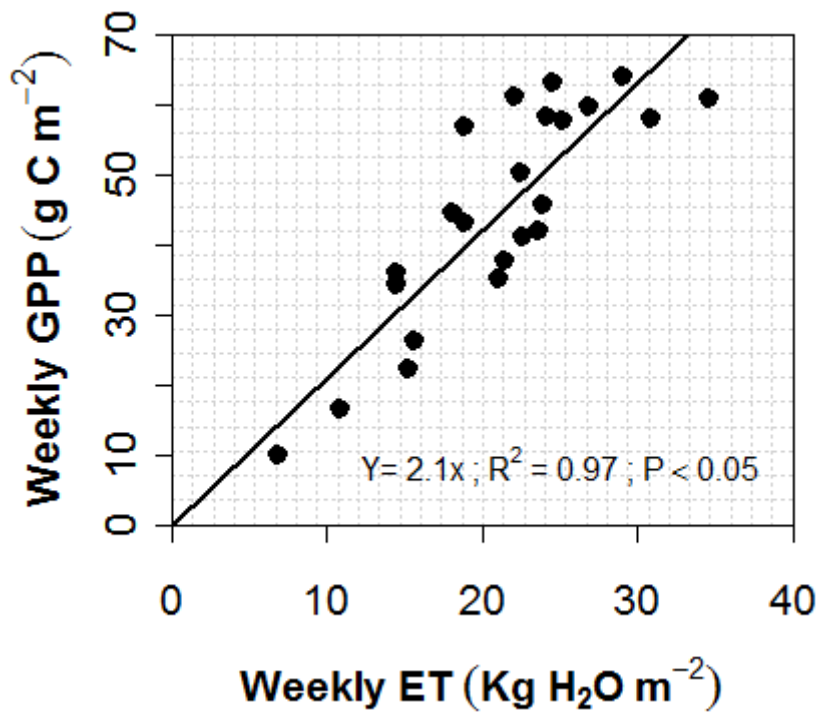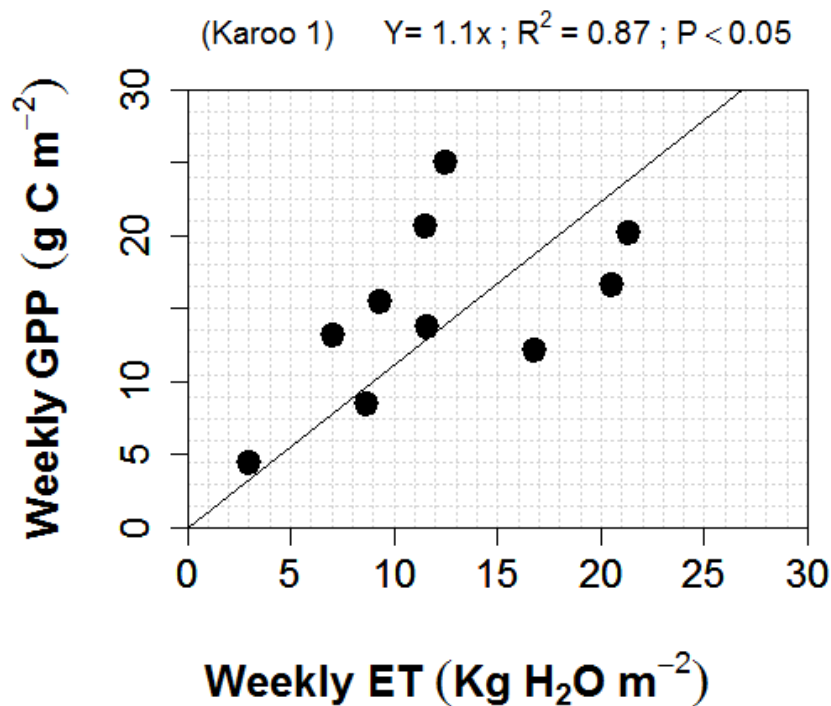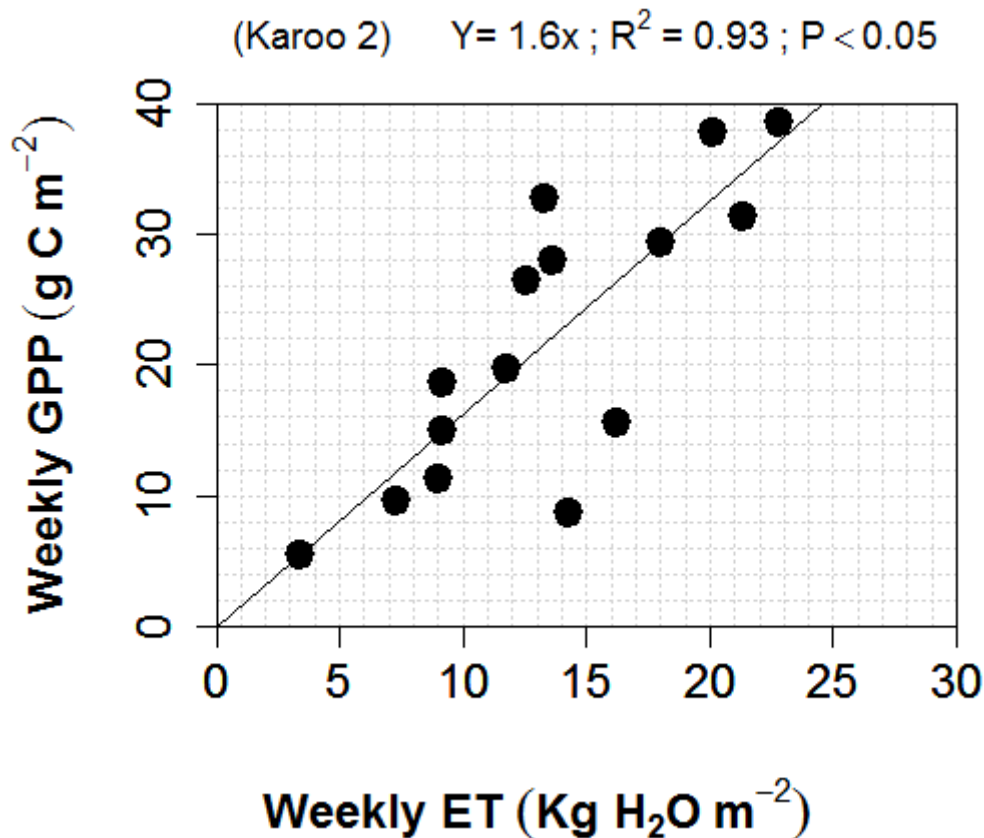
Figure 3.41: Karoo 2 ecosystem water use efficiency for vegetative functional season 2016/2017. Period of assessment from 29 December 2016 to 15 April 2017.

At Karoo 2, the increase in rainfall from year 1 to year 2 was also accompanied by augmentation of productivity and a slight increase in EWUE (from 1.2 to 1.6 g C kg^{-1} H_2O) although the difference in EWUE between the years was not significant ($P > 0.05$).

In summary, yearly comparisons of EWUE between the gently grazed site (Karoo 1) and the rested site (Karoo 2) showed no significant differences between the two Karoo sites and between the years for each Karoo site. Nevertheless, an increase in rainfall and productivity from year 1 to year 2 at the Karoo sites slightly increased EWUE. At the Skukuza site, with relatively higher rainfall and productivity compared to the Karoo sites, EWUE was higher than at the Karoo sites. Ecosystem water use efficiency for the vegetative functional season ranged from 1.1 to 1.6 g C kg^{-1} H_2O at the semi-arid Karoo sites to a range of 2.1 to 2.2 g C kg^{-1} H_2O at the semi-arid Skukuza site. A significant difference in EWUE was found between Skukuza and the Karoo sites ($P < 0.05$).

Micro-climatic conditions and rates of ecosystem productivity between the Karoo and Skukuza sites seemed to have influenced the significant differences in EWUE. Triggs et al. (2004) found a higher increase in EWUE under wet conditions compared to under dry conditions. A lower EWUE is expected with decreasing soil moisture conditions and increasing vapor pressure deficit (Massmann et al., 2018). Yu et al. (2017) also observed drought-induced reductions in EWUE in a wider range of land cover types, although in some cases (under water-limitation) plants may increase EWUE as an adaptation to unfavorable environmental conditions (Yu et al., 2017). Yang et al. (2016) found contrasting responses of EWUE to drought between arid and semi-arid ecosystems whereby EWUE increased with drought in many arid ecosystems and decreased with drought in many semi-arid ecosystems. The variability of EWUE can be influenced by plant functional types and environmental conditions (Schulze et al., 1987; Tang et al., 2015).

Plant functional types (mainly dwarf shrubs mixed with grasses and herbs) and meteorological conditions were generally similar. There were no significant differences in EWUE (P < 0.05) between Karoo 1 and Karoo 2 for year 1 and year 2. However, Karoo 2 had relatively higher EWUE compared to Karoo 1 most likely due to the observed differences in vegetation structure, composition and cover (see appendix 1) as a result of livestock grazing intensity differences. The longer rest of about 8 years at Karoo 2 had relatively improved vegetation cover and occurrence of grasses while Karoo 1 appeared to be shrubbier due to the current grazing. The ratio of grasses to woody vegetation may cause differences in carbon uptake behaviour (Scanlon and Albertson, 2004). Pickup (1996) observed that lower water use efficiency is associated with land degradation and loss of resilience.

In a semi-arid Demokeya site in Sudan, with a long-term annual rainfall of 320 mm, water use efficiencies of 3.9 g C kg^{-1} H$_2$O and 2.4 g C kg^{-1} H$_2$O, based on daily data, were observed during the dry and wet seasons, respectively (Ardö et al., 2008). In the study by Yang et al. (2016), EWUE ranged from 0.5 g C kg^{-1} H$_2$O in arid regions of North Africa, Central Euro-Asia and South America to 4 g C kg^{-1} H$_2$O in humid areas of Western Europe. The EWUE of Karoo and Skukuza sites seemed to fall within the ranges found in similar ecosystems elsewhere according to Yang et al. (2016). The wet season EWUE of Demokeya was higher than the EWUE at Karoo

sites, which had a relatively higher mean long-term annual rainfall of 374 mm. The wet season EWUE of Demokeya was also slightly higher than the EWUE at a much more relatively wetter Skukuza site (with long-term annual rainfall of 550 mm) for both 2009/2010 and 2010/2011 vegetative functional seasons. Demokeya is a sparse acacia savanna ecosystem (Sjöström et al., 2009) while Skukuza is a savanna dominated by broad-leaved *Combretum apiculatum* and fine-leaved *Acacia nigrescens*. Similarly, Scanlon and Albertson, (2004) found a lower EWUE at a wetter site, Mongu in Zambia – a Mopane woodland with mean annual rainfall of 879 mm, compared to EWUE at a dryer site, Tshane in Botswana – with mean annual rainfall of 365 mm. This further demonstrates that factors like vegetation type may pose a much stronger effect which can override the effects of site climatic differences on EWUE.

3.8 Surface energy balance at Karoo sites

The effect of livestock grazing intensity on surface energy balance closure (EBC) was examined at the Karoo sites for year 1 and year 2. The EBC offers the possibility to evaluate whether there was an under-estimation of the turbulent energy fluxes (H + LE) or over-estimation of the available energy ($Rn - G_0$). In addition, it also makes it possible to determine the effect of livestock grazing intensity (Karoo 1 vs Karoo 2) on EBC, as site differences can cause variability in energy balance closure (Wilson et al., 2002).

Soil heat storage was accounted for in the analysis of EBC as it is an important parameter in arid and semi-arid areas generally characterized by dry soils and low canopy cover or largely bare soils (Liebethal et al., 2005; Verhoef, 2004). As expected, ground heat flux (G_0, a combination of soil heat flux + soil heat storage) closely followed the net radiation (Rn) in a linear fashion (graphs not presented here) as the Karoo vegetation is short and homogeneous and there is not much shading from the vegetation. The ground heat flux followed the seasonal pattern of temperature changes at the Karoo sites. By comparison, Karoo 1 had relatively higher ground heat flux compared to Karoo 2. Nevertheless, the differences in ground heat flux between Karoo 1 and Karoo 2 for year 1 and year 2 were not significant ($P > 0.05$). Similarly, soil heat flux and soil heat storage were relatively higher in magnitude at Karoo 1 compared to Karoo 2, although the differences were not significant ($P > 0.05$) for year 1 and year 2.

It should also be noted that due to unavailability of soil temperature data for some of the periods, year 1 experienced more gaps of soil heat storage/ground heat flux than year 2 at Karoo 1 and Karoo 2 (Fig. 3.42). For instance, percentage gaps for soil heat storage for year 1 were 76 % and 74 % for Karoo 1 and Karoo 2, respectively. For year 2, percentage gaps for soil heat storage were 36 % and 35 % for Karoo 1 and Karoo 2, respectively.

Figure 3.42 shows the time series of the half hourly soil heat flux, soil heat storage and ground heat flux from 01 November 2015 to 31 October 2017. At Karoo 1 and Karoo 2, ground heat flux over the 2-year course of measurement ranged from -70 W m^{-2} to 132 W m^{-2} and -54 W m^{-2} to 128 W m^{-2}, respectively. Soil heat flux ranged from -55 W m^{-2} to 115 W m^{-2} and -49 W m^{-2} to 110 W m^{-2}, at Karoo 1 and Karoo 2, respectively. The range of soil heat storage at Karoo 1 and Karoo 2 were -36 W m^{-2} to 34 W m^{-2} and -24 W m^{-2} to 24 W m^{-2}, respectively.
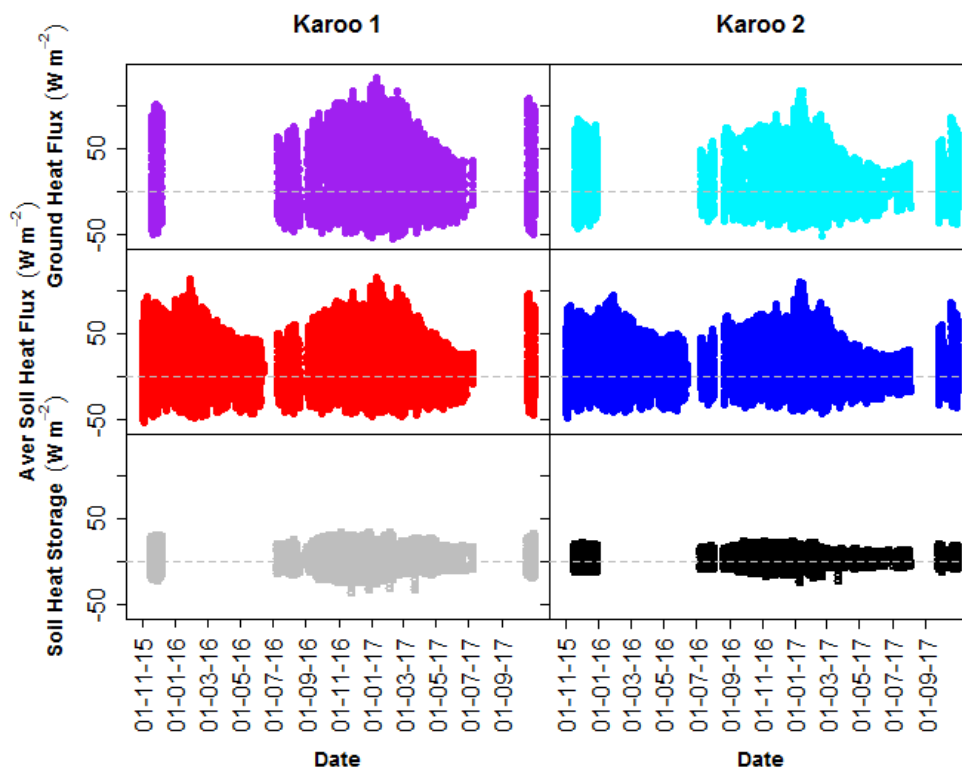
Figure 3.42: Time series of half hourly surface energy balance components (Ground heat flux, average soil heat flux and soil heat storage within 10 cm soil depth) over a 2-year period at Karoo 1 and Karoo 2. The average (aver) soil heat flux is based on four soil heat flux plates buried at 10 cm depth.

Since Karoo 1 and Karoo 2 had similar climatic conditions, the slight difference in ground heat flux between Karoo 1 and Karoo 2 may be an indication of the potential influence of livestock grazing intensity on vegetation characteristics and soil thermal properties that ultimately controls the dynamics of ground heat flux. As Gan et al. (2012) found, grazing pressure may alter fluxes of mass and energy in an ecosystem.

With regards to EBC, the slope of the regression fits of available energy (Rn-G_0) and turbulent energy flux (H+LE) was considered as the percentage of the EBC. The regression fits for all cases examined were significant ($P < 0.05$). When soil heat storage was included in energy balance calculations, energy balance closures of Karoo 1 and Karoo 2 during year 1 were 65 % and 60 %, respectively, which is a small difference of 5 % between the two Karoo sites. Despite the short vegetation at both Karoo sites, Karoo 2 seemed to have relatively higher vegetation cover compared to Karoo 1 due to resting (see appendix 1). Future studies may therefore need to investigate canopy heat storage at Karoo 1 and Karoo 2 in order to ascertain if small differences in vegetation cover may also have an influence on the overall energy balance. Generally, soil heat storage is considered as the most important storage flux but Masseroni et al. (2014) also showed an improvement in EBC when all storage terms are accounted for.

Figure 3.43 shows EBC of Karoo 1 (K1) and Karoo 2 (K2) for hydro-ecological years 2015/2016 (year 1) and 2016/2017 (year 2); after inclusion of soil heat storage, without inclusion of soil heat storage and the effect of rainfall on EBC of selected days at the two sites.
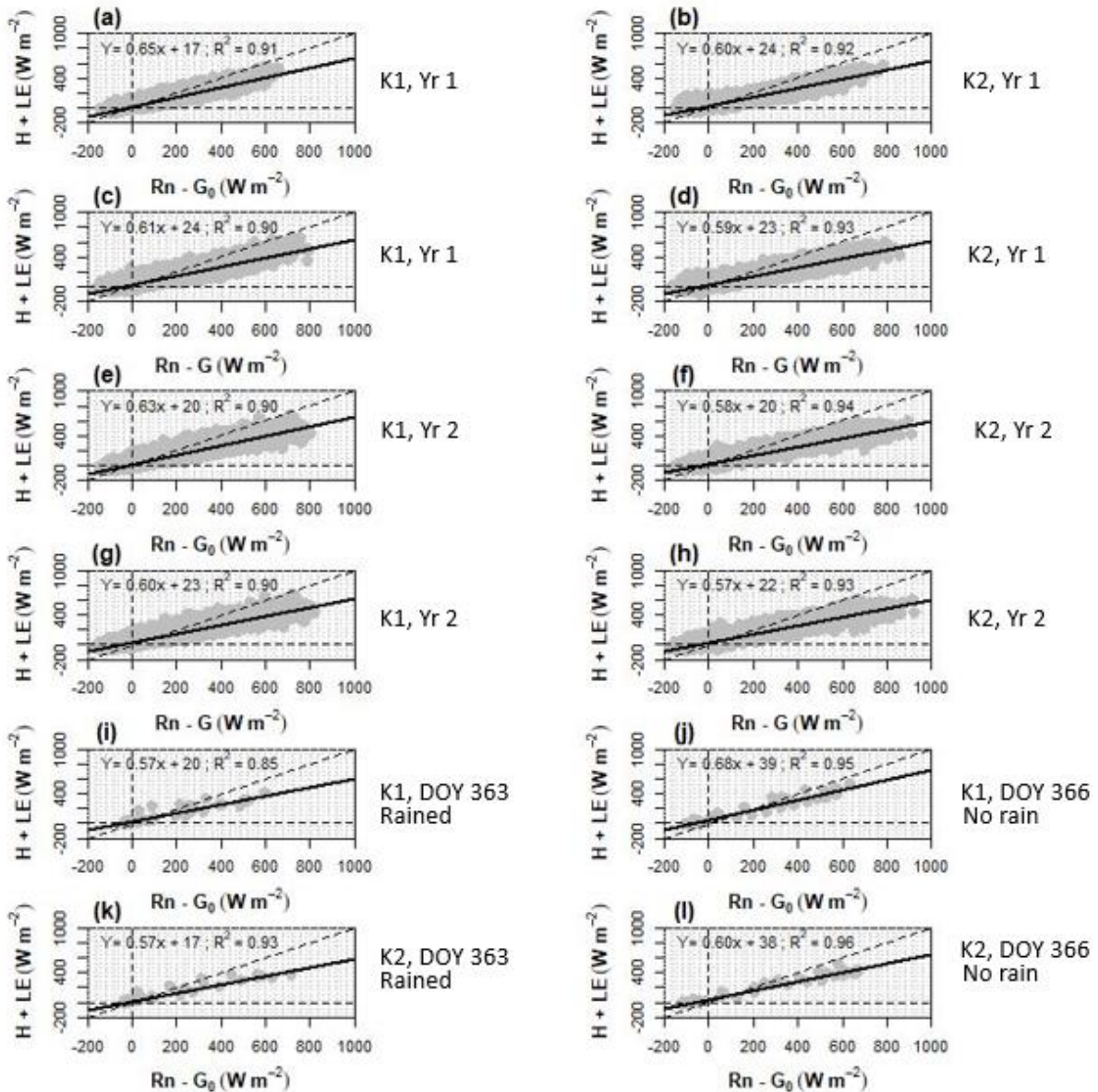
Fig. 3.43. Energy balance closures for Karoo 1 and Karoo 2: (i) with inclusion of soil heat storage component for hydro-ecological years 2015/2016 (a, b) and 2016/2017 (e, f); (ii) without inclusion of soil heat storage component for hydro-ecological years 2015/2016 (c, d) and 2016/2017 (g, h); and (iii) energy balance closures of two selected days with rain and without rain at Karoo 1 during year 2 (i, j) and at Karoo 2 during year 2 (k, l). Day of year (DOY) 363 in 2016 received a total rainfall of 23.7 mm and DOY 366 in 2016 was without rain at Karoo 1. Day of year (DOY) 363 in 2016 received a total rainfall of 25.8 mm and DOY 366 in 2016 was without rain at Karoo 2. Plots (a – h) are based on half hourly data from 01.11.2015 to 31.10.2016. Rn = net radiation, G_0 = Ground heat flux, H = sensible heat flux and LE = latent heat flux, Yr 1 = year 1, Yr 2 = year 2.

After inclusion of soil heat storage during year 1, the turbulent and available energy fluxes were positively linearly correlated, with coefficients of determination of $R^2 = 0.91$ and $R^2 = 0.92$ and intercepts of 17 W/m^2 and 24 W/m^2 for Karoo 1 and Karoo 2, respectively (Fig. 3.43 a, b). By not accounting for soil heat storage in the soil layer above the soil heat flux plates at 10 cm depth, lower surface energy balance closures of 61 % and 59 % were obtained at Karoo 1 and Karoo 2, respectively, during year 1 (Fig. 3.43 c, d). The turbulent energy flux linearly correlated with the available energy flux with coefficients of determination of $R^2 = 0.90$ and $R^2 = 0.93$ and intercepts of 24 W/m^2 and 23 W/m^2 for Karoo 1 and Karoo 2, respectively (Fig. 3.43 c, d).

During the second year and after inclusion of soil heat storage, the surface energy balance closures of Karoo 1 and Karoo 2 were 63 % and 58 %, respectively (Fig. 3.43 e, f). Like in year 1, a difference of 5 % in EBC between Karoo 1 and Karoo 2 was found during year 2. A positive linear correlation was found between turbulent and availably energy fluxes with coefficients of determination of $R^2 = 0.90$ and $R^2 = 0.94$ and intercepts of 20 W/m^2 and 20 W/m^2 for Karoo 1 and Karoo 2, respectively (Fig. 3.43 e, f).

Without accounting for soil heat storage during year 2, lower surface energy balance closures of 60 % and 57 % were obtained for Karoo 1 and Karoo 2, respectively, giving a 3 % difference in EBC between the two sites (Fig. 3.43 g, h). The turbulent energy flux was positively linearly correlated with the available energy flux with coefficients of determination of $R^2 = 0.90$ and $R^2 = 0.93$ and intercepts of 23 W/m^2 and 22 W/m^2 for Karoo 1 and Karoo 2, respectively.

In summary, it appears that the EBC of the rested site (Karoo 2) was lower than that of the gently grazed site (Karoo 1) by 5 % for both year 1 and year 2 when soil heat storage was accounted for in energy balance closure assessment. Energy balance closures of 65 % (Karoo 1) and 60 % (Karoo 2) were obtained during year 1 while the EBCs of year 2 were 63 % and 58 % for karoo 1 and Karoo 2, respectively. The EBCs of Karoo 1 and Karoo 2 for year 2 were relatively lower than the Year 1 EBC estimates by 2 %. The fact that year 2 was wetter than year 1 at the Karoo sites could be the reason why the EBCs of year 2 were relatively lower than the EBCs of year 1 by 2 %. By not accounting for soil heat storage, EBCs of Karoo 1 and Karoo 2 for year 1 were 61 % and 59 %, respectively, while the EBCs of Karoo 1 and Karoo 2 for year

2 were 60 % and 57 %, respectively. Accounting for soil heat storage between the surface and the heat flux plate at 10 cm depth improved EBC of Karoo 1 by 4 % and 3 % for year 1 and year 2, respectively. At Karoo 2, accounting for soil heat storage improved EBC slightly by 1 % for both year 1 and year 2. Soil heat storage is considered as an important component that can improve EBC (Foken, 2008; Masseroni et al., 2014). In a study conducted by Majozi et al. (2017a) in an African semi-arid savanna ecosystem, exclusion of soil heat storage resulted in underestimation of the EBC by 7 %. In a boreal ecosystem Sánchez et al. (2010) reported an EBC improvement of 6 % after inclusion of the storage term.

The linear regression intercept is a reflection of systematic errors in fluxes (Masseroni et al., 2014). To a greater extent accounting for soil heat storage generally decreased the regression intercepts. For instance, with the exception of Karoo 2 during year 1 (Figs 3.43 b, d), after inclusion of soil heat storage, the regression intercepts for Karoo 1 (year 1) decreased from 24 W/m^2 (Fig. 3.43 c) to 17 W/m^2 (Fig. 3.43 a). For year 2, the inclusion of soil heat storage decreased the regression intercepts from 23 W/m^2 (Fig. 3.43 g) to 20 W/m^2 (Fig. 3.43 e) and from 22 W/m^2 (Fig. 3.43 h) to 20 W/m^2 (Fig. 3.43 f) for Karoo 1 and Karoo 2, respectively. A general decrease of the regression intercept with inclusion of storage terms was also reported by Masseroni et al. (2014).

Using the annual datasets and accounting for soil heat storage, the overall EBC error (or imbalance) ranged from 35 % to 37 % at Karoo 1 and 40 % to 42 % at Karoo 2. At a woodland savanna site in Maun (Botswana), an imbalance of 25 % of the EBC was found (Veenendaal et al., 2004). At various flux measurement sites, non-closure of the energy balance has been reported as a common problem and EBC imbalance range of 10 to 40 % has been observed (Foken, 2008; Foken and Oncley, 1995; Wilson et al., 2002).

While Karoo 1 (gently grazed site) had a relatively higher EBC estimate compared to Karoo 2 (rested site), livestock grazing intensity cannot be regarded as the main cause of the small difference in EBC between the two Karoo sites. Additionally, grazing intensity may also not be the main reason for the high EBC error at the Karoo sites as there are numerous other possible causes of energy imbalance that were not examined in this study due to time constraints.

Besides investigating soil heat storage, an attempt was made to examine the effect of rain on EBC. Bagayoko et al. (2006) mentioned that precipitation events may also cause errors in measurement of fluxes due to sensitivity of the EC system to rain. On a rainy-day (DOY 363), the coefficient of determination (R^2) and EBC were lower than on DOY 366 (with no rain) during year 2 at Karoo 1 (i.e., 0.85 and 57 % compared to 0.95 and 68 %, respectively) (Figure 3.43 i, j). Similarly, at Karoo 2 the EBC and coefficient of determination on DOY 363 (rainy day) during year 2 were 57 % and 0.93, respectively, while on DOY 366 (with no rain) they increased to 60 % and 0.96, respectively (Figure 3.43 k, l). This implies that further improvement in the energy balance closure of the Karoo sites can be possible by addressing additional sources of errors that were not scrutinized in this study.

4.0 Conclusion and outlook

This study looks at the land-atmosphere fluxes of carbon dioxide and energy using the eddy covariance method. The study sites, located in South Africa, were 2 arid Karoo sites (Karoo 1 and Karoo 2) managed under different livestock grazing intensities; and Skukuza, a near-natural semi-arid savanna site under wildlife conservation. The Karoo sites were established in October 2015 and flux measurements over a period of two years were used in this study. The Skukuza site has long-term flux datasets of over a decade but data from 6 hydro-ecological years were used in further analyses after data screening.

The main foci of this study at Skukuza and Karoo sites were; i) to characterize 'hot moments' of ecosystem respiration efflux, which are triggered by rain pulses following the dry season; ii) to show connectivity between precipitation and carbon fluxes in determining vegetative functional seasons; and iii) to quantify the variability of EWUE at these sites. Important additional site-specific issues that were studied separately on individual sites were temporal dynamics and drivers of carbon and energy flux components at the Karoo sites, and explaining inter-annual variability and influence of main meteorological controls on light response parameters (GPP_{opt} and NEE_{offset}) at Skukuza.

Overall, this study showed a similarity in carbon fluxes (NEE, GPP, R_{eco}), EWUE and ground heat flux between the gently grazed site (Karoo 1) and the rested site (Karoo 2) for hydro-ecological years 2015/2016 and 2016/2017. The observed relative differences in carbon and energy fluxes at the Karoo sites were attributed to site management, without confounding influences of meteorological variability, as the meteorological conditions of Karoo 1 and Karoo 2 were similar. Notwithstanding the resemblance in the magnitudes of CO_2 fluxes between the Karoo sites, Karoo 2 (rested site) showed signs of improvement in vegetation cover as depicted by a relatively higher carbon sink strength compared to Karoo 1 during year 2. A long rest of 8 years at Karoo 2 may have improved carbon sequestration as fixed-point photos showed a higher ground cover at Karoo 2 compared to Karoo 1. Thus, in the long term, land use management may have an effect on plant physiological processes that may lead to significant changes in the rates of carbon metabolism at the dry Karoo ecosystems. Understanding the carbon sink/source strengths of the Karoo sites under the influence of climate change and land use disturbance is not only important for understanding the role of such ecosystems in the global carbon cycle, but also for developing sustainable livestock management practices and policies that protect the ecosystems in the long term. However, in order to determine the optimum resting period for maximum carbon sequestration, sustainable grazing and pasture improvement, continuous monitoring and further trials on the effects of various levels of grazing intensities on carbon and energy exchange components are needed. Other considerations which were overlooked in this study include veld condition assessment, among others.

Mean daily net carbon uptake at Karoo 1 and Karoo 2 during the vegetative functional season were generally similar to those of other semi-arid areas such as Demokeya (Sudan) and Hapex (Niger) in Africa. Interestingly, a drier desert shrub ecosystem in Mexico (which had received annual precipitation of 197 mm in 2003) produced an annual carbon balance estimate similar to that of Karoo 2 during the 2016/2017 hydro-ecological year (which had received an annual precipitation of 406 mm). The desert shrub ecosystem also had a similar mean daily carbon uptake similar to Karoo 1 during the wet season of 2015/2016 hydro-ecological year (which had received an annual precipitation of 352 mm). This shows that the magnitude of annual rainfall alone may not be adequate to explain differences in carbon fluxes among sites, but consideration of other ecosystem characteristics and functional properties may be needed.

The inclusion of soil heat storage resulted in improvement of the EBC by a range from $1 - 4$ % at the Karoo sites over the 2 years of measurement proving that it is an important component to consider in energy balance closure assessments. The exclusion of rain days, which may cause errors in measurement of fluxes, also slightly improved the EBC. In this study, a slight difference in EBC error between the Karoo sites could not be ascribed to livestock grazing intensity as there were other possible causes of energy imbalance that were not examined in this study due to time constraints. Therefore, further improvement in the energy balance closure of the Karoo sites can be possible by addressing additional sources of errors that were not examined in this study.

Over the two years of measurements at the Karoo sites, EWUE was similar between the rested site and the gently grazed site, leading to the conclusion that livestock grazing intensity had an insignificant impact in modifying either site hydrological aspects such as ET, or carbon assimilation rates at Karoo. The EWUE of Skukuza, a near-natural semi-arid savanna ecosystem with a mean annual precipitation of 550 mm, surpassed that observed at both Karoo sites in a significant manner demonstrating that an increase in rainfall and change in vegetation type may influence ecosystem function and govern the dynamics of productivity in semi-arid areas.

Regarding the connectivity between precipitation and CO_2 fluxes, a minimum precipitation threshold of at least 3 mm triggered a hot moment of CO_2 efflux at the gently grazed site while a minimum precipitation threshold of at least 1 mm triggered CO_2 efflux at the rested site. Hot moments of CO_2 efflux were not distinct in Skukuza due to increased rainfall and less occurrence of isolated rain pulses. The findings of this study on rain pulses and ecosystem respiration spikes under the influence of livestock grazing at the Karoo sites have implications on estimating annual carbon budgets under different livestock grazing intensities.

Establishing the connectivity between precipitation and CO_2 fluxes in timing the onset of vegetative functional seasons at Skukuza and Karoo sites is an approach that can also be applied in modelling primary productivity of dry and semi-arid areas. Methods that use accumulated

rainfall totals (Marteau et al., 2009; Sivakumar, 1988) provided the basis for separating 'false starts' of the growing season and the onset of productive rains leading to the onset of vegetative functional seasons. As a result, precipitation thresholds that triggered the onset of vegetative functional seasons from the onset of productive rains were determined. For instance, this study identified minimum precipitation thresholds of 33.9 mm, 40.8 mm and 52.8 mm for Karoo1, Karoo 2 and Skukuza, respectively, by way of relating productive precipitation and CO_2 fluxes. In order to obtain long-term average precipitation thresholds for the onset of vegetative functional seasons, continuous long-term monitoring of precipitation and CO_2 fluxes is needed.

The NDVI and EVI during the vegetative functional seasons of year 1 and year 2 showed no significant differences between Karoo 1 and Karoo 2. However, more work may be needed on the ground to compliment the basic information provided by the MODIS remote sensing products. Additional field verifications and vegetation assessments may include measurements of vegetation floristic composition, leaf area index, canopy type and structure, and status of land degradation. To increase the accuracy in measurement of vegetation greenness metrics for dry and semi-arid savanna areas, future studies may also need to explore the new possibilities of using high resolution optical remote sensing datasets such as Landsat (e.g., 30 m, 15 m pan-sharpened) or Sentinel-2 (e.g., 10 m, 20 m and 60 m), among others. These tools may prove particularly useful considering that the typical spectral mixing within the heterogeneous savanna - with mixed grasses, herbs, shrubs and trees - might not be well captured at coarse resolutions by MODIS.

Finally, flux measurements over a period of 6 hydro-ecological years at Skukuza revealed clear distinctions in the annual variability of light response parameters (i.e., GPP_{opt} and NEE_{offset}), especially between years of above-average precipitation and drought years. The uniqueness of this study was the stratification of vegetative functional seasons' dataset into various soil moisture and air temperature classes before the estimation of GPP_{opt} and NEE_{offset} in order to separate physiologically active periods from non-active periods and separate temperature effects on NEE response to light. The main control of the variability of GPP_{opt} and NEE_{offset} was found to be soil moisture, while air temperature and vapour pressure deficit did not show a clear relationship with the light response parameters. These results are consistent with previous studies in semi-arid savannas that mentioned water as the main driver of ecosystem processes. This study provides novel insight that could also be important for benchmarking

models of ecosystem function. Monitoring of GPP_{opt} and NEE_{offset} is also of importance for studies of land-atmosphere carbon exchange processes and may contribute to climate policy-making.

References

Abu-Hamdeh, N.H., 2003. Thermal properties of soils as affected by density and water content. Biosyst. Eng. 86, 97–102. https://doi.org/10.1016/S1537-5110(03)00112-0

Acocks, J.P.H., 1988. Veld types of South Africa, Third. ed. Botanical Research Institute, Pretoria, South Africa.

Adole, T., Dash, J., Atkinson, P.M., 2018. Large-scale prerain vegetation green-up across Africa. Glob. Change Biol. 24, 4054–4068. https://doi.org/10.1111/gcb.14310

Ago, E.E., Agbossou, E.K., Cohard, J.-M., Galle, S., Aubinet, M., 2016. Response of CO_2 fluxes and productivity to water availability in two contrasting ecosystems in northern Benin (West Africa). Ann. For. Sci. 73, 483–500. https://doi.org/10.1007/s13595-016-0542-9

Ago, E.E., Agbossou, E.K., Galle, S., Cohard, J.-M., Heinesch, B., Aubinet, M., 2014. Long term observations of carbon dioxide exchange over cultivated savanna under a Sudanian climate in Benin (West Africa). Agric. For. Meteorol. 197, 13–25. https://doi.org/10.1016/j.agrformet.2014.06.005

Ahlström, A., Raupach, M.R., Schurgers, G., Smith, B., Arneth, A., Jung, M., Reichstein, M., Canadell, J.G., Friedlingstein, P., Jain, A.K., Kato, E., Poulter, B., Sitch, S., Stocker, B.D., Viovy, N., Wang, Y.P., Wiltshire, A., Zaehle, S., Zeng, N., 2015. The dominant role of semi-arid ecosystems in the trend and variability of the land CO2 sink. Science 348, 895–899. https://doi.org/10.1126/science.aaa1668

Archibald, S., Kirton, A., Merwe, M. van der, Scholes, R.J., Williams, C.A., Hanan, N., 2008. Drivers of interannual variability in Net Ecosystem Exchange in a semi-arid savanna ecosystem, South Africa. Biogeosciences Discuss. 5, 3221–3266.

Archibald, S., Scholes, R. j., 2007. Leaf green-up in a semi-arid African savanna -separating tree and grass responses to environmental cues. J. Veg. Sci. 18, 583–594. https://doi.org/10.1111/j.1654-1103.2007.tb02572.x

Archibald, S.A., Kirton, A., van Der Merwe, M.R., Scholes, R.J., Williams, C.A., Hanan, N., 2009. Drivers of inter-annual variability in Net Ecosystem Exchange in a semi-arid savanna ecosystem, South Africa. Biogeosciences 251–266.

Ardö, J., Mölder, M., El-Tahir, B.A., Elkhidir, H.A.M., 2008. Seasonal variation of carbon fluxes in a sparse savanna in semi arid Sudan. Carbon Balance Manag. 3. https://doi.org/10.1186/1750-0680-3-7

Arneth, A., Veenendaal, E.M., Best, C., Timmermans, W., Kolle, O., Montagnani, L., Shibistova, O., 2006. Water use strategies and ecosystem-atmosphere exchange of CO_2 in two highly seasonal environments. Biogeosciences Eur. Geosci. Union 3, 421–437. https://doi.org/10.5194/bg-3-421-2006

Arora, V., 2002. Modeling vegetation as a dynamic component in soil-vegetation-atmosphere transfer schemes and hydrological models. Rev Geophys 40, 1006. https://doi.org/10.1029/2001RG000103

Asner, G.P., Elmore, A.J., Olander, L.P., Martin, R.E., Harris, A.T., 2004. Grazing systems, ecosystem responses, and global change. Annu. Rev. Environ. Resour. 29, 261–299. https://doi.org/10.1146/annurev.energy.29.062403.102142

Ati, O.F., Stigter, C.J., Oladipo, E.O., 2002. A comparison of methods to determine the onset of the growing season in northern Nigeria. Int. J. Climatol. 22, 731–742. https://doi.org/10.1002/joc.712

Aubinet, M., Grelle, A., Ibrom, A., Rannik, Ü., Moncrieff, J., Foken, T., Kowalski, A.S., Martin, P., Berbigier, P., Bernhofer, C., Clement, R., Elbers, J.A., Granier, A., Grünwald, T., Morgenstern, K., Pilegaard, K., Rebmann, C., Snijders, W., Valentini,

R., Vesala, T., 2000. Estimates of the Annual Net Carbon and Water Exchange of Forests: The UROFLUX Methodology. Adv. Ecol. Res. 30, 113–175. https://doi.org/10.1016/S0065-2504(08)60018-5

Aubinet, M., Vesala, T., Papale, D., 2012. Eddy Covariance: A Practical Guide to Measurement and Data Analysis. Springer Science & Business Media. ISBN: 978-94-007-2350-4. Springer Dordrecht, Heidelberg, London, New York.

Austin, A.T., Yahdjian, L., Stark, J.M., Belnap, J., Porporato, A., Norton, U., Ravetta, D.A., Schaeffer, S.M., 2004. Water pulses and biogeochemical cycles in arid and semiarid ecosystems. Oecologia 141, 221–235. https://doi.org/10.1007/s00442-004-1519-1

Bagayoko, F., Yonkeu, S., van de Giesen, N.C., 2006. Energy balance closure and footprint analysis using Eddy Covariance measurements in Eastern Burkina Faso, West Africa. Hydrol. Earth Syst. Sci. Discuss. 3, 2789–2812. https://doi.org/10.5194/hessd-3-2789-2006

Bahn, M., Schmitt, M., Siegwolf, R., Richter, A., Brüggemann, N., 2009. Does photosynthesis affect grassland soil-respired CO_2 and its carbon isotope composition on a diurnal timescale? New Phytol 182, 451 – 460. https://doi.org/10.1111/j.1469-8137.2008.02755.x

Bajgain, R., Xiao, X., Wagle, P., Basara, J., Zhou, Y., 2015. Sensitivity analysis of vegetation indices to drought over two tallgrass prairie sites. ISPRS J. Photogramm. Remote Sens. 108, 151–160. https://doi.org/10.1016/j.isprsjprs.2015.07.004

Baldocchi, D., Falge, E., Gu, L., Olson, R., Hollinger, D., Running, S., Anthoni, P., Bernhofer, C., Davis, K., Evans, R., Fuentes, J., Goldstein, A., Katul, G., Law, B., Lee, X., Malhi, Y., Meyers, T., Munger, W., Oechel, W., Paw U, K.T., Pilegaard, K., Schmid, H.P., Valentini, R., Verma, S., Vesala, T., Wilson, K., Wofsy, S., 2001. FLUXNET: A New Tool to Study the Temporal and Spatial Variability of Ecosystem-Scale Carbon Dioxide, Water Vapor, and Energy Flux Densities. Bull. Am. Meteorol. Soc. 82, 2415–2434. https://doi.org/10.1175/1520-0477(2001)082<2415: FANTTS>2.3.CO;2

Baldocchi, D., Ryu, Y., Keenan, T., 2016. Terrestrial carbon cycle variability. F1000Research 5, 2371. https://doi.org/10.12688/f1000research.8962.1

Baldocchi, D.D., 2003. Assessing the eddy covariance technique for evaluating carbon dioxide exchange rates of ecosystems: past, present and future. Glob. Change Biol. 9, 479–492. https://doi.org/10.1046/j.1365-2486.2003.00629.x

Barba, J., Cueva, A., Bahn, M., Barron-Gafford, G. A., Bond-Lamberty, B., Hanson, P. J., Jaimes, A., Kulmala, L., Pumpanen, J., Scott, R. L., Wohlfahrt, G., Vargas, R. 2018. Comparing ecosystem and soil respiration: Review and key challenges of tower-based and soil measurements. Agricultural and Forest Meteorology. Volume 249. Pages 434-443. https://doi.org/10.1016/j.agrformet.2017.10.028

Barnard, P., Brown, C.J., Jarvis, A.M., Robertson, A., 1998. Extending the Namibian protected area network to safeguard hotspots of endemism and divers. Biodivers. Conserv. 7, 531–547. https://doi.org/10.1023/A:1008831829574

Biederman, J.A., Scott, R.L., Goulden, M.L., Vargas, R., Litvak, M.E., Kolb, T.E., Yepez, E.A., Oechel, W.C., Blanken, P.D., Bell, T.W., Garatuza-Payan, J., Maurer, G.E., Dore, S., Burns, S.P., 2016. Terrestrial carbon balance in a drier world: the effects of water availability in southwestern North America. Glob. Change Biol. 22, 1867–1879. https://doi.org/10.1111/gcb.13222

Birch, H.F., 1958. The effect of soil dying on humus decomposition and nitrogen availability 10, 9–31. https://doi.org/10.1007/BF01343734

Blanco, L.J., Aguilera, M.O., Paruelo, J.M., Biurrun, F.N., 2008. Grazing effect on NDVI across an aridity gradient in Argentina. J Arid Env. 72, 764–776. https://doi.org/10.1016/j.jaridenv.2007.10.003

Blunden, J., Arndt, D.S., 2016. State of the climate in 2015. Bull. Am. Meteorol. Soc. 97, Si – S275. https://doi.org/10.1175/2016BAMSStateoftheClimate.1

Bombelli, A., Henry, M., Castaldi, S., Adu-Bredu, S., Arneth, A., de Grandcourt, A., Grieco, E., Kutsch, W.L., Lehsten, V., Rasile, A., Reichstein, M., Tansey, K., Weber, U., Valentini, R., 2009. An outlook on the Sub-Saharan Africa carbon balance. Biogeosciences 6, 2193–2205. https://doi.org/10.5194/bg-6-2193-2009

Brümmer, C., Black, T.A., Jassal, R.S., Grant, N.J., Spittlehouse, D.L., Chen, B., Nesic, Z., Amiro, B.D., Arain, M.A., Barr, A.G., Bourque, C.P.-A., Coursolle, C., Dunn, A.L., Flanagan, L.B., Humphreys, E.R., Lafleur, P.M., Margolis, H.A., McCaughey, J.H., Wofsy, S.C., 2012. How climate and vegetation type influence evapotranspiration and water use efficiency in Canadian forest, peatland and grassland ecosystems. Agric. For. Meteorol. 153, 14–30. https://doi.org/10.1016/j.agrformet.2011.04.008

Brümmer, C., Falk, U., Papen, H., Szarzynski, J., Wassmann, R., Brüggemann, N., 2008. Diurnal, seasonal, and interannual variation in carbon dioxide and energy exchange in shrub savanna in Burkina Faso (West Africa). J. Geophys. Res. Biogeosciences 113, 1–11. https://doi.org/10.1029/2007JG000583

Buitenwerf, R., Swemmer, A.M., Peel, M.J.S., 2011. Long-term dynamics of herbaceous vegetation structure and composition in two African savanna reserves: Effects of rainfall on herbaceous vegetation. J. Appl. Ecol. 48, 238–246. https://doi.org/10.1111/j.1365-2664.2010.01895.x

Burba, G., 2013. Eddy covariance method for scientific, industrial, agricultural, and regulatory applications: a field book on measuring ecosystem gas exchange and areal emission rates. LI-COR Biosciences, Lincoln, Nebraska, 331pp. ISBN: 978-0-615-76827-4.

Burba, G., Anderson, D., 2010. A Brief Practical Guide to Eddy Covariance Flux Measurements: Principles and Workflow Examples for Scientific and Industrial Applications. LI-COR Biosciences, Lincoln, USA, Hard- and Softbound, 211pp. ISBN: 978-0-61543013-3.

Carbone, M.S., Still, C.J., Ambrose, A.R., Dawson, T.E., Williams, A.P., Boot, C.M., Schaeffer, S.M., Schimel, J.P., 2011. Seasonal and episodic moisture controls on plant and microbial contributions to soil respiration. Oecologia 167, 265–278. https://doi.org/10.1007/s00442-011-1975-3

Cava, D., Contini, D., Donateo, A., Martano, 2008. Analysis of short-term closure of the surface energy balance above short vegetation. Agric. For. Meteorol. 148, 82–93.

Cernusak, L.A., Winter, K., Dalling, J.W., Holtum, J.A.M., Jaramillo, C., Körner, C., Leakey, A.D.B., Norby, R.J., Poulter, B., Turner, B.L., Wright, S.J., 2013. Tropical forest responses to increasing atmospheric CO_2: current knowledge and opportunities for future research. Funct. Plant Biol. 40, 531. https://doi.org/10.1071/FP12309

Chapin, F.S., Woodwell, G.M., Randerson, J.T., Rastetter, E.B., Lovett, G.M., Baldocchi, D.D., Clark, D.A., Harmon, M.E., Schimel, D.S., Valentini, R., Wirth, C., Aber, J.D., Cole, J.J., Goulden, M.L., Harden, J.W., Heimann, M., Howarth, R.W., Matson, P.A., McGuire, A.D., Melillo, J.M., Mooney, H.A., Neff, J.C., Houghton, R.A., Pace, M.L., Ryan, M.G., Running, S.W., Sala, O.E., Schlesinger, W.H., Schulze, E.-D., 2006. Reconciling carbon-cycle concepts, terminology, and methods. Ecosystems 9, 1041–1050. https://doi.org/10.1007/s10021-005-0105-7

Chen, S., Lin, G., Huang, J., He, M., 2008. Responses of soil respiration to simulated precipitation pulses in semiarid steppe under different grazing regimes. J. Plant Ecol. 1, 237–246. https://doi.org/10.1093/jpe/rtn020

Chen, Z., Yu, G., Ge, J., Sun, X., Hirano, T., Saigusa, N., Wang, Q., Zhu, X., Zhang, Y., Zhang, J., Yan, J., Wang, H., Zhao, L., Wang, Y., Shi, P., Zhao, F., 2013. Temperature and precipitation control of the spatial variation of terrestrial ecosystem carbon

exchange in the Asian region 182–183, 266–276.
https://doi.org/10.1016/j.agrformet.2013.04.026

Ciais, P., Bombelli, A., Williams, M., Piao, S.L., Chave, J., Ryan, C.M., Henry, M., Brender, P., Valentini, R., 2011. The carbon balance of Africa: synthesis of recent research studies. Philos. Trans. R. Soc. Math. Phys. Eng. Sci. 369, 2038–2057. https://doi.org/10.1098/rsta.2010.0328

Davis-Reddy, C.L., Vincent, K., 2017. Climate Risk and Vulnerability: a Handbook for Southern Africa (2nd edition). CSIR, Pretoria, South Africa.

Dean, W.R.J., Milton, S.J., 1999. The Karoo ecological patterns and processes. Cambridge University Press, Cambridge, UK.; New York, NY, USA.

Devine, A.P., McDonald, R.A., Quaife, T., Maclean, I.M.D., 2017. Determinants of woody encroachment and cover in African savannas. Oecologia 183, 939–951. https://doi.org/10.1007/s00442-017-3807-6

Diaz, S., Lavorel, S., de Bello, F., Quetier, F., Grigulis, K., Robson, T.M., 2007. Incorporating plant functional diversity effects in ecosystem service assessments. Proc. Natl. Acad. Sci. 104, 20684–20689. https://doi.org/10.1073/pnas.0704716104

Du Toit, J.C.O., 2010. An analysis of long-term daily rainfall data from Grootfontein, 1916 to 2008. Grootfontein Agric 10, 24–36.

Du Toit, J.C.O., O'Connor, T.G., 2014. Changes in rainfall pattern in the eastern Karoo, South Africa over the past 123 years. Water SA 40, 453 – 460. http://dx.doi.org/10.4314/wsa.v40i3.8

Du Toit, J.C.O., van den Berg, L., O'Connor, T.G., 2015. Fire effects on vegetation in a grassy dwarf shrubland at a site in the eastern Karoo, South Africa. Afr. J. Range Forage Sci. 32, 13–20. https://doi.org/10.2989/10220119.2014.913077

Du Toit, G. vanN., Snyman, H.A., Malan, P.J., 2011. Physical impact of sheep grazing on arid Karoo subshrub/grass rangeland, South Africa. South Afr. J. Anim. Sci. 41. https://doi.org/10.4314/sajas.v41i3.11

Emmerich, W.E., 2007. Ecosystem Water Use Efficiency in a Semiarid Shrubland and Grassland Community. Rangel. Ecol. Manag. 60, 464–470. https://doi.org/10.2111/1551-5028(2007)60[464:EWUEIA]2.0.CO;2

Esler, K.J., Milton, S.J., Dean, W.R.J., 2006. Karoo Veld - Ecology and Management. Briza Press, Pretoria.

Everson, C.S., 2001. The water balance of a first order catchment in the montane grasslands of South Africa. J. Hydrol. 241, 110–123. https://doi.org/10.1016/S0022-1694(00)00376-0

Falge, E., Baldocchi, D., Tenhunen, J., Aubinet, M., Bakwin, P., Berbigier, P., Bernhofer, C., Burba, G., Clement, R., Davis, K.J., Elbers, J.A., Goldstein, A.H., Grelle, A., Granier, A., Guðmundsson, J., Hollinger, D., Kowalski, A.S., Katul, G., Law, B.E., Malhi, Y., Meyers, T., Monson, R.K., Munger, J.W., Oechel, W., Paw U, K.T., Pilegaard, K., Rannik, Ü., Rebmann, C., Suyker, A., Valentini, R., Wilson, K., Wofsy, S., 2002. Seasonality of ecosystem respiration and gross primary production as derived from FLUXNET measurements. Agric. For. Meteorol. 113, 53–74. https://doi.org/10.1016/S0168-1923(02)00102-8

Fei, X., Jin, Y., Zhang, Y., Sha, L., Liu, Y., Song, Q., Zhou, W., Liang, N., Yu, G., Zhang, L., Zhou, R., Li, J., Zhang, S., Li, P., 2017. Eddy covariance and biometric measurements show that a savanna ecosystem in Southwest China is a carbon sink. Sci. Rep. 7. https://doi.org/10.1038/srep41025

Feig, G.T., Joubert, W.R., Mudau, A.E., Monteiro, P.M.S., 2017. South African carbon observations: CO_2 measurements for land, atmosphere and ocean. South Afr. J. Sci. 113. https://doi.org/10.17159/sajs.2017/a0237

Finkelstein, P.L., Sims, P.F., 2001. Sampling error in eddy correlation flux measurements. J Geophys Res 106, 3503–3509.

Foken, T., 2008. The energy balance closure problem: An overview. Ecol. Appl. 18, 1351–1367.

Foken, T., Oncley, S.P., 1995. Results of the workshop 'Instrumental and methodical problems of land surface flux measurements.' Bull Am Meteorol Soc 76, 1191–1193.

Foley, J.A., Coe, M.T., Scheffer, M., Wang, G., 2003. Regime Shifts in the Sahara and Sahel: Interactions between Ecological and Climatic Systems in Northern Africa. Ecosystems 6, 524–532. https://doi.org/10.1007/s10021-002-0227-0

Frost, P., Medina, E., Menaut, J.C., Solbrig, O., Swift, M., Walker, B., 1986. Responses of savannas to stress and disturbance: a proposal for a collaborative programme for research. Rep. IUBS Work. Group Decade Trop. Savanna Ecosyst. Spec. Issue 10 Biol. Int. IUBS Paris.

Gan, L., Peng, X., Peth, S., Horn, R., 2012. Effects of grazing intensity on soil thermal properties and heat flux under Leymus chinensis and Stipa grandis vegetation in Inner Mongolia, China. Soil Tillage Res. 118, 147–158. https://doi.org/10.1016/j.still.2011.11.005

Gillson, L., Midgley, G.F., Wakeling, J.L., 2012. Exploring the significance of land-cover change in South Africa. South Afr. J. Sci. 108. https://doi.org/10.4102/sajs.v108i5/6.1247

Gilmanov, T.G., Verma, S.B., Sims, P.L., Meyers, T.P., Bradford, J.A., Burba, G.G., Suyker, A.E., 2003. Gross primary production and light response parameters of four Southern Plains ecosystems estimated using long-term CO_2 flux tower measurements. Glob. Biogeochem. Cycles 17, 1071. https://doi.org/10.1029/2002GB002023

Goldewijk, K.K., 2001. Estimating global land use change over the past 300 years: The HYDE Database. Glob. Biogeochem. Cycles 15, 417–433. https://doi.org/10.1029/1999GB001232

Goodchild, M.S., Kühn, K.D., Nicholl, C., Jenkins, M.D., 2018. Temperature correction of substrate moisture measurements made in coir in polytunnel-grown strawberries. Acta Hortic. 147–154. https://doi.org/10.17660/ActaHortic.2018.1197.20

Guan, X., Huang, J., Guo, N., Bi, J., Wang, G., 2009. Variability of soil moisture and its relationship with surface albedo and soil thermal parameters over the Loess Plateau. Adv. Atmospheric Sci. 26, 692–700. https://doi.org/10.1007/s00376-009-8198-0

Guo, Q., Hu, Z., Li, S., Yu, G., Sun, X., Zhang, L., Mu, S., Zhu, X., Wang, Y., Li, Y., Zhao, W., 2015. Contrasting responses of gross primary productivity to precipitation events in a water-limited and a temperature-limited grassland ecosystem. Agric. For. Meteorol. 214–215, 169–177. https://doi.org/10.1016/j.agrformet.2015.08.251

Hagan, J.G., du Toit, J.C., Cramer, M.D., 2017. Long-term livestock grazing increases the recruitment success of epigeal termites: insights from a >75-year grazing experiment in the Karoo, South Africa. Afr. J. Range Forage Sci. 34, 123–132. https://doi.org/10.2989/10220119.2017.1314981

Hanan, N.P., Boulain, N., Williams, C.A., Scholes, R.J., Archibald, S., 2010. Functional convergence in ecosystem carbon exchange in adjacent savanna vegetation types of the Kruger National Park, South Africa. In: Hill, M. J and Hanan, N. P (ed), Ecosystem function in savannas: Measurement and modelling at landscape to global scales. Ecosystem Function in Savannas: Measurement and Modeling at Landscape to Global Scales, CRC Press, 77 – 95, Boca Raton, FL, U.

Hanan, N.P., Kabat, P., Dolman, A.J., Elbers, J.A., 1998. Photosynthesis and carbon balance of a Sahelian fallow savanna. Glob. Change Biol. 4, 523–538.

Hashimoto, H., Wang, W., Milesi, C., White, M.A., Ganguly, S., Gamo, M., Hirata, R., Myneni, R.B., Nemani, R.R., 2012. Exploring Simple Algorithms for Estimating

Gross Primary Production in Forested Areas from Satellite Data. Remote Sens 4, 303–326. https://doi.org/10.3390/rs4010303

Hastings, Oechel, W.C., Muhlia-Melo, A., 2005. Diurnal, seasonal and annual variation in the net ecosystem CO_2 exchange of a desert shrub community (Sarcocaulescent) in Baja California, Mexico. Glob. Change Biol. 11, 927–939. https://doi.org/10.1111/j.1365-2486.2005.00951.x

He, B., Wang, H., Huang, L., Liu, J., Chen, Z., 2017. A new indicator of ecosystem water use efficiency based on surface soil moisture retrieved from remote sensing. Ecol. Indic. 75, 10–16. https://doi.org/10.1016/j.ecolind.2016.12.017

Held, I.M., Soden, B.J., 2000. Water vapor feedback and global warming. Annu. Rev. Energy Environ. 25, 441–475. https://doi.org/10.1146/annurev.energy.25.1.441

Hess, T., Stephens, W., Maryah, U.M., 1995. Rainfall trends in the North East Arid Zone of Nigeria 1961-1990. Agric. For. Meteorol. 74, 87–97. https://doi.org/10.1016/0168-1923(94)02179-N

Hickler, T., Eklundh, L., Seaquist, J.W., Smith, B., Ardö, J., Olsson, L., Sykes, M.T., Sjöström, M., 2005. Precipitation controls Sahel greening trend. Geophys. Res. Lett. 32, L21415. https://doi.org/10.1029/2005GL024370

Higgins, S.I., Scheiter, S., 2012. Atmospheric CO_2 forces abrupt vegetation shifts locally, but not globally. Nature 488, 209–212. https://doi.org/10.1038/nature11238

Higgins, S.I., Scheiter, S., Sankaran, M., 2010. The stability of African savannas: insights from the indirect estimation of the parameters of a dynamic model. Ecology 91, 1682–1692. https://doi.org/10.1890/08-1368.1

Hoffmann, M., Jurisch, N., Albiac Borraz, E., Hagemann, U., Drösler, M., Sommer, M., Augustin, J., 2015. Automated modeling of ecosystem CO_2 fluxes based on periodic closed chamber measurements: A standardized conceptual and practical approach. Agric. For. Meteorol. 200, 30–45. https://doi.org/10.1016/j.agrformet.2014.09.005

Houghton, R.A., House, J.I., Pongratz, J., van der Werf, G.R., DeFries, R.S., Hansen, M.C., Le Quéré, C., Ramankutty, N., 2012. Carbon emissions from land use and land-cover change. Biogeosciences 9, 5125–5142. https://doi.org/10.5194/bg-9-5125-2012

Huang, L., He, B., Chen, A., Wang, H., Liu, J., Lů, A., Chen, Z., 2016. Drought dominates the interannual variability in global terrestrial net primary production by controlling semi-arid ecosystems. Sci. Rep. 6. https://doi.org/10.1038/srep24639

Huang, L., He, B., Han, L., Liu, J., Wang, H., Chen, Z., 2017. A global examination of the response of ecosystem water-use efficiency to drought based on MODIS data. Sci. Total Environ. 601–602. https://doi.org/10.1016/j.scitotenv.2017.05.084

Huete, A., Justice, C., van Leeuwen, W., 1999. MODIS Vegetation Index (MOD13) Algorithm Theoretical Basis Document. Version 3

Hui, D., Luo, Y., Katul, G., 2003. Partitioning interannual variability in net ecosystem exchange between climatic variability and functional change. Tree Physiol. 23, 433–442. https://doi.org/10.1093/treephys/23.7.433

Huizhi, L., Jianwu, F., 2012. Seasonal and Interannual Variations of Evapotranspiration and Energy Exchange over Different Land Surfaces in a Semiarid Area of China. J. Appl. Meteorol. Climatol. 51, 1875–1888. https://doi.org/10.1175/JAMC-D-11-0229.1

Huxman, T.E., Snyder, K.A., Tissue, D., Leffler, A.J., Ogle, K., Pockman, W.T., Sandquist, D.R., Potts, D.L., Schwinning, S., 2004. Precipitation pulses and carbon fluxes in semiarid and arid ecosystems. Oecologia 141, 254–268. https://doi.org/10.1007/s00442-004-1682-4

IPCC, 2013. Climate Change 2013: The Physical Science Basis. Contribution of Working Group I to the Fifth Assessment Report of the Intergovernmental Panel on Climate Change [Stocker, T. F., D. Qin, G. K. Plattner, M. Tignor, S. K. Allen, J. Boschung,

A. Nauels, Y. Xia, V. Bex and P. M. Midgley (eds.)]. Cambridge University Press, Cambridge, United Kingdom and New York, NY, USA, 1535 pp.

IPCC, 2007. Climate change 2007: The Physical Science Basis; Contribution of Working Group I to the Fourth Assessment Report of the Intergovernmental Panel on Climate Change, [Solomon, S., D. Qin, M. Manning, Z. Chen, M. Marquis, K.B. Averyt, M. Tignor and H.L. Miller (eds.)]. ed. Cambridge University Press, Cambridge, United Kingdom and New York, NY, USA, 996 pp.

IPCC, 2001. Climate Change 2001: The Scientific Basis. Contribution of Working Group I to the Third Assessment Report of the Intergovernmental Panel on Climate Change [Houghton, J. T., Y. Ding, D. J. Griggs, M. Noguer, P. J. van der Linden, X. Dai, K. Maskell, and C. A. Johnson (eds.)]. Cambridge University Press, Cambridge, United Kingdom and New York, NY, USA, 881pp.

Jafari, R., Bashari, H., Tarkesh, M., 2016. Discriminating and monitoring rangeland condition classes with MODIS NDVI and EVI indices in Iranian arid and semi-arid lands 31, 1–17. https://doi.org/10.1080/15324982.2016.1224955

Jaweed, T.H., Hussain, K., Kadam, A.K., Saptarshi, P.G., Gaikwad, S.W., 2018. Characterization of piospheres in Northern Liddar Valley of Kashmir Himalaya. Earth Syst. Environ. 2, 387–400. https://doi.org/10.1007/s41748-018-0056-8

Jenerette, G.D., Scott, R.L., Barron-Gafford, G.A., Huxman, T.E., 2009. Gross primary production variability associated with meteorology, physiology, leaf area, and water supply in contrasting woodland and grassland semiarid riparian ecosystems. J. Geophys. Res. Biogeosciences 114. https://doi.org/10.1029/2009JG001074

Jia, X., 2017. Dynamics and biophysical controls of carbon, water and energy exchange over a semiarid shrubland in northern China. Diss. For. 2017, 1–36. https://doi.org/10.14214/df.238

Jin, C., Xiao, X., Merbold, L., Arneth, A., Veenendaal, E., Kutsch, W.L., 2013. Phenology and gross primary production of two dominant savanna woodland ecosystems in Southern Africa. Remote Sens. Environ. 135, 189–201. https://doi.org/10.1016/j.rse.2013.03.033

Jung, M., Verstraete, M., Gobron, N., Reichstein, M., Papale, D., Bondeau, A., Robustelli, M., Pinty, B., 2008. Diagnostic assessment of European gross primary production. Glob. Change Biol. 14, 1–16. https://doi.org/10.1111/j.1365-2486.2008.01647.x

Junges, A.H., Bremm, C., Fontana, D.C., Oliveira, C.A.O. de, Schaparini, L.P., Carvalho, P.C. de F., 2016. Temporal profiles of vegetation indices for characterizing grazing intensity on natural grasslands in Pampa biome. Sci. Agric. 73, 332–337. https://doi.org/10.1590/0103-9016-2015-0213

Kato, T., Tang, Y., Gu, S., Hirota, M., Cui, X., Du, M., Li, Y., Zhao, X., Oikawa, T., 2004. Seasonal patterns of gross primary production and ecosystem respiration in an alpine meadow ecosystem on the Qinghai-Tibetan Plateau. J. Geophys. Res. 109. https://doi.org/10.1029/2003JD003951

Kgosikoma, O.E., Mojereman, W., Harvie, B.A., 2013. Grazing management systems and their effects on savanna ecosystem dynamics: A review. J. Ecol. Nat. Environ. 5, 88–94. https://doi.org/10.5897/JENE2013.0364

Kidson, J., Brümmer, C., Black, T.A., Morgenstern, K., Nesic, Z., McCaughey, J.H., Barr, A.G., 2010. Energy balance closure using eddy covariance above two different land surfaces and implications for CO_2 flux measurements. Bound.-Layer Meteorol. 136, 193–218. https://doi.org/10.1007/s10546-010-9507-y

Kleemann, J., Baysal, G., Bulley, H.N.N., Fürst, C., 2017. Assessing driving forces of land use and land cover change by a mixed-method approach in north-eastern Ghana, West Africa. J. Environ. Manage. 196, 411–442. https://doi.org/10.1016/j.jenvman.2017.01.053

Kotir, J.H., 2011. Climate change and variability in Sub-Saharan Africa: a review of current and future trends and impacts on agriculture and food securit. Env. Dev Sustain 13, 587– 605. https://doi.org/10.1007/s10668-010-9278-0

Kusangaya, S., Warburton, M.L., Archer van Garderen, E., Jewitt, G.P.W., 2014. Impacts of climate change on water resources in southern Africa: A review. Phys. Chem. Earth Parts ABC 67–69, 47–54. https://doi.org/10.1016/j.pce.2013.09.014

Kutsch, W.L., Hanan, N., Scholes, B., McHugh, I., Kubheka, W., Eckhardt, H., Williams, C., 2008. Response of carbon fluxes to water relations in a savanna ecosystem in South Africa 12.

Lambin, E.F., Geist, H.J., Lepers, E., 2003. Dynamics of land-use and land-cover change in tropical regions. Annu. Rev. Environ. Resour. 28, 205–241. https://doi.org/10.1146/annurev.energy.28.050302.105459

Lambin, E.F., Meyfroidt, P., 2011. Global land use change, economic globalization, and the looming land scarcity. Proc. Natl. Acad. Sci. 108, 3465–3472. https://doi.org/10.1073/pnas.1100480108

Lambin, E.F., Turner, B.L., Geist, H.J., Agbola, S.B., Angelsen, A., Bruce, J.W., Coomes, O.T., Dirzo, R., Fischer, G., Folke, C., George, P.S., Homewood, K., Imbernon, J., Leemans, R., Li, X., Moran, E.F., Mortimore, M., Ramakrishnan, P.S., Richards, J.F., Skånes, H., Steffen, W., Stone, G.D., Svedin, U., Veldkamp, T.A., Vogel, C., Xu, J., 2001. The causes of land-use and land-cover change: moving beyond the myths. Glob. Environ. Change 11, 261–269. https://doi.org/10.1016/S0959-3780(01)00007-3

Lasslop, G., Reichstein, M., Papale, D., Richardson, A.D., Arneth, A., Barr, A., Stoy, P., Wohlfahrt, G., 2010. Separation of net ecosystem exchange into assimilation and respiration using a light response curve approach: critical issues and global evaluation: SEPARATION OF NEE INTO GPP AND RECO. Glob. Change Biol. 16, 187–208. https://doi.org/10.1111/j.1365-2486.2009.02041.x

Law, B.., Falge, E., Gu, L., Baldocchi, D.., Bakwin, P., Berbigier, P., Davis, K., Dolman, A.., Falk, M., Fuentes, J.., Goldstein, A., Granier, A., Grelle, A., Hollinger, D., Janssens, I.., Jarvis, P., Jensen, N.., Katul, G., Mahli, Y., Matteucci, G., Meyers, T., Monson, R., Munger, W., Oechel, W., Olson, R., Pilegaard, K., Paw U, K.., Thorgeirsson, H., Valentini, R., Verma, S., Vesala, T., Wilson, K., Wofsy, S., 2002. Environmental controls over carbon dioxide and water vapor exchange of terrestrial vegetation. Agric. For. Meteorol. 113, 97–120. https://doi.org/10.1016/S0168-1923(02)00104-1

Leon, E., Vargas, R., Bullock, S., Lopez, E., Panosso, A.R., La Scala, N., 2014. Hot spots, hot moments, and spatio-temporal controls on soil CO_2 efflux in a water-limited ecosystem. Soil Biol. Biochem. 77, 12–21. https://doi.org/10.1016/j.soilbio.2014.05.029

Li, W., Ciais, P., Wang, Y., Peng, S., Broquet, G., Ballantyne, A.P., Canadell, J.G., Cooper, L., Friedlingstein, P., Le Quéré, C., Myneni, R.B., Peters, G.P., Piao, S., Pongratz, J., 2016. Reducing uncertainties in decadal variability of the global carbon budget with multiple datasets. Proc. Natl. Acad. Sci. 113, 13104–13108. https://doi.org/10.1073/pnas.1603956113

Liebethal, C., Huwe, B., Foken, T., 2005. Sensitivity analysis for two ground heat flux calculation approaches. Agric. For. Meteorol. 132, 253–262. https://doi.org/10.1016/j.agrformet.2005.08.001

Liu, H., Wang, B., Fu, C., 2008. Relationships between surface albedo, soil thermal parameters and soil moisture in the semi-arid area of Tongyu, northeastern China. Adv. Atmospheric Sci. 25, 757–764. https://doi.org/10.1007/s00376-008-0757-2

Liu, H. Q., Huete, A. R. 1995. A feedback based modification of the NDV I to minimize canopy background and atmospheric noise. IEEE Transactions on Geoscience and Remote Sensing, 33, 457–465

Liu, S., Chadwick, O.A., Roberts, D.A., Still, C.J., 2011. Relationships between GPP, Satellite Measures of Greenness and Canopy Water Content with Soil Moisture in Mediterranean-Climate Grassland and Oak Savanna. Appl. Environ. Soil Sci. 2011, 1–14. https://doi.org/10.1155/2011/839028

Loescher, H.W., Law, B.E., Mahrt, L., Hollinger, D.Y., Campbell, J., Wofsy, S.C., 2006. Uncertainties in, and interpretation of, carbon flux estimates using the eddy covariance technique. J. Geophys. Res. 111. https://doi.org/10.1029/2005JD006932

Lohmann, D., Tietjen, B., Blaum, N., Joubert, D.F., Jeltsch, F., 2012. Shifting thresholds and changing degradation patterns: climate change effects on the simulated long-term response of a semi-arid savanna to grazing: *Climate change and land use in savannas*. J. Appl. Ecol. 49, 814–823. https://doi.org/10.1111/j.1365-2664.2012.02157.x

López-Ballesteros, A., Beck, J., Bombelli, A., Grieco, E., Lorencová, E.K., Merbold, L., Brümmer, C., Hugo, W., Scholes, R., Vačkář, D., Vermeulen, A., Acosta, M., Butterbach-Bahl, K., Helmschrot, J., Kim, D.-G., Jones, M., Jorch, V., Pavelka, M., Skjelvan, I., Saunders, M., 2018. Towards a feasible and representative pan-African research infrastructure network for GHG observations. Environ. Res. Lett. 13, 085003. https://doi.org/10.1088/1748-9326/aad66c

Lovegrove, B., Siegfried, R., 1993. The living deserts of southern Africa. Fernwood Press, Cape Town, South Africa.

Lubke, R.A., Everard, D.A., Jackson, S., 1986. The biomes of the Eastern Cape with emphasis on their conservation. Bothalia 16. https://doi.org/10.4102/abc.v16i2.1099

Lucas-Moffat, A.M., Huth, V., Augustin, J., Brümmer, C., Herbst, M., Kutsch, W.L., 2018. Towards pairing plot and field scale measurements in managed ecosystems: Using eddy covariance to cross-validate CO_2 fluxes modeled from manual chamber campaigns. Agric. For. Meteorol. 256–257, 362–378. https://doi.org/10.1016/j.agrformet.2018.01.023

Lutz, W., Kc, S., 2010. Dimensions of global population projections: what do we know about future population trends and structures? Philos. Trans. R. Soc. B Biol. Sci. 365, 2779–2791. https://doi.org/10.1098/rstb.2010.0133

Ma, S., Baldocchi, D.D., Xu, L., Hehn, T., 2007. Inter-annual variability in carbon dioxide exchange of an oak/grass savanna and open grassland in California. Agric. For. Meteorol. 147, 157–171. https://doi.org/10.1016/j.agrformet.2007.07.008

MacDonald, D.J., Cowling, R.M., Boucher, C., 1996. Vegetation-environment relationships on a species rich coastal mountain range in the fynbos biome (South Africa). Vegetatio 123, 165–182. https://doi.org/10.1007/BF00118269

Magadza, C.H.D., 1994. Climate change: some likely multiple impacts in Southern Africa. Food Policy 19, 165–191.

Majozi, N., Mannaerts, C., Ramoelo, A., Mathieu, R., Mudau, A., Verhoef, W., 2017b. An Intercomparison of satellite-based daily evapotranspiration estimates under different eco-climatic regions in South Africa. Remote Sens. 9, 307. https://doi.org/10.3390/rs9040307

Majozi, N.P., Mannaerts, C.M., Ramoelo, A., Mathieu, R., Nickless, A., Verhoef, W., 2017a. Analysing surface energy balance closure and partitioning over a semi-arid savanna FLUXNET site in Skukuza, Kruger National Park, South Africa. Hydrol. Earth Syst. Sci. 21, 3401–3415. https://doi.org/10.5194/hess-21-3401-2017

Makhado, R.A., Scholes, R.J., 2011. Determinants of soil respiration in a semi-arid savanna ecosystem, Kruger National Park, South Africa. Koedoe 53.

Mallick, K., Jarvis, A., Wohlfahrt, G., Kiely, G., Hirano, T., Miyata, A., Yamamoto, S., Hoffmann, L., 2015. Components of near-surface energy balance derived from satellite soundings – Part 1: Noontime net available energy. Biogeosciences 12, 433–451. https://doi.org/10.5194/bg-12-433-2015

Marteau, R., Moron, V., Philippon, N., 2009. Spatial Coherence of Monsoon Onset over Western and Central Sahel (1950–2000). J. Clim. 22, 1313–1324. https://doi.org/10.1175/2008JCLI2383.1

Masseroni, D., Corbari, C., Mancini, M., 2014. Limitations and improvements of the energy balance closure with reference to experimental data measured over a maize field. Atmósfera 27, 335–352. https://doi.org/10.1016/S0187-6236(14)70033-5

Massmann, A., Gentine, P., Lin, C., 2018. When does vapor pressure deficit drive or reduce evapotranspiration? Hydrol. Earth Syst. Sci. Discuss. 1–38. https://doi.org/10.5194/hess-2018-553

Matsushita, B., Yang, W., Chen, J., Onda, Y., Qiu, G., 2007. Sensitivity of the Enhanced Vegetation Index (EVI) and Normalized Difference Vegetation Index (NDVI) to Topographic Effects: A Case Study in High-Density Cypress Forest. *Sensors*, 7, 2636-2651. ISSN 1424-8220. doi: https://doi.org/10.3390/s7112636

Mauder, M., Cuntz, M., Drüe, C., Graf, A., Rebmann, C., Schmid, H.P., Schmidt, M., Steinbrecher, R., 2013. A strategy for quality and uncertainty assessment of long-term eddy-covariance measurements. Agric. For. Meteorol. 169, 122–135. https://doi.org/10.1016/j.agrformet.2012.09.006

Mauder, M., Foken, T., 2004. Documentation and instruction manual of the eddy covariance software package TK2. Arbeitsergebn. Univ Bayreuth Abt Mikrometeorol 26, 42 pp.

McClain, M.E., Boyer, E.W., Dent, C.L., Gergel, S.E., Grimm, N.B., Groffman, P.M., Hart, S.C., Harvey, J.W., Johnston, C.A., Mayorga, E., McDowell, W.H., Pinay, G., 2003. Biogeochemical hot spots and hot moments at the interface of terrestrial and aquatic ecosystems. Ecosystems 6, 301–312. https://doi.org/10.1007/s10021-003-0161-9

McGuire, A.D., Sitch, S., Clein, J.S., Dargaville, R., Esser, G., Foley, J., Heimann, M., Joos, F., Kaplan, J., Kicklighter, D.W., Meier, R.A., Melillo, J.M., Moore, B., Prentice, I.C., Ramankutty, N., Reichenau, T., Schloss, A., Tian, H., Williams, L.J., Wittenberg, U., 2001. Carbon balance of the terrestrial biosphere in the twentieth century: Analyses of CO_2, climate and land use effects with four process-based ecosytem models. Glob. Biogeochem. Cycles 15, 183–206. https://doi.org/10.1029/2000GB001298

Merbold, L., Ardö, J., Arneth, A., Scholes, R.J., Nouvellon, Y., De Grandcourt, A., Archibald, S., Bonnefond, J.M., Boulain, N., Brueggemann, N., Bruemmer, C., Cappelaere, B., Ceschia, E., El-Khidir, H. a. M., El-Tahir, B.A., Falk, U., Lloyd, J., Kergoat, L., Le Dantec, V., Mougin, E., Muchinda, M., Mukelabai, M.M., Ramier, D., Roupsard, O., Timouk, F., Veenendaal, E.M., Kutsch, W.L., 2009. Precipitation as driver of carbon fluxes in 11 African ecosystems. Biogeosciences 6, 1027–1041. https://doi.org/10.5194/bg-6-1027-2009

Miao, F., Guo, Z., Xue, R., Wang, X., Shen, Y., 2015. Effects of Grazing and Precipitation on Herbage Biomass, Herbage Nutritive Value, and Yak Performance in an Alpine Meadow on the Qinghai–Tibetan Plateau. PLOS ONE 10, e0127275. https://doi.org/10.1371/journal.pone.0127275

Mintz, Y., Walker, G.K., 1993. Global Fields of Soil Moisture and Land Surface Evapotranspiration Derived from Observed Precipitation and Surface Air Temperature. J. Appl. Meteorol. 32, 1305–1334. https://doi.org/10.1175/1520-0450(1993)032<1305:GFOSMA>2.0.CO;2

Mitchell, L.E., Lin, J.C., Bowling, D.R., Pataki, D.E., Strong, C., Schauer, A.J., Bares, R., Bush, S.E., Stephens, B.B., Mendoza, D., Mallia, D., Holland, L., Gurney, K.R., Ehleringer, J.R., 2018. Long-term urban carbon dioxide observations reveal spatial and temporal dynamics related to urban characteristics and growth. Proc. Natl. Acad. Sci. 115, 2912–2917. https://doi.org/10.1073/pnas.1702393115

Moffat, A.M., Papale, D., Reichstein, M., Hollinger, D.Y., Richardson, A.D., Barr, A.G., Beckstein, C., Braswell, B.H., Churkina, G., Desai, A.R., Falge, E., Gove, J.H.,

Heimann, M., Hui, D., Jarvis, A.J., Kattge, J., Noormets, A., Stauch, V.J., 2007. Comprehensive comparison of gap-filling techniques for eddy covariance net carbon fluxes. Agric. For. Meteorol. 147, 209–232. https://doi.org/10.1016/j.agrformet.2007.08.011

Moncrieff, J., Clement, R., Finnigan, J., Meyers, T., 2004. Averaging, detrending, and filtering of Eddy Covariance time series. In: Lee X., Massman W., Law B. (eds) Handbook of Micrometeorology. Atmospheric and Oceanographic Sciences Library, Vol 29, Springer, Dordrecht.

Moncrieff, J.B., Monteny, B., Verhoef, A., Friborg, T., Elbers, J., Kabat, P., de Bruin, H., Soegaard, H., Jarvis, P.G., Taupin, J.D., 1997. Spatial and temporal variations in net carbon flux during HAPEX-Sahel. J. Hydrol. 188–189, 563–588. https://doi.org/10.1016/S0022-1694(96)03193-9

Moyana, F.E., Kutsch, W.L., Rebmann, C., 2008. Soil respiration fluxes in relation to photosynthetic activity in broad-leaf and needle-leaf forest stands. Agric. For. Meteorol. 148, 135 – 143. https://doi.org/10.1016/j.agrformet.2007.09.006

Munang, R., Thiaw, I., Alverson, K., Liu, J., Han, Z., 2013. The role of ecosystem services in climate change adaptation and disaster risk reduction. Curr. Opin. Environ. Sustain. 5, 47–52. https://doi.org/10.1016/j.cosust.2013.02.002

Mupangwa, W., Walker, S., Twomlow, S., 2011. Start, end and dry spells of the growing season in semi-arid southern Zimbabwe. J. Arid Environ. 75, 1097–1104. https://doi.org/10.1016/j.jaridenv.2011.05.011

Nakano, T., Shinoda, M., 2015. Modeling gross primary production and ecosystem respiration in a semiarid grassland of Mongolia. Soil Sci. Plant Nutr. 61, 106–115. https://doi.org/10.1080/00380768.2014.966043

Nel, W., Sumner, P.D., 2006. Trends in rainfall total and variability (1970-2000) along the KwaZulu- Natal Drakensberg foothills. South Afr. Geogr. J. 88, 130–137.

Nelson, J.A., Carvalhais, N., Migliavacca, M., Reichstein, M., Jung, M., 2018. Water-stress-induced breakdown of carbon–water relations: indicators from diurnal FLUXNET patterns. Biogeosciences 15, 2433–2447. https://doi.org/10.5194/bg-15-2433-2018

Ngetich, K.F., Mucheru-Muna, M., Mugwe, J.N., Shisanya, C.A., Diels, J., Mugendi, D.N., 2014. Length of growing season, rainfall temporal distribution, onset and cessation dates in the Kenyan highlands. Agric. For. Meteorol. 188, 24–32. https://doi.org/10.1016/j.agrformet.2013.12.011

Niu, S., Fu, Z., Luo, Y., Stoy, P.C., Keenan, T.F., Poulter, B., Zhang, L., Piao, S., Zhou, X., Zheng, H., Han, J., Wang, Q., Yu, G., 2017. Interannual variability of ecosystem carbon exchange: From observation to prediction. Glob. Ecol. Biogeogr. 26, 1225–1237. https://doi.org/10.1111/geb.12633

Osborne, C.P., Charles-Dominique, T., Stevens, N., Bond, W.J., Midgley, G., Lehmann, C.E.R., 2018. Human impacts in African savannas are mediated by plant functional traits. New Phytol. 220, 10–24. https://doi.org/10.1111/nph.15236

Otieno, D.O., K'Otuto, G.O., Maina, J.N., Kuzyakov, Y., Onyango, J.C., 2010. Responses of ecosystem carbon dioxide fluxes to soil moisture fluctuations in a moist Kenyan savanna. J. Trop. Ecol. 26, 605–618. https://doi.org/10.1017/S0266467410000416

Pan, S., Dangal, S.R.S., Tao, B., Yang, J., Tian, H., 2015. Recent patterns of terrestrial net primary production in Africa influenced by multiple environmental changes. Ecosyst. Health Sustain. 1, 1–15. https://doi.org/18. http://dx.doi.org/10.1890/EHS14-0027.1

Papale, D., Reichstein, M., Aubinet, M., Canfora, E., Bernhofer, C., Kutsch, W., Longdoz, B., Rambal, S., Valentini, R., Vesala, T., Yakir, D., 2006. Towards a standardized processing of Net Ecosystem Exchange measured with eddy covariance technique: algorithms and uncertainty estimation. Biogeosciences 3, 571–583. https://doi.org/10.5194/bg-3-571-2006

Parton, W., Morgan, J., Smith, D., Del Grosso, S., Prihodko, L., LeCain, D., Kelly, R., Lutz, S., 2012. Impact of precipitation dynamics on net ecosystem productivity. Glob. Change Biol. 18, 915–927. https://doi.org/10.1111/j.1365-2486.2011.02611.x

Penner, J.E., 1994. Atmospheric chemistry and air quality. In: Changes in land use and land cover: A global perspective. Edited by W. B. Meyer and B. L. Turner. Cambridge University Press, Cambridge, pp. 175–210.

Pettorelli, N., 2013. Normalized Difference Vegetation Index. Oxford University Press.

Pickup, G., 1996. Estimating the Effects of Land Degradation and Rainfall Variation on Productivity in Rangelands: An Approach Using Remote Sensing and Models of Grazing and Herbage Dynamics. J. Appl. Ecol. 33, 819–832. https://doi.org/10.2307/2404952

Pinty, B., Andredakis, I., Clerici, M., Kaminski, T., Taberner, M., et al, 2011a. Exploiting the MODIS albedos with the Two-stream Inversion Package (JRC-TIP):1. Effective leaf area index, vegetation, and soil properties 116. https://doi.org/10.1029/2010JD015372

Pinty, B., Clerici, M., Andredakis, I., Kaminski, T., Taberner, M., et al, 2011b. Exploiting the MODIS albedos with the Two-stream Inversion Package (JRC-TIP): 2. Fractions of transmitted and absorbed fluxes in the vegetation and soil layers. J. Geophys. Res. 116. https://doi.org/10.1029/2010JD015373

Pinty, B., Lavergne, T., Dickinson, R.E., Widlowski, J.L., Gobron, N., et al, 2006. Simplifying the interaction of land surfaces with radiation for relating remote sensing products to climate models. J Geo-Phys Res 111. https://doi.org/10.1029/2005JD005952

Qi, Y., Xu, M., 2004. Separating the effects of moisture and temperature on soil CO_2 efflux in a coniferous forest in the Sierra Nevada Mountains. Plant Soil 153, 131–142. https://doi.org/10.1023/A:1013368800287

R Core Team, 2013. R- A language and environment for statistical computing, R Foundation for Statistical Computing, Vienna, Austria.

Raich, J.W., Schlesinger, W.H., 1992. The global carbon dioxide flux in soil respiration and its relationship to vegetation and climate. Tellus 44B, 81–99. https://doi.org/10.1034/j.1600-0889.1992.t01-1-00001.x

Ramankutty, N., Foley, J.A., 1999. Estimating historical changes in global land cover: Croplands from 1700 to 1992. Glob. Biogeochem. Cycles 13, 997–1027. https://doi.org/10.1029/1999GB900046

Ramoelo, A., Majozi, N., Mathieu, R., Jovanovic, N., Nickless, A., Dzikiti, S., 2014. Validation of Global Evapotranspiration Product (MOD16) using Flux Tower Data in the African Savanna, South Africa. Remote Sens. 6, 7406–7423. https://doi.org/10.3390/rs6087406

Räsänen, M., Aurela, M., Vakkari, V., Beukes, J.P., Tuovinen, J.-P., Van Zyl, P.G., Josipovic, M., Venter, A.D., Jaars, K., Siebert, S.J., Laurila, T., Rinne, J., Laakso, L., 2017. Carbon balance of a grazed savanna grassland ecosystem in South Africa. Biogeosciences 14, 1039–1054. https://doi.org/10.5194/bg-14-1039-2017

Reichstein, M., Falge, E., Baldocchi, D., Papale, D., Aubinet, M., Berbigier, P., Bernhofer, C., Buchmann, N., Gilmanov, T., Granier, A., Grünwald, T., Havrankova, K., Ilvesniemi, H., Janous, D., Knohl, A., Laurila, T., Lohila, A., Loustau, D., Matteucci, G., Meyers, T., Miglietta, F., Ourcival, J.-M., Pumpanen, J., Rambal, S., Rotenberg, E., Sanz, M., Tenhunen, J., Seufert, G., Vaccari, F., Vesala, T., Yakir, D., Valentini, R., 2005. On the separation of net ecosystem exchange into assimilation and ecosystem respiration: review and improved algorithm. Glob. Change Biol. 11, 1424–1439. https://doi.org/10.1111/j.1365-2486.2005.001002.x

Rouse, J. W., Haas, R. H., Schell, J. A., Deering, D. W., 1974. Monitoring vegetation system in the great plains with ERTS (Earth Resources Technology Satellite). Proceedings of

Third Earth Resources Technology Satellite-1 Symposium. Greenbelt. USA. NASA SP-351, pp. 309–317

Roux, P.W., Vorster, M., 1983. Vegetation change in the karoo. Proc. Annu. Congr. Grassl. Soc. South. Afr. 18, 25–29. https://doi.org/10.1080/00725560.1983.9648976

Sánchez, J.M., Caselles, V., Rubio, E.M., 2010. Analysis of the energy balance closure over a FLUXNET boreal forest in Finland. Hydrol. Earth Syst. Sci. 14, 1487–1497. https://doi.org/10.5194/hess-14-1487-2010

Scanlon, T.M., Albertson, J.D., 2004. Canopy scale measurements of CO_2 and water vapor exchange along a precipitation gradient in southern Africa. Glob. Change Biol. 10, 329–341. https://doi.org/10.1046/j.1365-2486.2003.00700.x

Scholes, R.J., Archer, S.R., 1997. Tree-grass interactions in savannas. Annu Rev Ecol Syst 28, 517–44.

Scholes, R.J., Biggs, R. (Eds.), 2004. Ecosystem services in southern Africa: a regional assessment. Millennium Ecosystem Assessment and Council for Scientific and Industrial Research, Pretoria, South Africa.

Scholes, R.J., Frost, P.G.H., Tian, Y., 2004. Canopy structure in savannas along a moisture gradient on Kalahari sands. Glob. Change Biol. 10, 292–302. https://doi.org/10.1046/j.1365-2486.2003.00703.x

Scholes, R.J., Gureja, N., Giannecchinni, M., Dovie, D., Wilson, N., Davidson, N., Piggott, K., Mcloughlin, C., Van der, V., Freeman, A., Bradley, Smart, R., Ndala, S., 2001. The environment and vegetation of the flux measurement site near Skukuza, Kruger National Park. Koedoe 44, 73–83.

Schulze, E.D., Robichaux, R.H., Grace, J., Rundel, P.W., Ehleringer, J.R., 1987. Plant Water Balance. BioScience 37, 30–37. https://doi.org/10.2307/1310175

Scott, R.L., Hamerlynck, E.P., Jenerette, G.D., Moran, M.S., Barron-Gafford, G.A., 2010. Carbon dioxide exchange in a semidesert grassland through drought-induced vegetation change. J. Geophys. Res. 115. https://doi.org/10.1029/2010JG001348

Scott, R.L., Jenerette, G.D., Potts, D.L., Huxman, T.E., 2009. Effects of seasonal drought on net carbon dioxide exchange from a woody-plant-encroached semiarid grassland. J. Geophys. Res. 114. https://doi.org/10.1029/2008JG000900

Seymour, C.L., Milton, S.J., Joseph, G.S., Dean, W.R.J., Ditlhobolo, T., Cumming, G.S., 2010. Twenty years of rest returns grazing potential, but not palatable plant diversity, to Karoo rangeland, South Africa: Recovery of arid rangelands over 20 years. J. Appl. Ecol. 47, 859–867. https://doi.org/10.1111/j.1365-2664.2010.01833.x

Sivakumar, M.V.K., 1988. Predicting rainy season potential from the onset of rains in Southern Sahelian and Sudanian climatic zones of West Africa. Agric. For. Meteorol. 42, 295–305. https://doi.org/10.1016/0168-1923(88)90039-1

Sjöström, M., Ardö, J., Eklundh, L., El-Tahir, B.A., El-Khidir, H.A.M., Hellström, M., Pilesjö, P., Seaquist, J., 2009. Evaluation of satellite based indices for gross primary production estimates in a sparse savanna in the Sudan. Biogeosciences 6, 129–138. https://doi.org/10.5194/bg-6-129-2009

Skarpe, C., 1991. Impact of Grazing in Savanna Ecosystems. Ambio 20, 351–356.

Skead, C.J., 1982. Historical Mammal Incidence in the Cape Province Volume 1: The Western and Northern Cape. Cape Town, South Africa.

Snyder, K.A., Tartowski, S.L., 2006. Multi-scale temporal variation in water availability: Implications for vegetation dynamics in arid and semi-arid ecosystems. J. Arid Environ. 65, 219–234. https://doi.org/10.1016/j.jaridenv.2005.06.023

Sponseller, R.A., 2006. Precipitation pulses and soil CO_2 flux in a Sonoran Desert ecosystem. Glob. Change Biol. 13, 426–436. https://doi.org/10.1111/j.1365-2486.2006.01307.x

Svensen, H., Planke, S., Malthe-Sørenssen, A., Jamtveit, B., Myklebust, R., Rasmussen Eidem, T., Rey, S.S., 2004. Release of methane from a volcanic basin as a mechanism

for initial Eocene global warming. Nature 429, 542–545. https://doi.org/10.1038/nature02566

Tagesson, T., Ardö, J., Guiro, I., Cropley, F., Mbow, C., Horion, S., Ehammer, A., Mougin, E., Delon, C., Galy-Lacaux, C., Fensholt, R., 2016. Very high CO_2 exchange fluxes at the peak of the rainy season in a West African grazed semi-arid savanna ecosystem. Geografisk Tidsskrift 116(2), 93–109. https://doi.org/10.1080/00167223.2016.1178072

Tang, X., Li, H., Desai, A.R., Nagy, Z., Luo, J., Kolb, T.E., Olioso, A., Xu, X., Yao, L., Kutsch, W., Pilegaard, K., Köstner, B., Ammann, C., 2015. How is water-use efficiency of terrestrial ecosystems distributed and changing on Earth? Sci. Rep. 4, 7483. https://doi.org/10.1038/srep07483

Thomas, C.K., Law, B.E., Irvine, J., Martin, J.G., Pettijohn, J.C., Davis, K.J., 2009. Seasonal hydrology explains interannual and seasonal variation in carbon and water exchange in a semiarid mature ponderosa pine forest in central Oregon. J. Geophys. Res. 114. https://doi.org/10.1029/2009JG001010

Thomas, C.K., Martin, J.G., Law, B.E., Davis, K., 2013. Toward biologically meaningful net carbon exchange estimates for tall, dense canopies: multi-level eddy covariance observations and canopy coupling regimes in a mature Douglas-fir forest in Oregon. Agric Meteorol 173, 14–27. https://doi.org/10.1016/j.agrformet.2013.01.001

Triggs, J.., Kimball, B.., Pinter, P.., Wall, G.., Conley, M.., Brooks, T.., LaMorte, R.., Adam, N.., Ottman, M.., Matthias, A.., Leavitt, S.., Cerveny, R.., 2004. Free-air CO_2 enrichment effects on the energy balance and evapotranspiration of sorghum. Agric. For. Meteorol. 124, 63–79. https://doi.org/10.1016/j.agrformet.2004.01.005

UN, 2017. World Population Prospects: The 2017 Revision (Department of Economic and Social Affairs, Population Division) (https://esa.un.org/unpd/wpp/DataQuery/) (Accessed: 22 February 2019).

UN, 2002. The least developed countries report 2002: Escaping the poverty trap. United Nations Conference on Trade and Development.

Unger, S., Máguas, C., Pereira, J.S., David, T.S., Werner, C., 2010. The influence of precipitation pulses on soil respiration e Assessing the "Birch effect" by stable carbon isotopes. Soil Biol. Biochem. 42, 1800–1810. https://doi.org/10.1016/j.soilbio.2010.06.019

USGCRP, 2017. Climate Science Special Report: Fourth National Climate Assessment, Volume I [Wuebbles, D. J., D. W. Fahey, K. A. Hibbard, D. J. Dokken, B. C. Stewart, and T. K. Maycock (eds.)]. U.S. Global Change Research Program, Washington, DC, USA, 470 pp.

Valentini, R., Arneth, A., Bombelli, A., Castaldi, S., Cazzolla Gatti, R., Chevallier, F., Ciais, P., Grieco, E., Hartmann, J., Henry, M., Houghton, R.A., Jung, M., Kutsch, W.L., Malhi, Y., Mayorga, E., Merbold, L., Murray-Tortarolo, G., Papale, D., Peylin, P., Poulter, B., Raymond, P.A., Santini, M., Sitch, S., Vaglio Laurin, G., van der Werf, G.R., Williams, C.A., Scholes, R.J., 2014. A full greenhouse gases budget of Africa: synthesis, uncertainties, and vulnerabilities. Biogeosciences 11, 381–407. https://doi.org/10.5194/bg-11-381-2014

Veenendaal, E.M., Kolle, O., Lloyd, J., 2004. Seasonal variation in energy fluxes and carbon dioxide exchange for a broad-leaved semi-arid savanna (Mopane woodland) in Southern Africa. Glob. Change Biol. 10, 318–328. https://doi.org/10.1111/j.1365-2486.2003.00699.x

Vegten van, J.A., 1981. Man-made vegetation changes: an example from botswana´s savanna. Natl. Inst. Dev. Cult. Res. Doc. Unit Work. Pap. No 40.

Verduzco, V.S., Garatuza-Payán, J., Yépez, E.A., Watts, C.J., Rodríguez, J.C., Robles-Morua, A., Vivoni, E.R., 2015. Variations of net ecosystem production due to seasonal
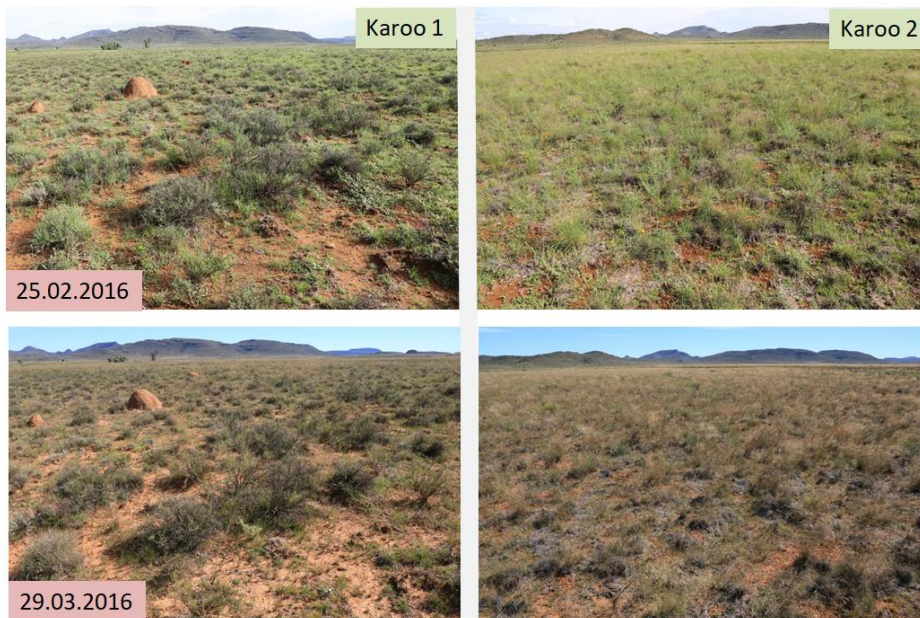
precipitation differences in a tropical dry forest of northwest Mexico: Carbon exchange at a tropical dry forest. J. Geophys. Res. Biogeosciences 120, 2081–2094. https://doi.org/10.1002/2015JG003119

Verhoef, A., 2004. Remote estimation of thermal inertia and soil heat flux for bare soil. Agric. For. Meteorol. 123, 221–236. https://doi.org/10.1016/j.agrformet.2003.11.005

Verhoef, A., Fernández-Gálvez, J., Diaz-Espejo, A., Main, B.E., El-Bishti, M., 2006. The diurnal course of soil moisture as measured by various dielectric sensors: Effects of soil temperature and the implications for evaporation estimates. J. Hydrol. 321, 147–162. https://doi.org/10.1016/j.jhydrol.2005.07.039

Verma, M., Friedl, M.A., Richardson, A.D., Kiely, G., Cescatti, A., Law, B.E., Wohlfahrt, G., Gielen, B., Roupsard, O., Moors, E.J., Toscano, P., Vaccari, F.P., Gianelle, D., Bohrer, G., Varlagin, A., Buchmann, N., van Gorsel, E., Montagnani, L., Propastin, P., 2014. Remote sensing of annual terrestrial gross primary productivity from MODIS: an assessment using the FLUXNET La Thuile data set. Biogeosciences 11, 2185–2200. https://doi.org/10.5194/bg-11-2185-2014

Verstraete, M.M., Hunt, L.A., Scholes, R.J., Clerici, M., Pinty, B., Nelson, D.L., 2012. Generating 275-m Resolution Land Surface Products From the Multi-Angle Imaging SpectroRadiometer Data. IEEE Trans. Geosci. Remote Sens. 50, 3980–3990. https://doi.org/10.1109/TGRS.2012.2189575

Vicca, S., Balzarolo, M., Filella, I., Granier, A., Herbst, M., Knohl, A., Longdoz, B., Mund, M., Nagy, Z., Pintér, K., Rambal, S., Verbesselt, J., Verger, A., Zeileis, A., Zhang, C., Peñuelas, J., 2016. Remotely-sensed detection of effects of extreme droughts on gross primary production. Sci. Rep. 6. https://doi.org/10.1038/srep28269

Vitousek, P.M., Mooney, H.A., Lubchenco, J., Melillo, J.M., 1997. Human Domination of Earth's Ecosystems. Science 277, 494–499.

Vittek, M., Brink, A., Donnay, F., Simonetti, D., Desclée, B., 2014. Land Cover Change Monitoring Using Landsat MSS/TM Satellite Image Data over West Africa between 1975 and 1990. Remote Sens. 6, 658–676. https://doi.org/10.3390/rs6010658

Vörösmarty, C.J., Green, P., Salisbury, J., Lammers, R.B., 2000. Global water resources: Vulnerability from climate change and population growth. Science 289, 284–288.

Vuichard, N., Papale, D., 2015. Filling the gaps in meteorological continuous data measured at FLUXNET sites with ERA-Interim reanalysis. Earth Syst. Sci. Data 7, 157–171.

Wang, X., Piao, S., Ciais, P., Janssens, I.A., Reichstein, M., Peng, S., Wang, T., 2010. Are ecological gradients in seasonal $Q10$ of soil respiration explained by climate or by vegetation seasonality? Soil Biol. Biochem. 42, 1728–1734. https://doi.org/10.1016/j.soilbio.2010.06.008

Weber, U., Jung, M., Reichstein, M., Beer, C., Braakhekke, M.C., Lehsten, V., Ghent, D., Kaduk, J., Viovy, N., Ciais, P., Gobron, N., Rodenbeck, C., 2009. The interannual variability of Africa's ecosystem productivity: a multi-model analysis. Biogeosciences 6, 285–295.

Whitehead, D., Gower, S.T., 2001. Photosynthesis and light-use efficiency by plants in a Canadian boreal forest ecosystem. Tree Physiol. 21, 925–929. https://doi.org/10.1093/treephys/21.12-13.925

Wigley, B.J., Bond, W.J., Hoffman, M.T., 2010. Thicket expansion in a South African savanna under divergent land use: local vs. global drivers? Glob. Change Biol. 16, 964–976. https://doi.org/10.1111/j.1365-2486.2009.02030.x

Wilczak, J.M., Oncley, S.P., Stage, S.A., 2001. Sonic anemometer tilt correction algorithms. Bound.-Layer Meteorol. 99, 127–150.

Williams, C.A., Albertson, J.D., 2004. Soil moisture controls on canopy-scale water and carbon fluxes in an African savanna. Water Resour. Res. 40. https://doi.org/10.1029/2004WR003208

Williams, C.A., Hanan, N., Scholes, R.J., Kutsch, W., 2009. Complexity in water and carbon dioxide fluxes following rain pulses in an African savanna. Oecologia 161, 469–480. https://doi.org/10.1007/s00442-009-1405-y

Williams, C.A., Hanan, N.P., Neff, J.C., Scholes, R.J., Berry, J.A., Denning, A.S., Baker, D.F., 2007. Africa and the global carbon cycle. Carbon Balance Manag. 2. https://doi.org/10.1186/1750-0680-2-3

Wilson, K., Goldstein, A., Falge, E., Aubinet, M., Baldocchi, D., Berbigier, P., Bernhofer, C., Ceulemans, R., Dolman, H., Field, C., Grelle, A., Ibrom, A., Law, B.., Kowalski, A., Meyers, T., Moncrieff, J., Monson, R., Oechel, W., Tenhunen, J., Valentini, R., Verma, S., 2002. Energy balance closure at FLUXNET sites. Agric. For. Meteorol. 113, 223–243. https://doi.org/10.1016/S0168-1923(02)00109-0

Wright, M.J., Teagle, D.A.H., Feetham, P.M., 2014. A quantitative evaluation of the public response to climate engineering. Nat. Clim. Change 4, 106–110. https://doi.org/10.1038/nclimate2087

Xue J., Su B., 2017, Significant Remote Sensing Vegetation Indices: A Review of Developments and Applications, Hindawi Journal of Sensors. Volume 2017, Article ID 1353691, 17 pages, https://doi.org/10.1155/2017/1353691

Yan, L., Chen, S., Huang, J., Lin, G., 2011. Water regulated effects of photosynthetic substrate supply on soil respiration in a semiarid steppe. Glob. Change Biol. 17, 1990–2001. https://doi.org/10.1111/j.1365-2486.2010.02365.x

Yan, L., Chen, S., Xia, J., Luo, Y., 2014. Precipitation Regime Shift Enhanced the Rain Pulse Effect on Soil Respiration in a Semi-Arid Steppe. PLoS ONE 9, e104217. https://doi.org/10.1371/journal.pone.0104217

Yang, F., Zhou, G., 2013. Sensitivity of temperate desert steppe carbon exchange to seasonal droughts and precipitation variations in Inner Mongolia, China. PLoS ONE 8, e55418. https://doi.org/10.1371/journal.pone.0055418

Yang, K., Wang, J., 2008. A temperature prediction-correction method for estimating surface soil heat flux from soil temperature and moisture data. Sci. China Ser. Earth Sci. 51, 721–729. https://doi.org/10.1007/s11430-008-0036-1

Yang, Y., Guan, H., Batelaan, O., McVicar, T.R., Long, D., Piao, S., Liang, W., Liu, B., Jin, Z., Simmons, C.T., 2016. Contrasting responses of water use efficiency to drought across global terrestrial ecosystems. Sci. Rep. 6, 23284. https://doi.org/10.1038/srep23284

Yu, Z., Wang, J., Liu, S., Rentch, J.S., Sun, P., Lu, C., 2017. Global gross primary productivity and water use efficiency changes under drought stress. Environ. Res. Lett. 12, 014016. https://doi.org/10.1088/1748-9326/aa5258

Zachos, J.C., Dickens, G.R., Zeebe, R.E., 2008. An early cenozoic perspective on greenhouse warming and carbon-cycle dynamics. Nature 451, 279–283. https://doi.org/10.1038/nature06588

Zhang, Q., Huang, R.H., 2004. Parameters of land-surface processes for Gobi in north-west China. Bound. Layer Meteorol. 110, 471–478.

Zhang, X., Zhai, P., Huang, J., Zhao, X., Dong, K., 2018. Responses of ecosystem water use efficiency to spring snow and summer water addition with or without nitrogen addition in a temperate steppe. PLOS ONE 13, e0194198. https://doi.org/10.1371/journal.pone.0194198

Zoungrana, B., Conrad, C., Amekudzi, L., Thiel, M., Da, E., 2014. Land Use/Cover Response to Rainfall Variability: A Comparing Analysis between NDVI and EVI in the Southwest of Burkina Faso. Climate 3, 63–77. https://doi.org/10.3390/cli3010063
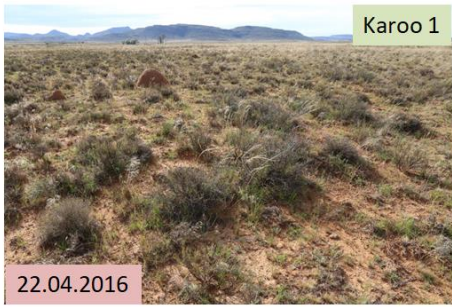
List of appendices

Appendix 1: Fixed-point photos at Karoo 1 and Karoo 2. Source: Justin Du Toit (GADI)

Fixed point photos taken on dates: 25.02.2016; 29.03.2016; 22.04.2016; 06.05.2016; 10.05.2016; 06.06.2016; 29.06.2016; 26.08.2016; 11.10.2016; 04.11.2016; 25.11.2016; 09.12.2016; 21.12.2016; 19.01.2017; 27.02.2017; 02.10.2017; 09.10.2017 and 23.10.2017 were an attempt to illustrate changes in biomass cover at the Karoo 1 and Karoo 2 study sites.
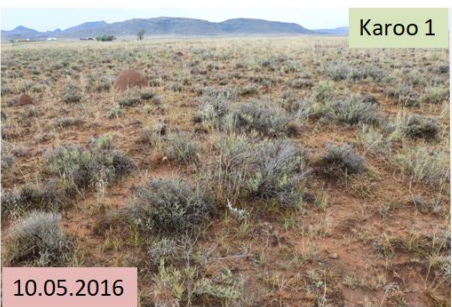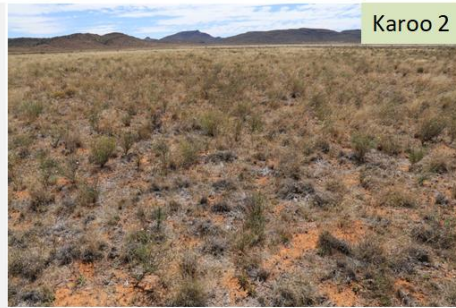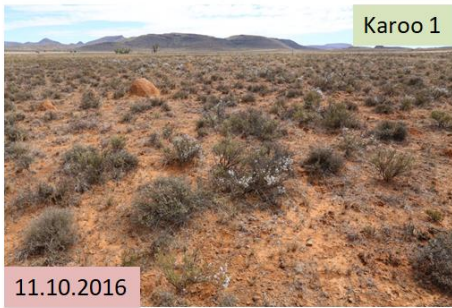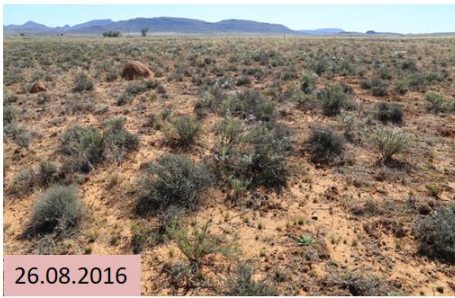
Karoo 1 · Karoo 2

22.04.2016 / 06.05.2016 / 10.05.2016 / 06.06.2016

154

Karoo 1 — 29.06.2016

Karoo 2

Karoo 1 — 26.08.2016

Karoo 1 — 11.10.2016

Karoo 2

Karoo 1 — 04.11.2016

Karoo 1

Karoo 2

25.11.2016

09.12.2016

Karoo 1

Karoo 2

21.12.2016

19.01.2017

Karoo 1

Karoo 2

27.02.2017

02.10.2017

Karoo 1

Karoo 2

09.10.2017

23.10.2017
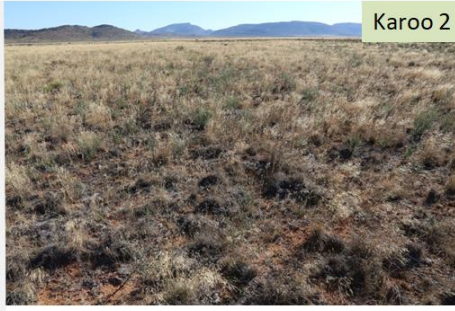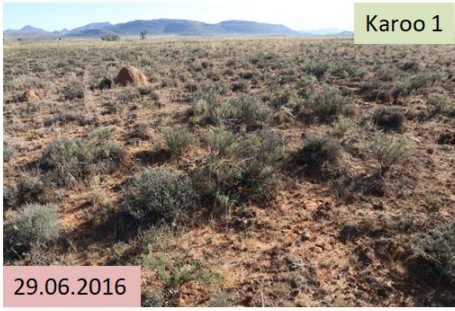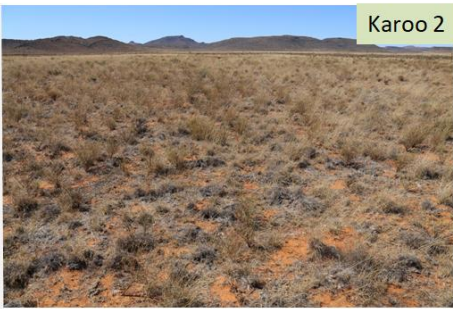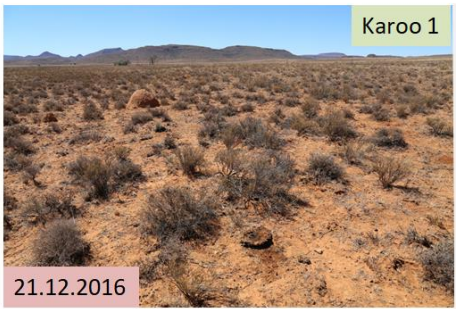
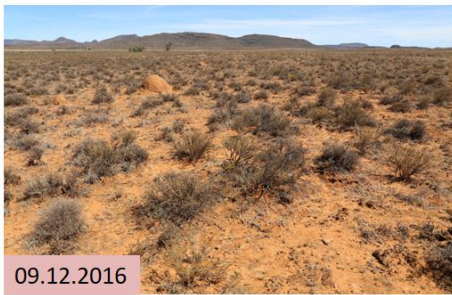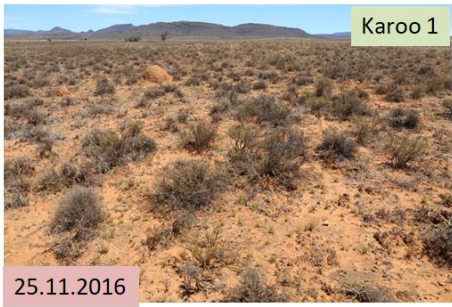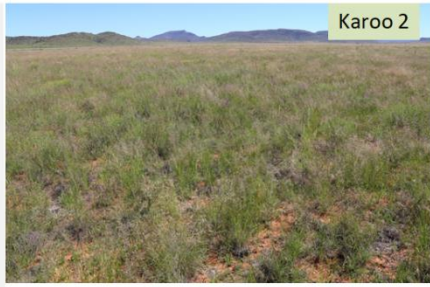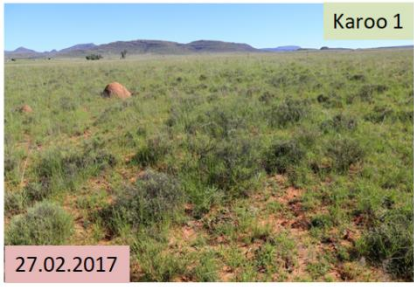# Appendix 2: Skukuza and Karoo instruments and measurement details

K – Karoo (1 and 2)   S – Skukuza

Meteorological variable		Instrument / sensor	No of sensors	Height /Depth (m)	Measurement frequency (Hz)	By who	Period
Soil Moisture (θ)	K	Soil Moisture Probe (ML3x Delta T)	2 x 2	0.08, 0.16	1	Thuenen Institute	01.11.2015 – 31.10.2018
	S	Soil Moisture Probe (CS615L)	8	0.06, 0.13; 0.29; 0.58	1	CSIR	2000 - 2014
Precipitation (P)	K	Tipping Bucket Rain Gauge (Texas Electronics TR 525)	1 x 2	3.5	1	Thuenen Institute	01.11.2015 – 31.10.2018
	S	Tipping Bucket Rain Gauge (Texas TR525M)	1	22	1	CSIR	2000 - 2014
Air Temperature (Tair)	K	Temperature/Humidity Probe (Rotronic HC2S3)	1 x 2	3.2	1	Thuenen Institute	01.11.2015 – 31.10.2018
	S	Temperature/Humidity Probe (Vaisalla HMP155, HMP50)	1	16	1	CSIR	2000 - 2014
Vapor Pressure Deficit (VPD)	K	Derived				Thuenen Institute	01.11.2015 – 31.10.2018
	S	Derived				CSIR	2000 - 2014
Relative Humidity (RH)	K	Temperature/Humidity Probe (Rotronic HC2S3)				Thuenen Institute	01.11.2015 – 31.10.2018
	S	Temperature/Humidity Probe (Vaisalla HMP155, HMP50)				CSIR	2000 - 2014
Net Radiation (Rn)	K	CNR4 Net Radiometer (Kipp and Zonen)	1 x 2	2.4	1	Thuenen Institute	01.11.2015 – 31.10.2018
	S	CNR2 and CNR4 Net Radiometer (Kipp and Zonen)	1	17	1	CSIR	2000 – 2014
Photosynthetically active radiation (PAR)	S	Licor LI 190R	1	17	1	CSIR	2000 - 2014

Soil Temperature (ST)	K	Soil Temperature Probe (UMS TH3 sdi12)	1 x 2	0.03(0.02);0.05(0.04); 0.07 (0.06); 0.1 (0.08); 0.17 (0.18); 0.3 (0.35)	1	Thuenen Institute	01.11.2015 – 31.10.2018
	S	Soil Temperature Probe (CS 108)	8	0.06, 0.13; 0.29; 0.58	1	CSIR	2000 - 2014
Soil Heat Flux (SHF)	K	Soil Heat Flux Plates (HFP01 + HFP01 SC)	6 x 2	0.1 and 0.2	1	Thuenen Institute	01.11.2015 – 31.10.2018
	S	Hukseflux HFP01	3	0.05	1	CSIR	2000 - 2014
Wind Speed (WS)	K	CSAT 3 Anemometer (Campbell Scientific)	1 x 2	3	20	Thuenen Institute	01.11.2015 – 31.10.2018
	S	RM young wind sentry, Climatronics Wind Sensor; Gill R3-50; CSAT 3 (Campbell Scientific)	1	16	20	CSIR	2000 - 2014
Wind Direction (WD)	K	CSAT 3 Anemometer (Campbell Scientific)				Thuenen Institute	01.11.2015 – 31.10.2018
	S	RM young wind sentry, Climatronics Wind Sensor; Gill R3-50; CSAT 3 (Campbell Scientific)				CSIR	2000 - 2014
Carbon (C) and turbulent energy (H, LE) fluxes	K	LI7200	1 x 2	3	20	Thuenen Institute	01.11.2015 – 31.10.2018
	S	LI6262 and LI7500	1 and 1	16	20	CSIR	2000 – 2005 and 2006 – 2014

(Eidesstattliche) Versicherungen und Erklärungen

(§ 9 Satz 2 Nr. 3 PromO BayNAT)

Hiermit versichere ich eidesstattlich, dass ich die Arbeit selbstständig verfasst und keine anderen als die von mir angegebenen Quellen und Hilfsmittel benutzt habe (vgl. Art. 64 Abs. 1 Satz 6 BayHSchG).

(§ 9 Satz 2 Nr. 3 PromO BayNAT)

Hiermit erkläre ich, dass ich die Dissertation nicht bereits zur Erlangung eines akademischen Grades eingereicht habe und dass ich nicht bereits diese oder eine gleichartige Doktorprüfung endgültig nicht bestanden habe.

(§ 9 Satz 2 Nr. 4 PromO BayNAT)

Hiermit erkläre ich, dass ich Hilfe von gewerblichen Promotionsberatern bzw. -vermittlern oder ähnlichen Dienstleistern weder bisher in Anspruch genommen habe noch künftig in Anspruch nehmen werde.

(§ 9 Satz 2 Nr. 7 PromO BayNAT)

Hiermit erkläre ich mein Einverständnis, dass die elektronische Fassung meiner Dissertation unter Wahrung meiner Urheberrechte und des Datenschutzes einer gesonderten Überprüfung unterzogen werden kann.

(§ 9 Satz 2 Nr. 8 PromO BayNAT)

Hiermit erkläre ich mein Einverständnis, dass bei Verdacht wissenschaftlichen Fehlverhaltens Ermittlungen durch universitätsinterne Organe der wissenschaftlichen Selbstkontrolle stattfinden können.

Braunschweig, 13.01.2020

………………………………………………………………………………………….

Ort, Datum, Unterschrift